Title
Bioinspired Adhesives for Fetal Membrane Presealing

Author
Winkler, Sara

Publication Date
2020

Peer reviewed|Thesis/dissertation

Bioinspired Adhesives for Fetal Membrane Presealing

By

Sara Winkler

A dissertation submitted in partial satisfaction of the

requirements for the degree of

Doctor of Philosophy

in

Bioengineering

in the

Graduate Division

of the

University of California, Berkeley

Committee in charge:

Professor Phillip B. Messersmith
Professor Tejal A. Desai
Professor Markita P. Landry

Summer 2020

Abstract

Bioinspired Adhesives for Fetal Membrane Presealing

by

Sara Winkler

Doctor of Philosophy in Bioengineering

University of California, Berkeley

Professor Phillip B. Messersmith, Chair

Fetal surgery can improve outcomes for severely affected fetuses, but carries a substantial risk of preterm birth. In order to perform surgery on the fetus, surgeons must breach the fetal membranes, a pair of fragile tissues that are susceptible to post-surgical rupture. Here, we sought to develop adhesives to seal this non-healing tissue, decreasing the overall risk of fetal surgery and making it an option for more families. The central challenge of fetal membrane sealing is achieving robust adhesion in a wet environment. In designing our adhesives, we took inspiration from marine mussels. Mussels secrete adhesive plaques rich in the amino acid 3,4- dihydroxyphenylalanine (DOPA) to adhere to diverse underwater surfaces, and we incorporated similar DOPA chemistry into our adhesives. We designed both injectable hydrogel adhesives and supramolecular adhesive patches and measured their adhesive strength and cytocompatibility. The adhesive hydrogels were also studied in a novel rabbit model of fetal membrane presealing. Membrane presealing is a proposed surgical approach in which the delicate fetal membranes are sealed prior to surgical puncture, stabilizing them, reducing the risk of membrane leakage and rupture, and decreasing the overall risk of fetal surgery. In this animal model, our mussel-inspired formulation appeared to be fetotoxic, but with an alternative adhesive, we found that fetal membrane presealing appeared facile and safe for mothers and fetuses. I also sought to understand how our materials interact with human fetal membrane tissues *in vitro*, and developed protocols to culture these tissues and their cells *ex vivo*. We used these cultures to analyze the cytocompatibility of our adhesives with clinically relevant primary cells and tissues, and took the initial steps to investigate the potential for a small molecule regenerative drug candidate (dihydrophenonthrolin-4-one-3-carboxylic acid, DPCA) to regenerate human fetal membranes *in vitro*. In this work, we created novel, mussel-inspired adhesive hydrogels and patches; established the feasibility of fetal membrane presealing *in vivo*; and developed human fetal membranes as an *ex vivo* tool for biomaterial-tissue compatibility evaluation.

Dedication

To my family: Mom, Dad, Marty, and especially Steven and Elizabeth.

I am not the first one of us to perform surgery on a pregnant patient, invent a new biomaterial, get a real engineering job, or earn a PhD, but I am grateful for the opportunity to follow in your footsteps while forging my own path. I am so privileged to have learned from and been loved by each of you.

Acknowledgements

This dissertation, and my entire graduate school experience, would not have been possible without the support of so many people. For technical help, experimental guidance, and project feedback, but also friendship, support, and love – thank you!

I am indebted to all Messersmith lab members, past and present. It has been so much fun to learn and work alongside you all. For expert technical assistance, input, and life wisdom I am thankful to postdocs and visiting scholars Cody Higginson, Kyueui Lee, Caroline Sugnaux, Suhair Sunoqrot, Helen Zha, Jing Cheng, Joakim Engstrom, Miriam Zintl, Yiran Li, Brylee Tiu, Patrick Rühs, Rafael Libanori, and Severin Sigg. Almost all of the experiments I did in grad school were totally new to me, so I am grateful to have learned from you all. Each of the graduate students I have overlapped with in the lab has helped shape me as a scientist and person. Many, many thanks to Angie Korpusik, Arianna Avellan, Peyman Delparastan, Katerina Malollari, Kelsey DeFrates, and Devang Amin for guiding me and for the many late nights and fun times we've shared. I can't wait to see what's next for each of you and all of the awesome things you will do. An extra special, eternal thanks to my postdoc project collaborators, Dirk Balkenende and Jisoo Shin – thank you for always guiding me, Dirk, and for taking my fetal membrane project across the finish line, Jisoo!

Of course, thank you so my undergraduate students Sarah Bhattacharjee, Sasha Demeulenaere, Sarah Spivack, Jacob Fisher, and Mason Kellogg for working alongside me so enthusiastically and excellently over the course of my grad school experience. I am so proud of all you accomplished in our lab, and what you've done since you left. Thank you for trusting me with your education, and sorry for all the times you had to clean the mussel tank.

Thanks to Phil for being a great mentor and sponsor and for trusting me with these projects. Besides being supportive of me and my career and always having new ideas for experiments and project directions to try, one of the greatest testaments to his leadership is that he always filled the lab with brilliant, kind, hardworking people. He fostered a strong spirit of collaboration in the group and supported us in pursuing our own ideas. Many of our postdocs have told me that this is the most collaborative, least competitive lab they've ever been in, and without this we're-all-in-it-together scientific outlook, I certainly would not have had nearly as successful of a PhD experience. I was introduced our group's work by a mentor in undergrad who recommended I look into the Messersmith lab because the research was cutting edge and because "Phil is a really nice guy." It's because of Phil's reputation and actions as good person and as a student advocate that I have been able to be so outspoken about systemic problems in academia; when I speak out against toxic mentorship, people know I'm not talking about Phil. Thanks for everything, Phil!!!!!

Thank you also to my committee members, Markita Landry and Tejal Desai, and to the collaborators outside our group for all your help and support! Huge thanks to Dr. Michael Harrison and his team, especially surgical fellows Vamsi Aribindi and Veeshal Patel. Working with the father of fetal surgery has been such an honor, and it is not an exaggeration to say that this project would have never happened (or been successful) without his input. Thanks to Dr. Diana Bauer and her team at the UCSF LARC facility for their expert work with our rabbits. Thank you to the Maternal Fetal Medicine research collections team, especially Jessica Amezcua and Nicole Rigler, and all the moms who donated their membranes to our research! Finally, an enormous thank you

to Diana Mountain and the entire team at Cornerstone Children's Center for remaining open during this pandemic and for providing such loving care to Elizabeth. Having a safe, loving place to send Elizabeth was absolutely critical to my finishing my PhD.

Thank you to my peers and friends in the Berkeley/UCSF Bioengineering program, especially Shaheen Jeeawoody, Christina Fuentes, Xinyi Zhou, and Kayla Wolf. I couldn't have done it without you, and am so excited for each of you on your post-PhD journey. Extra special thanks to Kayla for founding Double Shelix with me and being there for all our adventures along the way. This has been a bright light in my graduate school experience and it is so rewarding to light the way for future grad students and STEM leaders. I am stoked for our next episodes, and to explore post-PhD life with you.

My parents are a huge inspiration to me, the reason I pursued science from an early age, and the reason I wanted to get a PhD (and did!). Thank you so much, Mom and Dad, for everything you have done for me. I am enormously privileged to be your daughter. Both of you have helped so many patients over the course of your careers, both directly through your practices, and indirectly (but even more impactfully) through Compression Dynamics (Dad) and your work in Kenyan maternity wards (Mom). Over the course of my career, I aspire to live up to your impact. And thanks also to Marty for being a wonderful brother, and now uncle. I am grateful that we have been able to grow closer during these last years both in the Bay Area, and I am so proud (and envious!) of you and your real engineering job.

Thank you also to my in-laws, my extended family, and my Grandma Sue. I am grateful that the pandemic has provided an excuse for us to catch up more frequently, despite being farther away; I miss you all and can't wait to see you again soon.

Finally, infinite thanks and love to my husband, Steven. We are so lucky to have each other, and now, to have Elizabeth. Thank you for always supporting me, always loving me, and always cheering me on. You are the best husband I can ever imagine, and seeing almost no one except you and Elizabeth these past 6 months has only solidified this – further evidence of your love, patience, kindness, and big-heartedness. Also, Elizabeth is the best baby in the whole world. I would do anything for her, I am so proud of her, and I can't wait to see how her life unfolds. Thanks to Elizabeth, my strong, sweet, amazing daughter who came into our life at the perfect time and changed it forever. You're absolutely my greatest accomplishment, and being your mom is the privilege of a lifetime.

Sally Winkler
August 2020

Introduction

Fetal membranes surround the developing fetus and amniotic fluid and play a crucial role in maintaining a healthy pregnancy. For patients who undergo fetal surgery, the membranes are punctured to access the fetus, and this carries a substantial risk. About 30% of fetal surgery patients ultimately go into preterm labor, which is attributed to the surgical membrane puncture. The goal of my work was to develop novel ways to seal the fragile, non-healing fetal membranes. I designed a mussel-inspired injectable adhesive that confers robust adhesion, even in the wet fetal environment. In tandem with these sealant development efforts, I designed a pregnant rabbit model to study a new fetal surgery hypothesis proposed by our UCSF collaborators: fetal membrane presealing. In this approach, an injectable adhesive stabilizes the fetal membranes before they are punctured. We found that my mussel-inspired formulations were fetotoxic, but control adhesives performed well with no adverse maternal or fetal events, validating the presealing hypothesis. In addition, I collaborated with other lab members to develop mussel-inspired tissue adhesive patches with supramolecular crosslinkers. These patches also demonstrated robust adhesion to wet tissue in benchtop assays as well as dose-dependent cytocompatibility with fibroblast cell lines *in vitro*. Finally, I developed *ex vivo* tissue and cell culture models of human fetal membrane tissues from patients undergoing elective Cesarian sections. These cultures were used to conduct tissue- and cytocompatibilty assays of the adhesive biomaterials and study the effects of a small molecule regenerative drug candidate (dihydrophenonthrolin-4-one-3-carboxylic acid, DPCA) on human tissues for the first time.

This introduction highlights the key findings, enduring hurdles, and future opportunities of each chapter of my dissertation, as well as the overarching themes that tie the work together. I also identify emerging trends and give suggestions for the most promising and exciting areas for future exploration.

In **Chapter 1**, which was originally published as a review article titled “Biomaterials in Fetal Surgery” in *Biomaterials Science* [1], I outline the history and the clinical state-of-the-art of biomaterials in fetal surgery. This is, to my knowledge, the first and only published review on this topic. I also discuss ongoing bench research and animal studies in the field that show potential for eventual clinical translation. Today, much of the innovation centers on developing patches to protect neural tissue in fetal myelomeningocele (spina bifida) and adhesives to seal the fetal membranes following fetal surgery. Historically, most of the biomaterials and devices used in fetal surgery have been developed by fetal surgeons themselves, innovating when the tools they needed did not exist. In recent years, surgeon scientists and surgeon/scientist teams have developed novel biomaterials and devices for fetal surgery. I argue that these collaborative teams, especially with the input of biomaterials experts, are necessary for future innovations.

Themes of this review that especially resonate with other work in this dissertation include the importance of careful materials design and selection, the need for tissue- or surgery-specific biological characterization, and the challenges of maternal-fetal animal model development. One theme with a lot of promise for future exploration is potential for biomaterials engineers to exploit the immature fetal immune system. The fetus’s drastically reduced immune response, including to biomaterials, means that engineers could potentially utilize biomaterials in new and creative ways that would not be feasible in adult patients. An enduring hurdle to the field, which, realistically, may never be overcome, is simply that not many fetal surgeries are performed each year. This means that not only is clinical trial coordination is a challenge, but also that stakeholders are not financially incentivized to invest in innovation for fetal surgery. Nonetheless, new fetal surgery

and fetal treatment centers are opening around the world each year, including in the global south, as more countries and hospitals gain the technical skills and resources to accommodate these challenging and resource-intensive procedures. However, the development of adhesives to seal the fetal membranes, thus reducing the risk of preterm birth, may derisk the procedures enough to make the feasible options for more patients around the world.

Chapter 2 highlights the development of tissue adhesives inspired by marine organisms. This work was originally published with Dr. Diederik Balkenende, a postdoc in our lab, as "Marine-inspired polymers in medical adhesion," a review article in the *European Polymer Journal* [2]. In this work, we focus on innovative tissue sealants from the academic and patent literatures that are inspired by the chemical and structural adhesives of mussels (eg, *Mytilus*), sandcastle worms (eg, *Phragmatopoma californica*), and cephalopods. Of these three, mussels enjoy the longest research history; efforts to understand and replicate their unique underwater adhesive abilities span decades, with many research groups around the world attempting to create mussel-inspired adhesives for diverse applications, including wet tissue adhesion. While the unique adhesiveness of mussels has long been attributed to the amino acid DOPA (and its side chain, catechol) found in the adhesive plaques, an increasing body of evidence from biologists and biochemists has demonstrated that there is far more to the story of mussel adhesion. Other factors that play a role in mussel adhesion include synergy with the cationic amino acid lysine, the importance of the mussel's polymer processing and extrusion processes, and the role of cysteine in maintaining DOPA in its most reactive form at the adhesive interface. Understanding and recapitulation of the animals' materials processing abilities was also a key theme in the sandcastle worm- and cephalopod-inspired adhesives. From sandcastle worms' liquid-to-solid coacervate adhesives to the polymer gradients that make squid beaks both super hard and super tough, it is clear that materials engineers still have a lot of catching up to do. To be fair, evolution had quite the head start.

One of the themes in this review that resonates most strongly with the rest of the work in this thesis is the difficulty of comparing measured adhesive strength values across different labs and different publications. I encountered these challenges when measuring the adhesive strengths of hydrogel adhesives (Chapter 4) and tissue-adhesive patches (Chapter 5), and spent a significant amount of time optimizing these measurement protocols. In writing the review, it was impossible to identify the strongest adhesives as most authors deviate significantly from the ASTM standards in an effort to get more tissue- or surgery-specific data for their adhesive.

Notably, despite decades of effort, no mussel-inspired adhesive has reached the clinical trial stage, and surprisingly few have entered animal studies. In nature, catechol is extremely chemically reactive and, as such, is found in only a few places, including in marine structural adhesives and neuron synapses. However, these are isolated, confined environments with little opportunity for uncontrolled cellular interactions. It is becoming increasingly clear that outside these environments, the biological side effects of catechol's reactivity, including oxidation and H_2O_2 generation, may outweigh the benefits. Immediate oxidation of catechols *in situ* may be a workaround to these challenges (e.g., in catecholic adhesives activated with sodium periodate before adhering), but presents its own hurdles (namely, the introduction of an oxidant). I encountered firsthand the challenges of using unoxidized catechols *in vivo* in my rabbit studies – learn more in Chapter 4.

For **Chapter 3**, we are back to fetal surgery! In this Chapter, which has been submitted as a research article titled "Fetal membrane presealing: Initial *in vivo* study in rabbits," I describe the creation of a rabbit model of fetal membrane presealing. While we originally intended to use this animal model to study mussel-inspired presealants (Chapter 4), pilot surgeries showed that these materials were fetotoxic *in vivo*, so I pivoted this work and this manuscript to focus on presealing animal model development, using our control polymer (a previously-published PEG-based native chemical ligation hydrogel) as the membrane presealant. Past attempts to seal the fetal membranes following fetal surgery have focused on sealing the membranes at the end of the surgery, but our hypothesis, first proposed by our collaborator and co-author Dr. Michael Harrison (internationally renowned as the father of fetal surgery), is that by applying an adhesive between the membranes and uterus prior to puncture, the membranes are stabilized and defect size is reduced.

In developing our animal model, we found that presealing was quite straightforward and that the adhesive can reliably be delivered between the uterus and membranes without puncturing the membranes. We performed 15 survival and 1 acute surgeries, and overall the rabbit mothers did well with no maternal adverse events. Fetal survival was also excellent overall, but, surprisingly, there was no difference in fetal survival between fetuses in punctured fetal sacs, fetuses in presealed-then-punctured sacs, and fetuses who received no intervention. There were also no statistical differences between these groups when we analyzed fetal lung-to-body mass ratios, a marker of late-gestation fetal fitness. While this was disappointing, as we had expected to find a more robust benefit for presealing, this study does demonstrate that fetal membrane presealing is feasible, and that native chemical ligation hydrogels are appropriate for presealing applications. Future investigations could focus on tissue presealing for other clinical applications, for example to reduce leakage following bladder or dural surgery or to reduce hernias following abdominal surgeries. Past attempts to study presealing have failed because there was not a sealant with the appropriate adhesive properties, gelation kinetics, and biological properties. Now that we have identified one, the future of presealing is bright!

In **Chapter 4**, I detail the synthesis and characterization work I performed to develop mussel-inspired adhesive hydrogels. I modified the structure of the native chemical ligation hydrogels used in Chapter 3 to incorporate short mussel-inspired peptides containing DOPA and lysine to improve wet adhesive properties. Because the mussel-inspired formulations ultimately proved to be feto-toxic *in vivo,* most of the characterization work detailed herein was not published. Nonetheless, significant work went into developing adhesive characterization methods, especially obtaining reliable lap shear adhesion measurements. While this was instructive, ultimately, both the mussel-inspired formulations and the control hydrogels were more than sufficiently adhesive for fetal membrane presealing in our rabbit model. Thus, in hindsight, doing a single pilot animal trial very early on would have helped future research proceed more efficiently. Gratifyingly, some of this work developing accurate lap shear adhesive measurement protocols was used and published in Chapter 5 analyzing adhesive patches.

Another key contribution was the improved synthesis method I developed to couple amino acids sequentially to multi-arm PEGs. Past published protocols from our lab on similar syntheses reported 50% yield and 85% conversion, but I optimized the synthesis and purification to improve to ~95% conversion of each step and >60% yield after 3 coupling-deprotection cycles. Additionally, I studied these adhesives not only in conditioned media cytocompatibility studies with fibroblast cell lines, but also with fetal membrane cells and tissues from patients at UCSF.

The work with human fetal membranes is detailed in Chapter 6, and represents a unique contribution to the development of fetal surgery biomaterials.

In Chapter 4 I also summarize the work I did to develop a tissue-adhesive multi-lamellar patch. This work was done together with Dr. Diederik Balkenende, our team of Masters of Engineering students, and my undergraduate students Sarah Spivack and Sasha Demeulenaere. We sought to develop an elastomeric patch with a tissue-adhesive surface; a "universal" adhesive surface could be applied to an elastomer with the appropriate mechanical properties for a specific clinical application. We investigated a number of adhesive formulations, and we ultimately developed a formulation with moderate (20 kPa) adhesion to wet tissue. The limiting factor in this patch was the fact that, in a multi-layered patch (elastomer, polyphenol surface coating, adhesive surface polymers), the bulk adhesivity is determined by the strength of the weakest interface. In this case, the weak mechanical properties of the polyphenol coating layer are likely to blame. Our findings in the development of this patch informed the design of the supramolecular adhesive patch that we developed in Chapter 5.

Chapter 5 has been submitted as a manuscript titled "Supramolecular crosslinks in mussel-inspired tissue adhesives," that was co-authored with Dr. Diederik Balkenende (co-first author with me), Dr. Yiran Li, and Dr. Phil Messersmith. In this manuscript, we detail our efforts to design, synthesize, and characterize an adhesive patch that uses catechols for wet tissue adhesion and supramolecular ureido-4-pyrimidinone (UPy) as a supramolecular crosslinker. The key insight was the incorporation of hydrophobic and hydrophilic methacrylate comonomers. These enabled the entire material to phase separate on the nanoscale so that the cohesive supramolecular UPy monomers and adhesive dopamine methacrylamide monomers could be in their desired hydrophobic or hydrophilic environment, respectively. These adhesive patches exhibited robust adhesion to wet tissue, clinically-relevant burst strength, self-separated morphology upon AFM analysis, and dose-dependent cytocompatibility with fibroblasts *in vitro*. Our careful lap shear adhesion analysis, coupled with catechol-specific staining that allowed us to identify which polymer formulations were failing cohesively (indicating that the supramolecular polymer could be improved) vs. adhesively (indicating that the limit of catechol's wet adhesiveness had been reached) and to optimize and adjust the formulation accordingly to arrive at the best performer.

Many themes from this work are also echoed elsewhere in the thesis. For example, here we found that this mussel-inspired formulation did exhibit cytotoxicity at the higher studied doses; this tracks with other findings here (Chapter 4) and elsewhere that cast doubts about the extent of catechol's biocompatibility. Additionally, we noted substantial differences in measured lap shear adhesion strength of these materials depending on the incubation conditions used (under weights or clamped with binder clips). These seemingly small details track with findings from Chapters 2 and 4; it is really hard to reliably compare adhesive measurements from different labs, materials, publications, or even days. An enduring barrier to the clinical translation of these adhesives is the uncertainty that still surrounds catechol's *in vivo* safety. Other (unpublished) projects in the lab explored incorporating an n-hydroxysuccinimide esters into similar methacrylamide adhesives, and had promising early results (from Dirk Balkenende, Miriam Zintl, and Benzi Estipona); this is a good avenue for future exploration by other lab members, if desired.

In **Chapter 6**, I discuss my work developing human fetal membranes as a tool for biomaterials development and drug evaluation in our lab. I developed protocols for collecting human fetal membranes from UCSF patients and transporting them to our lab; *ex vivo* organ culture

of human fetal membranes, amnions, and chorions; and *in vitro* cell culture of extracted amnion cells. Once these methods were established, I used the cells and tissues for cytocompatibility evaluations with the polymer adhesives developed in Chapters 3 and 4. This unique and relatively accessible primary human tissue source could be used in cytocompatibility and tissue-compatibility analyses of other biomaterials. Few other models exist for whole-organ *ex vivo* culture, and this could be used to bridge the substantial gaps between cell culture, animal studies, and human clinical studies.

I also developed protocols to study the effect of the small molecule regenerative drug 1,4-dihydrophenonthrolin-4-one-3-carboxylic acid (DPCA) on the human fetal membranes. Fetal membranes do not heal after they rupture or are punctured, so they are an ideal candidate for mammalian tissue regeneration. My experiments did not show an effect on the expression of DPCA's downstream target, HIF1a, or of stem cell markers, which has been shown in animal models and other human cell lines *in vitro*. I attribute this to the low concentration of DPCA used in my studies. In fact, in the short time since the lab has reopened following coronavirus-19 campus closure, my colleague postdoctoral scholar Dr. Jisoo Shin has used my protocols, with increased DPCA concentrations over shorter times, to show that DPCA increases HIF1a and stem cell marker expression. Additional work to confirm these immunofluorescence staining results with qPCR and to study healing of punctured human fetal membrane tissue *ex vivo* is ongoing.

Moving forward, I see a huge potential for future growth of and expansion upon this work. Most of the labs studying and culturing human fetal membranes *ex vivo* are focused on the following areas: using intact or decellularized membranes for wound healing applications, studying the physiology of the fetal membranes, studying the cellular and immune trafficking and barrier functions of the amnion and placenta, developing placenta-on-a-chip applications, and using the fetal membranes as a source for human stem cells. However, few labs are using *ex vivo* fetal membranes to study tissue-biomaterial interactions or drug-tissue interactions. Now that our lab has established human fetal membrane culture protocols, we are poised to become a leader in this field.

Summary

The research presented here was all conducted in an attempt to solve a really scientifically and emotionally difficult problem faced by several hundred patients a year: the risk of preterm birth following fetal surgery. On the way to addressing this challenge, I have discovered new avenues of exploration in the fields of surgery, tissue adhesives, and regenerative medicine. While I will not be the one directly conducting the future work in any of these projects, I am optimistic that one day patients will receive presealants prior to surgery or be treated with a bioinspired adhesive. Meanwhile, I hope that scientists can continue to explore the awesome resource that is human fetal membrane tissues; like so many facets of women's health, there is still so much to be explored and discovered.

[1] S.M. Winkler, M.R. Harrison, P.B. Messersmith, Biomaterials in fetal surgery, Biomaterials science 7(8) (2019) 3092-3109.
[2] D.W.R. Balkenende, S.M. Winkler, P.B. Messersmith, Marine-inspired polymers in medical adhesion, European polymer journal 116 (2019) 134-143.

CHAPTER ONE – BIOMATERIALS IN FETAL SURGERY

N.B. *This chapter also appeared as a manuscript of the same title published in* Biomaterials Science*. I wrote the article with supervisory input from our UCSF collaborator Dr. Michael R. Harrison and Professor Phillip B. Messersmith. The ways that this chapter contribute to and inform my thesis as a whole are discussed in the Introduction.*

Sally M. Winkler, Michael R. Harrison, and Phillip B. Messersmith. "Biomaterials in fetal surgery." Biomaterials science *7.8 (2019): 3092-3109.*

Abstract

Fetal surgery and fetal therapy involve surgical interventions on the fetus *in utero* to correct or ameliorate congenital abnormalities and give a developing fetus the best chance at a healthy life. Historical use of biomaterials in fetal surgery has been limited, and most biomaterials used in fetal surgeries today were originally developed for adult or pediatric patients. However, as the field of fetal surgery moves from open surgeries to minimally invasive procedures, many opportunities exist for innovative biomaterials engineers to create materials designed specifically for the unique challenges and opportunities of maternal-fetal surgery. Here, we review biomaterials currently used in clinical fetal surgery as well as promising biomaterials in development for eventual clinical translation. We also highlight unmet challenges in fetal surgery that could particularly benefit from novel biomaterials, including fetal membrane sealing and minimally invasive myelomeningocele defect repair. Finally, we conclude with a discussion of the underdeveloped fetal immune system and opportunities for exploitation with novel immunomodulating biomaterials.

Introduction

Since the first successful surgery on a human fetus in the 1980s [4], fetal surgery has evolved from high-risk open surgeries, in which the uterus is opened, and the fetus partially exposed and operated on, to fetoscopic, minimally invasive procedures in which instruments or needles are inserted through small incisions in the mother's abdomen. The history, state of the art, and future potential of minimally invasive fetal surgery were expertly reviewed by Graves and colleagues [5]. While the number of fetal surgeries has increased, and the surgical techniques used in fetal surgery have advanced in the past 30 years, the materials used in these procedures have not seen such progress. For the most part, the materials and devices utilized in fetal surgeries have been modified from existing devices already in use in adults or neonates. The development of biomaterials tailored for fetal surgery represents a significant opportunity for biomaterials engineers to address an unmet clinical need. Furthermore, the immune privilege and relatively short duration of pregnancy present unique materials requirements and opportunities for fetal treatment compared to biomaterials used in adult patients.

For a patient to be a candidate for fetal surgery, the potential benefits of the surgery must outweigh the risk to the fetus and mother. Given the current limitations of fetal surgery, especially the risk of membrane rupture and subsequent preterm birth, surgical procedures have been limited to those conditions for which no intervention would mean fetal or perinatal death or loss of limb or organ function. For fetal surgery to be considered in a specific case, the fetus must be affected enough to merit intervention, but not so severely affected that the intervention would not improve chances of survival. Modalities for determining fetal health status include ultrasound, amniocentesis and other genetic diagnostics, fetal MRI, and fetal echocardiogram. Criteria to stage the severity of a condition, such as lung area to head circumference ratio measurements in

congenital diaphragmatic hernia, should be established before considering performing fetal surgeries to address that condition. Additionally, ample pre-clinical evidence of an intervention's success in animal models is necessary prior to deploying new strategies on human patients; animal models of fetal surgery were recently reviewed by Kabagambe and colleagues [6]. Patient-specific inclusion and exclusion criteria vary depending on the type of surgery being performed, and a representative set of criteria first established in 1982 [1] and still utilized today [2] is shown in **Box 1.**

Box 1. Criteria for fetal surgery, adapted from Harrison, et al. [1], Deprest et al. [2], and Adzick, et al [3].

- The disease must be diagnosable *in utero* and have no effective post-natal therapy.
- *In utero* disease staging criteria must be established to ensure that only severely affected fetuses undergo fetal surgery but also that surgery is not performed on fetuses too severely affected to benefit from intervention.
- Mothers and fetuses should be free of co-morbidities including fetal karyotype abnormalities.
- There must be proof in form of a clinical trial, or animal study evidence supporting a reasonable cause to assume (in case of pre-trial case studies), that the benefits of the therapy outweigh the risks of the procedure.
- Timing of the procedure must be optimized to provide maximum benefit to the fetus while decreasing the risk of preterm labor before the gestational limit of viability.
- Surgery and delivery should be performed at a specialty center with established ethical protocols, informed consent of parents, and an experienced multi-specialty team.

Maternal-fetal surgery also raises important ethical issues. These include establishment of clinical equipoise in clinical trials, determining "patienthood" in the context of maternal-fetal surgery, resisting the "urge to intervene," and ensuring accurate representation of a fetal surgery's risks and benefits to patients, especially in the context of potential fetal or neonatal palliative care [7-12]. Clinicians and engineers should take care that, whenever possible, potential fetal treatments are evaluated in the context of a randomized trial with multi-specialty clinical expertise. Due to small patient populations (made smaller by the fact that mothers may choose conservative management or pregnancy termination rather than enroll in a trial), many of the most successful randomized controlled trials are conducted as multi-center or even multi-national trials. Examples of such multi-center trials include Management of Myelomeningocele Study (MOMS), which compared outcomes from fetal vs. neonatal repair of myelomeningocele (spina bifida) neural tube defects [3]; the percutaneous vesicoamniotic shunting versus conservative management for fetal lower urinary tract obstruction (PLUTO) trial, which compared *in utero* bladder shunting to conservative management for urinary tract obstructions in utero [13, 14]; and a study from the EuroFoetus consortium that compared laser ablation of placental anastomoses versus serial amnioreduction for the treatment of twin-twin transfusion syndrome (TTTS) [15].

The use of biomaterials in fetal surgery has begun to improve clinical outcomes for human patients (**Figure 1**), for example the use of balloons for tracheal occlusion in congenital diaphragmatic hernia (**Figure 1a)** [16] and bladder shunts to drain lower urinary tract obstructions *in utero* (**Figure 1b**) [17]. Other biomaterials solutions are being actively explored in large animal models with promising results, such as patches to prevent damage to abnormally exposed neural tissue in cases of spina bifida (myelomeningocele, **Figure 1c**) [18]. Yet other materials are being developed and investigated in laboratory settings, such as novel fetal membrane sealant materials (**Figure 1d**) [19]. Efforts to design and test materials specifically for fetal surgery will not only spur materials innovation in an underexplored area of medicine but also provide the best chance at a healthy life for fetuses and infants with otherwise grim prognoses.

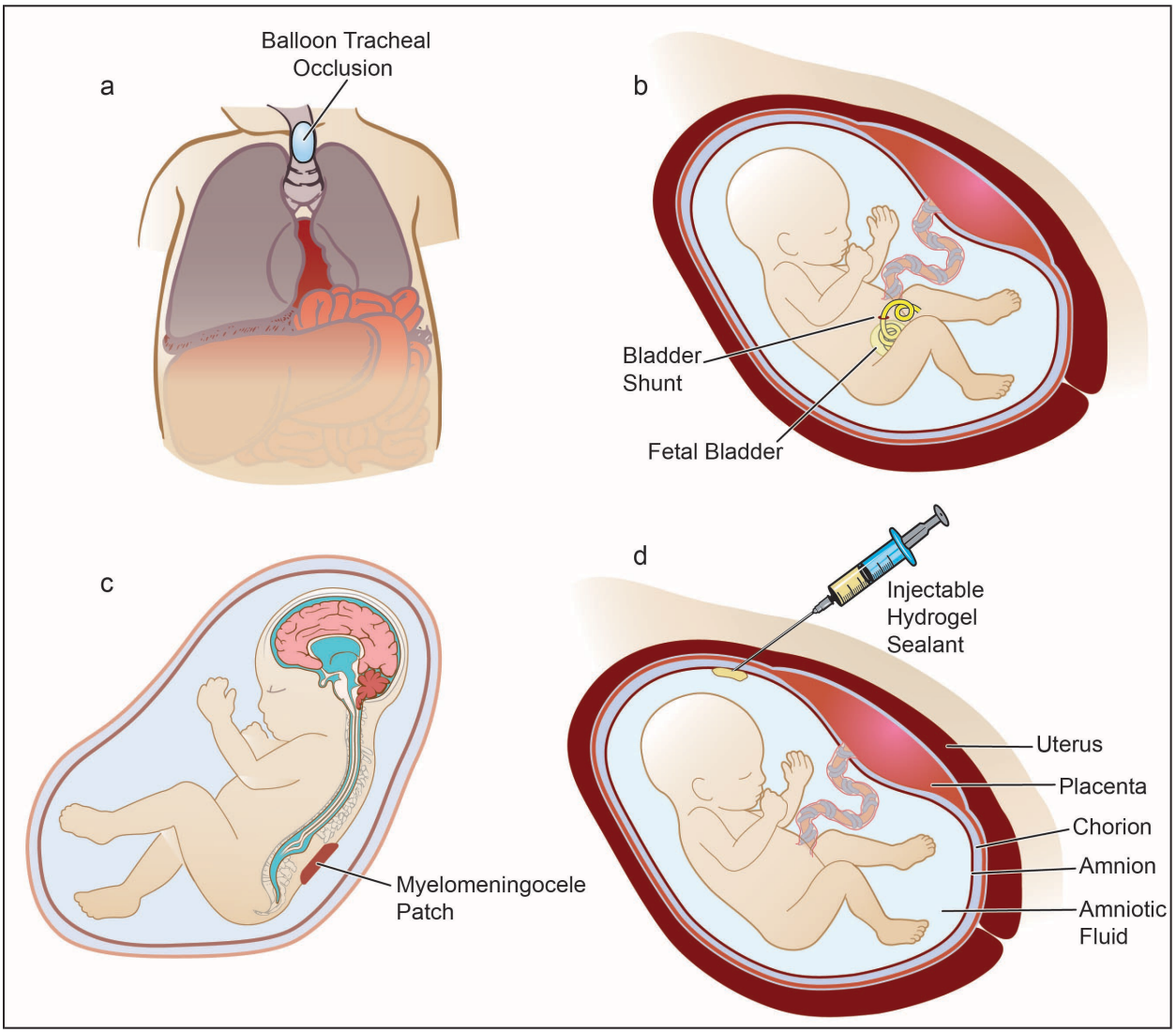

Figure 1. Examples of biomaterials in fetal surgery. (**A**) In cases of congenital diaphragmatic hernia, *in utero* occlusion of the trachea with a silicone balloon allows lungs to fill with fluid and expand, pushing abdominal organs out of the pleural cavity. (**B**) *In utero* shunting can be used to drain fluid from swollen organs into the amniotic sac. For example, in cases of lower urinary obstruction, double-pigtail shunts can be inserted to drain the bladder. (**C**) Biomaterial patches can prevent amniotic fluid enzymes from degrading abnormally exposed tissues *in utero*, for example, in covering exposed neural tissue in myelomeningocele. (**D**) Materials to seal the fetal membranes (chorion and amnion) and reduce the risk of membrane rupture following fetal surgery are currently in development. These injectable hydrogels can seal between the uterus and membranes (called presealing) or inside the amniotic sac (as shown).

Risk in fetal surgery

Risks associated with fetal surgery can be significantly reduced by decreasing the invasiveness of the procedure [20]. Recent trends in fetal surgery have transitioned away from open fetal surgery, in which the fetus is delivered in a partial Cesarean section (without disruption of placental blood supply), an intervention is performed, and the fetus is returned to the uterus for the duration of pregnancy [3]. In Fetoscopic surgery (Fetendo), small ports are placed in the amniotic space, an endoscope projects the image on a screen, and the surgeon manipulates small diameter instruments under endoscopic guidance to accomplish the surgery. Most Fetendo procedures are done percutaneously, but some require maternal laparotomy. Finally, in image guided fetal surgery, small instruments or needles deliver therapy or perform minor interventions under ultrasound guidance. Such minimally invasive interventions are often termed fetal therapy, and include fetal blood or stem cell transfusion [21], injection or aspiration of amniotic fluid [15], and some laser ablation procedures [22]. Instruments and devices used in fetal surgery and fetal therapy were expertly reviewed by Klaritsch and colleagues [23]. Most fetal procedures are performed in the first or second trimester of pregnancy, and many before the limit of viability (about 25 of a full 40 weeks of gestation) [3]. In its current form, fetal surgery still presents a significant risk to the fetus; thus, it is only performed on those fetuses at-risk for fetal or neonatal demise or loss of limb or organ function, but healthy enough that they will likely benefit from intervention. Major risks are discussed below.

Maternal morbidity in fetal surgery

Maternal morbidity is generally low in cases of fetal surgery and the underlying conditions that require fetal surgery. No maternal deaths following open fetal surgery have been reported [7, 24], but potential serious maternal sequalae of fetal surgery include placental abruption, premature rupture of membranes, premature birth, chorioamnionitis (infection of the membranes), loss of ability to carry future pregnancies, and sepsis [5]. Following open fetal surgery, delivery of the fetus in any future pregnancy must be via Cesarean section [25].

Fetal membrane rupture and preterm birth

In any fetal surgery, as well in fetal therapies and some diagnostic procedures like amniocentesis [26], the fetal membranes (amniotic sac) must be breached. The fetal membranes (FM) are the amnion and chorion, two closely associated membrane tissues that line the uterus and enclose the fetus and amniotic fluid during gestation (**Figure 1d)**. They are largely avascular and do not heal after rupture or surgical cut or puncture [27-30], though recent evidence suggests collagen remodeling may contribute to a small degree of re-sealing [31]. This breaching of the FM is what makes fetal surgery so risky, as it can lead to premature preterm rupture of membranes (PPROM) and preterm birth and its associated sequelae [32, 33]. Today, most fetal surgeries are performed via a minimally invasive approach; nonetheless iatrogenic (surgically caused) PPROM (iPPROM) occurs in about 30% of fetoscopic fetal surgery cases, but this rate varies from 11-50% depending on the intervention or practitioner [20, 34, 35]. iPPROM during the intervention is rare; iPPROM usually happens in the days or weeks following surgery, up to the 37th week, after which time the pregnancy is considered term [20]. Most fetal surgeries are performed during the second trimester, making the risk of iPPROM particularly high as fetuses are unable to survive outside the uterus prior to the limit of viability (25 weeks) [3], and delivery before 32 weeks' gestation carries

significant fetal and neonatal risk, including perinatal death [36]. iPPROM has accordingly been deemed the "Achilles heel" of fetal surgery; several materials strategies for reducing iPPROM have been investigated (detailed below), but no viable solution has been widely adopted. A solution to reduce iPPROM incidence would drastically decrease the overall risk of all fetal surgeries and make fetal surgery a viable option for more patients [20, 35].

Materials and devices in fetal surgery

Materials solutions for preventing fetal membrane rupture

To access the fetus, fetal surgeons necessarily must puncture the fetal membranes, and this puncture site can later rupture, leading to preterm birth. Over the past few decades, rates of neonatal survival and survival without impairment following preterm birth have remained steady, and the limit of viability relatively unchanged, indicating that the limits of post-natal intervention may have been reached [36]. For fetuses that undergo fetal surgery, there is still an unmet clinical need to keep the fetuses in the uterus until at least 37 of 40 weeks' gestation and to reduce the instances of membrane rupture and preterm birth.

Some attempted strategies for fetal membrane repair following fetal surgery (see **Table 1**) include mixtures of maternal platelets and fibrin cryoprecipitate with and without dry collagen/gelatin plugs ("amniopatch") [26, 37-39], synthetic polymer sealants [40, 41], laser welding [42], scaffold-type plugs manufactured directly from decellularized amnion [28, 43-45], and tissue engineering approaches [46]. These have had limited success, and no clear pathway to a clinically viable solution has emerged after more than a decade of research. These strategies rely on depositing a material at or near the defect site after the membranes have been punctured surgically. However, recent research on benchtop models of the fetal membranes suggests that applying an adhesive sealant material to the space between the fetal membranes and the uterus prior to surgical membrane puncture can help stabilize membranes during surgery, decrease the size of surgical membrane defects, maintain a watertight seal of the membranes during and after surgery, and decrease the probability of catastrophic membrane rupture [5, 47, 48]. Future development of adhesives for fetal membrane sealing could potentially use a seal-then-puncture membranes strategy ("presealing") with great success. We contend that an ideal material solution for membrane sealing may have some of the following properties: have similar mechanical properties to the fetal membranes, be fluid impenetrable, be nonimmunogenic and not cause an adverse tissue response, maintain adhesive and/or mechanical properties for an appropriate timescale to extend pregnancy (e.g., 4 weeks or up to 24 weeks), stabilize the membranes during and after surgery, be resistant to biofouling, or encourage cellular regrowth when applicable.

Some sealants and adhesives initially designed to seal tissues elsewhere in the body have been studied in benchtop, animal, or clinical models of fetal surgery [19, 49]; many such materials are summarized in **Table 1**, along with other materials designed specifically for fetal membrane sealing. Thus far, no material has become widely accepted as a clinical solution for fetal membrane sealing, and there exists an opportunity for biomaterials engineers to design or identify a material capable of strong, robust adhesion in the wet and biologically sensitive amniotic space.

Table 1: Selected materials approaches to sealing fetal membranes after surgical puncture

Material	Status	Notes	Selected Literature	Material Performance
Maternal platelets and fibrin cryoprecipitate, "amniopatch"	Human cases; mixed results	Used following fetal surgery *after iPPROM* but before onset of preterm labor. Slurry of platelets and cryoprecipitate injected into amniotic fluid, through FM at site distal to initial intervention hole. In some cases, transvaginal fluid leakage ceased, but FM seal at defect site hard to confirm. One series reported fetal or neonatal death of ≥1 fetus in 11 of 21 cases [38]. Some intrauterine fetal deaths attributed to platelet overactivation.	**Quintero** et al., 1999 [50]: n = 7 cases. 3 healthy infants. **Quintero**, 2001 [38]: n = 21. 11 pregnancies with ≥1 healthy infant. **O'Brien** et al., 2002 [51]: n = 1 case, amniopatch + gelatin sponge. Healthy infant. **Young** et al., 2004 [26]: n = 8 cases. 6 with no evidence of AF leakage from puncture site. **Richter**, et al. 2013 [52]: n = 24. 58% amniopatch success rate; 55% survival to discharge.	Formation of sealing plug at defect site difficult to document; mechanical properties akin to blood clot, not robust. Amniopatch method utilized only after onset of iPPROM; does not decrease incidence of membrane rupture.
Collagen or gelatin plug. For example decellularized amnion [41] or porcine-skin derived gelatin	Some in-human use; no improvement relative to the standard of care (no treatment)	As laparoscopic instruments are removed from the amniotic cavity, a small gelatin or collagen plug is left behind in the membrane defect, like a tampon.	**Chang**, et al., 2006 [37]: n = 27 TTTS laser coagulation cases. PPROM rate 4.2% attributed to "meticulous technique and atraumatic insertion and removal of ports." **Engels**, et al., 2014 [49]: n = 54 with plug; n = 87 without plug. No evidence that collagen reduces risk of PPROM after minimally invasive CDH repair. **Papanna** et al., 2010 [22]: n = 79 TTTS laser coagulation cases. PPROM rate = 34%.	Plug rapidly swells with amniotic fluid to occlude the defect site but does not form a water-tight seal.
Commercially available surgical glues				
Fibrin glues (e.g., Tisseal)	Benchtop evaluations and animal studies; some in-human use for other applications	Several groups have attempted to study the performance of commercially available surgical glues to seal the FM following surgical puncture. While some have been evaluated in animal or human trials and show promise, others were eliminated during phases of benchtop testing due to their poor biological or mechanical properties.	**Bilic**, et al., 2010 [19]: Compared biological and adhesive properties of surgical glues for FM sealing. **Burke**, et al., 2007 [53]: Compared adhesive properties of fibrin and mussel-inspired tissue adhesives. **Haller**, et al., 2012 [54]: Evaluated FM tissue sealing properties of glues using burst device. **Devaud**, et al., 2019 [55]: Comparative studies using novel delivery device to apply sealants to *ex vivo* human fetal membranes in benchtop uterine models.	Poor adhesion to wet tissues.
Cyanoacrylate (Dermabond, Histoacryl)			**Bilic**, et al., 2009 [19]. **Devaud**, et al., 2019 [55].	Dermabond: poor cytocompatibility, not for application to wet wounds (per manufacturer). Histoacryl: cytocompatible, adheres to tissues.

BioGlue (2-component bovine serum albumin/ glutaraldehyde glue)			**Azadani**, et al., 2009 [56]: Comparison of mechanical properties of vascular glues. **Bures**, et al., 2016 [57]: *In vitro* evaluation of BioGlue for sealing lung defects	Mismatch of mechanical properties relative to FM. When cured, BioGlue elastic modulus is 3.1 ± 1.6 MPa [56].
SprayGel (2-component multi-arm PEG modified with NHS ester and lysine)			**Bilic**, et al., 2009 [19]	Poor adhesion to wet tissues.
CoSeal (2-component multi-arm PEG with NHS esters and thiols)			**Spotnitz & Burks**, 2008 [58]	Swelling up to 400%; cannot be used in confined spaces such as the FM-uterus interface. Skin sensitization issues in animals.
Duraseal (2-component solution of PEG ester and trilysine amine)			**Spotnitz & Burks**, 2008 [58]	Swelling *in vivo* up to 50%; potential for wound-site infections.
Adhesives designed specifically for fetal membrane sealing				
Catechol-PEG (cPEG)	Promising animal data	Multi-arm PEG modified with mussel-inspired catechol groups.	**Bilic**, et al., 2009 [19]. **Haller**, et al., 2012 [54]: cPEG improved fetal survival in a rabbit model of fetal membrane sealing. **Kivelio**, et al., 2013 [59]. **Devaud**, et al., 2019 [55].	Catechol-mediated wet adhesion superior to other injectable glues. Biocompatibility and material cohesion could be improved.
Nanosilica coacervate glue + decellularized amnion (DAm)	Studied in porcine FM sealing model	Nanosilica coacervate glue was used to adhere sheets of DAm to seal swine FM defects, but no significant difference was found between treatment and control groups.	**Mann**, et al., 2012 [41]: Benchtop evaluation of coacervate glue. **Papanna**, et al, 2015 [60]: Mini-swine FM sealing study; inconclusive as swine membranes healed spontaneously.	Further work needed to identify the properties of this adhesive system and validate in a non-self-healing animal fetal membrane model.
Tissue engineering and other approaches				
Laser welding	Not suitable for FM sealing	Laser welding with albumin solders was attempted *in vitro* to seal a FM defect. This method was not effective in sealing membrane defects.	**Petratos**, et al., 2002 [42].	Laser welding produces worse adhesion than either sutures or polymeric sealants.
Membrane-mimetic sheets	Preliminary benchtop studies, some animal studies	Non-adhesive sheets are sutured, glued, or placed in or on membrane defects. Cell infiltration and sealing ability is assessed.	**Roman**, et al., 2016 [61]: Electrospum polymer bi-layer with elastic properties similar to the fetal membranes. Phase: Benchtop testing. **Ochsenbein-Kölble**, et al., 2006 [44]: Comparing decellularized amnion sheets to polyesterurethane	Most materials are non-adhesive, but approach is promising for both iatrogenic and spontaneous PPROM

			sheets in rabbit model of FM puncture. **Pensabene**, et al., 2015 [62]: Ultrathin poly-L-lactic acid film adheres to uterus and exposed FM following puncture in rabbit model. Adhesion mechanism unclear.	
Precipitated egg white	Bench top studies	Precipitated egg whites were assessed for ability to plug fluid leaks human FM in a benchtop model.	**Mendez-Figueroa**, et al., 2010 [63].	Translation potential unclear as unvalidated in animal work.
Tissue engineering *de novo* FM from hPSCs	Preliminary / basic science	**Shao,** et al., 2017 [64]: Protocol to differentiate human pluripotent stem cells (hPSCs) into amnion cells. In the future, this could be expanded to create implantable FM tissues for FM repair.		

Patches in Fetal Surgery

Myelomeningocele

One of the biggest success stories for fetal surgery is in the treatment of severe spina bifida, or myelomeningocele (MMC). Spina bifida affects about 3.5 per 10,000 live births in the US [65], and 25-40% of MMC-affected fetuses are aborted [66, 67]. Briefly, in this condition, the skin and vertebrae do not fully form around the lower portions of the spinal cord. Children with myelomeningocele often have limited lower limb function, develop Arnold-Chiari II malformations (hindbrain herniation), and accumulate excess cerebrospinal fluid in their brains (hydrocephalus), which often requires repeated shunting to drain the fluid throughout the patient's lifetime [3]. The development and progression of MMC follows the two-hit hypothesis where the first "hit" is the failure of the neural tube to become fully enclosed and the second "hit" is the damage to spinal tissue that occurs during gestation due to degradation by enzymes in the amniotic fluid [68, 69]. Fetuses with myelomeningocele can sometimes move their lower limbs during early gestation, but they are often born with total or partial loss of lower limb function because enzymes in the amniotic fluid degrade the spinal cord tissue [70]. It was hypothesized that repairing the defect *in utero* would protect it from such degradation. A large, multi-site clinical trial, the Management of Myelomeningocele Study (MOMS), demonstrated the benefits of open fetal surgery for myelomeningocele repair compared to traditional postnatal repair: increased use of lower limbs and decreased need for cerebrospinal fluid (CSF) shunting due to hydrocephalus. Risks of the repair surgery included membrane rupture leading to preterm birth and its associated complications [3]. In the MOMS trial, most cases were performed via an open surgical access technique, and the fetus's skin surrounding the spinal cord defect was stretched to cover the exposed neural tissue and sutured in place. This trial, as well as the preceding animal trials and human case studies, was excellently reviewed by Adzick [68] and the state of the field of *in utero* repair of MMC defects in the post-MOMS era was reviewed by Moldenhauer and Adizick [71].

Researchers have also investigated endoscopic and other minimally invasive approaches to tissue closure of MMC defects [72, 73]; tissue engineering approaches towards minimally invasive MMC repair were reviewed by Watanabe, et al. [18]. Recent animal data suggest the potential for the use of materials to aid in closure of MMC defects and to isolate exposed neural tissue from amniotic fluid enzymes and from surrounding tissues to prevent spinal cord tethering and its long-term sequelae [18, 74-82]. **Table 2** describes some of this preliminary work. Materials utilized as scaffolds and/or defect coverings for *in utero* MMC defect repair in animal models

include collagen- or gelatin-based scaffolds, small intestinal submucosa, and polymeric materials including silicone, high density poly ethylene, and polypropylene [18]. Covering MMC defects with a biomaterial could drastically reduce the FM defect size necessary to perform MMC closures compared to open surgery. In one example of biomaterials use for MMC defect coverage, Watanabe and colleagues used an ovine model of *in utero* myelomeningocele [83]. Fetal lambs with surgically-created MMC defects were treated with gelatin or gelatin-collagen sponges laced with bFGF (basic fibroblast growth factor) secured around the defect site with Dermabond cyanoacrylate adhesive with or without a gelatin sheet atop the sponge. Though all sheets detached from the defect site, sponges remained, and compared with sham-operated control animals, treated animals had less hindbrain herniation and more neural tube coverage. Animals treated with bFGF-laced sponges had more granulation and epithelial tissue covering the neural tube compared to non-bFGF controls. This work suggests the potential for eventual clinical translation, though more studies are required to assess the toxicity of the materials used, perfect minimally invasive surgical technique, improve or maintain a water-tight seal, and investigate the potential for spinal cord tethering at the defect site.

Table 2: Materials approaches for defect repair in MMC and gastroschisis.

Material	Status	Selected Literature	Material Performance
Surrounding tissue stretched to cover defect	Standard of care in fetal surgery to correct MMC; used postnatally to cover gastroschisis & omphalocele defects	**Adzick** et al., 2011 [3]: Repairing human MMC defects *in utero via* open fetal was surgery superior to post-natal repair in large randomized controlled trial. **Stephenson**, et al., 2010 [84]: Gastrochisis repair successful in 2/2 fetal sheep via open surgery.	Surrounding tissue can successfully be used to cover MMC or gastroschisis defects, but *in utero*, this approach may necessitate an open surgery approach. Also, in some gastroschisis and omphalocele cases, surrounding tissue is not large enough to stretch across the defect.
Gelatin/collagen sponges laced with bFGF and adhered to defect with cyanoacrylate adhesive	Successful rat and sheep studies	**Watanabe,** et al., 2010 [74]: Successful repair of MMC defect in fetal rat model using gelatin sheet/gelatin sponge combination, adhered to tissue with cyanoacrylate and laced with bFGF. Epithelial and vascular cell ingrowth into sponges. **Watanabe,** et al., 2016 [83]: Successful repair of MMC defect in ovine model using gelatin/collagen sponges laced with bFGF and with or without gelatin sheet covering. Histology revealed epithelial layers covering the defect as well as neovascularization.	Promising. Further work needed to fully characterize materials properties of sponge, including mechanical properties and cellular response to biomaterial, and to investigate if these findings could be reproduced using laparoscopic surgery. Materials did not cause inflammation of MMC defect site.
Biocellulose film	Sheep studies	**Oliveira**, et al., 2007 [85]: In sheep model, biocellulose films were placed atop exposed spinal tissue before skin was closed around the defect *in utero.* Film used to prevent cord tethering sometimes associated with MMC repair. **Papanna,** et al., 2016 (1) [86]: In sheep model, biocellulose films were attached with sandcastle worm-inspired sealants [41] that were cured with 532 nm laser light at 200 mW for 10 s/cm^2. Films dislodged, and no defect repair was seen.	Biocellulose films are still candidate materials, but attachment method is important. This sandcastle-worm inspired adhesive seems unsuitable for this application.
Cryopreserved human umbilical cord (HUC) + sutures	Sheep studies promising and ongoing; early human case reports successful	**Papanna,** et al., 2016 (1) [86]: In sheep model, HUC was used to patch MMC defect *in utero*. Repair was excellent, including almost full skin coverage and layered tissue regeneration. **Papanna,** et al., 2016 (2) [87]: Case report in 2 human patients. Promising results. Hindbrain herniation was reversed and minimal cord tethering was found at birth.	Promising. Further studies to validate the method and compare to *in utero* repair without patches are needed.
Placenta-derived mesenchymal stromal cells seeded onto porcine small intestine submucosa-derived ECM	Fetal rat study yielded promising results	**Chen** et al., 2018 [88]: In rat MMC model, decreased spinal cord deformity and apoptosis seen in placental mesenchymal stromal cell-seeded ECM compared to ECM-only scaffold repair in fetal rats.	Promising. More work needed in larger animal models.

Gastroschisis and omphalocele

Gastroschisis and omphalocele are abdominal wall defect conditions that are promising targets for fetal surgery. In gastroschisis, muscles of the fetal abdomen do not fully close around the internal organs, and the abdominal organs are exposed to the amniotic fluid [89]. Omphalocele is a similar condition, except that the organs are surrounded by a thin sac and not exposed directly to amniotic fluid. These conditions are diagnosed and staged *in utero* using ultrasound imaging,

with more severe cases presenting with a larger defect and more organs developing outside the abdominal cavity. Most patients have good outcomes following post-natal intervention. However, in 10-20% of fetal gastroschisis patients, prolapsed organs experience long-term damage. Experiments in fetal sheep demonstrate that intestinal damage at birth is likely due to restricted blood flow and enzymatic degradation of the tissues by the amniotic fluid [90-92]. Gastroschisis cases with severe intestinal evisceration are also at risk for oligohydramnios (insufficient amniotic fluid) [89]. Animal models of gastroschisis have been established in fetal chickens [93], rats [94], rabbits [95], and sheep [84, 90, 96]. Biomaterial patches developed for myelomeningocele may also be adapted for use treating gastroschisis or omphalocele. However, minimally invasive large animal models must first be developed to confirm the efficacy and improve the safety of procedures to deploy biomaterial tissue patches to cover gastroschisis or omphalocele defects in utero before they are attempted in human patients [97].

Materials considerations for tissue patch materials

Several considerations must be made in the development of biomaterials for direct application to internal fetal tissues, such as in the repair of myelomeningocele or gastroschisis defects or, potentially, sealing of FM defects. Materials should be deliverable via a minimally invasive surgical approach, for example a liquid adhesive that cures *in situ* or a patch that can be rolled up to fit into a 4 mm trocar. As these materials will be in direct contact with internal fetal organs, cytocompatibility is an extremely important consideration. Materials should be able to accommodate the fetus's growth throughout pregnancy and should isolate the exposed tissue from the surrounding amniotic fluid in a fluid-impenetrable manner. Attention should be paid to the post-natal and long-term role of the materials implanted *in utero*, and decisions about whether to design removable, degradable, or permanent materials should be application- and tissue-specific. Tatu and Lin [98] present a set of materials characterization experiments that should be considered when developing new fetal patch materials or choosing existing materials to use for these applications.

Occlusion and ablation in fetal surgery and fetal therapy

Congenital diaphragmatic hernia

Congenital diaphragmatic hernia (CDH) occurs in about 1 in 3000 live births when the diaphragm fails to form properly during development, allowing the liver, intestines, stomach, and/or other abdominal organs to invade the lung cavity. Thus, development of one or both lungs is restricted. Most infants with severe CDH defects undergo corrective surgery after birth, but in the most severe cases, prenatal treatment is considered to increase the lung volume of affected neonates at birth. Fetal lung area to head circumference ratio (LHR) is used to stage the severity of CDH, with severely affected fetuses having lower LHRs [99]. Saxena expertly reviewed the materials used for post-natal repair of large congenital diaphragmatic hernia defects [100]; none of the materials used were developed specifically for CDH repair, a trend also seen in fetal surgery and in the pediatric medical device industry in general. Jeanty, et al., reviewed non-surgical strategies with promise to address CDH *in utero*, including stem cell and pharmacologic methods [101], and Eastwood reviewed strategies that have been pursued in *in utero* animal models for reducing pulmonary hypoplasia resulting from CDH [102]. Over the years, several different types of biomaterials have been investigated for use addressing CDH *in utero* (**Figure 2**) including polymer fabrics [103], balloons [104], metal clips [99], hydrogels [105], and tissue engineered

materials [106]. The first successful in utero CDH repair was reported in 1990 [103]; a Gore-Tex (PTFE fabric) patch was used to repair the diaphragm and another to cover the abdomen (**Figure 2a**). However, *in utero* repair of fetal CDH defects did not prove superior to the standard of care, post-natal surgery and monitoring [103, 107].

Eventually, *in utero* hernia repair was replaced with *in utero* tracheal occlusion. Occluding the trachea allows fluid to build up in the lungs, and the lungs expand, pushing the abdominal organs out of lung cavity. Initially, open surgery was performed to clamp Silastic-coated titanium clips around the trachea to occlude it (**Figure 2b**). This was replaced by the less invasive Fetendo approach, in which a maternal laparotomy is performed to expose the uterus [99, 108, 109]. Then, endoscopic tools were used to place titanium clips around the trachea. In 2005, Deprest and colleagues published the first successful FETO balloon trial, in which an inter-tracheal silicone balloon is deployed laparoscopically and inflated to approximately 2 cm long and 0.5 mm in diameter to occlude the trachea (**Figure 2c**), eliminating the need for a maternal laparotomy [16, 104]. The timing and removal of tracheal occlusions is an ongoing area of research; titanium clips are removed via a neck incision at birth via an EXIT procedure, whereas balloons can be punctured transcutaneously *in utero* or punctured and removed at birth (vaginal or EXIT). Recently, *in situ* gelating hydrogels have been pursued as an alternative to balloon occlusion. Muensterer and colleagues tested fibrin glue (Tisseel), porcine gelatin, bovine collagen, cyanoacrylate, perfluorocarbon gel, and recombinant thrombin for their abilities to plug tracheal lumens *ex vivo* and found that fibrin glue performed best [110]. Fibrin glue was further studied in a fetal rabbit model of tracheal occlusion; it increased lung mass (beneficial) and airway resistance (detrimental) [110]. Similarly, in another study of fibrin glue on a fetal rabbit tracheal occlusion model, lung performance measures were not improved with tracheal occlusion [105]. Nevertheless, given the minimally invasive potential of this intervention, opportunities exist for further investigation and development of hydrogel sealants for intrauterine tracheal occlusion. Recent animal data suggest that the use of a hydrogel sealant to secure the balloon in the trachea and prevent balloon dislodgement [111] could be a promising strategy. Additional strategies that incorporate biomaterials are currently under development in animal and preclinical studies. In one example, researchers are looking to repair congenital diaphragmatic hernias postnatally with autologous tendon tissue seeded with circulating cells from the amniotic fluid [106].

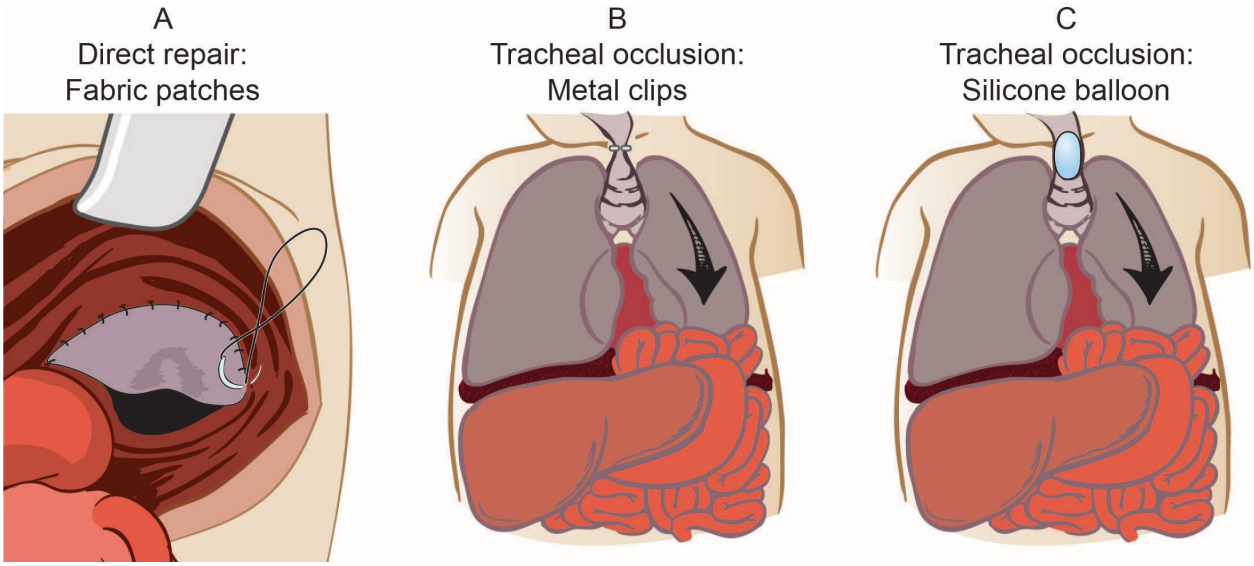

Figure 2. Biomaterials methods to address congenital diaphragmatic hernia *in utero*. (A) In early fetal surgeries, Gore-Tex patches were used to repair the diaphragm defect and to patch the abdomen. (B) In later attempts, fetal tracheal occlusion was achieved by clamping the fetal trachea with a metal clip to occlude it and allow lung volume to expand. (C) Currently, tracheal occlusion is achieved by inserting a silicone balloon into the fetal trachea and inflating it with saline to occlude the trachea.

Monochorionic twin conditions

In twin pregnancies, several circulation-related abnormalities sometimes indicate the use of fetal surgery. In a monochorionic twin pregnancy (about 70% of monozygotic, or identical, twin pregnancies), the fetuses share a placenta, but each has their own amniotic sac [112]. Vessels of the shared placenta sometimes anastomose abnormally, leading to twin-twin transfusion syndrome (TTTS) in 8-10% of monochorionic pregnancies [112]. Blood from one twin (donor) crosses into the other twin (recipient). In TTTS, one twin's heart pumps blood to both twins and causes delayed organ development in the donor twin and polyhydramnios and fetal hydrops (accumulation of excess fluid in fetal organs) in the recipient twin. Untreated, 70-80% of TTTS twins will die, and survivors may have severe organ damage [113]. The standard of care for TTTS is radiofrequency ablation of the vessels connecting the two twins. A 2004 multinational randomized controlled trial of 142 pregnant women with TTTS demonstrated that this method is more effective than serial amnioreduction of the polyhydramniotic sac [15]. Twins treated with laser coagulation (via a 3.3-mm cannula and a neodymium:yttrium–aluminum–garnet or diode laser under fetoscopic guidance) had significantly higher survival rates and lower rates of neurologic complications. However, survival of at least 1 twin to 6 months was still only 76% in the treatment group.

In Twin Reversed Arterial Perfusion (TRAP), which affects around 3% of monochorionic twin pregnancies, one twin is structurally normal, but, due to aberrant blood vessel formation in the placenta, the other twin lacks a heart and head. Untreated, 50% of normal "pump" twins, whose heart pumps blood both to themselves as well as to their acardiac twin, die *in utero* or as neonates

[114]. To treat TRAP, a 1 mm diameter needle is inserted through the maternal abdomen and into the abdomen of the acardiac twin. Radiofrequency ablation is performed through needle to heat and coagulate the vessels of the acardiac twin. This serves to stop blood flow between the twins without exposing the pump twin to the potentially harmful byproducts of the dying acardiac twin. Initial reports suggest a pump twin survival rate of around 90% [115].

Selective intrauterine growth restriction (SIUGR) is another twin abnormality in which unequal sharing of placental blood between monochorionic twins can result in an extreme difference in weight between the twins. In the most severe cases, one twin is drastically underdeveloped and poses a risk to the healthy twin because intrauterine death of the smaller twin could lead to neurological impairment of the healthy twin. In these cases, selective termination of the underdeveloped twin in a way that does not damage the healthy twin is considered [116]. When termination of the non-thriving twin is indicated and desired, similar care is needed to prevent harm to the healthy twin. Radiofrequency ablation is also used in this case, as is bipolar cord coagulation. Bipolar cord coagulation is more invasive (>3mm FM incision) and involves using ultrasound guidance to clamp the umbilical cord of the unhealthy twin and ablate it with radiofrequecy [117, 118].

Shunting in fetal surgery

Fetal Urinary Tract Obstruction

Lower urinary tract obstruction (LUTO) occurs in approximately 1-5 of 10,000 live births when the lower urinary tract fails to develop properly, and urine swells the fetal bladder. This can lead to fluid accumulation in the kidneys or other parts of the renal system (eg. hydronephrosis), renal failure, and oligohydramnios, and is associated with high rates of premature birth and/or perinatal death due to pulmonary hypoplasia (underdeveloped lungs). LUTO affects lung development because amniotic fluid is largely composed of fetal urine; when urinary outflow is obstructed, insufficient amniotic fluid hinders lung maturation. Postnatal repair to address urinary blockage remains the standard of care for this condition, but since severely affected infants often die of pulmonary hypoplasia soon after birth, fetal surgery to place a shunt to allow fluid to flow from the bladder to amniotic fluid during gestation (vesicoamniotic shunting) is an active area of research [119]. Current state of the art for fetal interventions for urinary tract obstructions were recently reviewed by Brock and Clayton [17]. After many case studies in human patients suggested that shunting may improve perinatal outcomes in fetuses with a poor outlook [120-122], a randomized controlled trial was conducted to study LUTO shunting in male fetuses, the percutaneous vesicoamniotic shunting versus conservative management for fetal lower urinary tract obstruction (PLUTO) trial [123, 124]. Though the PLUTO trial was terminated early due to low recruitment, the infants treated with *in utero* shunting had lower rates of perinatal lung failure-related death. However, shunt treatment did not appear to have a drastic benefit on renal function; two of seven treated and zero of three untreated infants alive at 2 years had normal renal function, respectively. Issues including membrane rupture, shunt dislodging, and shunt blockage were cited as contributing to fetal or infant demise in the treatment group. Further work to develop shunts specifically for fetal bladder shunting is needed.

Unfortunately, little attention has been paid to the materials of the shunts themselves, in urinary tract obstruction, as well as in shunting to address fetal hydrocephalus and drain fetal lungs (see below). In fact, the identity and physicochemical properties of materials used for shunting are often not mentioned in the medical literature. In a report of all 73 fetal obstructive uropathy cases

reported to International Fetal Surgery Registry between 1982 and 1985, for example, shunt architecture and materials were not reported [120]. In the PLUTO prenatal urinary tract obstruction clinical trial, a pigtail catheter was inserted with a King's College/Rocket introducer (n = 5) or a Harrison shunting set (n = 10). Double pigtail shunts are commonly used in fetal surgery as they are designed to stay in place and are unlikely to interfere with fetal development. However, a recent analysis revealed that half of shunts used to correct fetal urinary tract obstructions become dislodged [125]. And while shunts have multiple holes on each side, shunt failure due to clogging is common [120, 126, 127]. Future research should focus on the development of shunts with an internal antibiofouling surface coating to reduce biomolecule fouling and clogging of the shunt and valves, and alternative shunt architectures, such as the double basket catheter [128], to ensure the shunt stays in place for the duration of pregnancy.

More than half of fetal lower urinary tract obstructions are caused by posterior urethral valves (PUV) that occlude or block urine flow; this occurs in 1 of 8000 live births [129]. To repair urine flow and reduce fluid buildup in kidneys, some researchers have begun to use fetal cystoscopy and laser ablation to remove the aberrant valves [130]. In a series of 40 cases of diagnostic fetal cystoscopy to enable visualization of PUV formation, 23 fetuses received laser ablation to correct PUV, 14 fetuses survived to birth, and 12 survived with intact renal function. However, in addition to the risks associated with all fetal surgeries (maternal morbidity, preterm birth, spontaneous membrane rupture, etc.), laser fulguration was also associated with the development of urological fistulas (4 fetuses). Fistulae development was found to be associated ($P < 0.01$) with the materials and instruments used in the procedure, including catheter sheath shape and laser type, power, and energy [131]. Other opportunities for valve disruption for this indication include micro scissors, balloon disruption, or guidewires [131]. At least one case of successful in utero urethral stenting with a 0.9mm stent has been reported in a fetus with fetal cystoscopy-confirmed urethral stenosis [132]; the stent material was not reported. In a retrospective analysis comparing fetal cystoscopy and vesicoamniotic shunting in the treatment of severe LUTO cases, Ruano and colleagues found that while both therapies increase the 6-month survival rate, only fetal cystoscopy improves renal function in PUV patients [133]. A randomized controlled trial to compare the efficacy of fetal cystoscopy and vesicoamniotic shunting is planned (trial ID: NCT01552824).

Fetal pleural and pericardial fluid

Similar double-pigtail shunts are also sometimes used *in utero* to drain fluid from the lungs and chest cavity into the amniotic space. Pleural effusion (PE) and macrocystic congenital cystic adenomatoid malformation (CCAM) are rare conditions in which fluid builds up in the pleural sac surrounding the lungs and in cystic lung tissue, respectively [134]. Untreated, severe fetal pleural effusion can have a mortality rate between 57-100% [135]. In a retrospective of 48 cases of fetal hydrothorax (PE of lymphatic fluid) in the Netherlands from 2001-16, overall fetal survival through the neonatal period following *in utero* thoracoamniotic shunting was 75% [136]. A retrospective study from Children's Hospital of Philadelphia (1998-2001) found postnatal survival of treated fetuses to be 67% (6 of 9 fetuses) for PE and 70% (7 of 10 fetuses) for CCAM [134]. These survival rates and rates of adequate lung function following fetal thoracoamniotic shunt placement are similar to those first reported in 1988, 75% survival of 8 treated fetuses [135]. Many fetuses with fluid accumulation in the chest will not need fetal surgery, but the procedure is considered when the fetus develops severe fetal hydrops and/or the fluid accumulation constricts surrounding organs.

Fetal Hydrocephalus

Severe cerebrospinal fluid (CSF) buildup in the ventricles of the fetal brain (ventriculomegaly) can delay the development of other brain structures and often requires post-natal placement of a ventricoperitoneal shunt to drain excess CSF to the abodmen. These shunts are prone to infection and clogging, and serial shunt replacement throughout the child's lifetime is often required. Some cases of fetal vesicoamniotic shunting (between brain ventricles and AF) have been reported in human patients [120, 137, 138], though overall prognoses remain grim. One factor that contributes to poor outcomes in these fetuses is that most cases of hydrocephalus are accompanied by co-morbidities including neural tube defects, oligo- or polyhydramnios, and other congenital abnormalities [138]. A 2014 report of 222 cases in Poland of fetal hydrocephalus repair conducted between 1992-2012 used Orbis-Sigma and Accu-Flow valves and Cook's shunts to drain fluid from the ventricles into the amniotic sac. In this study, 44% of neonates were preterm, and only 12.5% had normal mental development at age 3 [139]. The study demonstrated that fetal shunting decreased ventricular size, but as this was not a randomized trial, it cannot be fully established that this treatment is better than the standard of care. Other case studies show similarly inconclusive results [126], and a retrospective case study suggests that fetal shunting results in higher rates of severe neurological impairment [140]. A voluntary moratorium against *in utero* shunting for fetal hydrocephalus has since been imposed until more information about the natural progression of fetal hydrocephalus could be established. In many of these early studies, patient selection was poor as it was difficult to identify which fetuses may benefit most from intervention, however improved fetal diagnostic methods may allow for advances fetal surgery for hydrocephalus in the future [140].

Immune tolerance and exploitation in fetal surgery and fetal therapy

Biomaterial interaction with the innate and adaptive immune systems has long been an area of research in adult patients, but less is known about the response of the fetal immune system to implanted biomaterials. The fetal immune system develops throughout gestation and continues to develop after birth; preterm infants are likely to be born with more immature immune systems, making them especially susceptible to bacterial or viral infections [141]. A certain degree of fetal immune tolerance or immaturity is necessary to accommodate the presence of maternal alloantigens in the fetal circulation [141, 142]. However, recent evidence in mouse models suggests that fetal interventions, including fetal surgery, increase trafficking of maternal T cells to the uterus and increase maternal T cell recognition of the fetus. This trafficking could contribute to adverse outcomes like preterm birth and immune-mediated fetal demise [143, 144]. Nonetheless, the fetus's lack of a complete immune system could present a unique opportunity for biomaterials development. For example, the complement activation system is incomplete; circulating complement factors in newborns are 10-80% lower than in adults [141]. To our knowledge no study has set out to specifically address questions of long-term biomaterial interactions in the fetus. However, in studies in which materials were implanted in human or animal fetuses, little to no evidence of negative immune response (inflammation, fibrous capsule formation, foreign body response, etc.) was detected, though analysis of tissue-material interactions is underreported in the clinical fetal surgery literature [3, 13, 59, 83]. Though further investigation is needed, it seems that some immune responses elicited by implanted biomaterials

are less pronounced in fetuses, possibly creating a more permissive environment for biomaterials in the fetal patient.

Researchers have begun to take advantage of the immature fetal immune system to develop stem cell treatments for alpha thassalemia major (ATM, Hemoglobin Bart's) and other inherited genetic conditions that are incompatible with life and detectable *in utero* [21, 145-147]. Fetal stem cell and genetic therapies, and initial animal and clinical data thereof, were reviewed by Witt and colleagues [148]. Without intrauterine treatment, fetuses with ATM are severely anemic and will die *in utero* or during the neonatal period or, rarely, survive with major neurological impairments. ATM also presents with significant maternal morbidities including pre-eclampsia and hypertension. Intrauterine blood transfusions to reduce fetal anemia have led to improved outcomes in severely affected patients [149, 150]; transfused fetuses who survive to infancy generally have a good outlook but are reliant on lifelong blood transfusions, medications, and/or bone marrow stem cell transplantations from matched donors [151]. An emerging strategy to combat ATM (and other inherited genetic diseases incompatible with life) is *in utero* hematopoietic cell transplantation (IUHCTx). By introducing donor stem cells before immune maturity, donor specific tolerance could be induced to improve outcomes in affected fetuses [145]. However, only limited cases have been reported in human patients, and maternal rejection of donor cells is an issue [145, 152]. One promising area of investigation is the use of maternal cells as donor cells in fetal transplantation because fetal cells are already de-sensitized to the antigens of the mother [143, 153]. The first news report of a fetus with ATM surviving to birth after serial *in utero* blood transfusions and a bone marrow stem cell transplant from maternal cells was released in May 2018 from the UCSF Fetal Treatment Center [154]; the clinical trial, from which this is the first reported case, is ongoing (ClinicalTrials.gov ID NCT02986698) [152]. Additionally, MacKenzie and colleagues published a consensus statement about the future of fetal stem cell transplantation and gene therapy [155]. Beyond ATM, other candidate conditions include sickle cell anemia and osteogenesis imperfecta. Future work in IUHCTx could utilize novel materials for delivery of stem cells or other therapies to the fetus as cell engraftment remains low.

Early fetal surgeons observed that fetuses exhibit gestational age-dependent scarless healing following fetal surgery [156]. The mechanism underlying this scarless healing has been an active area of investigation [157] and piqued interest in the potential of fetal surgery to improve infant outcomes relative to post-natal (scar-inducing) intervention. This regenerative-type healing could also be used to the advantage of engineers designing biomaterials for the fetal milieu.

Conclusion

Fetal surgery is a growing and promising field of medicine that has the potential to drastically improve or save lives of children with debilitating or terminal diagnoses. In this review, we have presented the progress of several biomaterials solutions for fetal surgery and have suggested potential avenues for further exploration. As the field continues to transition from open surgeries to minimally invasive procedures, biomaterials are poised to become more widely used; for example, in the prenatal repair of myelomeningocele defects, it could be far easier to insert a biomaterial patch through a cannula than to do a full surgical repair of the MMC defect *in utero*. Similarly, successful *in utero* gastroschisis repair may also rely on the development of an appropriate biomaterial patch. Perhaps biomaterials can have the greatest impact on fetal surgery and fetal therapy through the development of adhesives to prevent fetal membrane rupture following fetal surgery. The risk of iatrogenic membrane rupture, the "Achilles heel" of fetal surgery, is still the riskiest part of most fetal surgeries; a robust method to prevent membrane

rupture (and thus subsequent preterm birth) would make fetal surgery accessible to more families by decreasing the overall risk of the procedure, tipping the balance on the risk-benefit analysis. Fetal blood transplantation and stem cell therapy remain an ongoing area of clinical and basic science research; in the future, biomaterials strategies may be useful to improve engraftment or delivery of these cells. As prenatal diagnostic technologies improve, clinicians will be better able to identify patients well-suited for fetal surgery; this trend has already started and demand for fetal surgery centers at major pediatric hospitals is growing. Today, over 30 hospitals have fetal therapy programs registered with NAFTANet (North American Fetal Therapy Network), and other fetal treatment centers exist internationally outside the NAFTANet system. As recently as the 1980s, fetal surgery was accessible to only 10s of patients a year; today it is the standard of care for thousands of patients per year in the United States. Moving forward, targeted biomaterial development will enable fetal surgery to help even more families deliver healthy, thriving children.

Glossary

Clinical equipoise – The assumption that it is unknown which of two or more treatment options is better. In the context of clinical trials, it is ethical to establish clinical equipoise between treatment groups.

EXIT procedure – *Ex Utero* Intrapartum Treatment, a type of Cesarean section in which the baby is kept attached to the umbilical cord to receive oxygenated blood from the placenta until breathing or breathing support can be established. Used in cases where fetal airway obstruction is known or suspected.

Fetal surgery vs. fetal therapy – Fetal therapy usually refers to procedures that have limited number of instruments entering the uterus, for example fetal blood transfusions, while fetal surgery often is used to refer to more complicated invasive procedures like shunt placement or open surgery.

Iatrogenic – Used to describe symptoms or conditions that are caused by medical intervention or treatment. For example, iatrogenic membrane rupture is membrane rupture that results from *in utero* interventions.

Laparotomy – Surgical incision into the abdominal cavity, for example to expose the uterus for fetal surgery.

Amnioreduction – Insertion of a needle to aspirate amniotic fluid from the uterus to reduce amniotic fluid volumes in cases of polyhydramnios.

Oligohydramnios – Insufficient amniotic fluid present during gestation. This can hinder lung maturation and lead to perinatal morbidity.

Polyhydramnios – Excess amniotic fluid present during gestation. This can lead to poor perinatal outcomes.

Acknowledgements and Contributions

The authors thank Vamsi K. Aribindi, M.D., for helpful feedback on the manuscript and Colin Fahrion for illustrations. This work was supported by the National Science Foundation (Graduate Research Fellowship DGE 1752814 to SMW) and the National Institutes of Health (1R01EB022031-01). S.M.W. wrote the manuscript with input from P.B.M. and M.R.H.

References

[1] M.R. Harrison, R.A. Filly, M.S. Golbus, R.L. Berkowitz, P.W. Callen, T.G. Canty, C. Catz, W.H. Clewell, R. Depp, M.S. Edwards, J.C. Fletcher, F.D. Frigoletto, W.J. Garrett, M.L. Johnson, A. Jonsen, A.A. De Lorimier, W.A. Liley, M.J. Mahoney, F.D. Manning, P.R. Meier, M. Michejda, D.K. Nakayama, L. Nelson, J.B. Newkirk, K. Pringle, C. Rodeck, M.A. Rosen, J.D. Schulman, Fetal treatment 1982, N Engl J Med 307(26) (1982) 1651-2.
[2] J.A. Deprest, R. Devlieger, K. Srisupundit, V. Beck, I. Sandaite, S. Rusconi, F. Claus, G. Naulaers, M. Van de Velde, P. Brady, K. Devriendt, J. Vermeesch, J. Toelen, M. Carlon, Z. Debyser, L. De Catte, L. Lewi, Fetal surgery is a clinical reality, Semin Fetal Neonat M 15(1) (2010) 58-67.
[3] N.S. Adzick, E.A. Thom, C.Y. Spong, J.W. Brock, P.K. Burrows, M.P. Johnson, L.J. Howell, J.A. Farrell, M.E. Dabrowiak, L.N. Sutton, N. Gupta, N.B. Tulipan, M.E. D'Alton, D.L. Farmer, M. Investigators, A Randomized Trial of Prenatal versus Postnatal Repair of Myelomeningocele, New Engl J Med 364(11) (2011) 993-1004.
[4] M.S. Golbus, M.R. Harrison, R.A. Filly, P.W. Callen, M. Katz, In utero treatment of urinary tract obstruction, Am J Obstet Gynecol 142(4) (1982) 383-8.
[5] C.E. Graves, M.R. Harrison, B.E. Padilla, Minimally Invasive Fetal Surgery, Clinics in Perinatology 44(4) (2017) 729.
[6] S.K. Kabagambe, C.J. Lee, L.F. Goodman, Y.J. Chen, M.A. Vanover, D.L. Farmer, Lessons from the Barn to the Operating Suite: A Comprehensive Review of Animal Models for Fetal Surgery, Annu Rev Anim Biosci 6 (2018) 99-119.
[7] R.M. Antiel, Ethical challenges in the new world of maternal-fetal surgery, Semin Perinatol 40(4) (2016) 227-33.
[8] D. Munson, The intersection of fetal palliative care and fetal surgery: Addressing mortality and quality of life, Seminars in Perinatology 41(2) (2017) 101-105.
[9] H. Kitagawa, K.C. Pringle, Fetal surgery: a critical review, Pediatr Surg Int 33(4) (2017) 421-433.
[10] F.A. Chervenak, L.B. McCullough, The ethics of maternal-fetal surgery, Semin Fetal Neonat M 23(1) (2018) 64-67.
[11] R.M. Antiel, A.W. Flake, C.A. Collura, M.P. Johnson, N.E. Rintoul, J.D. Lantos, F.A. Curlin, J.C. Tilburt, S.D. Brown, C. Feudtner, Weighing the Social and Ethical Considerations of Maternal-Fetal Surgery, Pediatrics 140(6) (2017) e20170608.
[12] R.M. Antiel, A.W. Flake, Responsible surgical innovation and research in maternal-fetal surgery, Semin Fetal Neonat M 22(6) (2017) 423-427.
[13] R. Morris, M. Kilby, The PLUTO trial: percutaneous shunting in lower urinary tract obstruction, American Journal of Obstetrics and Gynecology 206(1) (2012) S14-S14.
[14] Pluto Collaborative Study Group, M. Kilby, K. Khan, K. Morris, J. Daniels, R. Gray, L. Magill, B. Martin, P. Thompson, Z. Alfirevic, S. Kenny, S. Bower, S. Sturgiss, D. Anumba, G. Mason, G. Tydeman, P. Soothill, K. Brackley, P. Loughna, A. Cameron, S. Kumar, P. Bullen, PLUTO trial protocol: percutaneous shunting for lower urinary tract obstruction randomised controlled trial, BJOG 114(7) (2007) 904-5, e1-4.
[15] M.V. Senat, J. Deprest, M. Boulvain, A. Paupe, N. Winer, Y. Ville, Endoscopic laser surgery versus serial amnioreduction for severe twin-to-twin transfusion syndrome, N Engl J Med 351(2) (2004) 136-44.

[16] J. Deprest, J. Jani, E. Gratacos, H. Vandecruys, G. Naulaers, J. Delgado, A. Greenough, K. Nicolaides, F.T. Grp, Fetal intervention for congenital diaphragmatic hernia: The European experience, Seminars in Perinatology 29(2) (2005) 94-103.
[17] D.B. Clayton, J.W. Brock, Current State of Fetal Intervention for Lower Urinary Tract Obstruction, Curr Urol Rep 19(1) (2018) 12.
[18] M. Watanabe, A.G. Kim, A.W. Flake, Tissue engineering strategies for fetal myelomeningocele repair in animal models, Fetal Diagn Ther 37(3) (2015) 197-205.
[19] G. Bilic, C. Brubaker, P.B. Messersmith, A.S. Mallik, T.M. Quinn, C. Haller, E. Done, L. Gucciardo, S.M. Zeisberger, R. Zimmermann, J. Deprest, A.H. Zisch, Injectable candidate sealants for fetal membrane repair: bonding and toxicity in vitro, American Journal of Obstetrics and Gynecology 202(1) (2010) 85.e1-85.e9.
[20] V. Beck, P. Lewi, L. Gucciardo, R. Devlieger, Preterm prelabor rupture of membranes and fetal survival after minimally invasive fetal surgery: a systematic review of the literature, Fetal Diagn Ther 31(1) (2012) 1-9.
[21] D. Merianos, T. Heaton, A.W. Flake, In Utero Hematopoietic Stem Cell Transplantation: Progress toward Clinical Application, Biology of Blood and Marrow Transplantation 14(7) (2008) 729-740.
[22] R. Papanna, S. Molina, K.Y. Moise, K.J. Moise, A. Johnson, Chorioamnion plugging and the risk of preterm premature rupture of membranes after laser surgery in twin-twin transfusion syndrome, Ultrasound Obst Gyn 35(3) (2010) 337-343.
[23] P. Klaritsch, K. Albert, T. Van Mieghem, L. Gucciardo, E. Done, B. Bynens, J. Deprest, Instrumental requirements for minimal invasive fetal surgery, Bjog-Int J Obstet Gy 116(2) (2009) 188-197.
[24] K. Golombeck, R.H. Ball, H. Lee, J.A. Farrell, D.L. Farmer, V.R. Jacobs, M.A. Rosen, R.A. Filly, M.R. Harrison, Maternal morbidity after maternal-fetal surgery, Am J Obstet Gynecol 194(3) (2006) 834-9.
[25] R.D. Wilson, K. Lemerand, M.P. Johnson, A.W. Flake, M. Bebbington, H.L. Hedrick, N.S. Adzick, Reproductive outcomes in subsequent pregnancies after a pregnancy complicated by open maternal-fetal surgery (1996-2007), American Journal of Obstetrics and Gynecology 203(3) (2010) 209.e1-209.e6.
[26] B.K. Young, A.S. Roman, A.P. MacKenzie, C.D. Stephenson, V. Minior, A. Rebarber, I. Timor-Tritsch, The closure of iatrogenic membrane defects after amniocentesis and endoscopic intrauterine procedures, Fetal Diagn Ther 19(3) (2004) 296-300.
[27] R. Devlieger, E. Gratacos, J. Wu, L. Verbist, R. Pijnenborg, J.A. Deprest, An organ-culture for in vitro evaluation of fetal membrane healing capacity, Eur J Obstet Gynecol Reprod Biol 92(1) (2000) 145-50.
[28] R. Devlieger, L.K. Millar, G. Bryant-Greenwood, L. Lewi, J.A. Deprest, Fetal membrane healing after spontaneous and iatrogenic membrane rupture: A review of current evidence, American Journal of Obstetrics and Gynecology 195(6) (2006) 1512-1520.
[29] E. Gratacos, J. Sanin-Blair, L. Lewi, N. Toran, G. Verbist, L. Cabero, A histological study of fetoscopic membrane defects to document membrane healing, Placenta 27 (2006) 452-6.
[30] R.M. Moore, J.M. Mansour, R.W. Redline, B.M. Mercer, J.J. Moore, The physiology of fetal membrane rupture: insight gained from the determination of physical properties, Placenta 27(11-12) (2006) 1037-51.
[31] N.S. Carvalho, A.F. Moron, R. Menon, S. Cavalheiro, M.M. Barbosa, H.J. Milani, M.M. Ishigai, Histological evidence of reparative activity in chorioamniotic membrane following open

fetal surgery for myelomeningocele, Experimental and Therapeutic Medicine 14(4) (2017) 3732-3736.
[32] B.M. Mercer, Preterm premature rupture of the membranes, Obstet Gynecol 101(1) (2003) 178-93.
[33] S. Saigal, L.W. Doyle, Preterm birth 3 - An overview of mortality and sequelae of preterm birth from infancy to adulthood, Lancet 371(9608) (2008) 261-269.
[34] L. Rüegg, M. Hüsler, F. Krähenmann, G. Natalucci, R. Zimmermann, N. Ochsenbein-Kölble, Outcome after fetoscopic laser coagulation in twin–twin transfusion syndrome – is the survival rate of at least one child at 6 months of age dependent on preoperative cervical length and preterm prelabour rupture of fetal membranes?, The Journal of Maternal-Fetal & Neonatal Medicine (2018) 1-9.
[35] G. Bryant-Greenwood, L.K. Millar, Human fetal membranes: Their preterm premature rupture, Biology of Reproduction 63 (2000) 1575-79.
[36] D.J. Field, J.S. Dorling, B.N. Manktelow, E.S. Draper, Survival of extremely premature babies in a geographically defined population: prospective cohort study of 1994-9 compared with 2000-5, BMJ 336(7655) (2008) 1221-3.
[37] J. Chang, T.F. Tracy, S.R. Carr, D.L. Sorrells, F.I. Luks, Port insertion and removal techniques to minimize premature rupture of the membranes in endoscopic fetal surgery, Journal of Pediatric Surgery 41(5) (2006) 905-909.
[38] R. Quintero, New horizons in the treatment of preterm premature rupture of membranes, Clin Perinatol 28 (2001) 861-75.
[39] R. Quintero, Treatment of previable premature ruptured membranes, Clin Perinatol 30 (2003) 573-89.
[40] F. Breathnach, S. Daly, E. Griffin, N. Gleeson, Intracervical application of synthetic hydrogel sealant for preterm prelabor rupture of membranes: a case report, Journal of Perinatal Medicine 33(5) (2005) 458-460.
[41] L.K. Mann, R. Papanna, K.J. Moise, Jr., R.H. Byrd, E.J. Popek, S. Kaur, S.C.G. Tseng, R.J. Stewart, Fetal membrane patch and biomimetic adhesive coacervates as a sealant for fetoscopic defects, Acta Biomaterialia 8(6) (2012) 2160-2165.
[42] P.B. Petratos, R.N. Baergen, C.B. Bleustein, D. Felsen, D.P. Poppas, Ex vivo evaluation of human fetal membrane closure, Lasers in Surgery and Medicine 30(1) (2002) 48-53.
[43] A. Mallik, M. Fichter, S. Rieder, G. Bilic, S. Stergioula, J. Henke, Fetoscopic closure of punctured fetal membranes with acellular human amnion plugs in a rabbit model, Obstet Gynecol 110 (2007) 1121-9.
[44] N. Ochsenbein-Kölble, J. Jani, L. Lewi, G. Verbist, L. Vercruysse, B. Portmann-Lanz, M. Marquardt, R. Zimmermann, J. Deprest, Enhancing sealing of fetal membrane defects using tissue engineered native amniotic-scaffolds in the rabbit model, American Journal of Obstetrics and Gynecology 196(3) (2007) 263-265.
[45] A. Zisch, R. Zimmermann, Bioengineering of foetal membrane repair, Swiss Med Wkly 138 (2008) 596-601.
[46] A. Kivelio, N. Ochsenbein-Koelble, R. Zimmermann, M. Ehrbar, Engineered cell instructive matrices for fetal membrane healing, Acta Biomater 15 (2015) 1-10.
[47] H.K. Carnaghan, M.R. Harrison, Presealing of the chorioamniotic membranes prior to fetoscopic surgery: preliminary study with unfertilized chicken egg models, Eur J Obstet Gynecol Reprod Biol 144 Suppl 1 (2009) S142-5.

[48] R.A. Cortes, A.J. Wagner, H. Lee, M.S. Clifton, E. Grethel, S.H. Yang, R. Ball, M.R. Harrison, Pre-emptive placement of a presealant for amniotic access, American Journal of Obstetrics and Gynecology 193(3) (2005) 1197-1203.
[49] A.C. Engels, B. Van Calster, J. Richter, P. DeKoninck, L. Lewi, L. De Catte, R. Devlieger, J.A. Deprest, Collagen plug sealing of iatrogenic fetal membrane defects after fetoscopic surgery for congenital diaphragmatic hernia, Ultrasound Obstet Gynecol 43(1) (2014) 54-9.
[50] R.A. Quintero, W.J. Morales, M. Allen, P.W. Bornick, J. Arroyo, G. LeParc, Treatment of iatrogenic previable premature rupture of membranes with intra-amniotic injection of platelets and cryoprecipitate (amniopatch): Preliminary experience, American Journal of Obstetrics and Gynecology 181(3) (1999) 744-749.
[51] J.M. O'Brien, D.A. Milligan, J.R. Barton, Gelatin sponge embolization. a method for the management of iatrogenic preterm premature rupture of the membranes, Fetal Diagn Ther 17(1) (2002) 8-10.
[52] J. Richter, A. Henry, G. Ryan, P. DeKoninck, L. Lewi, J. Deprest, Amniopatch procedure after previable iatrogenic rupture of the membranes: a two-center review, Prenat. Diagn. 33(4) (2013) 391-396.
[53] S.A. Burke, M. Ritter-Jones, B.P. Lee, P.B. Messersmith, Thermal gelation and tissue adhesion of biomimetic hydrogels, Biomed Mater 2(4) (2007) 203-10.
[54] C.M. Haller, W. Buerzle, A. Kivelio, M. Perrini, C.E. Brubaker, R.J. Gubeli, A.S. Mallik, W. Weber, P.B. Messersmith, E. Mazza, N. Ochsenbein-Koelble, R. Zimmermann, M. Ehrbar, Mussel-mimetic tissue adhesive for fetal membrane repair: an ex vivo evaluation, Acta Biomater 8(12) (2012) 4365-70.
[55] Y.R. Devaud, S. Zuger, R. Zimmermann, M. Ehrbar, N. Ochsenbein-Kölble, Minimally Invasive Surgical Device for Precise Application of Bioadhesives to Prevent iPPROM, Fetal Diagnosis and Therapy 45(2) (2019) 102-110.
[56] A.N. Azadani, P.B. Matthews, L. Ge, Y. Shen, C.S. Jhun, T.S. Guy, E.E. Tseng, Mechanical Properties of Surgical Glues Used in Aortic Root Replacement, Ann Thorac Surg 87(4) (2009) 1154-1160.
[57] M. Bures, H.K. Hoffler, G. Friedel, T. Kyriss, E. Boedeker, F. Langer, P. Zardo, R.Y. Zhang, Albumin-glutaraldehyde glue for repair of superficial lung defect: an in vitro experiment, J Cardiothorac Surg 11(1) (2016) 63.
[58] W.D. Spotnitz, S. Burks, Hemostats, sealants, and adhesives: components of the surgical toolbox, Transfusion 48(7) (2008) 1502-1516.
[59] A. Kivelio, P. Dekoninck, M. Perrini, C.E. Brubaker, P.B. Messersmith, E. Mazza, J. Deprest, R. Zimmermann, M. Ehrbar, N. Ochsenbein-Koelble, Mussel mimetic tissue adhesive for fetal membrane repair: initial in vivo investigation in rabbits, Eur J Obstet Gynecol Reprod Biol 171(2) (2013) 240-5.
[60] R. Papanna, L.K. Mann, S.C. Tseng, R.J. Stewart, S.S. Kaur, M.M. Swindle, T.R. Kyriakides, N. Tatevian, K.J. Moise, Jr., Cryopreserved human amniotic membrane and a bioinspired underwater adhesive to seal and promote healing of iatrogenic fetal membrane defect sites, Placenta 36(8) (2015) 888-94.
[61] S. Roman, A.J. Bullock, D.O. Anumba, S. MacNeil, Development of an implantable synthetic membrane for the treatment of preterm premature rupture of fetal membranes, J Biomater Appl 30(7) (2016) 995-1003.

[62] V. Pensabene, P.P. Patel, P. Williams, T.L. Cooper, K.C. Kirkbride, T.D. Giorgio, N.B. Tulipan, Repairing Fetal Membranes with a Self-adhesive Ultrathin Polymeric Film: Evaluation in Mid-gestational Rabbit Model, Ann Biomed Eng 43(8) (2015) 1978-1988.
[63] H. Mendez-Figueroa, R. Papanna, D.L. Berry, K.J. Moise, Precipitated egg white as a sealant for iatrogenic preterm premature rupture of the membranes, American Journal of Obstetrics and Gynecology 202(2) (2010) 191.e1-6.
[64] Y. Shao, K. Taniguchi, K. Gurdziel, R.F. Townshend, X. Xue, K.M. Yong, J. Sang, J.R. Spence, D.L. Gumucio, J. Fu, Self-organized amniogenesis by human pluripotent stem cells in a biomimetic implantation-like niche, Nat Mater 16(4) (2017) 419-425.
[65] S.E. Parker, C.T. Mai, M.A. Canfield, R. Rickard, Y. Wang, R.E. Meyer, P. Anderson, C.A. Mason, J.S. Collins, R.S. Kirby, A. Correa, N. National Birth Defects Prevention, Updated National Birth Prevalence estimates for selected birth defects in the United States, 2004-2006, Birth Defects Res A Clin Mol Teratol 88(12) (2010) 1008-16.
[66] E.M. Velie, G.M. Shaw, Impact of prenatal diagnosis and elective termination on prevalence and risk estimates of neural tube defects in California, 1989-1991, Am J Epidemiol 144(5) (1996) 473-479.
[67] J.M. Lary, L.D. Edmonds, Prevalence of Spina Bifida at Birth -- United States, 1983-1990: a Comparison of Two Surveillance Systems, MMWR CDC Surveill Summ 42(2) (1996) 15-26.
[68] N.S. Adzick, Fetal myelomeningocele: Natural history, pathophysiology, and in-utero intervention, Semin Fetal Neonat M 15(1) (2010) 9-14.
[69] D.S. Heffez, J. Aryanpur, G.M. Hutchins, J.M. Freeman, The paralysis associated with myelomeningocele: clinical and experimental data implicating a preventable spinal cord injury, Neurosurgery 26(6) (1990) 987-92.
[70] J.P. Bruner, N. Tulipan, R.L. Paschall, F.H. Boehm, W.F. Walsh, S.R. Silva, M. Hernanz-Schulman, L.H. Lowe, G.W. Reed, Fetal surgery for myelomeningocele and the incidence of shunt-dependent hydrocephalus, JAMA 282(19) (1999) 1819-25.
[71] J.S. Moldenhauer, N.S. Adzick, Fetal surgery for myelomeningocele: After the Management of Myelomeningocele Study (MOMS), Semin Fetal Neonat M 22(6) (2017) 360-366.
[72] J.P. Bruner, W.O. Richards, N.B. Tulipan, T.L. Arney, Endoscopic coverage of fetal myelomeningocele in utero, Am J Obstet Gynecol 180(1 Pt 1) (1999) 153-8.
[73] J.P. Bruner, N.E. Tulipan, W.O. Richards, Endoscopic coverage of fetal open myelomeningocele in utero, Am J Obstet Gynecol 176(1 Pt 1) (1997) 256-7.
[74] M. Watanabe, J. Jo, A. Radu, M. Kaneko, Y. Tabata, A.W. Flake, A tissue engineering approach for prenatal closure of myelomeningocele with gelatin sponges incorporating basic fibroblast growth factor, Tissue Eng Part A 16(5) (2010) 1645-55.
[75] M. Watanabe, H. Li, J. Roybal, M. Santore, A. Radu, J. Jo, M. Kaneko, Y. Tabata, A. Flake, A tissue engineering approach for prenatal closure of myelomeningocele: comparison of gelatin sponge and microsphere scaffolds and bioactive protein coatings, Tissue Eng Part A 17(7-8) (2011) 1099-110.
[76] A.J. Eggink, L.A. Roelofs, W.F. Feitz, R.M. Wijnen, R.A. Mullaart, J.A. Grotenhuis, T.H. van Kuppevelt, M.M. Lammens, A.J. Crevels, A. Hanssen, P.P. van den Berg, In utero repair of an experimental neural tube defect in a chronic sheep model using biomatrices, Fetal Diagn Ther 20(5) (2005) 335-40.
[77] A.J. Eggink, L.A. Roelofs, M.M. Lammens, W.F. Feitz, R.M. Wijnen, R.A. Mullaart, H.T. van Moerkerk, T.H. van Kuppevelt, A.J. Crevels, A. Hanssen, F.K. Lotgering, P.P. van den

Berg, Histological evaluation of acute covering of an experimental neural tube defect with biomatrices in fetal sheep, Fetal Diagn Ther 21(2) (2006) 210-6.
[78] A.J. Eggink, L.A. Roelofs, W.F. Feitz, R.M. Wijnen, M.M. Lammens, R.A. Mullaart, H.T. van Moerkerk, T.H. van Kuppevelt, A.J. Crevels, K. Verrijp, F.K. Lotgering, P.P. van den Berg, Delayed intrauterine repair of an experimental spina bifida with a collagen biomatrix, Pediatr Neurosurg 44(1) (2008) 29-35.
[79] C.G. Fontecha, J.L. Peiro, M. Aguirre, F. Soldado, S. Anor, L. Fresno, V. Martinez-Ibanez, Inert patch with bioadhesive for gentle fetal surgery of myelomeningocele in a sheep model, Eur J Obstet Gynecol Reprod Biol 146(2) (2009) 174-9.
[80] C.G. Fontecha, J.L. Peiro, J.J. Sevilla, M. Aguirre, F. Soldado, L. Fresno, C. Fonseca, A. Chacaltana, V. Martinez, Fetoscopic coverage of experimental myelomeningocele in sheep using a patch with surgical sealant, Eur J Obstet Gynecol Reprod Biol 156(2) (2011) 171-6.
[81] J.L. Peiro, C.G. Fontecha, R. Ruano, M. Esteves, C. Fonseca, M. Marotta, S. Haeri, M.A. Belfort, Single-Access Fetal Endoscopy (SAFE) for myelomeningocele in sheep model I: amniotic carbon dioxide gas approach, Surg Endosc 27(10) (2013) 3835-40.
[82] L. Joyeux, F. De Bie, E. Danzer, T. Van Mieghem, A.W. Flake, J. Deprest, Safety and efficacy of fetal surgery techniques to close a spina bifida defect in the fetal lamb model: A systematic review, Prenat. Diagn. 38(4) (2018) 231-242.
[83] M. Watanabe, H.Y. Li, A.G. Kim, A. Weilerstein, A. Radu, M. Davey, S. Loukogeorgakis, M.D. Sanchez, K. Sumita, N. Morimoto, M. Yamamoto, Y. Tabata, A.W. Flake, Complete tissue coverage achieved by scaffold-based tissue engineering in the fetal sheep model of Myelomeningocele, Biomaterials 76 (2016) 133-143.
[84] J.T. Stephenson, K.O. Pichakron, L. Vu, T. Jancelewicz, R. Jamshidi, J.K. Grayson, K.K. Nobuhara, In utero repair of gastroschisis in the sheep (Ovis aries) model, Journal of Pediatric Surgery 45(1) (2010) 65-69.
[85] R.C.S. Oliveira, P.R. Valente, R.C. Abou-Jamra, A. Araujo, P.H. Saldiva, D.A. Pedreira, Biosynthetic cellulose induces the formation of a neoduramater following pre-natal correction of meningomyelocele in fetal sheep, Acta Cir Bras 22(3) (2007) 174-81.
[86] R. Papanna, K.J. Moise, Jr., L.K. Mann, S. Fletcher, R. Schniederjan, M.B. Bhattacharjee, R.J. Stewart, S. Kaur, S.P. Prabhu, S.C. Tseng, Cryopreserved human umbilical cord patch for in-utero spina bifida repair, Ultrasound Obstet Gynecol 47(2) (2016) 168-76.
[87] R. Papanna, S. Fletcher, K.J. Moise, Jr., L.K. Mann, S.C. Tseng, Cryopreserved Human Umbilical Cord for In Utero Myeloschisis Repair, Obstet Gynecol 128(2) (2016) 325-30.
[88] Y.J. Chen, K.R. Chung, C. Pivetti, L. Lankford, S.K. Kabagambe, M. Vanover, J. Becker, C. Lee, J. Tsang, A.J. Wang, D.L. Farmer, Fetal surgical repair with placenta-derived mesenchymal stromal cell engineered patch in a rodent model of myelomeningocele, Journal of Pediatric Surgery 53(1) (2018) 183-188.
[89] A.J.A. Holland, K. Walker, N. Badawi, Gastroschisis: an update, Pediatr Surg Int 26(9) (2010) 871-878.
[90] J.C. Langer, M.T. Longaker, T.M. Crombleholme, S.J. Bond, W.E. Finkbeiner, C.A. Rudolph, E.D. Verrier, M.R. Harrison, Etiology of Intestinal Damage in Gastroschisis 1. Effects of Amniotic-Fluid Exposure and Bowel Constriction in a Fetal Lamb Model, Journal of Pediatric Surgery 24(10) (1989) 992-997.
[91] J.C. Langer, J.G. Bell, R.O. Castillo, T.M. Crombleholme, M.T. Longaker, B.W. Duncan, S.M. Bradley, W.E. Finkbeiner, E.D. Verrier, M.R. Harrison, Etiology of intestinal damage in

gastroschisis, II. Timing and reversibility of histological changes, mucosal function, and contractility, Journal of Pediatric Surgery 25(11) (1990) 1122-1126.
[92] S.K. Srinathan, J.C. Langer, M.G. Blennerhassett, M.R. Harrison, G.J. Pelletier, D. Lagunoff, Etiology of intestinal damage in gastroschisis. III: Morphometric analysis of the smooth muscle and submucosa, J Pediatr Surg 30(3) (1995) 379-83.
[93] P. Klück, D. Tibboel, A.W. van der Kamp, J.C. Molenaar, The effect of fetal urine on the development of the bowel in gastroschisis, Journal of pediatric surgery 18(1) (1983) 47-50.
[94] J. Correia-Pinto, M.L. Tavares, M.J. Baptista, J. Estevão-Costa, A.W. Flake, A.F. Leite-Moreira, A new fetal rat model of gastroschisis: Development and early characterization, Journal of Pediatric Surgery 36(1) (2001) 213-216.
[95] J.D. Phillips, R.E. Kelly, Jr., E.W. Fonkalsrud, A. Mirzayan, C.S. Kim, An improved model of experimental gastroschisis in fetal rabbits, J Pediatr Surg 26(7) (1991) 784-7.
[96] L.A.J. Roelofs, P.J. Geutjes, C.A. Hulsbergen-van de Kaa, A.J. Eggink, T.H. van Kuppevelt, W.F. Daamen, A.J. Crevels, P.P. van den Berg, W.F.J. Feitz, R.M.H. Wijnen, Prenatal coverage of experimental gastroschisis with a collagen scaffold to protect the bowel, Journal of Pediatric Surgery 48(3) (2013) 516-524.
[97] R. Bergholz, T. Krebs, K. Wenke, T. Andreas, B. Tiemann, J. Paetzel, B. Jacobsen, R. Fahje, C. Schmitz, O. Mann, B. Roth, B. Appl, K. Hecher, Fetoscopic management of gastroschisis in a lamb model, Surgical Endoscopy and Other Interventional Techniques 26(5) (2012) 1412-1416.
[98] R. Tatu, C.Y. Lin, Characterization of Biomaterial Patches as Fetal Surgery Implants, Front Nanobiomed Res 10 (2018) 29-47.
[99] M.R. Harrison, G.B. Mychaliska, C.T. Albanese, R.W. Jennings, J.A. Farrell, S. Hawgood, P. Sandberg, A.H. Levine, E. Lobo, R.A. Filly, Correction of congenital diaphragmatic hernia in utero IX: Fetuses with poor prognosis (liver herniation and low lung-to-head ratio) can be saved by fetoscopic temporary tracheal occlusion, Journal of Pediatric Surgery 33(7) (1998) 1017-1022.
[100] A.K. Saxena, Surgical perspectives regarding application of biomaterials for the management of large congenital diaphragmatic hernia defects, Pediatr Surg Int 34(5) (2018) 475-489.
[101] C. Jeanty, S.M. Kunisaki, T.C. MacKenzie, Novel non-surgical prenatal approaches to treating congenital diaphragmatic hernia, Semin Fetal Neonat M 19(6) (2014) 349-356.
[102] M.P. Eastwood, F.M. Russo, J. Toelen, J. Deprest, Medical interventions to reverse pulmonary hypoplasia in the animal model of congenital diaphragmatic hernia: A systematic review, Pediatr Pulm 50(8) (2015) 820-838.
[103] M.R. Harrison, J.C. Langer, N.S. Adzick, M.S. Golbus, R.A. Filly, R.L. Anderson, M.A. Rosen, P.W. Callen, R.B. Goldstein, A.A. Delorimier, Correction of Congenital Diaphragmatic-Hernia in Utero 5. Initial Clinical-Experience, Journal of Pediatric Surgery 25(1) (1990) 47-57.
[104] J. Deprest, E. Gratacos, K.H. Nicolaides, F.T. Grp, Fetoscopic tracheal occlusion (FETO) for severe congenital diaphragmatic hernia: evolution of a technique and preliminary results, Ultrasound Obst Gyn 24(2) (2004) 121-126.
[105] R. Elattal, B.S. Rich, C.M. Harmon, O.J. Muensterer, Pulmonary alveolar and vascular morphometry after gel plug occlusion of the trachea in a fetal rabbit model of CDH, Int J Surg 11(7) (2013) 558-561.
[106] D.O. Fauza, J.J. Marler, R. Koka, R.A. Forse, J.E. Mayer, J.P. Vacanti, Fetal tissue engineering: diaphragmatic replacement, J Pediatr Surg 36(1) (2001) 146-51.

[107] M.R. Harrison, N.S. Adzick, A.W. Flake, R.W. Jennings, J.M. Estes, T.E. Macgilivray, J.T. Chueh, J.D. Goldberg, R.A. Filly, R.B. Goldstein, M.A. Rosen, C. Cauldwell, A.H. Levine, L.J. Howell, Correction of Congenital Diaphragmatic-Hernia in-Utero 6. Hard-Earned Lessons, Journal of Pediatric Surgery 28(10) (1993) 1411-1418.
[108] M.R. Harrison, R.M. Sydorak, J.A. Farrell, J.A. Kitterman, R.A. Filly, C.T. Albanese, Fetoscopic temporary tracheal occlusion for congenital diaphragmatic hernia: Prelude to a randomized, controlled trial, Journal of Pediatric Surgery 38(7) (2003) 1012-1020.
[109] K.J. VanderWall, S.W. Bruch, M. Meuli, T. Kohl, Z. Szabo, N.S. Adzick, M.R. Harrison, Fetal endoscopic ('Fetendo') tracheal clip, Journal of Pediatric Surgery 31(8) (1996) 1101-1103.
[110] O.J. Muensterer, T. Nicola, S. Farmer, C.M. Harmon, N. Ambalavanan, Temporary fetal tracheal occlusion using a gel plug in a rabbit model of congenital diaphragmatic hernia, Journal of Pediatric Surgery 47(6) (2012) 1063-1066.
[111] R. Chang, M. Komura, S. Andreoli, R. Jennings, J. Wilson, D. Fauza, Rapidly polymerizing hydrogel prevents balloon dislodgement in a model of fetal tracheal occlusion, J Pediatr Surg 39(4) (2004) 557-60.
[112] L. Lewi, L. Gucciardo, T. Van Mieghem, P. de Koninck, V. Beck, H. Medek, D. Van Schoubroeck, R. Devlieger, L. De Catte, J. Deprest, Monochorionic diamniotic twin pregnancies: natural history and risk stratification, Fetal Diagn Ther 27(3) (2010) 121-33.
[113] G.E. Chalouhi, M. Essaoui, J. Stirnemann, T. Quibel, B. Deloison, L. Salomon, Y. Ville, Laser therapy for twin-to-twin transfusion syndrome (TTTS), Prenat. Diagn. 31(7) (2011) 637-646.
[114] M.J.C. van Gemert, J.P.H.M. van den Wijngaard, F.P.H.A. Vandenbussche, Twin reversed arterial perfusion sequence is more common than generally accepted, Birth Defects Res A 103(7) (2015) 641-643.
[115] H. Lee, A.J. Wagner, E. Sy, R. Ball, V.A. Feldstein, R.B. Goldstein, D.L. Farmer, Efficacy of radiofrequency ablation for twin-reversed arterial perfusion sequence, Am J Obstet Gynecol 196(5) (2007) 459 e1-4.
[116] Z. Russell, R.A. Quintero, E.V. Kontopoulos, Intrauterine growth restriction in monochorionic twins, Semin Fetal Neonat M 12(6) (2007) 439-449.
[117] R. Robyr, M. Yamamoto, Y. Ville, Selective feticide in complicated monochorionic twin pregnancies using ultrasound-guided bipolar cord coagulation, Bjog-Int J Obstet Gy 112(10) (2005) 1344-1348.
[118] M.M. Lanna, M.A. Rustico, M. Dell'Avanzo, V. Schena, S. Faiola, D. Consonni, A. Righini, B. Scelsa, E.M. Ferrazzi, Bipolar cord coagulation for selective feticide in complicated monochorionic twin pregnancies: 118 consecutive cases at a single center, Ultrasound Obstet Gynecol 39(4) (2012) 407-13.
[119] R.K. Morris, G.L. Malin, E. Quinlan-Jones, L.J. Middleton, L. Diwakar, K. Hemming, D. Burke, J. Daniels, E. Denny, P. Barton, T.E. Roberts, K.S. Khan, J.J. Deeks, M.D. Kilby, P.C. Grp, Fetal bladder obstruction and its treatment, Health Technol Asses 17(59) (2013) 1.
[120] F.A. Manning, M.R. Harrison, C. Rodeck, Catheter Shunts for Fetal Hydronephrosis and Hydrocephalus - Report of the International Fetal Surgery Registry, New Engl J Med 315(5) (1986) 336-340.
[121] J.S. Elder, J.W. Duckett, H.M. Snyder, Intervention for Fetal Obstructive Uropathy - Has It Been Effective, Lancet 2(8566) (1987) 1007-1010.

[122] T.J. Clark, W.L. Martin, T.G. Divakaran, M.J. Whittle, M.D. Kilby, K.S. Khan, Prenatal bladder drainage in the management of fetal lower urinary tract obstruction: A systematic review and meta-analysis, Obstetrics and Gynecology 102(2) (2003) 367-382.
[123] R.K. Morris, G.L. Malin, E. Quinlan-Jones, L.J. Middleton, K. Hemming, D. Burke, J.P. Daniels, K.S. Khan, J. Deeks, M.D. Kilby, P.V. Shunti, Percutaneous vesicoamniotic shunting versus conservative management for fetal lower urinary tract obstruction (PLUTO): a randomised trial, Lancet 382(9903) (2013) 1496-1506.
[124] R.K. Morris, G.L. Malin, E. Quinlan-Jones, L.J. Middleton, L. Diwakar, K. Hemming, D. Burke, J. Daniels, E. Denny, P. Barton, T.E. Roberts, K.S. Khan, J.J. Deeks, M.D. Kilby, The Percutaneous shunting in Lower Urinary Tract Obstruction (PLUTO) study and randomised controlled trial: evaluation of the effectiveness, cost-effectiveness and acceptability of percutaneous vesicoamniotic shunting for lower urinary tract obstruction, Health Technol Assess 17(59) (2013) 1-232.
[125] M.P. Kurtz, C.J. Koh, G.A. Jamail, H. Sangi-Haghpeykar, A.A. Shamshirsaz, J. Espinoza, D.L. Cass, O.O. Olutoye, O.A. Olutoye, M.C. Braun, D.R. Roth, M.A. Belfort, R. Ruano, Factors associated with fetal shunt dislodgement in lower urinary tract obstruction, Prenat. Diagn. 36(8) (2016) 720-725.
[126] J.P. Bruner, G. Davis, N. Tulipan, Intrauterine shunt for obstructive hydrocephalus--still not ready, Fetal Diagn Ther 21(6) (2006) 532-9.
[127] M.L. Johnson, D. Pretorius, W.H. Clewell, P.R. Meier, D. Manchester, Fetal hydrocephalus: diagnosis and management, Semin Perinatol 7(2) (1983) 83-9.
[128] B.D. Jeong, H.S. Won, M.Y. Lee, Perinatal Outcomes of Fetal Lower Urinary Tract Obstruction After Vesicoamniotic Shunting Using a Double-Basket Catheter, J Ultrasound Med 37(9) (2018) 2147-2156.
[129] I. Stanasel, E. Gonzales, Posterior Urethral Valves, Curr Bladder Dysfunct Rep 10(3) (2015) 250–255.
[130] R.A. Quintero, A.R. Shukla, Y.L. Homsy, R. Bukkapatnam, Successful in utero endoscopic ablation of posterior urethral valves: a new dimension in fetal urology, Urology 55(5) (2000) 774.
[131] N. Sananes, R. Favre, C.J. Koh, A. Zaloszyc, M.C. Braun, D.R. Roth, R. Moog, F. Becmeur, M.A. Belfort, R. Ruano, Urological fistulas after fetal cystoscopic laser ablation of posterior urethral valves: surgical technical aspects, Ultrasound Obstet Gynecol 45(2) (2015) 183-9.
[132] R. Ruano, C.T. Yoshizaki, A.M. Giron, M. Srougi, M. Zugaib, Cystoscopic placement of transurethral stent in a fetus with urethral stenosis, Ultrasound Obstet Gynecol 44(2) (2014) 238-40.
[133] R. Ruano, N. Sananes, H. Sangi-Haghpeykar, S. Hernandez-Ruano, R. Moog, F. Becmeur, A. Zaloszyc, A.M. Giron, B. Morin, R. Favre, Fetal intervention for severe lower urinary tract obstruction: a multicenter case-control study comparing fetal cystoscopy with vesicoamniotic shunting, Ultrasound Obstet Gynecol 45(4) (2015) 452-8.
[134] R.D. Wilson, J.K. Baxter, M.P. Johnson, M. King, S. Kasperski, T.M. Crombleholme, A.W. Flake, H.L. Hedrick, L.J. Howell, N.S. Adzick, Thoracoamniotic shunts: fetal treatment of pleural effusions and congenital cystic adenomatoid malformations, Fetal Diagn Ther 19(5) (2004) 413-20.
[135] C.H. Rodeck, N.M. Fisk, D.I. Fraser, U. Nicolini, Long-term in utero drainage of fetal hydrothorax, N Engl J Med 319(17) (1988) 1135-8.

[136] R. Witlox, F. Klumper, A.B. Te Pas, E.W. van Zwet, D. Oepkes, E. Lopriore, Neonatal management and outcome after thoracoamniotic shunt placement for fetal hydrothorax, Arch Dis Child Fetal Neonatal Ed 103(3) (2018) F245-F249.
[137] W.H. Clewell, M.L. Johnson, P.R. Meier, J.B. Newkirk, S.L. Zide, R.W. Hendee, W.A. Bowes, Jr., F. Hecht, D. O'Keeffe, G.P. Henry, R.H. Shikes, A surgical approach to the treatment of fetal hydrocephalus, N Engl J Med 306(22) (1982) 1320-5.
[138] D.H. Pretorius, K. Davis, M.L. Manco-Johnson, D. Manchester, P.R. Meier, W.H. Clewell, Clinical course of fetal hydrocephalus: 40 cases, AJR Am J Roentgenol 144(4) (1985) 827-31.
[139] K. Szaflik, M. Czaj, L. Polis, J. Wojtera, W. Szmanski, W. Krzeszowski, B. Polis, M. Litwinska, W. Mikolajczyk, K. Janiak, I. Maroszynska, E. Gulczynska, Fetal therapy--evaluation of ventriculo-amniotic shunts in the treatment of hydrocephalus, Ginekol Pol 85(12) (2014) 16-22.
[140] C.S. von Koch, N. Gupta, L.N. Sutton, P.P. Sun, In utero surgery for hydrocephalus, Childs Nerv Syst 19(7-8) (2003) 574-86.
[141] A.K. Simon, G.A. Hollander, A. McMichael, Evolution of the immune system in humans from infancy to old age, Proc Biol Sci 282(1821) (2015) 20143085.
[142] J.M. Anderson, A. Rodriguez, D.T. Chang, Foreign body reaction to biomaterials, Semin Immunol 20(2) (2008) 86-100.
[143] T.C. MacKenzie, Fetal Surgical conditions and the unraveling of maternal-fetal tolerance, J Pediatr Surg 51(2) (2016) 197-9.
[144] M. Wegorzewska, A. Nijagal, C.M. Wong, T. Le, N. Lescano, Q. Tang, T.C. MacKenzie, Fetal intervention increases maternal T cell awareness of the foreign conceptus and can lead to immune-mediated fetal demise, J Immunol 192(4) (2014) 1938-45.
[145] S.C. Derderian, C. Jeanty, M.C. Walters, E. Vichinsky, T.C. MacKenzie, In utero hematopoietic cell transplantation for hemoglobinopathies, Front Pharmacol 5 (2014) 278.
[146] A.W. Flake, In utero stem cell transplantation, Best Practice & Research Clinical Obstetrics & Gynaecology 18(6) (2004) 941-958.
[147] J.L. Roybal, M.T. Santore, A.W. Flake, Stem cell and genetic therapies for the fetus, Seminars in Fetal and Neonatal Medicine 15(1) (2010) 46-51.
[148] R. Witt, T.C. MacKenzie, W.H. Peranteau, Fetal stem cell and gene therapy, Semin Fetal Neonat M 22(6) (2017) 410-414.
[149] B. Weisz, O. Rosenbaum, B. Chayen, R. Peltz, B. Feldman, S. Lipitz, Outcome of severely anaemic fetuses treated by intrauterine transfusions, Arch Dis Child Fetal Neonatal Ed 94(3) (2009) F201-4.
[150] E.P. Vichinsky, Alpha thalassemia major--new mutations, intrauterine management, and outcomes, Hematology Am Soc Hematol Educ Program (2009) 35-41.
[151] M.Y. Elsaid, C.M. Capitini, C.A. Diamond, M. Porte, M. Otto, K.B. DeSantes, Successful matched unrelated donor stem cell transplant in Hemoglobin Bart's disease, Bone Marrow Transplant 51(11) (2016) 1522-1523.
[152] E.M. Kreger, S.T. Singer, R.G. Witt, N. Sweeters, B. Lianoglou, A. Lal, T.C. Mackenzie, E. Vichinsky, Favorable outcomes after in utero transfusion in fetuses with alpha thalassemia major: a case series and review of the literature, Prenat. Diagn. 36(13) (2016) 1242-1249.
[153] R. Witt, Q.-H.L. Nguyen, T. MacKenzie, In Utero Hematopoietic Cell Transplantation: Past Clinical Experience and Future Clinical Trials, Current Stem Cell Reports 4(1) (2018) 74-80.

[154] D. Grady, Five Blood Transfusions, One Bone Marrow Transplant — All Before Birth, The New York Times (2018) https://www.nytimes.com/2018/05/25/health/fetal-bone-marrow-transplant.html.
[155] T.C. MacKenzie, A.L. David, A.W. Flake, G. Almeida-Porada, Consensus statement from the first international conference for in utero stem cell transplantation and gene therapy, Front Pharmacol 6 (2015) 15.
[156] B.J. Larson, M.T. Longaker, H.P. Lorenz, Scarless Fetal Wound Healing: A Basic Science Review, Plastic and reconstructive surgery 126(4) (2010) 1172-1180.
[157] S.Y. Chen, B. Han, Y.T. Zhu, M. Mahabole, J. Huang, D.C. Beebe, S.C.G. Tseng, HC-HA/PTX3 Purified from Amniotic Membrane Promotes BMP Signaling in Limbal Niche Cells to Maintain Quiescence of Limbal Epithelial Progenitor/Stem Cells, Stem Cells 33(11) (2015) 3341-3355.

CHAPTER TWO – MARINE-INSPIRED POLYMERS IN MEDICAL ADHESION

N.B. *This chapter first appeared as a review manuscript of the same title as part of a special issue on biomimetic polymers in the* European Polymer Journal*. Please see the Introduction for more on how this manuscript relates to the dissertation as a whole.*

Diederik WR Balkenende, Sally M. Winkler, and Phillip B. Messersmith. "Marine-inspired polymers in medical adhesion." European Polymer Journal *116 (2019): 134-143.*

Abstract

Medical adhesives that are strong, easy to apply and biocompatible are promising alternatives to sutures and staples in a large variety of surgical and clinical procedures. Despite progress in the development and regulatory approval of adhesives for use in the clinic, adhesion to wet tissue remains challenging. Marine organisms have evolved a diverse set of highly effective wet adhesive approaches that have inspired the design of new medical adhesives. Here we provide an overview of selected marine animals and their chemical and physical adhesion strategies, the state of clinical translation of adhesives inspired by these organisms, and target applications where marine-inspired adhesives can have a significant impact. We will focus on medical adhesive polymers inspired by mussels, sandcastle worms, and cephalopods, emphasize the history of bioinspired medical adhesives from the peer reviewed and patent literature, and explore future directions including overlooked sources of bioinspiration and materials that exploit multiple bioinspired strategies.

Introduction

Medical adhesives that are easy to apply to seal wet tissues during surgery have enormous potential to replace invasive mechanical fixations such as sutures and staples, or to provide fluid-impenetrable sealing of a suture line.[1] Most engineering and consumer adhesives exploit non-specific interactions (e.g. van der Waals), but these adhesive interactions are dramatically weakened in the presence of the high dielectric and ionic strength of physiological fluids.[2, 3] Despite these challenges, a myriad of biological and synthetic adhesives have been developed and approved for specific surgical procedures.[4] Clinically used tissue adhesives include fibrin, gelatin resorcinol, and cyanoacrylates, all of which are considered to have shortcomings with respect to toxicity or mechanical performance.[4] They suffer from poor adhesion or biocompatibility and fail to meet the requirements of many surgical procedures including sealing leaks in the lungs and gastrointestinal system, fetal surgery, and most musculoskeletal repairs. This unmet clinical need has motivated the development of synthetic and bioderived adhesives, including polysaccharide and polyethylene glycol (PEG) based materials with improved adhesive strength and biocompatibility relative to clinically available formulations.

Here, our focus is on marine animals that firmly attach to biological or mineral surfaces underwater and the medical adhesive materials they have inspired. For a more general treatment of bioinspiration and bioinspired materials development, the reader is referred to several excellent reviews.[3-10] Well-studied underwater adhesion specialists include the mussel, sandcastle worm, and octopus (**Fig. 1**).[11-14] Basic science research has elucidated these animals' highly-evolved wet adhesion mechanisms, and researchers have since incorporated these chemical and physical wet adhesion strategies into medical adhesives. Much of the work in mussel-inspired adhesion has focused on understanding and mimicking the unusual adhesive proteins found in the terminal plaque of the mussel byssus.[15] Sandcastle worms employ coacervate-forming protein adhesives

to construct their sand grain dwellings.[12] Cephalopods, on the other hand, rely on shape and structure, in the form of suction cups, to adhere robustly onto wet surfaces.[14] Moving forward, promising strategies in bioinspired adhesives will likely involve incorporating multiple bioinspired elements, for example mussel-inspired motifs together with a cephalopod-inspired suction cup microstructure or other combinations of chemical and physical adhesive strategies. Animals have evolved many strategies for adhering underwater, and incorporating these strategies into medical adhesives offers a tremendous opportunity to address unmet clinical challenges.

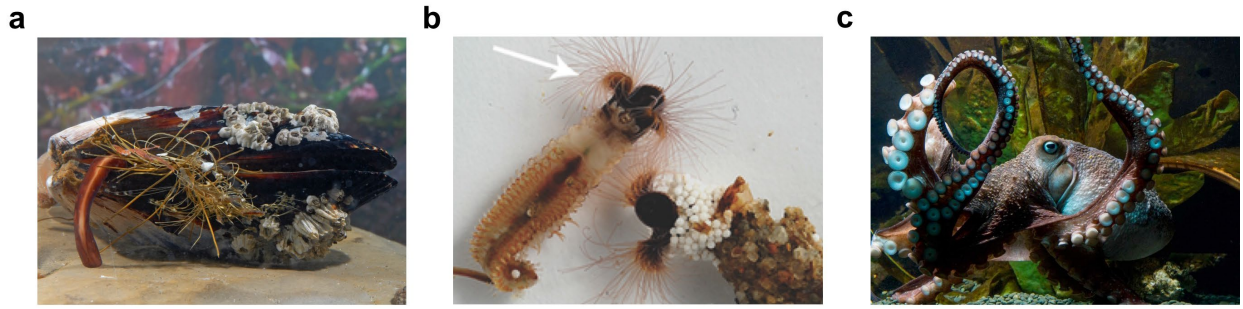

Fig. 1. Underwater bioinspiration for medical adhesives. **(**a) Mussels strongly attach to underwater surfaces with a protein-based plaque and can withstand the strong forces of crashing waves. Image was generously provided by and reused with permission from Gary McDonald. (b) The sandcastle worm builds tubular dwellings of sand particles cemented together with adhesive proteins. Photo of a sandcastle worm (left, arrow) and a worm inside a tubular dwelling in construction. The (untanned) white granules contain the coacervated and un-cured adhesive. Reproduced under the terms of the Creative Commons Attribution 4.0 International License [7] Copyright 2016, John Wiley & Sons, Inc. (c) A common New Zealand octopus uses suction cups to reversibly adhere to diverse surfaces and can use this attachment to move around its environment. Courtesy of the National Aquarium of New Zealand.

Mussel-inspired adhesion

Biology of mussel adhesion

The mussel's adhesive plaque is arguably the most well-studied marine bioadhesive (**Fig. 2**). Mussels secrete protein threads called byssal threads to anchor themselves to diverse underwater surfaces, including rocks, ships, and other organisms. At the distal end of these threads, adhesive proteins form an adhesive plaque that securely attaches the thread (and thus the mussel) to the surface, allowing the mussel to withstand the high shear forces of waves.[15-22] A landmark 1981 paper from the Waite lab identified a mussel adhesive protein in the byssus that had repetitive decapeptide sequences with a high concentration of 3,4-dihydroxypheny-l-alanine (DOPA), a post-translational modification of tyrosine. DOPA was hypothesized to mediate the high adhesion strength of these proteins.[23] Waite and colleagues went on to identify numerous other byssal proteins, each with a specific sequence, biodistribution and function.[22]

In particular, mussel foot proteins (mfps) found at the adhesive interface have high DOPA content. Surface force apparatus measurements of extracted and recombinant mfps clearly demonstrated the contribution of DOPA to bioadhesion.[21, 24] In another fundamental study, single molecule force spectroscopy experiments demonstrated the high adhesion strength of an isolated DOPA amino acid, furthering the hypothesis that DOPA, specifically its catechol side chain, mediates robust adhesion.[25] In the interfacial proteins with the highest DOPA content,

DOPA was often flanked by the positively-charged, nitrogen-containing amino acids lysine and arginine.[26] Experiments with model siderophores (proteins that chelate iron) confirmed that catechol and amino functional groups contribute synergistically to wet adhesion in a spatially-dependent manner.[26] In addition to amino acid composition and protein sequence, recent research has shown that other chemical and physical phenomena including iron crosslinking, phase inversion and temporospatial control during byssal thread fabrication are essential to overall mussel adhesion.[11, 27, 28] A fundamental understanding of mussel adhesion has inspired many scientists to improve the performance of medical adhesives.[29]

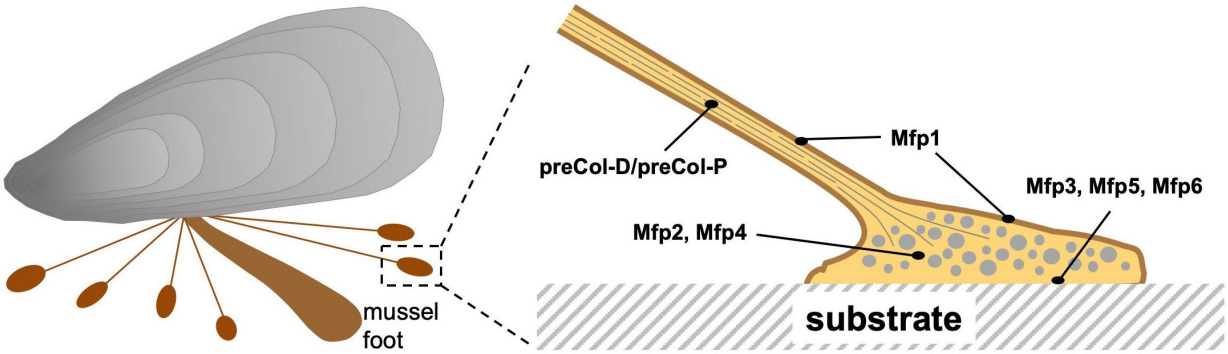

Fig. 2. The mussel byssus. Mussels secrete many byssal threads to securely attach to underwater surfaces and withstand the high forces exerted by waves. During formation of a byssal thread, glands along the mussel foot secrete a mixture of byssal collagens and mfps that self-assemble and solidify into the thread shaft and the adhesive plaque. The core of the adhesive plaque consists of a porous complex coacervate with mfps with low DOPA concentrations (mpf 2, 4). Mfps at the adhesive interface (mfp 3, 5, 6) have high DOPA content.

Mussel-inspired tissue adhesives

DOPA oxidation, crosslinking and interactions with tissue surfaces

In theory, a robust medical adhesive would form covalent interfacial interactions with the tissue surface. Thus, many clinically approved synthetic adhesives rely on reactive motifs (e.g. aldehyde, N-hydroxysuccinimide (NHS) esters) that target lysine and cysteine residues that are omnipresent at the surface of most targeted tissues.[30] In the mussel and in mussel-inspired medical adhesives, DOPA facilitates wet adhesion to the substrate. As an amino acid, DOPA has thus far only been identified in the proteins of marine adhesives, likely due to its versatile reactivity which could interfere with organisms' biochemical processes.[11]

In alkaline seawater or after the addition of a strong oxidant (e.g., $NaIO_4$), catechols convert to reactive *o*-quinone species and can covalently conjugate with tissue surfaces via many possible reaction pathways (**Fig. 3**). A similar pathway in the bulk of the plaque leads to protein crosslinking, thereby contributing to elastic properties of the mussel byssus.[11] Importantly for tissue adhesion and perhaps also for mussel adhesion, *o*-quinone is highly reactive towards tissue bound lysine and cysteine residues via nucleophilic addition or imine formation (**Fig. 3**). [31] Although the exact reaction pathways are still under investigation, it is clear that DOPA can form covalent bonds with nucleophilic substrates.

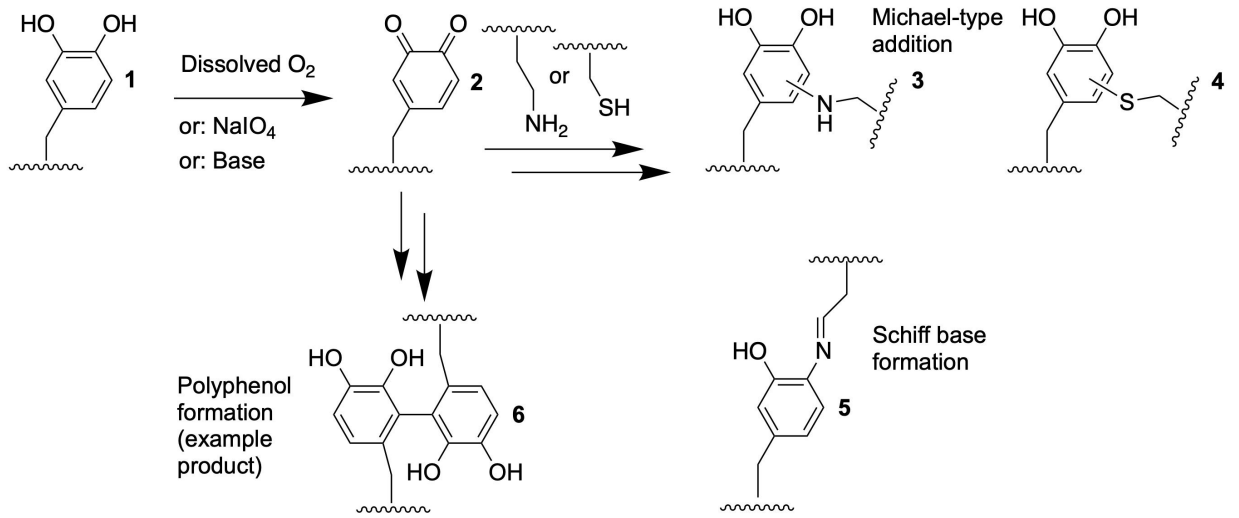

Fig. 3. DOPA's reactivity leads to multiple chemical pathways relevant to wet tissue adhesion. DOPA's side chain, catechol (1), forms the highly reactive *o*-quinone (2) intermediate upon (auto)oxidation with dissolved oxygen, a strong oxidant (e.g. $NaIO_4$) or basic conditions. *o*-Quinone can then react with tissue pendent lysine or cysteine residues to form covalent interfacial bonds via Michael-type addition (3, 4) or Schiff base formation (5). Alternatively, tanning of *o*-quinone also results in polyphenol crosslinks (6), which contribute to the elastic properties of the byssus or synthetic wet adhesives.

In synthetic materials, DOPA or catechol is often used for both adhesion (binding to substrates) and cohesion (crosslinking of the adhesive material), and there are several common strategies for oxidizing or crosslinking DOPA. The formation of coordination bonds between DOPA and Fe^{3+} has been extensively studied as a crosslinking and toughening mechanism in the mussel byssus and in mussel-inspired materials.[32, 33] However, for medical applications, iron should be used with caution, since soluble iron salts may increase bacterial growth and result in localized or systemic infection.[34-36] Swelling is an additional concern in iron-coordinated catechol gels; due to the dynamic nature of metal coordination bonds, hydrogels that are only crosslinked via metal-DOPA coordination may swell, causing the gel to dissipate.[37] Oxidizing agents such as $NaIO_4$ are regularly used to crosslink DOPA. However, when using such oxidizers with DOPA-functionalized polysaccharides, aldehyde formation via oxidative carbohydrate ring opening is important but often overlooked as a side reaction in these studies. Indeed, relying only on oxidative aldehyde formation in polysaccharides is enough to establish good tissue adhesion. This was exemplified by a study from the Elisseeff group in which methacrylated chondroitin sulphate was treated with $NaIO_4$ and resulted in the carbohydrate ring opening to yield aldehyde motifs.[38] Upon UV irradiation, the methacrylate motifs form a covalent network and the aldehydes form interfacial bonds resulting in a horizontal shear adhesive strength of 46 kPa to cartilage. $NaIO_4$ oxidation and Fe^{+3} coordination are ubiquitous in the mussel-inspired adhesives literature, but the benefits and drawbacks of each approach should be carefully considered in the context of the intended application.

Materials with mussel-inspired proteins and peptides

As Waite and colleagues discovered and characterized the proteins responsible for mussel adhesion, research teams have been striving to develop synthetic versions of mussel glue. Early efforts involved extracted mussel adhesive proteins intended for a range of applications including

ligament reconstruction, skin grafts and dental restoration.[39] Extracting adhesive proteins from mussels proved to be impractical and expensive; thousands of mussels are needed to obtain even 1g of pure adhesive protein.[10] Therefore, a polymer with grafted DOPA-containing decapeptides was synthesized in an effort to mimic the high molecular weight of mussel adhesive proteins.[40] Tissue adhesive experiments on bovine corneal tissue revealed a shear adhesive strength of up to 32 kPa; however, unintended DOPA reactivity resulted in a short shelf life and large variation in observed adhesion strengths.[40] Despite this early research effort, neither material progressed to clinical use. Later, Biopolymer Products of Sweden disclosed in a patent the use of small, bioderived mussel adhesive decapeptides that were combined with charged polysaccharides (e.g. heparin, chitosan) and tested these as corneal adhesives.[41, 42]. For this particular application, the use of strong oxidizers or aldehyde compounds could be avoided, thus greatly increasing the biocompatibility. The only remaining commercial outcome of this early appears to be Cell-Tak™, an extract of adhesive proteins from the mussel byssus that is available for non-medical applications including attaching non-adherent cells to surfaces for microscopy.[43]

In subsequent efforts, the Yamamoto group synthesized numerous polypeptides as mussel-inspired tissue adhesives.[44-47] For example, the addition of tyrosinase $(X\text{-}Tyr\text{-}Lys)_n$, (X = Gly, Ala, Pro, Ser, Leu, Ile, or Phe) resulted in the post translational modification of tyrosine into DOPA and subsequent oxidative crosslinking.[48] Tissue adhesion experiments on dry pig skin with concentrated solutions of the polytripeptides showed a shear tissue adhesion strength of 11 kPa. In an elegant approach, Deming and colleagues copolymerized lysine- and DOPA-functionalized α-amino acid N-carboxyanhydride (NCA) monomers into high molecular weight random polypeptides (>100 kg mol^{-1}).[49-51] This material was used to prepare moisture resistant bonds to aluminum, steel, glass, and plastics. In a related patent, Deming and coworkers hinted at the potential biomedical adhesive applications.[52] Taken together, early bioinspired research efforts focused on precise mimicry of the polypeptides of the mussel foot proteins and, while they informed future investigations, they were later replaced with efforts to develop materials with simplified designs.

Catechol-PEG materials

After Deming's influential work, the focus of the field of mussel-inspired materials shifted towards designs in which only one or a few bioadhesive elements are used to enhance wet adhesion. These approaches facilitate clinical translation but admittedly suffer from isolating one or more components (e.g. DOPA) from a complex protein adhesive. In an effort to obtain adhesive hydrogels, Lee *et al.* reported a 4-arm PEG macromer that was end-functionalized with DOPA motifs (cPEG, **Fig. 4a**).[53] The addition of an oxidizing agent ($NaIO_4$) to a solution of this polymer led to rapid gelation and adhesion to tissue. cPEG was tested as a tissue adhesive and showed a shear adhesion strength of 35.1 kPa towards porcine dermal tissue, a five-fold improvement over fibrin glue (**Fig. 4b**).[54] In the first *in vivo* use of cPEG, Brubaker, et al., secured transplanted islets to the liver or epididymal fat pad of diabetic mice with cPEG.[55] The material secured the islets in place *in vivo* for up to a year, with little evidence of inflammatory response or fibrotic capsule formation. Islet transplantation with cPEG and in sutured controls led to normoglycemia, reversal of the diabetic phenotype, in the mice.

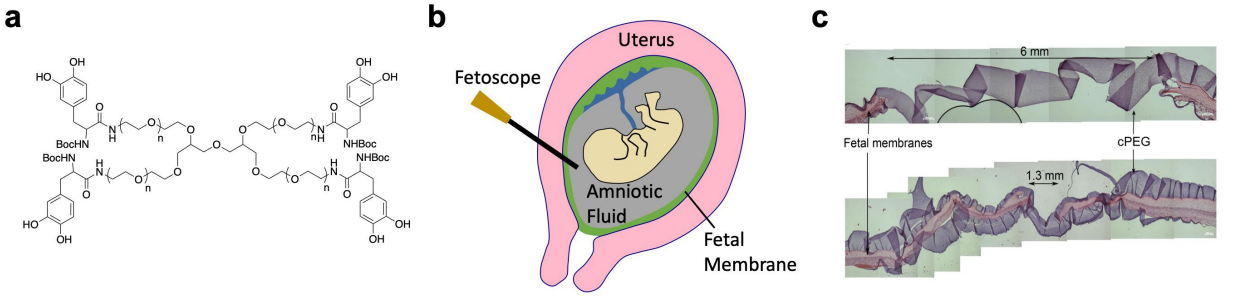

Fig. 4. Mussel-inspired adhesives for fetal surgery. (a) Chemical structure of DOPA functionalized branched PEG polymer (cPEG). (b) Insertion of a fetoscopic instrument during fetal surgery. After removal of instrument, a small defect is left in the uterus and the amniotic sac (fetal membranes). The sac defect does not heal, leading to postoperative complications including membrane rupture and preterm birth. (c) Histology of the fetal membrane (pink) shows that the mussel inspired sealant (purple) successfully sealed a trocar-induced defect. Reprinted from [56], Copyright 2010, with permission from Elsevier.

Sealing of the amniotic sac after fetal surgery has been an important strategic focus for marine-inspired adhesives. Fetal surgery can correct some severe congenital abnormalities like spina bifida and twin-twin transfusion syndrome *in utero*, but to access the fetus, surgeons must puncture the amniotic sac (fetal membranes).[57] This fragile membrane does not heal or withstand suturing, and can rupture, leading to high risk of preterm birth (**Fig. 4c**).[57] Common commercial tissue adhesives were unsuccessful in this application;[58] however, marine-inspired adhesives excel at sealing in wet environments and are well-poised to address this unmet clinical need. With collaborators at the University Hospital Zurich, our group reported cPEG based hydrogels as a promising material to seal induced amniotic sac defects (**Fig. 4d**).[56, 59, 60] *Ex vivo* evaluation of the sealant showed a comparable acute tissue toxicity response to fibrin sealants.[56]

Nerites Corporation explored PEG-catechols as synthetic mussel-inspired tissue adhesives for medical applications. In a comparative study, the authors compared 4-arm PEG based adhesives functionalized with a single DOPA motif, tetra DOPA sequences and short DOPA-lysine sequences, respectively.[61] Surprisingly, they did not observe a significant difference in tissue shear adhesion strength between adhesives carrying a single DOPA versus tetra DOPA sequences. However, upon addition of short DOPA-lysine sequences, a marked increase in lap shear tissue adhesion strength was found, confirming the synergy between DOPA and lysine. Lee and colleagues also developed a library of linear copolymers of polycaprolactone (PCL) and 4-arm PEG macromers in which two PEG-arms are functionalized with DOPA.[62, 63] With hernia repair as a target application, these functionalized PEGs were coated onto surgical meshes and biological scaffolds to form materials with high adhesive strengths.[62] The authors showed that adding an oxidant is necessary to form a strong adhesive interface. In another approach from the same team, unreacted $NaIO_4$ was incorporated into the polymer coating via a solvent casting process, rendering the patches immediately adhesive upon contact with tissue.[62] While strong oxidants such as $NaIO_4$ are perceived as potential biotoxins, biocompatibility studies showed acceptable cell viability (> 70% cell survival per ISO standard 10993-1).[62] On a cautionary note, cytotoxicity of mussel-inspired hydrogels was mainly attributed to the generation of H_2O_2 during oxidation of aromatic diols.[64, 65] This effect could be reversed with the addition of catalase to suppress oxidative stress.

To introduce degradability into PEG-catechol hydrogels, one can exploit linkers that are photo- or hydrolytically labile or that are susceptible to enzymatic cleavage. Our group introduced di-alanine (Ala-Ala) as spacer in DOPA functionalized 4-arm PEG macromers in order to exploit peptide cleavage by tissue elastase *in vivo*.[66] In another attempt to obtain degradable 4-arm PEG hydrogels, Zahid and coworkers functionalized 4-arm PEG polymers with photocleavable ortho-nitro substituted catechol groups.[67] After oxidative formation of the hydrogel, irradiation with UV light resulted in photocleavage of the crosslinks and hence debonding of the adhesive.

One drawback of PEG-based hydrogels is significant swelling which has the potential for postoperative complications such as blocked nerves. To address swelling, Barrett *et al.* reported the synthesis of 4-arm polypropylene-PEG (Tetronic) functionalized with DOPA (cT).[68] Subsequent oxidative crosslinking ($NaIO_4$) yielded a hydrogel that displayed a shear adhesion strength of 49 kPa and an absence of swelling due to a thermally induced hydrophobic transition of the PPO domains. Interestingly, a comparative investigation between cPEG and cT as amniotic sealant did not reveal a significant difference in critical burst pressure when sealants were used to seal a membrane that was inflated until rupture.[58]

Polysaccharide materials

Polysaccharides are strong candidates for mussel-inspired modification because they have a range of modifiable substitutions such as primary amines (e.g. chitosan) and carboxylic acids (e.g. alginate, hyaluronic acid) to derivatize with phenolic motifs.[4, 69] In one example with hyaluronic acid, Cho and Haeshin Lee formed hydrogels of dopamine-conjugated hyaluronic acid oxidized with $NaIO_4$.[70] Although these hydrogels could also be formed by photo crosslinking of methacrylated hyaluronic acid, the authors showed that catechol was essential for the formation of an adhesive interface. While such DOPA containing hydrogels did not show appreciable pull-off adhesion to liver tissue (1.4 kPa), the authors observed an adhesive strength of 48 kPa to heart tissue. In a similar fashion, the Cho group formed hydrogels of hyaluronic acid functionalized with aromatic triols in alkaline conditions or after addition of $NaIO_4$.[71] Interestingly, rheological tack tests were used to qualitatively show that alkaline conditions lead to higher adhesion strengths. This observation may indicate that adhesion of DOPA-containing materials is sensitive to the oxidation method and suggests different oxidation method-dependent kinetics or reaction pathways. Additionally, hyaluronic acid conjugated with dopamine was combined with thermo-responsive PEO-PPO-PEO (Pluronic) to prepare a lightly crosslinked injectable hydrogel.[72] Upon increasing the temperature to 37 ^{o}C, adhesive hydrogels were formed. Tissue adhesion experiments on mouse skin revealed a pull-off adhesion strength of 7 kPa.

Another polysaccharide of high interest for medical applications is chitosan, a (partly) deacylated chitin that is commercially derived from crustaceans. One important commercial medical application of chitosan films is hemostatic wound dressings (e.g. HemCon®).[73] Taking advantage of the hemostatic ability of chitosan, Lee, Park, and colleagues prepared hydrogels by reacting catechol functionalized chitosan (Chi-C) with thiol endcapped Pluronic.[74] These hydrogels had a pull-off adhesive strength of 15 kPa, and reduced blood loss when applied as a hemostat. InnoTherapy is currently pursuing these materials commercially.[75, 76] To improve the mechanical properties of bioinspired chitosan hydrogels, Hwang and colleagues synthesized pyrogallol-functionalized chitin fibers that formed adhesive hydrogels after oxidation with $NaIO_4$ or chelation with Fe^{3+}.[77] In another innovation from Lee and coworkers, oxidatively crosslinked Chi-C was drop casted onto needle shafts to form hemostatic needles. [76, 78] Intravenous and intramuscular injection into mice using these coated needles revealed a complete prevention of blood loss due to self-sealing of Chi-C. Likewise, the same authors also coated cotton swabs with

Chi-C.[79] Simply swiping coated swabs onto a bleeding wound reduced blood loss in both normal and coagulopathic (diabetic) mice.

Alginate, a polysaccharide found in certain bacterial biofilms and brown seaweed, is also a promising material for medical adhesives. Upon addition of Ca^{2+}, alginate will form weak hydrogels due to the formation of ionic bonds. Inspired by the tanning of brown algae, Bianco-Peled and colleagues oxidized a solution containing phloroglucinol, alginate and Ca^{2+} to form adhesive hydrogels.[80] Depending on the concentration of each component, the authors observed tissue shear adhesive strengths from 17 to 25 kPa. In a subsequent report, the same authors investigated the influence of alginate concentration in combination with various phenolic compounds as a sealant using a burst device.[81] In such a device, a hole in a fluid-filled chamber is covered with cellulose and the sealant. Then, the chamber is inflated and the pressure at which the sealant bursts is recorded. Contrary to their previous results, no significant difference in burst pressure was detected in the presence or absence of phenolic compounds. In addition, two of the polyphenolic compounds (epicatechin and morin) appeared to reduce the adhesive performance.

To increase the tissue adhesive strength of alginate gels, Mooney and coworkers prepared a family of double network hydrogels that contain alginate, Ca^{2+} and a second covalently crosslinked polymer such as poly(acrylamide) or NHS-crosslinked chitosan. These materials adhered to diverse tissues.[82] In a control experiment using chitosan labeled with fluorescein, the authors observed significant tissue penetration (30 μm), suggesting that mechanical interlocking of cationic polymers into tissue surfaces is at least partly responsible for the adhesive interfacial strength of these chitosan adhesives.

Gelatin-based materials

The use of DOPA or catechol to mediate adhesion in wet environments is usually considered to be mussel-inspired, but, to the best of our knowledge, the first reported example of a marine-inspired medical adhesive was actually inspired by the strong underwater adhesion of barnacles. Barnacle adhesive plaques had been found to contain tyrosine and polyphenol oxidase enzymes that were hypothesized to be responsible for the strong interfacial adhesion. [83, 84] Based on the assumption that catechol-lysine crosslinks serve an essential role in barnacle adhesion, the Erhan group reported the first marine-inspired medical adhesive – gelatin functionalized with aromatic diols.[84, 85] Adding polyphenol oxidase to a solution of functionalized gelatin resulted in a material that adhered to bone slices. However, protein analysis of barnacle adhesives subsequently showed an absence of DOPA,[86] and Rittschof and Wahl reported that tyrosine and polyphenol oxidase enzymes are connected to surface priming: eliminating marine biofilms before the establishment of permanent adhesion.[13, 86-88] Since the early barnacle-inspired work, Wang and coworkers crosslinked DOPA-functionalized gelatin using Fe^{3+} or genipin, resulting in an adhesive hydrogel.[89] Shear adhesion studies on moist porcine dermal tissue and cartilage showed an adhesion strength up to 25 and 194 kPa respectively.

Polymethacrylate materials

There is a large research effort to incorporate DOPA into polymethacrylates to develop wet adhesives for engineering and tissue sealing applications. The Grubbs group prepared adhesive hydrogels by reacting poly(dopamine methacrylamide (DMA) - NHS ester acrylate - acrylic acid) with thiol end-functionalized three-arm PEG, revealing a shear adhesive strength of approximately 12 kPa towards porcine dermal tissue. [90] In a report from Kuroda and coworkers, poly(DMA-methoxyethyl acrylate (MEA)) was tested as dental adhesive with and without the addition of Fe^{3+} salts.[91] The authors observed especially strong adhesive bonds to dentin in the presence of Fe^{3+}, and the presence of saliva during adhesive application did not significantly reduce the bonding

strength. In an elegant approach to render methacrylate based polymers biodegradable, Agarwal and coworkers copolymerized a mixture of 2-methylene-1,3-dioxepane, DMA and PEG methacrylate monomers, resulting in randomly distributed degradable ester bonds in the polymer backbone.[92] Tissue adhesion experiments on fresh porcine skin revealed a shear adhesive strength of 6 kPa, with a further increase to 8 kPa and 13 kPa after the addition of H_2O_2 or Fe^{3+} salts, respectively.

Polymethacrylates containing catechol were also used in a combined mussel- and gecko-inspired adhesive material in which the wet adhesive capabilities of the catechol were combined with the dry, structural adhesive strategies used by many organisms including geckos.[93-95] Geckos' impressive climbing abilities are due in large part to nanofibers on their foot pads that provide a large surface area for non-specific interactions like van der Waals forces. However, gecko feet, as well as many synthetic gecko-inspired materials, have limited adhesive abilities in wet environments as water disrupts these non-specific interactions. [93, 96, 97] It is likely for this reason that geckos are less active during rainy weather.[98] To overcome the reduced wet adhesion of synthetic nanofibrillar-patterned materials, our lab reported the first gecko- and mussel- inspired wet adhesive: nanopatterned PDMS coated with a DOPA-containing poly(DMA-co-MEA).[99] In dry conditions, adhesion was doubled compared to uncoated nanostructures, and in wet conditions, the coated samples could maintain the adhesive strength during 1000 contact cycles. The combination (nanofibers and polymer coating) material exerted stronger adhesion forces in wet conditions than the gecko-inspired (nanofibers only) material. This is one example of researchers combining multiple bioinspired strategies to create materials to address challenging problems.

Materials for mucoadhesion

Mfps extracted from the threads and plaques of mussel byssal threads were found to have mucoadhesive properties, but, at first, the exact contribution of DOPA to this adhesion was unclear.[39, 100] Experiments with cPEG revealed significant mucoadhesion that could be attributed more definitively to catechol, since PEG alone is not mucoadhesive; this demonstrated DOPA's ability to form effective interfacial bonds with mucosa.[101] Several other DOPA-containing materials have been tested for mucoadhesive properties. Cerruti and colleagues infiltrated or conjugated chitosan with DOPA, hydrocaffeic acid or dopamine. These materials were mucoadhesive, and oxidation was initiated upon contact with mucosa.[102, 103] Likewise, Haeshin Lee and coworkers observed increased gastrointestinal (GI) tract retention due to mucoadhesive properties of Chi-C.[104] In addition to DOPA-functionalized materials, oxidative coatings of polydopamine have also been evaluated. Sunoqrot and coworkers tested the mucoadhesive properties of polydopamine coated mPEG-PCL nanoparticles, targeting gastric mucosa for controlled drug release. Compared to uncoated particles, the authors observed an increase in mucosal retention and a similar drug release profile.[105] Mussel-inspired chemistries and materials are promising mucoadhesives and poised to address many clinical mucosal adhesion challenges.

Sandcastle worm inspired medical adhesives

Chemistry of sandcastle worm adhesion

Sandcastle worms, *Phragmatopoma californica*, are small marine worms that build their own underwater dwellings out of sand particles that they cement together with protein coacervate glue that they excrete (**Fig. 1b**). [7, 12, 27, 106] Coacervate formation is a thermodynamically driven liquid-liquid phase separation in which oppositely charged (amino acids in) proteins are

triggered to phase separate by a change in temperature, pH or ionic strength. The exclusion of water during coacervation results in the formation of a concentrated macromolecular liquid that can solidify into a porous solid.[107] The rapid formation of solid coacervates by marine organisms has been hypothesized to be triggered by injection of proteins from acidic storage glands into seawater (pH ~ 8.1) while, simultaneously, Ca^{2+} and Mg^{2+} ions coordinate with phosphorylated serine residues.[108] As the sandcastle worm constructs its dwelling, after initial coacervate formation, the excreted adhesive is further slow-cured via oxidative DOPA crosslinking.[12] While the proteinaceous cement of the sandcastle worm contains DOPA residues (**Fig. 1b**), these reactive amino acids are mainly indicated for cohesive protein crosslinking via polyphenol formation and DOPA-cysteine crosslinks. This suggests that the adhesive interface mostly relies on non-specific interactions.[12, 108] Inspiration from marine coacervate formation has led to the development of several medical adhesives.

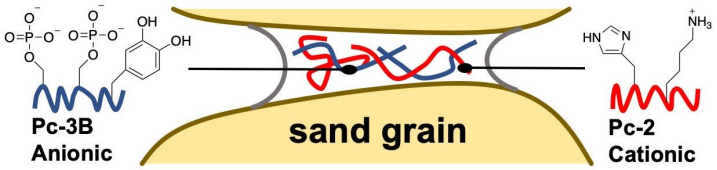

Fig. 5. Inspiration from the sandcastle worm. The sandcastle worm connects sand grains to build tubular dwellings. The load bearing bioadhesive that connects sand particles consists of a complex coacervate of highly phosphorylated anionic proteins (Pc-3B) and cationic proteins (Pc-2).

Sandcastle worm-inspired materials

Inspired by the proteins involved in complex coacervate formation in sandcastle worms, Stewart and coworkers developed several complex coacervate tissue adhesives. As an analog to the phosphorylated anionic proteins of the sandcastle worm's coacervate, the authors synthesized poly(monoacryloxyethyl phosphate-co-DMA). To mimic the cationic protein, gelatin was functionalized with primary amines (**Fig. 5b**).[109] A fluid coacervate was observed upon addition of Ca^{2+} to an acidic solution that contained both polyelectrolytes at low pH (**Fig. 5c**). Mimicking sandcastle worms' adhesive secretion into basic seawater, a shift to basic pH led to solidification of the synthetic coacervate. The coacervated adhesive was well tolerated *in vivo* and adhered to bone in a rat model of craniofacial reconstruction.[110] To improve the adhesive strength, the same authors also prepared a double network hydrogel that combined a complex coacervate consisting of poly(monoacryloxyethyl phosphate-co-DMA) and poly(acrylamide-co-aminopropyl methacrylamide) with a PEG diacrylate hydrogel.[111]

While the presence of DOPA in sandcastle worm glue is hypothesized to primarily serve a cohesive role, synthetic sandcastle worm-inspired materials can become adhesive to tissue when oxidized with $NaIO_4$. In collaboration with TissueTech, the Stewart group tested these adhesive hydrogels to seal defects after fetal surgery.[56, 112] In an *ex vivo* experimental setup, they demonstrated that complex coacervate-coated fetal membrane patches outperformed uncoated patches in their ability to withstand pressure when inflated with fluid. In an *in vivo* model of fetal membrane sealing in Yucatan pics, the same authors were unable to detect a difference in efficacy between a bioinspired coacervate gel and a human amniotic membrane patch because the fetal membranes of Yucatan pigs healed spontaneously, a phenomenon not seen in human fetal membranes.[113] The complex coacervate glue was also tested for *in utero* spina bifida repair in a sheep model, but this study showed fetal neuronal degeneration or necrosis.[114] While the

reasons for the negative response in this animal trial remain unclear, this body of work shows promise for the development of coacervate based injectable tissue adhesives.

Researchers have also taken inspiration from the mechanisms that sandcastle worms use to process their adhesive and its precursors. Before coacervate formation, the sandcastle worm stores the two oppositely charged proteins in separate secretory granules inside its glands.[12] Because proteins are stored in granules, the proteins are stable at the acidic pH of the glands but destabilize upon contact with seawater. This strategy is a practical approach to overcome high protein viscosity and prevents premature coacervate formation inside the glands. Inspired by this secretion approach, a collaboration between the groups of Langer, Lin and Karp coated particles of a highly viscous polymer, poly(glycerol sebacate acrylate) (PGSA), in alginate, resulting in a low viscosity, injectable aqueous dispersion.[115, 116] After injection of the nanoprecipitate dispersion, positively charged protamines were added, and the material rapidly coalesced. Formation of a solid was achieved after rapid crosslinking of the viscous polymer using high intensity UV irradiation (10s, 380 mW cm^{-2}). Tissue adhesion studies onto epicardium tissue showed a pull-off adhesive strength of 14 kPa and cell viability studies indicated cytocompatibility. Commercial application of PGSA is currently pursued by Gecko Biomedical with a recent approval for clinical use in Europe.

Adhesives inspired by cephalopods

Anatomy of cephalopod adhesion

Mussels and sandcastle worms secrete proteinaceous adhesives that are intended to form a permanent holdfast. However, in nature, as in the clinic, adhering reversibly or temporarily can be quite useful. Cephalopods, a class of mollusks that includes octopus, squid, cuttlefish, and nautilus, adhere to underwater surfaces temporarily for numerous purposes including prey capture, mating, camouflage, and locomotion. [117] As in gecko and sea star adhesion, most cephalopod adhesion is the result of anatomical features, like muscular suction cups, or suckers, that adhere reversibly to surfaces [14]. However, some species in four cephalopod genera secrete adhesives from epithelial gland structures in different parts of the body to accomplish specially evolved functions including camouflage (*Euprymna),* attaching to underwater plants (*Idiosepius*), enhancing adhesion of the digital tentacles (*Nautilus*), and improving mechanical adhesion (*Sepia*) [117]. The biochemical makeup of these adhesives in each genus is still an active area of investigation, but early evidence suggests that they are composed of carbohydrates or protein. [117-119] As the biochemistry of these adhesives is elucidated, they may inspire synthetic mimics, but thus far, most cephalopod-inspired tissue adhesives have mimicked the suckers that serve as muscular hydrostats to allow cephalopods to grasp objects and attach reversibly to underwater surfaces, including living tissue (prey) and irregular surfaces.[14]

Materials inspired by octopus suckers

Octopus arms are covered suckers that serve as muscular hydrostats. In *Octopus vulgaris*, there is an unusual small round protuberance inside each flexible suction cup. It is hypothesized that compression of this protuberance against a surface leads to a spatial separation between water at the top of the chamber and at the surface, effectively creating a vacuum that attaches the cup to the surface (**Fig. 6a**).[14, 120, 121] Importantly, this type of adhesion is only strong perpendicular to the surface. When a force in the plane of the surface is applied, water can easily re-enter and eliminate the pressure difference. Pang and coworkers reported patterned surfaces that are inspired by octopus suction cups.[14] The adhesive patches were prepared by reactive molding of a polyurethane acrylate-based polymer into an inverted silicon master. The authors compared

various patterned geometries including perforated cylinders, cylindrical pillars, cylindrical holes and the *vulgaris* inspired sphere-in-cup architecture. In wet conditions, the octopus inspired architecture outperformed other geometries.

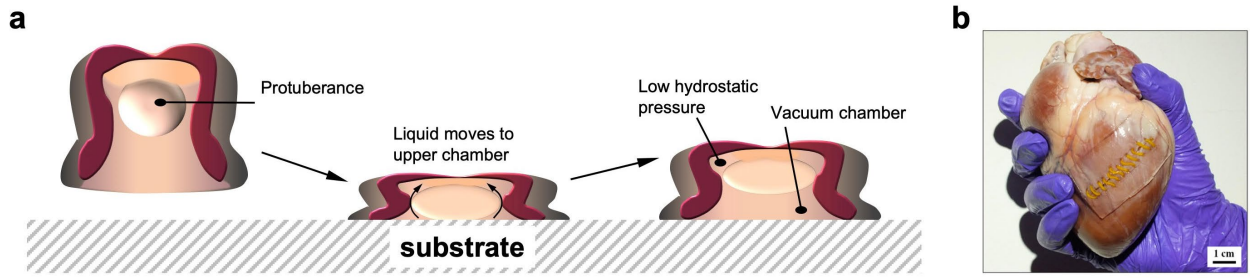

Fig. 6. *Octopus*-inspired tissue adhesive patches. (a) It is hypothesized that *Octopus vulgaris* muscular hydrostats reversibly adhere to surfaces by compressing suction cups, causing liquid to flow to the upper chamber, above the protuberance resulting in a low hydrostatic pressure. A vacuum is created in the lower chamber. Adapted from [14]. (b) A simplified biomimetic suction cup patch showed wet tissue adhesion to a porcine heart. Reprinted with permission from [122] Copyright 2017 American Chemical Society.

Yang and colleagues also created sucker-inspired tissue adhesives with a simplified cup architecture with no protuberance (**Fig. 6b**).[122] Silicon substrates were patterned with nanosucker geometries and tested on porcine epicardium tissue. Pull-off experiments showed the patches had an adhesive strength of around 28 kPa on a wet glass substrate, and the patches maintained the initial adhesion strength for at least 80 min when submerged. Due to plastic deformation of PDMS, the authors found that the suction cups showed a significant loss of adhesion after 30 contact cycles. Patterned arrays of nanosuckers were also used to develop a multilayer skin adhesive patch that could serve as a wearable temperature sensor.[123] Similar to observations of Pang, et al., the authors found that a cylindrical hole pattern only results in appreciable dry adhesion.[14, 123] Taken together, octopus inspired patterned surfaces are an exciting new avenue of exploration for reversible tissue adhesive materials.

Inspiration from squid sucker ring teeth

Like octopus, squid also use suction cups on their tentacles to capture prey, but some squid species have a set of tough sucker ring teeth inside each sucker that they use to grip escaping prey. These sucker ring teeth attracted attention from materials engineers after Miserez and coworkers discovered that sucker ring teeth (SRT) were mainly composed of proteins, not chitin as previously suspected.[124-126] The authors showed that SRT proteins contain randomly oriented β-sheet nanocrystals dispersed in an amorphous matrix. This protein structure gives SRT their relatively high elastic modulus.[124] In the absence of covalent crosslinks, SRT proteins are readily soluble and melt processable, which is distinctive for natural load bearing materials. Pena-Francesch and colleagues demonstrated that SRT protein (suckerin) extracted from squid SRT have pressure-sensitive adhesive properties, with a tensile adhesive strength of 1.1-1.5 MPa underwater. Lap shear adhesive strength to various underwater surfaces was up to was 2.5 MPa (to glass).[127] The promise of suckerin and suckerin-inspired materials as bioadhesives was furthered when Ding and colleagues produced recombinant suckerin that could be crosslinked into gels (40-500 Pa) and films (GPa) across a range of stiffnesses. When human primary cells, stem cells, or embryonic kidney cells were cultured on these suckerin materials, cells attached, were viable, and proliferated.[128] Together, this preliminary work demonstrates that suckerin materials are

adhesive and biocompatible, promising first steps towards making suckerin adhesives for biomedical applications.[127]

Outlook

Future research to develop bioinspired adhesives for clinical use may take inspiration from other sources, for example animals' materials processing strategies, or may combine multiple adhesive strategies. Future research efforts should address the mechanical mismatch often found between tissue adhesives and target tissues. To achieve high tissue adhesive strengths, it is essential to avoid a mechanical mismatch between the tissue and adhesive. This mismatch exists in most commercial tissue adhesives because the focus of development is usually on the formation of an adhesive interface rather than on the cohesive properties of the adhesive itself. In nature, adhesive interfaces feature sophisticated mechanical gradients to eliminate mechanical mismatch, however such approaches are hard to mimic by simply focusing on the biomimicry of protein structures.[20] For example, squid beaks are relatively unique in nature because they are extremely hard yet unmineralized, and because the gradient of hardness and toughness present in the material between the hard tooth surface and the underlying soft tissue spans two orders of magnitude.[129] Squid beak gradients have inspired synthetic mimics,[130, 131] and squid beak-inspired materials could address the unmet challenge in tissue engineering of adhering tissues with different mechanical properties together, for example attaching ligament to bone or tendon to muscle.[132, 133] Developing adhesives whose mechanical properties closely match those of the target tissue may necessitate development of different glue formulations for different applications, but the improved adhesive performance would likely be appreciable.

Another focus of future work should be to better understand processing methods used by marine creatures to store, process, and deliver the adhesive to the interface. Indeed, biomimicry of sandcastle worm complex coacervate formation described above is an early example of this. However, further research into coacervate formation is necessary to relate phase behavior to mechanical properties as a function of pH, concentration, temperature and ionic strength. For most surgical procedures it is desirable to prepare injectable formulations, which require a combination of low viscosity and rapid setting kinetics to form a load bearing adhesive. An often-used strategy is injection of two solutions through a mixing chamber, one containing an adhesive polymer and the other a (macromolecular) crosslinker. Notably, oxidative curing of DOPA-containing proteins (e.g. mussel plaque, marine egg cases) is slow in nature. Slow oxidation combined with tissue penetrating polymers may significantly increase (long term) interfacial adhesion via mechanical interlocking and anchoring. Therefore, it may be desirable to combine rapid initial gelation with slow curing.

Besides injectable formulations, tissue-adhesive patches are also valuable for medical applications. Gecko-inspired adhesive patches cannot adhere in wet environments unless an adhesive coating is applied or swellable amphiphilic blockcopolymers are used.[134] On the other hand, octopus-inspired patches do not require such a coating.[123] Like the gecko inspired wet adhesive patches, adding a wet-adhesive coating to octopus sucker-inspired patches may further improve their adhesion. Unlike in cephalopod adhesion, reversibility is not desired for most internal surgical applications, though it may be desirable in treatment of skin wounds. One advantage of patch-based adhesives is that the adhesive properties of patterned adhesive patches are largely substrate independent. Thus, adhesiveness can, for the most part, be decoupled from the bulk mechanical properties of the patch, improving material tunability.

The ability to bond or de-bond on demand and other stimuli-responsive properties may also be desirable in medical adhesives. Nitro-catechols have been incorporated into mussel inspired materials, and these adhesives de-bond upon exposure to UV irradiation. **[67, 135]** Another promising strategy to achieve de-bonding on demand in catecholic materials is to incorporate catechol-boronate chemistry; changing the pH changes the adhesiveness of the material, and the material can cycle between adhesive and non-adhesive states.[136] These strategies may improve mussel-inspired adhesives, but other animals could inspire additional stimuli-responsiveness. For example, the skin of many cephalopod species can respond to physical and chemical stimuli and rapidly change color or texture.[137] Researchers have developed cephalopod skin-inspired materials for applications including films that change color when stretched, innovations towards the development of wearable electronics, dynamic patterning, and materials that can change shape and texture.[137-139] Phan, et al., expertly reviewed dynamic materials inspired by cephalopod skin.[139] Many such technologies have the potential for eventual clinical translation to enhance tissue adhesives, especially those on the skin. Dynamic adhesives may be able to report strain or respond to skin temperature, and materials that can de-bond on demand (e.g. after exposure to specific wavelengths of light) may be valuable as, for example, adhesives to attach monitor leads to neonates, the elderly, or other patients with compromised skin.

It is important to note that the mussel and the sandcastle worm evolved primarily to adhere to stiff inorganic surfaces and particles. For the development of tissue adhesives, it would be relevant to investigate bioadhesive organisms that attach to soft and living surfaces. Potential sources of bioinspiration include several species of barnacles that can strongly attach to the skin of whales, reversible adhesion of sea star tube feet, and the pressure sensitive adhesive properties of squid sucker rings.[95, 127, 140] Analysis of the responsible protein sequences and subsequent biomimicry could lead to superior tissue adhesives. It was recently discovered that barnacle larvae secrete enzymes and lipids to clear omnipresent biofilms from marine surfaces before they establish permanent adhesion.[13] While the exact components that are responsible for this surface priming are not yet fully understood, the addition of a primer can be easily implemented to improve adhesion of bioinspired tissue adhesives.

Summary

Marine animals have evolved numerous methods for adhering underwater, and researchers have adapted many of these approaches into adhesive materials with promise for clinical tissue adhesion. Critical to the development of these and future materials is a deep understanding of the basic science underlying these natural adhesives and the marine organisms that create them. Early work in the field of mussel-inspired adhesives focused on direct replication of whole or fragmented mussel adhesive proteins. Over time, researchers have identified the chemical groups that most strongly contribute to mussels' wet adhesion (DOPA and, to a lesser extent, lysine) and created synthetic adhesive polymers using just these moieties to render natural and synthetic polymers adhesive towards wet tissue. Impressive progress in wet tissue adhesion has been achieved with this approach. Similarly, in the cases of sandcastle worm and cephalopod inspired materials, mimetic strategies that utilize only the most essential adhesive elements may surpass more thorough mimicry attempts. This strategy also allows for the incorporation of additional chemical functionality. In fact, taking inspiration from multiple biological sources, incorporating synergistic elements inspired by the mussel, sandcastle worm, octopus, or other animals as yet unexplored, may give ample opportunity for future advancement.

In mimicking and taking inspiration from the ocean's adhesives, researchers have developed materials with remarkable adhesion to wet mammalian tissues. Moving forward, engineers developing novel materials are buoyed by basic science researchers, who are discovering and characterizing the wet adhesives of the natural world. This biological understanding is paired with new breakthroughs from the lab bench, including new polymer synthesis strategies, nanofabrication techniques, and crosslinking chemistries. In developing adhesives for the clinic, tissue wetness is an enduring hurdle. Researchers and clinicians alike should continue to turn to the seas, where this challenging problem has been solved many times over.

Acknowledgements
The authors acknowledge the National Institutes of Health (1R01EB022031-01) for supporting this work. D. W. R. B. is grateful for support from the Swiss National Science Foundation early and advanced postdoc mobility grant (P2FRP2_165141 and P300P2_174468). S. M. W. acknowledges the National Science Foundation (Graduate Research Fellowship DGE 1752814) for support.

References

[1] F. Scognamiglio, A. Travan, I. Rustighi, P. Tarchi, S. Palmisano, E. Marsich, M. Borgogna, I. Donati, N. de Manzini, S. Paoletti, Adhesive and sealant interfaces for general surgery applications, J. Biomed. Mater. Res. B Appl. Biomater. 104(3) (2016) 626-39.
[2] D.A. Hammer, M. Tirrell, Biological adhesion at interfaces, Annu Rev Mater Sci 26(1) (1996) 651-691.
[3] B.P. Lee, P.B. Messersmith, J.N. Israelachvili, J.H. Waite, Mussel-Inspired Adhesives and Coatings, Annu. Rev. Mater. Res. 41(1) (2011) 99-132.
[4] A.P. Duarte, J.F. Coelho, J.C. Bordado, M.T. Cidade, M.H. Gil, Surgical adhesives: Systematic review of the main types and development forecast, Prog. Polym. Sci. 37(8) (2012) 1031-1050.
[5] U.G. Wegst, H. Bai, E. Saiz, A.P. Tomsia, R.O. Ritchie, Bioinspired structural materials, Nat. Mater. 14(1) (2015) 23-36.
[6] R. Schirhagl, C. Weder, J. Lei, C. Werner, H.M. Textor, Bioinspired surfaces and materials, Chem. Soc. Rev. 45(2) (2016) 234-6.
[7] A.H. Hofman, I.A. van Hees, J. Yang, M. Kamperman, Bioinspired Underwater Adhesives by Using the Supramolecular Toolbox, Adv. Mater. 30(19) (2018) e1704640.
[8] J.H. Ryu, P.B. Messersmith, H. Lee, Polydopamine Surface Chemistry: A Decade of Discovery, ACS Appl. Mater. Interfaces 10(9) (2018) 7523-7540.
[9] L.P. Bre, Y. Zheng, A.P. Pego, W.X. Wang, Taking tissue adhesives to the future: from traditional synthetic to new biomimetic approaches, Biomater. Sci. 1(3) (2013) 239-253.
[10] J.H. Waite, Nature's underwater adhesive specialist, Int. J. Adhesion Adhesives 7(1) (1987) 9-14.
[11] J.H. Waite, Mussel adhesion - essential footwork, J. Exp. Biol. 220(Pt 4) (2017) 517-530.
[12] R.J. Stewart, C.S. Wang, H. Shao, Complex coacervates as a foundation for synthetic underwater adhesives, Adv. Colloid Interface Sci. 167(1-2) (2011) 85-93.
[13] K.P. Fears, B. Orihuela, D. Rittschof, K.J. Wahl, Acorn Barnacles Secrete Phase-Separating Fluid to Clear Surfaces Ahead of Cement Deposition, Adv. Sci. 5(6) (2018) 1700762.

[14] S. Baik, D.W. Kim, Y. Park, T.J. Lee, S. Ho Bhang, C. Pang, A wet-tolerant adhesive patch inspired by protuberances in suction cups of octopi, Nature 546(7658) (2017) 396-400.
[15] J.H. Waite, N.H. Andersen, S. Jewhurst, C.J. Sun, Mussel adhesion: Finding the tricks worth mimicking, J Adhesion 81(3-4) (2005) 297-317.
[16] M.V. Rapp, G.P. Maier, H.A. Dobbs, N.J. Higdon, J.H. Waite, A. Butler, J.N. Israelachvili, Defining the Catechol-Cation Synergy for Enhanced Wet Adhesion to Mineral Surfaces, J. Am. Chem. Soc. 138(29) (2016) 9013-6.
[17] D.R. Miller, J.E. Spahn, J.H. Waite, The staying power of adhesion-associated antioxidant activity in Mytilus californianus, J. R. Soc. Interface 12(111) (2015) 20150614.
[18] Y. Akdogan, W. Wei, K.Y. Huang, Y. Kageyama, E.W. Danner, D.R. Miller, N.R. Martinez Rodriguez, J.H. Waite, S. Han, Intrinsic surface-drying properties of bioadhesive proteins, Angew. Chem. Int. Ed. 53(42) (2014) 11253-6.
[19] W. Wei, J. Yu, C. Broomell, J.N. Israelachvili, J.H. Waite, Hydrophobic enhancement of Dopa-mediated adhesion in a mussel foot protein, J. Am. Chem. Soc. 135(1) (2013) 377-83.
[20] M.J. Harrington, J.H. Waite, Holdfast heroics: comparing the molecular and mechanical properties of Mytilus californianus byssal threads, J. Exp. Biol. 210(Pt 24) (2007) 4307-18.
[21] Q. Lin, D. Gourdon, C. Sun, N. Holten-Andersen, T.H. Anderson, J.H. Waite, J.N. Israelachvili, Adhesion mechanisms of the mussel foot proteins mfp-1 and mfp-3, Proc. Natl. Acad. Sci. USA 104(10) (2007) 3782-6.
[22] D.G. DeMartini, J.M. Errico, S. Sjoestroem, A. Fenster, J.H. Waite, A cohort of new adhesive proteins identified from transcriptomic analysis of mussel foot glands, 14(131) (2017) 20170151.
[23] J.H. Waite, M.L. Tanzer, Polyphenolic Substance of Mytilus edulis: Novel Adhesive Containing L-Dopa and Hydroxyproline, Science 212(4498) (1981) 1038-40.
[24] J. Yu, W. Wei, E. Danner, R.K. Ashley, J.N. Israelachvili, J.H. Waite, Mussel protein adhesion depends on interprotein thiol-mediated redox modulation, Nat. Chem. Biol. 7(9) (2011) 588-90.
[25] H. Lee, N.F. Scherer, P.B. Messersmith, Single-molecule mechanics of mussel adhesion, Proc. Natl. Acad. Sci. USA 103(35) (2006) 12999-3003.
[26] G.P. Maier, M.V. Rapp, J.H. Waite, J.N. Israelachvili, A. Butler, Adaptive synergy between catechol and lysine promotes wet adhesion by surface salt displacement, Science 349(6248) (2015) 628-632.
[27] T. Priemel, E. Degtyar, M.N. Dean, M.J. Harrington, Rapid self-assembly of complex biomolecular architectures during mussel byssus biofabrication, Nat. Commun. 8 (2017) 14539.
[28] M.J. Harrington, A. Masic, N. Holten-Andersen, J.H. Waite, P. Fratzl, Iron-clad fibers: a metal-based biological strategy for hard flexible coatings, Science 328(5975) (2010) 216-20.
[29] S. Moulay, Dopa/Catechol-Tethered Polymers: Bioadhesives and Biomimetic Adhesive Materials, Polym Rev 54(3) (2014) 436-513.
[30] C. Ghobril, M.W. Grinstaff, The chemistry and engineering of polymeric hydrogel adhesives for wound closure: a tutorial, Chem. Soc. Rev. 44(7) (2015) 1820-35.
[31] J. Yang, V. Saggiomo, A.H. Velders, M.A. Cohen Stuart, M. Kamperman, Reaction Pathways in Catechol/Primary Amine Mixtures: A Window on Crosslinking Chemistry, Plos One 11(12) (2016) e0166490.
[32] N. Holten-Andersen, M.J. Harrington, H. Birkedal, B.P. Lee, P.B. Messersmith, K.Y. Lee, J.H. Waite, pH-induced metal-ligand cross-links inspired by mussel yield self-healing polymer networks with near-covalent elastic moduli, Proc. Natl. Acad. Sci. USA 108(7) (2011) 2651-5.

[33] C.A. Monnier, D.G. DeMartini, J.H. Waite, Intertidal exposure favors the soft-studded armor of adaptive mussel coatings, Nat. Commun. 9(1) (2018) 3424.
[34] D.M. Wiseman, Possible Intergel reaction syndrome (pIRS), Ann. Surg. 244(4) (2006) 630-632.
[35] C.L. Tang, D.G. Jayne, F.A. Seow-Choen, Y.Y. Ng, K.W. Eu, N. Mustapha, A randomized controlled trial of 0.5% ferric hyaluronate gel (Intergel) in the prevention of adhesions following abdominal surgery, Ann. Surg. 243(4) (2006) 449-455.
[36] J.W. Kuo, Practical Aspects of Hyaluronan Based Medical Products, 1 ed., CRC Press2005.
[37] N. Holten-Andersen, A. Jaishankar, M.J. Harrington, D.E. Fullenkamp, G. DiMarco, L.H. He, G.H. McKinley, P.B. Messersmith, K.Y.C. Leei, Metal-coordination: using one of nature's tricks to control soft material mechanics, J. Mater. Chem. B 2(17) (2014) 2467-2472.
[38] D.A. Wang, S. Varghese, B. Sharma, I. Strehin, S. Fermanian, J. Gorham, D.H. Fairbrother, B. Cascio, J.H. Elisseeff, Multifunctional chondroitin sulphate for cartilage tissue-biomaterial integration, Nat. Mater. 6(5) (2007) 385-92.
[39] J. Schnurrer, C.M. Lehr, Mucoadhesive properties of the mussel adhesive protein, Int J Pharm 141(1-2) (1996) 251-256.
[40] C.V. Benedict, N. Chaturvedi, Preparation of polymers containing dihydroxyphenylalanine and their adhesiveness, Bio-Polymers, Inc., USA . 1990, p. 15 pp.
[41] M. Qvist, H.A. Hansson, New use of a bioadhesive composition comprising a polyphenolic protein in ophthalmic therapy, BioPolymer Products of Sweden AB, WO2001044401A1, 2001.
[42] M. Qvist, Improved coating comprising a bioadhesive polyphenolic protein derived from a byssus-forming mussel, Bio Polymer Products of Sweden AB, WO2006038866A1, 2006.
[43] M.F. Notter, Selective attachment of neural cells to specific substrates including Cell-Tak, a new cellular adhesive, Experimental cell research 177(2) (1988) 237-46.
[44] H. Tatehata, A. Mochizuki, T. Kawashima, S. Yamashita, K. Ohkawa, H. Yamamoto, Oxidative reaction and conformational studies on synthetic sequential polypeptides of mussel adhesive proteins, Curr. Trends Polym. Sci. 5 (2000) 91-96.
[45] A. Nagai, H. Yamamoto, Insolubilizing Studies of Water-Soluble Poly(Lys Tyr) by Tyrosinase, B Chem Soc Jpn 62(7) (1989) 2410-2412.
[46] H. Yamamoto, Adhesive studies of synthetic polypeptides: A model for marine adhesive proteins, J. Adhesion Sci. Tech. 1(1) (1987) 177-183.
[47] H. Yamamoto, T. Hayakawa, Conformational studies of sequential polypeptides containing L-β-(3,4-dihydroxyphenyl)-α-alanine (Dopa) and L-lysine, Macromolecules 16(7) (1983) 1058-1063.
[48] H. Tatehata, A. Mochizuki, T. Kawashima, S. Yamashita, H. Yamamoto, Model polypeptide of mussel adhesive protein. I. Synthesis and adhesive studies of sequential polypeptides (X-Tyr-Lys)(n) and (Y-Lys)(n), J. Appl. Polym. Sci. 76(6) (2000) 929-937.
[49] M.E. Yu, J.Y. Hwang, T.J. Deming, Role of L-3,4-dihydroxyphenylalanine in mussel adhesive proteins, J. Am. Chem. Soc. 121(24) (1999) 5825-5826.
[50] T.J. Deming, Mussel byssus and biomolecular materials, Curr. Opin. Chem. Biol. 3(1) (1999) 100-5.
[51] M. Yu, T.J. Deming, Synthetic Polypeptide Mimics of Marine Adhesives, Macromolecules 31(15) (1998) 4739-45.
[52] T.J. Deming, M. Yu, Crosslinking of catechol-containing copolypeptide adhesives, The Regents of the University of California, USA . 2003, p. 13 pp.

[53] B.P. Lee, J.L. Dalsin, P.B. Messersmith, Synthesis and gelation of DOPA-modified poly(ethylene glycol) hydrogels, Biomacromolecules 3(5) (2002) 1038-47.
[54] A.B. Sean, R.-J. Marsha, P.L. Bruce, B.M. Phillip, Thermal gelation and tissue adhesion of biomimetic hydrogels, Biomed. Mater. 2(4) (2007) 203.
[55] C.E. Brubaker, H. Kissler, L.J. Wang, D.B. Kaufman, P.B. Messersmith, Biological performance of mussel-inspired adhesive in extrahepatic islet transplantation, Biomaterials 31(3) (2010) 420-7.
[56] G. Bilic, C. Brubaker, P.B. Messersmith, A.S. Mallik, T.M. Quinn, C. Haller, E. Done, L. Gucciardo, S.M. Zeisberger, R. Zimmermann, J. Deprest, A.H. Zisch, Injectable candidate sealants for fetal membrane repair: bonding and toxicity in vitro, Am. J. Obstet. Gynecol. 202(1) (2010) 85 e1-9.
[57] T. Jancelewicz, M.R. Harrison, A history of fetal surgery, Clin. Perinatol. 36(2) (2009) 227-36, vii.
[58] M. Perrini, D. Barrett, N. Ochsenbein-Koelble, R. Zimmermann, P. Messersmith, M. Ehrbar, A comparative investigation of mussel-mimetic sealants for fetal membrane repair, J. Mech. Behav. Biomed. Mater. 58 (2016) 57-64.
[59] A. Kivelio, P. Dekoninck, M. Perrini, C.E. Brubaker, P.B. Messersmith, E. Mazza, J. Deprest, R. Zimmermann, M. Ehrbar, N. Ochsenbein-Koelble, Mussel mimetic tissue adhesive for fetal membrane repair: initial in vivo investigation in rabbits, Eur. J. Obstet. Gynecol. Reprod. Biol. 171(2) (2013) 240-5.
[60] C.M. Haller, W. Buerzle, A. Kivelio, M. Perrini, C.E. Brubaker, R.J. Gubeli, A.S. Mallik, W. Weber, P.B. Messersmith, E. Mazza, N. Ochsenbein-Koelble, R. Zimmermann, M. Ehrbar, Mussel-mimetic tissue adhesive for fetal membrane repair: an ex vivo evaluation, Acta Biomater. 8(12) (2012) 4365-70.
[61] P.B. Messersmith, J.L. Dalsin, B.P. Lee, S.A. Burke, Dopa-functionalized, branched, poly(alkylene oxide) adhesives, Nerites Corporation, USA; Northwestern University . 2008, p. 41pp.
[62] B.P. Lee, J.L. Dalsin, J.L. Murphy, L. Vollenweider, A. Lyman, F. Xu, J. White, W. Lew, M. Brodie, Polymer medical adhesives for hernia repair, KNC Ner Acquisition Sub, Inc., USA . 2012, p. 394pp.
[63] J.L. Murphy, L. Vollenweider, F. Xu, B.P. Lee, Adhesive performance of biomimetic adhesive-coated biologic scaffolds, Biomacromolecules 11(11) (2010) 2976-84.
[64] H. Meng, Y. Li, M. Faust, S. Konst, B.P. Lee, Hydrogen peroxide generation and biocompatibility of hydrogel-bound mussel adhesive moiety, Acta Biomater. 17 (2015) 160-9.
[65] H. Meng, Y. Liu, B.P. Lee, Model polymer system for investigating the generation of hydrogen peroxide and its biological responses during the crosslinking of mussel adhesive moiety, Acta Biomaterialia 48 (2017) 144-156.
[66] C.E. Brubaker, P.B. Messersmith, Enzymatically Degradable Mussel-Inspired Adhesive Hydrogel, Biomacromolecules 12(12) (2011) 4326-4334.
[67] Z. Shafiq, J. Cui, L. Pastor-Perez, V. San Miguel, R.A. Gropeanu, C. Serrano, A. del Campo, Bioinspired underwater bonding and debonding on demand, Angew. Chem. Int. Ed. 51(18) (2012) 4332-5.
[68] D.G. Barrett, G.G. Bushnell, P.B. Messersmith, Mechanically robust, negative-swelling, mussel-inspired tissue adhesives, Adv. Healthc. Mater. 2(5) (2013) 745-55.
[69] J.H. Ryu, S. Hong, H. Lee, Bio-inspired adhesive catechol-conjugated chitosan for biomedical applications: A mini review, Acta Biomater. 27 (2015) 101-115.

[70] J. Shin, J.S. Lee, C. Lee, H.J. Park, K. Yang, Y. Jin, J.H. Ryu, K.S. Hong, S.H. Moon, H.M. Chung, H.S. Yang, S.H. Um, J.W. Oh, D.I. Kim, H. Lee, S.W. Cho, Tissue Adhesive Catechol-Modified Hyaluronic Acid Hydrogel for Effective, Minimally Invasive Cell Therapy, Adv. Funct. Mater. 25(25) (2015) 3814-3824.
[71] J.H. Cho, J.S. Lee, J. Shin, E.J. Jeon, S. An, Y.S. Choi, S.W. Cho, Ascidian-Inspired Fast-Forming Hydrogel System for Versatile Biomedical Applications: Pyrogallol Chemistry for Dual Modes of Crosslinking Mechanism, Adv. Funct. Mater. 28(6) (2018) 1705244.
[72] Y. Lee, H.J. Chung, S. Yeo, C.H. Ahn, H. Lee, P.B. Messersmith, T.G. Park, Thermo-sensitive, injectable, and tissue adhesive sol-gel transition hyaluronic acid/pluronic composite hydrogels prepared from bio-inspired catechol-thiol reaction, Soft matter 6(5) (2010) 977-983.
[73] S.J. McCarthy, K.W. Gregory, J.W. Morgan, Tissue dressing assemblies, systems, and methods formed from hydrophilic polymer sponge structures such as chitosan, HemCon, Inc., USA . 2005, pp. 41 pp., Cont.-in-part of U.S. Ser. No. 480,827.
[74] J.H. Ryu, Y. Lee, W.H. Kong, T.G. Kim, T.G. Park, H. Lee, Catechol-functionalized chitosan/pluronic hydrogels for tissue adhesives and hemostatic materials, Biomacromolecules 12(7) (2011) 2653-9.
[75] H. Lee, M.S. Lee, J.H. Ryu, Hydrogel comprising catechol group-coupled chitosan or polyamine and poloxamer comprising thiol group coupled to end thereof, preparation method thereof, and hemostatic using the same, Korea Advanced Institute of Science and Technology, S. Korea; InnoTherapy Inc. . 2013, p. 33pp.; Chemical Indexing Equivalent to 159:63670 (KR).
[76] H. Lee, M. Shin, M.S. Lee, S.S. Oh, Hemostatic injection needle coated with crosslinked chitosan functionalized with catechol derivative, InnoTherapy Inc., S. Korea . 2016, p. 30pp.; Chemical Indexing Equivalent to 164:107545 (KR).
[77] D.X. Oh, S. Kim, D. Lee, D.S. Hwang, Tunicate-mimetic nanofibrous hydrogel adhesive with improved wet adhesion, Acta Biomater. 20 (2015) 104-112.
[78] M. Shin, S.G. Park, B.C. Oh, K. Kim, S. Jo, M.S. Lee, S.S. Oh, S.H. Hong, E.C. Shin, K.S. Kim, S.W. Kang, H. Lee, Complete prevention of blood loss with self-sealing haemostatic needles, Nat. Mater. 16(1) (2017) 147-152.
[79] M. Shin, J.H. Ryu, K. Kim, M.J. Kim, S. Jo, M.S. Lee, D.Y. Lee, H. Lee, Hemostatic Swabs Containing Polydopamine-like Catecholamine Chitosan-Catechol for Normal and Coagulopathic Animal Models, ACS Biomater. Sci. Eng. 4(7) (2018) 2314-2318.
[80] R. Bitton, H. Bianco-Peled, Novel biomimetic adhesives based on algae glue, Macromol. Biosci. 8(5) (2008) 393-400.
[81] Y. Rozen, H. Bianco-Peled, Studies of Phenol-Based Bioinspired Sealants, J Adhesion 90(8) (2014) 667-681.
[82] J. Li, A.D. Celiz, J. Yang, Q. Yang, I. Wamala, W. Whyte, B.R. Seo, N.V. Vasilyev, J.J. Vlassak, Z. Suo, D.J. Mooney, Tough adhesives for diverse wet surfaces, Science 357(6349) (2017) 378-381.
[83] P.J. Cheung, G.D. Ruggieri, R.F. Nigrelli, A new method for obtaining barnacle cement in the liquid state for polymerization studies, Marine Biology 43(2) (1977) 157-163.
[84] K. Kaleem, F. Chertok, S. Erhan, Collagen-based bioadhesive barnacle cement mimic. I. Chemical and enzymic studies, Angew. Makromol. Chem. 155 (1987) 31-43.
[85] K. Kaleem, F. Chertok, S. Erhan, Novel materials from protein-polymer grafts, Nature 325(6102) (1987) 328-9.

[86] C.R. So, K.P. Fears, D.H. Leary, J.M. Scancella, Z. Wang, J.L. Liu, B. Orihuela, D. Rittschof, C.M. Spillmann, K.J. Wahl, Sequence basis of Barnacle Cement Nanostructure is Defined by Proteins with Silk Homology, Scientific Reports 6 (2016) 36219.
[87] T. Essock-Burns, N.V. Gohad, B. Orihuela, A.S. Mount, C.M. Spillmann, K.J. Wahl, D. Rittschof, Barnacle biology before, during and after settlement and metamorphosis: a study of the interface, J. Exp. Biol. 220(2) (2017) 194-207.
[88] N.V. Gohad, N. Aldred, C.M. Hartshorn, Y. Jong Lee, M.T. Cicerone, B. Orihuela, A.S. Clare, D. Rittschof, A.S. Mount, Synergistic roles for lipids and proteins in the permanent adhesive of barnacle larvae, Nat. Commun. 5 (2014) 4414.
[89] C. Fan, J. Fu, W. Zhu, D.A. Wang, A mussel-inspired double-crosslinked tissue adhesive intended for internal medical use, Acta Biomater. 33 (2016) 51-63.
[90] H.Y. Chung, R.H. Grubbs, Rapidly Cross-Linkable DOPA Containing Terpolymer Adhesives and PEG-Based Cross-Linkers for Biomedical Applications, Macromolecules 45(24) (2012) 9666-9673.
[91] S.B. Lee, C. Gonzalez-Cabezas, K.M. Kim, K.N. Kim, K. Kuroda, Catechol-Functionalized Synthetic Polymer as a Dental Adhesive to Contaminated Dentin Surface for a Composite Restoration, Biomacromolecules 16(8) (2015) 2265-75.
[92] Y.F. Shi, P.R. Zhou, V. Jerome, R. Freitag, S. Agarwal, Enzymatically Degradable Polyester-Based Adhesives, ACS Biomater. Sci. Eng. 1(10) (2015) 971-977.
[93] Y.S. Li, J. Krahn, C. Menon, Bioinspired Dry Adhesive Materials and Their Application in Robotics: A Review, J Bionic Eng 13(2) (2016) 181-199.
[94] W. Adlassnig, T. Lendl, M. Peroutka, I. Lang, Deadly Glue — Adhesive Traps of Carnivorous Plants, in: J. von Byern, I. Grunwald (Eds.), Biological Adhesive Systems: From Nature to Technical and Medical Application, Springer Vienna, Vienna, 2010, pp. 15-28.
[95] E. Hennebert, R. Wattiez, M. Demeuldre, P. Ladurner, D.S. Hwang, J.H. Waite, P. Flammang, Sea star tenacity mediated by a protein that fragments, then aggregates, Proc. Natl. Acad. Sci. USA 111(17) (2014) 6317-22.
[96] S.H. Chen, H.J. Gao, Bio-inspired mechanics of reversible adhesion: Orientation-dependent adhesion strength for non-slipping adhesive contact with transversely isotropic elastic materials, J. Mech. Phys. Solids 55(5) (2007) 1001-1015.
[97] B.N.J. Persson, On the mechanism of adhesion in biological systems, J. Chem. Phys. 118(16) (2003) 7614-7621.
[98] A.Y. Stark, T.W. Sullivan, P.H. Niewiarowski, The effect of surface water and wetting on gecko adhesion, J. Exp. Biol. 215(Pt 17) (2012) 3080-6.
[99] H. Lee, B.P. Lee, P.B. Messersmith, A reversible wet/dry adhesive inspired by mussels and geckos, Nature 448(7151) (2007) 338-U4.
[100] M.P. Deacon, S.S. Davis, J.H. Waite, S.E. Harding, Structure and mucoadhesion of mussel glue protein in dilute solution, Biochemistry 37(40) (1998) 14108-12.
[101] N.D. Catron, H. Lee, P.B. Messersmith, Enhancement of poly(ethylene glycol) mucoadsorption by biomimetic end group functionalization, Biointerphases 1(4) (2006) 134-141.
[102] J. Xu, G.M. Soliman, J. Barralet, M. Cerruti, Mollusk glue inspired mucoadhesives for biomedical applications, Langmuir 28(39) (2012) 14010-7.
[103] G.M. Soliman, Y.L. Zhang, G. Merle, M. Cerruti, J. Barralet, Hydrocaffeic acid-chitosan nanoparticles with enhanced stability, mucoadhesion and permeation properties, Eur. J. Pharm. Biopharm. 88(3) (2014) 1026-37.

[104] K. Kim, K. Kim, J.H. Ryu, H. Lee, Chitosan-catechol: a polymer with long-lasting mucoadhesive properties, Biomaterials 52 (2015) 161-70.
[105] S. Sunoqrot, L. Hasan, A. Alsadi, R. Hamed, O. Tarawneh, Interactions of mussel-inspired polymeric nanoparticles with gastric mucin: Implications for gastro-retentive drug delivery, Colloids Surf. B Biointerfaces 156 (2017) 1-8.
[106] W. Wei, L. Petrone, Y. Tan, H. Cai, J.N. Israelachvili, A. Miserez, J.H. Waite, An Underwater Surface-Drying Peptide Inspired by a Mussel Adhesive Protein, Adv. Funct. Mater. 26(20) (2016) 3496-3507.
[107] Q. Zhao, D.W. Lee, B.K. Ahn, S. Seo, Y. Kaufman, J.N. Israelachvili, J.H. Waite, Underwater contact adhesion and microarchitecture in polyelectrolyte complexes actuated by solvent exchange, Nat. Mater. 15(4) (2016) 407-412.
[108] C. Sun, G.E. Fantner, J. Adams, P.K. Hansma, J.H. Waite, The role of calcium and magnesium in the concrete tubes of the sandcastle worm, J. Exp. Biol. 210(Pt 8) (2007) 1481-8.
[109] H. Shao, R.J. Stewart, Biomimetic underwater adhesives with environmentally triggered setting mechanisms, Adv. Mater. 22(6) (2010) 729-33.
[110] B.D. Winslow, H. Shao, R.J. Stewart, P.A. Tresco, Biocompatibility of adhesive complex coacervates modeled after the sandcastle glue of Phragmatopoma californica for craniofacial reconstruction, Biomaterials 31(36) (2010) 9373-81.
[111] S. Kaur, G.M. Weerasekare, R.J. Stewart, Multiphase adhesive coacervates inspired by the Sandcastle worm, ACS Appl. Mater. Interfaces 3(4) (2011) 941-4.
[112] L.K. Mann, R. Papanna, K.J. Moise, Jr., R.H. Byrd, E.J. Popek, S. Kaur, S.C. Tseng, R.J. Stewart, Fetal membrane patch and biomimetic adhesive coacervates as a sealant for fetoscopic defects, Acta Biomater. 8(6) (2012) 2160-5.
[113] R. Papanna, L.K. Mann, S.C. Tseng, R.J. Stewart, S.S. Kaur, M.M. Swindle, T.R. Kyriakides, N. Tatevian, K.J. Moise, Jr., Cryopreserved human amniotic membrane and a bioinspired underwater adhesive to seal and promote healing of iatrogenic fetal membrane defect sites, Placenta 36(8) (2015) 888-94.
[114] R. Papanna, K.J. Moise, Jr., L.K. Mann, S. Fletcher, R. Schniederjan, M.B. Bhattacharjee, R.J. Stewart, S. Kaur, S.P. Prabhu, S.C. Tseng, Cryopreserved human umbilical cord patch for in-utero spina bifida repair, Ultrasound. Obstet. Gynecol. 47(2) (2016) 168-76.
[115] Y. Lee, C. Xu, M. Sebastin, A. Lee, N. Holwell, C. Xu, D. Miranda Nieves, L. Mu, R.S. Langer, C. Lin, J.M. Karp, Bioinspired Nanoparticulate Medical Glues for Minimally Invasive Tissue Repair, Adv Healthc Mater 4(16) (2015) 2587-96.
[116] N. Lang, M.J. Pereira, Y. Lee, I. Friehs, N.V. Vasilyev, E.N. Feins, K. Ablasser, E.D. O'Cearbhaill, C. Xu, A. Fabozzo, R. Padera, S. Wasserman, F. Freudenthal, L.S. Ferreira, R. Langer, J.M. Karp, P.J. del Nido, A blood-resistant surgical glue for minimally invasive repair of vessels and heart defects, Sci. Transl. Med. 6(218) (2014) 218ra6.
[117] N. Cyran, L. Klinger, R. Scott, C. Griffiths, T. Schwaha, V. Zheden, L. Ploszcanski, J.v. Byren, Characterization of the Adhesive Systems in Cephalopods in: J.v. Byren, I. Grunwald (Eds.) Biological Adhesive Systems: From Nature to Technical and Medical Application, SpringerWeinNewYork, Wien, 2010, pp. 54-82.
[118] J. Von Byern, W. Klepal, Adhesive mechanisms in cephalopods: a review, Biofouling 22(5) (2006) 329-338.
[119] N. Cyran, W. Klepal, J. von Byern, Ultrastructural characterization of the adhesive organ of Idiosepius biserialis and Idiosepius pygmaeus (Mollusca: Cephalopoda), J. Mar. Biol. Assoc. U. K. 91(7) (2011) 1499-1510.

[120] F. Tramacere, N.M. Pugno, M.J. Kuba, B. Mazzolai, Unveiling the morphology of the acetabulum in octopus suckers and its role in attachment, Interface Focus 5(1) (2015).
[121] F. Tramacere, L. Beccai, M. Kuba, A. Gozzi, A. Bifone, B. Mazzolai, The Morphology and Adhesion Mechanism of Octopus vulgaris Suckers, Plos One 8(6) (2013).
[122] Y.C. Chen, H. Yang, Octopus-Inspired Assembly of Nanosucker Arrays for Dry/Wet Adhesion, Acs Nano 11(6) (2017) 5332-5338.
[123] J.H. Oh, S.Y. Hong, H. Park, S.W. Jin, Y.R. Jeong, S.Y. Oh, J. Yun, H. Lee, J.W. Kim, J.S. Ha, Fabrication of High-Sensitivity Skin-Attachable Temperature Sensors with Bioinspired Microstructured Adhesive, ACS Appl. Mater. Interfaces 10(8) (2018) 7263-7270.
[124] S.H. Hiew, A. Miserez, Squid Sucker Ring Teeth: Multiscale Structure-Property Relationships, Sequencing, and Protein Engineering of a Thermoplastic Biopolymer, ACS Biomater. Sci. Eng. 3(5) (2017) 680-693.
[125] A. Miserez, J.C. Weaver, O. Chaudhuri, Biological materials and molecular biomimetics - filling up the empty soft materials space for tissue engineering applications, J. Mater. Chem. B 3(1) (2015) 13-24.
[126] A. Miserez, J.C. Weaver, P.B. Pedersen, T. Schneeberk, R.T. Hanlon, D. Kisailus, H. Birkedal, Microstructural and Biochemical Characterization of the Nanoporous Sucker Rings from Dosidicus gigas, Adv. Mater. 21(4) (2009) 401-406.
[127] A. Pena-Francesch, B. Akgun, A. Miserez, W.P. Zhu, H.J. Gao, M.C. Demirel, Pressure Sensitive Adhesion of an Elastomeric Protein Complex Extracted From Squid Ring Teeth, Adv. Funct. Mater. 24(39) (2014) 6227-6233.
[128] D. Ding, P.A. Guerette, J. Fu, L. Zhang, S.A. Irvine, A. Miserez, From Soft Self-Healing Gels to Stiff Films in Suckerin-Based Materials Through Modulation of Crosslink Density and β-Sheet Content, 27(26) (2015) 3953-3961.
[129] A. Miserez, T. Schneberk, C. Sun, F.W. Zok, J.H. Waite, The transition from stiff to compliant materials in squid beaks, Science 319(5871) (2008) 1816-9.
[130] J.D. Fox, J.R. Capadona, P.D. Marasco, S.J. Rowan, Bioinspired water-enhanced mechanical gradient nanocomposite films that mimic the architecture and properties of the squid beak, J. Am. Chem. Soc. 135(13) (2013) 5167-74.
[131] R. Libanori, R.M. Erb, A. Reiser, H. Le Ferrand, M.J. Suess, R. Spolenak, A.R. Studart, Stretchable heterogeneous composites with extreme mechanical gradients, Nat. Commun. 3 (2012).
[132] A. Seidi, M. Ramalingam, I. Elloumi-Hannachi, S. Ostrovidov, A. Khademhosseini, Gradient biomaterials for soft-to-hard interface tissue engineering, Acta Biomater. 7(4) (2011) 1441-1451.
[133] Z.Q. Liu, M.A. Meyers, Z.F. Zhang, R.O. Ritchie, Functional gradients and heterogeneities in biological materials: Design principles, functions, and bioinspired applications, Prog. Mater. Sci. 88 (2017) 467-498.
[134] N. Annabi, A. Tamayol, S.R. Shin, A.M. Ghaemmaghami, N.A. Peppas, A. Khademhosseini, Surgical materials: Current challenges and nano-enabled solutions, Nano Today 9(5) (2014) 574-589.
[135] Y.-Z. Wang, L. Li, F.-S. Du, Z.-C. Li, A facile approach to catechol containing UV dismantlable adhesives, Polymer 68 (2015) 270-278.
[136] A.R. Narkar, B. Barker, M. Clisch, J. Jiang, B.P. Lee, pH Responsive and Oxidation Resistant Wet Adhesive based on Reversible Catechol–Boronate Complexation, Chemistry of Materials 28(15) (2016) 5432-5439.

[137] D. Osorio, Cephalopod Behaviour: Skin Flicks, Curr. Biol. 24(15) (2014) R684-R685.
[138] A. Fishman, J. Rossiter, M. Homer, Hiding the squid: patterns in artificial cephalopod skin, J. R. Soc. Interface 12(108) (2015) 20150281.
[139] L. Phan, R. Kautz, E.M. Leung, K.L. Naughton, Y. Van Dyke, A.A. Gorodetsky, Dynamic Materials Inspired by Cephalopods, Chem. Mater. 28(19) (2016) 6804-6816.
[140] Y. Nogata, K. Matsumura, Larval development and settlement of a whale barnacle, Biol. Lett. 2(1) (2006) 92-3.

CHAPTER THREE – FETAL MEMBRANE PRESEALING: INITIAL *IN VIVO* STUDY IN RABBITS

N.B. *This chapter also appeared in a manuscript of the same title that has been submitted for publication; I wrote the manuscript with feedback from all authors. Co-investigators on this study include Vamsi K. Aribindi (surgery, surgical design), Jisoo Shin (polymer preparation), Phillip H. Kim (surgery), Kristina L. Hicks (veterinary surgery), and Sasha G. Demeulenaere (polymer preparation), along with senior investigators Diana Bauer, Michael R. Harrison, and Phillip B. Messersmith. For more about details about how the work in this chapter relates to the other studies in this dissertation, please see the Introduction.*

3.1 Abstract

Introduction: Fetal surgery can improve health outcomes for severely affected fetuses, but surgical fetal membrane puncture remains risky due to the potential for peri- or post-surgical membrane rupture, leading to preterm birth. Here we investigate a new surgical approach, fetal membrane presealing, in which an injectable liquid sealant is placed between the uterus and fetal membranes, stabilizing them prior to surgical membrane puncture.

Methods: An experimental polyethylene glycol (PEG)-based fetal membrane adhesive was studied in a rabbit model of fetal membrane presealing. Midgestational fetal sacs of 15 rabbit does were sealed and punctured to emulate fetal surgery; fetuses in non-sealed punctured sacs served as controls. Fetal viability and lung-to-body mass ratio (LBR) were assessed after 6-7d.

Results: Fetal survival was high for fetuses in each group (presealed-and-punctured sacs, punctured sacs, and no intervention). No significant differences in viability or LBR, adverse materials-related events, or toxicity were noted.

Discussion/Conclusion: We demonstrate the potential of a PEG-based adhesive for fetal membrane presealing. In a pilot animal study in pregnant rabbits, fetal membrane presealing with our adhesives appeared safe, straightforward, reliable, and biocompatible with mothers and fetuses.

3.2 Introduction

Fetal surgery has drastically improved outcomes for some fetuses with severe conditions like myelomeningocele, congenital diaphragmatic hernia, and urinary tract obstructions. However, the risk of post-surgical membrane rupture and preterm birth, which is around 30%, can often outweigh the potential benefits of fetal surgery [1-4]. Central to this risk is damage to the fetal membranes during the surgery. Human fetal membranes do not heal after puncture [5-9], but several strategies (reviewed elsewhere [10]) have been attempted to seal the fetal membranes following surgery including fibrin glue [11-13], tissue engineering approaches [14], patches [15-18], commercially available surgical glues [11], and novel polymer adhesives [11, 13, 19-21]. However, none of these approaches have been clinically adopted. We propose a new surgical strategy, fetal membrane presealing [10, 22], in which an adhesive is applied to the delicate fetal membranes prior to surgical access, stabilizing them during and after surgery and improving fetal outcomes.

As shown in Figure 1, to preseal the fetal membranes, a liquid adhesive is injected into the potential space between the uterus and fetal membranes. After ~1 minute, the material solidifies into a soft, adhesive hydrogel. To access the fetus, surgical tools puncture through the uterus, the adhesive, and the fetal membranes. During surgery, the adhesive would support the membrane, decreasing overall defect size, reducing amniotic fluid leakage, and ultimately improving fetal outcomes, for example reducing preterm birth and improving fetal/neonatal fitness. As a first step towards demonstrating this presealing hypothesis, we developed a rabbit model to study the efficacy of fetal membrane presealing and potential presealants.

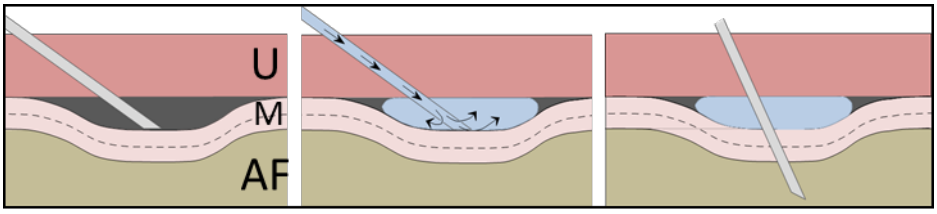

Fig. 1. Schematic figure illustrating pre-sealing concept. 1) "Tenting" of membranes using oblique needle insertion (uterus, U; membranes, M; amniotic fluid, AF). 2) Injection of liquid sealant between membranes and uterine wall. 3) Intervention through pre-sealed membranes, stabilizing membranes and reducing leakage.

While animal models of fetal membrane sealing have been developed [17, 21, 23, 24], to our knowledge no animal model of fetal membrane presealing has been published. However, the presealing hypothesis has been tested in benchtop studies, including on chicken egg fetal membranes [22]. Researchers demonstrated that applying an adhesive gel to the delicate membranes prior to puncture with a 2mm biopsy needle greatly reduced membrane leakage. We sought to develop an animal model of fetal membrane presealing. Rabbits have been used as animal models for various fetal surgeries including membrane and uterine post-sealing [21, 24, 25], congenital diaphragmatic hernia [26], and spina bifida [26]. Rabbit fetuses are large enough for surgical manipulation, and unlike many larger species, they have many fetuses per litter and short (~32 d) gestations, which makes them relatively resource-efficient. In addition to fetal survival, fetal lung-to-body mass ratio (LBR) is a proxy for the amount of amniotic fluid present in late gestation [27], which is a useful metric for assessing potential leakage and fetal fitness.

The ideal adhesive for a fetal membrane presealing application would be injectable but rapidly solidify *in situ*, adhere well to wet tissues, and have cyto- and bio-compatible properties suitable for the delicate fetal niche. Tissue adhesives, including commercially available surgical glues, that have been considered as potential fetal membrane sealants have been studied and reviewed elsewhere; however, these materials have a number of shortcomings including cytotoxicity, poor adhesivity, use of harsh oxidants, or poor mechanical properties [10, 11, 21, 28, 29]. One adhesive with physical properties that may be appropriate for fetal membrane presealing is the hydrogel formed upon mixing of an aqueous solution of multi-arm PEG end-functionalized with cysteine (20 kDa, 8 arms, PEG-Cys) and multi-arm PEG end-functionalized with n-hydroxysuccinimide ester (20 kDa, 8 arms, PEG-NHS) (Fig. 2) [30, 31]. This material has been shown to have suitable gelation kinetics (~1 minute), exhibit adhesion to wet tissue (46 kPa), be

cytocompatible with mammalian cells *in vitro*, and was used *in vivo* in a mouse drug delivery model with no adverse biocompatibility events at any studied doses [31].

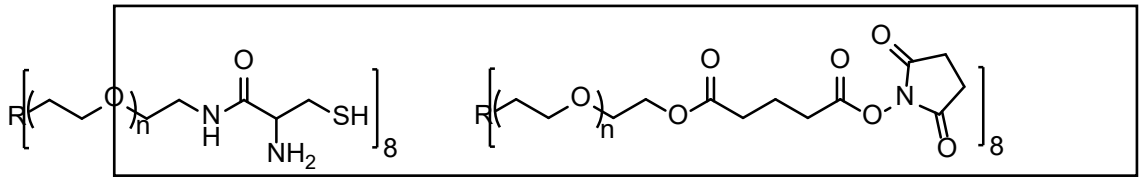

Fig. 2. Structure of 8-arm PEG-Cys (left) and 8-arm PEG-NHS (right). Each polymer has molecular weight 20 kDa.

3.3 Results

3.3.1 Materials for sealing the fetal membrane

Previous reports indicated that PEG-Cys/PEG-NHS would be a promising adhesive for sealing wet, internal tissues [30]. PEG-Cys was synthesized from PEG-NH_2 (8 arm, 20 kDa) and PEG-NHS was purchased. All polymers were purified and prepared for use *in vivo*. To form adhesive hydrogels, PEG-Cys and PEG-NHS polymers were dissolved separately at 15 wt% in tissue culture PBS (1x), and mixed 1:1 to form adhesive gels that formed in 50-70 seconds. Each batch of material was also evaluated for cytocompatibility with NIH 3T3 and CCD32-sk cells *in vitro* following ISO 10993-05, and all were found to be cytocompatible (Supplemental Fig. S3.3).

3.3.2 Rabbit model development

We sought to develop a rabbit model of fetal membrane presealing to establish the surgical feasibility of presealing tissues *in vivo*, determine the fetotoxicity of the adhesive formulation, and investigate the efficacy of fetal membrane presealing relative to the membranes that were punctured with no sealant, the clinical standard of care for most human patients. New Zealand white rabbits were chosen because they have fetuses large enough for surgical manipulation but are relatively cost-effective compared to most large-animal models. Additionally, their bicornate uteruses, which have around 2-5 fetuses on each uterine horn, enable each rabbit doe to serve as an internal control, puncturing 2-4 fetal sacs on one horn and presealing and puncturing 2-4 sacs on the opposite horn. Remaining fetuses (if any), on whom no intervention is performed, can serve as an internal control to account for maternal factors. Previous studies have assigned all fetuses in the same mother to the same intervention [17, 21]. However, this can leave the data subject to catastrophic events where all fetuses are delivered prematurely or die and are resorbed, and it can be difficult to tell if the fetal loss is the result of the intervention or maternal factors. Maternal fitness and wellbeing could also contribute to variability. Thus, we perform each intervention (puncture or preseal-then-puncture) on a different uterine horn in the same doe.

Animal study followed an IACUC-approved protocol. Pregnant rabbits were obtained from Western Oregon Rabbit Co., housed in an AAALAC accredited facility, and acclimated to the facility for at least 72 h prior to study inception. At day 21-26 of the 31-32 day gestation, rabbits were anesthetized and abdomens were carefully shaved and aseptically prepared for surgery. An approximately 5-7 cm abdominal incision was created, and the uterus was removed from the abdominal cavity so fetuses on each uterine horn could be counted (**Fig. 3A**). The uterus was then carefully replaced back in the abdomen. During fetal presealing trials, the individual fetuses in the uterus were sequentially exposed to prevent dehydration and maintain body temperature of non-operative fetuses. Following surgery, the abdomen was closed in layers.

Acute surgery

In the first approach, we performed an acute (non-survival) surgery to study the feasibility of delivering PEG-Cys/PEG-NHS gels to the uterine-membrane interface in a minimally invasive manner. The adhesive was delivered at this interface with a beveled 23-gauge needle. We found that a shallow injection angle resulted in more reliable adhesive placement (**Fig. 3B**). This same study also demonstrated the adhesiveness of PEG-Cys/PEG-NHS to wet uterine and fetal membrane tissue. When the adhesive was applied to the surface of the fetal membrane (with or without overlying uterine tissue) (**Fig. 3D**), sacs did not leak when punctured with an 18 or 14 g needle (**Fig. 3C**). Sacs that were not presealed showed significant leakage of amniotic fluid when punctured while still inside the uterus and ruptured when punctured without overlying uterine tissue. Presealed-then-punctured sacs did not leak at the presealed puncture site when fluorescein dye was injected at a distal site with a 23 g needle (**Fig. 3E**); dye leakage assays were not performed in subsequent survival surgeries for fetal safety.

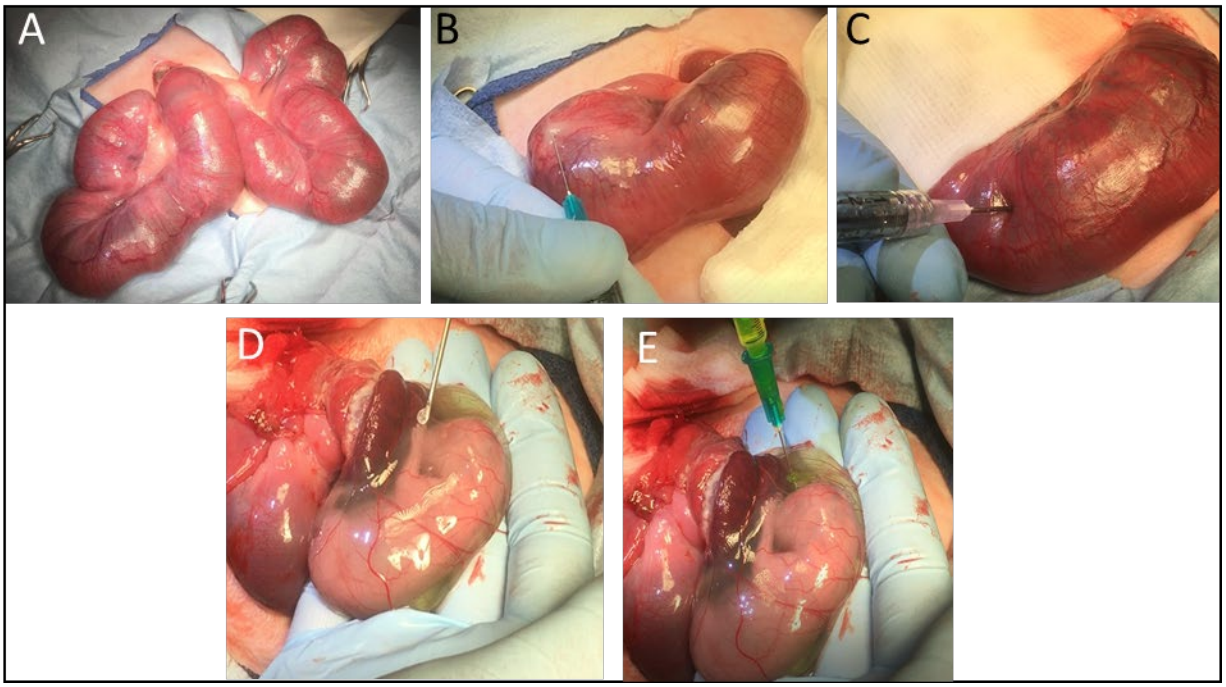

Fig. 3. Photos from acute surgery. A. Rabbit uterus exposed through abdominal opening to count and identify fetal sacs. B. Presealing between uterus and fetal membranes with 23 g needle. C. Puncture through uterus and presealing bolus with 18 g needle. D. Direct application of adhesive to fetal membranes; adhesive adheres strongly and cannot be removed without damage to membranes. E. Dye injection into sac.

Survival surgeries

We sought to develop an animal model that showed significant differences in fetal outcomes for fetuses in presealed-then-punctured sacs relative to puncture-only controls. Primary outcomes evaluated were fetal survival and fetal lung to body mass ratio, a marker of lung maturity and an indicator of amniotic fluid levels present at end-gestation [27]. Methods studied in the 6-7 day *in vivo* studies include 1.) The experimental adhesive was applied between uterus and membranes with a 23 gauge needle; subsequently, a 14 gauge needle was used to puncture through the uterus, sealant bolus, and membranes. 2.) The experimental adhesive was applied as in 1 and

the uterus, sealant bolus, and membranes were punctured with an 11-blade scalpel (5mm). 3.) Two stay sutures were placed on the fundus of the uterus, 1-1.5 cm apart, to use as anchors. As an assistant held the stay sutures, a 1 cm opening in the uterus was carefully cut between the sutures to reveal underlying membranes. Then presealant was applied directly to the membranes, the membranes and adhesive bolus were punctured with a no. 11 scalpel blade, and the uterus defect was sutured closed (**Fig. 4, Supplemental Video**).

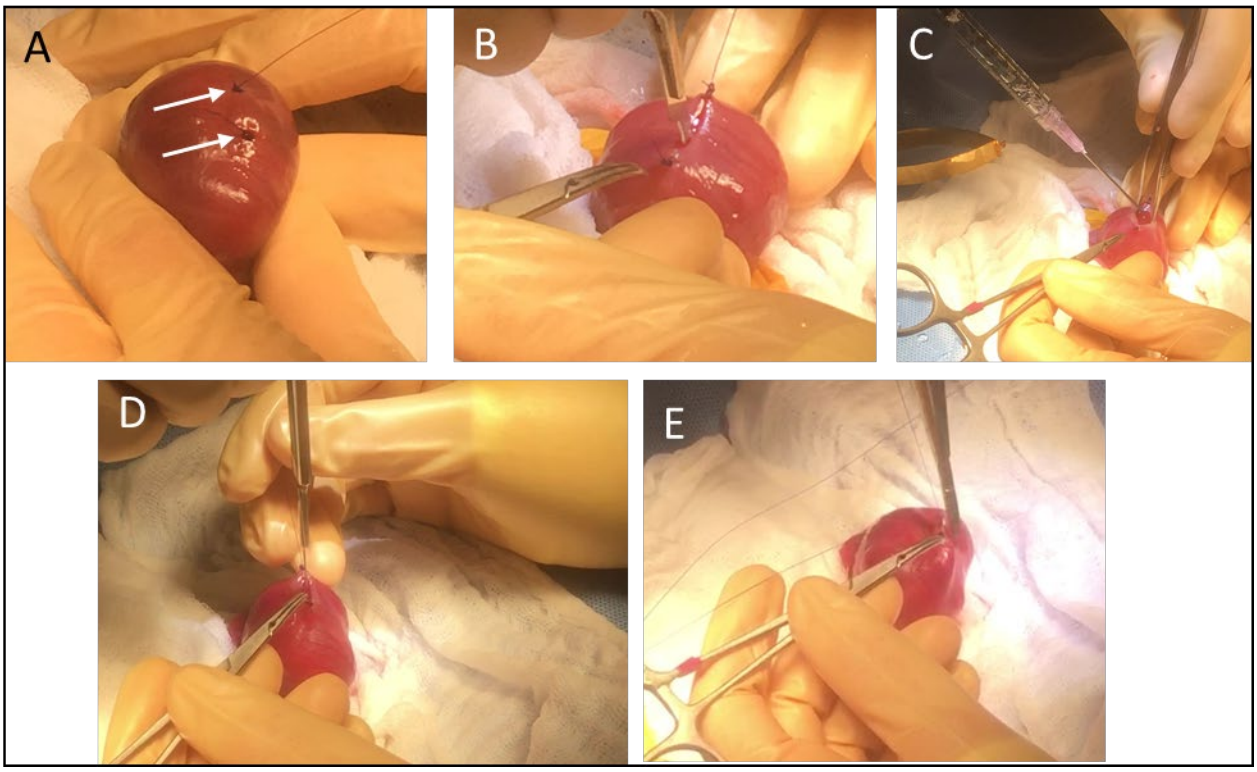

Fig. 4. Photos from survival membrane puncture surgery. A. Rabbit uterus partially exposed with 2 stay sutures (arrows). B. Cutting through uterus between stay sutures; care taken to avoid puncturing underlying fetal membrane. C. Presealing of fetal membrane through uterus opening. D. Puncture through adhesive and fetal membranes with 11-blade scalpel. E. Closure of uterus with running sutures.

In all surgical approaches, adhesives were identified *in situ* between the uterus and membranes at sacrifice. The less invasive presealing methods (n = 1 rabbit each for methods 1 and 2) exhibited excellent fetal survival with all fetuses surviving (6 preseal-puncture, 6 puncture only, and 10 no intervention). In each doe, LBR was very similar in presealed and puncture only fetuses (see **Table S3.2**). This lack of differentiation in fetal survival between control and experimental fetuses was unexpected, given literature reports of low survival rates in control fetuses in a similar rabbit post-sealing model [21]. We then pursued the more invasive presealing surgical approach, method 3 above. In early trials of this method, fetal lung to body weight ratios showed promising differentiation between presealed and puncture only fetuses. This method was then used to study the efficacy of presealing in a total of 13 rabbit litters.

3.3.3 Efficacy of fetal membrane presealing.

Thirteen rabbit does underwent fetal membrane presealing which included laparotomy, an approximately 1cm uterus cut, direct adhesive application to the fetal membranes, scalpel puncture, and uterine closure (surgical method 3). Does remained clinically normal throughout the study timeline. Two does miscarried the entire litter, with fetal material found in cages on post-surgical day 4 and day 5, respectively, and no fetal or placental remnants found in the uterus at sacrifice. Two does gave birth to live litters of 5 and 7 fetuses (one doe also had fetal remains found in her cage at post-surgical day 1) at gestational day 32. Neonates appeared morphologically normal. One rabbit was excluded from analysis because only 4 undersized fetuses were identified at the first surgery, all in the same uterine horn. The remaining 8 rabbits and fetuses were sacrificed and analyzed at post-surgery day 6 or 7. Fetal body and lung masses were weighed and mummified fetuses were noted. From a total of 66 fetuses (21 no intervention, 24 preseal and puncture, 21 puncture only), 8 were mummified (3 no intervention, 3 preseal and puncture, and 2 puncture only) and 58 were analyzed for LBR. Overall fetal survival to sacrifice was 88%, with no statistical difference between treatment groups ($p = 1$, Fisher's exact test). Average LBR for fetuses whose sacs had no intervention was 3.03%, LBR in fetuses in presealed and punctured sacs was 3.15%, and in puncture-only sacs, 2.88%. While the overall trends were promising and as hypothesized, i.e. presealing leads to increased LBR relative to puncture-only sacs, these two groups were not significantly different ($p=0.15$, one-way ANOVA).

In this study, we found that the mother had a significant impact of fetal LBR and body mass**.** One-way ANOVA comparing LBR of all fetuses in each litter was significant at $p <0.001$. The maternal influence on fetal LBR held even when fetuses in the preseal/puncture ($p<0.001$) and puncture only ($p<0.01$) groups were compared by litter; litter assignment did not appear to statistically impact fetuses that received no intervention. Similarly, intervention had no effect on fetal body mass. However, litter assignment did significantly impact body mass ($p < 0.001$). These differences are likely the result of differing maternal fitness and slight differences in gestational age. Qualitatively, these differences are also seen in fetal survival with some mothers carrying a large litter, and others miscarrying all fetuses. The impact of the mother on the ultimate litter fitness validates our experimental design to assign both control and experimental fetuses to each doe.

3.4 Conclusion

The robust fitness of control fetuses in this animal model made it challenging to demonstrate the benefit of fetal membrane presealing compared relative to the clinical standard of care in human patients (no membrane sealing). However, these results are an encouraging first steps towards the eventual translation of tissue presealing. We demonstrated that PEG-Cys/PEG-NHS gels can be injected *in situ* between delicate tissue layers into potential (tented) space and solidify in a surgically relevant timescale. The adhesive adheres well to wet uterine and fetal membrane tissue and did not appear to contribute to fetotoxicity or adverse maternal response. This confirms past findings that PEG-based adhesives are well-tolerated in fetal membrane sealing application in animals *in vivo* [21]. However, the high rate of survival in punctured but unsealed (control) rabbit fetuses contradicts some previous reports, but is concordant with others [21, 24]; this may be a result of our study design to include both experimental and control fetuses in the same litter. Future investigations of tissue presealing would benefit from an animal model with poor fetal viability of fetuses in punctured sacs, or could explore tissue presealing for a different clinical indication, such as bladder surgery or dural sealing. Whatever the application, the adhesive studied herein would be appropriate for trials of tissue presealing.

3.5 Materials and Methods

PEG-Cys synthesis

Synthesis scheme of cysteine-terminated PEG (PEG-Cys) was based on previous reports [30]. 4 g of 8 arm PEG-amine (20 kDa, JenKem Technology USA) was dissolved in excess toluene; toluene was evaporated off to azeotrope away excess water three times. Then, 20 mL dry DMF was added under inert conditions. In a separate vessel, HBTU (2 equivalents per NH_2 endgroup) and Boc-Cys(TRT)-OH (3.5 equivalents) were dissolved in 20 mL dry DMF. 2.5 mL DIPEA was added to each vessel and each was stirred for 5 minutes and then the contents of the two vessels were combined and reacted under argon overnight. Subsequently, 3x volume of DCM was added to the reaction mixture, stirred briefly, added to a separation funnel, and extracted against NaCl brine three times. The brine was then backwashed with fresh DCM. The DCM solution was dried with Na_2SO_4, filtered, and the reaction volume reduced to ~30 mL on a rotary evaporator and precipitated into ice cold diethyl ether. Precipitate and supernatant were chilled at -80 C for 10 minutes and then centrifuged at 4000 g for 5 minutes; mother liquor was decanted. Then, product was redissolved in methanol, mixed 1:1 with diethyl ether and chilled at -20 C overnight to precipitate PEG. Centrifugation and reprecipitation was repeated, after which the product was dried under nitrogen stream and then vacuum. Deprotection of Boc was accomplished by dissolving the dried product in minimal DMF before adding to a 50 mL solution of 95:2.5:2.5 TEA:TIPS:EDTA for 4 h. The solution was evaporated on a rotary evaporator and then precipitated in cold diethyl ether, frozen, centrifuged, and redissolved as above. A total of 4 precipitation steps were performed. Finally, the product was dried under a stream of nitrogen briefly and then on a high vacuum. The dry product was weighed, dissolved at 75 mg/ml in a 70:30 ethanol:water solution, aliquoted into cryovials, flash frozen in liquid nitrogen, lyophilized and stored under inert gas at -20 C until use. Amino acid coupling and deprotection was confirmed using NMR.

PEG-NHS preparation

PEG-n-hydroxysuccinimide (PEG-NHS, 8 arm, 20 kDa) was purchased from JenKem Technology USA. To remove impurities, PEG-NHS was dissolved in excess methanol, mixed 1:1 with diethyl ether, and precipitated at -20 C overnight. Three total cycles of precipitation and centrifugation (as above) were performed. Product was dried on a high vacuum, aliquoted, lyophilized, analyzed, and stored as above.

Gel formation

PEG-Cys and PEG-NHS gels were formed by first dissolving each polymer separately at 15 wt% in 1x PBS, and then mixing the two solutions 1:1 to form adhesive gels. As needed, buffer strength was adjusted with molecular biology grade water to achieve a gelation time of 50-70s. Gelation time was measured as time to clogging of a 200 µl pipette tip when mixing [30].

Cytocompatibility analysis

Per ISO 10993-05 standard for cytocompatibility, gels from each batch were cast into disk-shaped molds and were then incubated in cell culture media (DMEM, 10% fetal bovine serum, 1% penicillin/streptavidin) at 37 C for 24 h (30 mg gel per 200 µl media). This conditioned media was added to subconfluent cultures of NIH 3T3 or CCD32-sk cells and cultured for 24 h at 37 C, 5% CO_2. Then, viability was assessed with a 3-hour neutral red dye uptake assay and compared with

cells conditioned with 0.2% SLS (negative control) and normal media (positive control). Data from a representative batch is shown in Figure S1.

Surgery details and animal care

Rabbits were housed in an AAALAC accredited facility and allowed free access to feed and water. All procedures followed an Institutional Animal Care and Use Committee approved protocol. During procedures, the rabbits were anesthetized with a combination of buprenorphine, ketamine, xylazine, and isoflurane, with dosages and delivery rates as deemed appropriate by veterinary staff. The abdomen was shaved, aseptically prepared, and draped for surgery. An Ioban (3M) drape was applied to the skin

The abdomen was entered via an approximately 5-7 cm incision. The subcutaneous tissue was dissected through using a combination of blunt and sharp dissection. The linea alba was opened sharply with scissors and the uterus exposed. The uterus was fully exteriorized and inspected, total fetuses and position counted, and sides selected for intervention and control arms. The uterus was then replaced into the animal, and uterine horn at the point of the first fetus, typically the ovarian most fetus on the intervention arm, was exteriorized. Two 5-0 polydioxanone stay sutures were placed on the fundus of the uterus, approximately 1-1.5 cm apart, along the longitudinal axis running from fetus to fetus along the horn, minimizing transection of blood vessels. The uterine muscle was then carefully incised, with a 15-blade scalpel, and the fetal membranes exposed.

For surgical application, PEG-Cys and PEG-NHS polymer aliquots were each dissolved at 15 wt% in 0.5 ml sterile PBS. Then, solutions were combined in a sterile tube using a 1mL pipette and mixed up and down 3x. 1 mL of the solution was quickly drawn into a sterile 1mL luer lock syringe and rapidly injected *in situ* onto the relevant tissues. After approximately 60s (to allow for the adhesive to solidify), an 11-blade scalpel was used to puncture through both the glue and the uterine membranes. In the control arm, an identical procedure but without the application of glue was followed.

Following the completion of each puncture, the uterus was closed with running sutures (5-0 polydioxanone). After all fetal interventions were performed, typically 3 fetuses in the uterine horn selected for intervention and 3 fetuses in the uterine horn selected as a control, the abdomen was closed in layers using a running 3-0 polyglactin suture for the linea alba, a running 3-0 polyglactin suture for the subcutaneous tissue, and a subcuticular 5-0 polydioxanone suture for the skin. Post-surgery, rabbits were monitored until fully ambulatory, treated with postoperative analgesics and antibiotics as needed, and monitored daily for signs of pain or distress. At sacrifice, does were anesthetized using the same anesthetic protocol as for surgery, followed by intravenous veterinary euthanasia solution.

Fetal viability determination and lung analysis

At the first surgery, the uterus was closely examined, and fetuses on each uterine horn were enumerated and examined for viability. Fetuses that had begun to mummify or resorb or were noticeably smaller than siblings were excluded from further study. At the sacrifice surgery, after the does were euthanized, the laparotomy was reopened, and the uterus was removed and fetuses were again counted. Presealing sites were examined for abnormalities. Then, the uterus was carefully dissected, opposite the suture sites. Fetal sacs were examined and fetuses were removed and weighed. Lung tissue was carefully dissected and weighed.

Acknowledgements, ethics, conflicts, funding, and contributions.

The authors thank the UCSF LARC surgery and husbandry staff for their excellent contributions to the health and care of our animals.

Study was approved by the UCSF Institutional Animal Care and Use Committee.

P.B.M. holds a patent for the use of PEG-Cys/PEG-NHS gels in regenerative medicine.

This work was supported by the National Institutes of Health (1R01EB022031-01). S.M.W. acknowledges fellowship support from the National Science Foundation (GRFP DGE 1752814) and the Siebel Foundation. The funders had no role in data or manuscript preparation.

S.M.W. designed experiments with input from P.B.M., M.R.H., D.B., and V.K.A.. S.M.W., J.S., and S.G.D. prepared adhesives. V.K.A., D.B., P.K., and K.L. performed surgeries. S.M.W wrote manuscript with input from all authors.

3.6 Supplemental information

S3.1 List of abbreviations
LBR – Lung:body mass ratio
PEG – Poly(ethylene) glycol
DMF – Dimethyl formamide
DIPEA – N,N-Diisopropylethylamine
HBTU – Hexafluorophosphate benzotriazole tetramethyl uranium
Boc-Cys(trt)-OH – N-(tert-Butoxycarbonyl)-S-trityl-L-cysteine
DCM – Dichloromethane
TEA – Triethyl amine
TIPS – Triisopropyl silane
EDTA – Ethylenediaminetetraacetic acid

Table S3.2 – Lung-to-body mass ratios in early trials of minimally invasive presealing

Presealing method	**Preseal-puncture** Survival Avg. lung-to-body ratio	**Puncture only**	**No intervention**
Tented presealing, 14g needle puncture	3/3 2.65% ± 0.29%	3/3 2.79% ± 0.83%	7/7 2.71% ± 0.18%
Tented presealing, scalpel puncture	3/3 2.36% ± 0.05%	3/3 2.37% ± 0.19%	3/3 3.35% ± 0.54%

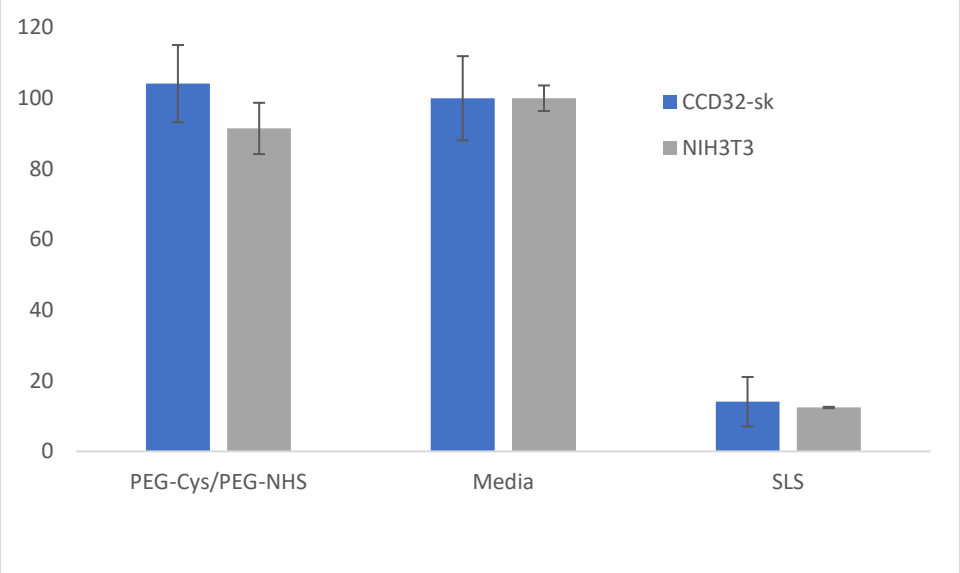

Supplemental Figure S3.3. Cytocompatibility of NIH 3T3 (grey) and CCD32-sk (blue) cells treated with media conditioned with PEG-Cys/PEG-NHS gels. Media-only and SLS-treated cells are controls (mean ± SD of triplicate samples).

References

[1] V. Beck, P. Lewi, L. Gucciardo, R. Devlieger, Preterm prelabor rupture of membranes and fetal survival after minimally invasive fetal surgery: a systematic review of the literature, Fetal Diagn Ther 31(1) (2012) 1-9.

[2] G. Bryant-Greenwood, L.K. Millar, Human fetal membranes: Their preterm premature rupture, Biology of Reproduction 63 (2000) 1575-79.

[3] C.E. Graves, M.R. Harrison, B.E. Padilla, Minimally Invasive Fetal Surgery, Clinics in Perinatology 44(4) (2017) 729.

[4] H. Kitagawa, K.C. Pringle, Fetal surgery: a critical review, Pediatr Surg Int 33(4) (2017) 421-433.

[5] E. Gratacos, J. Sanin-Blair, L. Lewi, N. Toran, G. Verbist, L. Cabero, A histological study of fetoscopic membrane defects to document membrane healing, Placenta 27 (2006) 452-6.

[6] S.J. Fortunato, R. Menon, K.F. Swan, T.W. Lyden, Organ culture of amniochorionic membrane in vitro, Am J Reprod Immunol 32(3) (1994) 184-7.

[7] R. Devlieger, E. Gratacos, J. Wu, L. Verbist, R. Pijnenborg, J.A. Deprest, An organ-culture for in vitro evaluation of fetal membrane healing capacity, Eur J Obstet Gynecol Reprod Biol 92(1) (2000) 145-50.

[8] R. Devlieger, L.K. Millar, G. Bryant-Greenwood, L. Lewi, J.A. Deprest, Fetal membrane healing after spontaneous and iatrogenic membrane rupture: A review of current evidence, American Journal of Obstetrics and Gynecology 195(6) (2006) 1512-1520.

[9] R.M. Moore, J.M. Mansour, R.W. Redline, B.M. Mercer, J.J. Moore, The physiology of fetal membrane rupture: insight gained from the determination of physical properties, Placenta 27(11-12) (2006) 1037-51.

[10] S.M. Winkler, M.R. Harrison, P.B. Messersmith, Biomaterials in fetal surgery, Biomaterials science 7(8) (2019) 3092-3109.

[11] G. Bilic, C. Brubaker, P.B. Messersmith, A.S. Mallik, T.M. Quinn, C. Haller, E. Done, L. Gucciardo, S.M. Zeisberger, R. Zimmermann, J. Deprest, A.H. Zisch, Injectable candidate sealants for fetal membrane repair: bonding and toxicity in vitro, American Journal of Obstetrics and Gynecology 202(1) (2010).

[12] S.A. Burke, M. Ritter-Jones, B.P. Lee, P.B. Messersmith, Thermal gelation and tissue adhesion of biomimetic hydrogels, Biomed Mater 2(4) (2007) 203-10.

[13] C.M. Haller, W. Buerzle, A. Kivelio, M. Perrini, C.E. Brubaker, R.J. Gubeli, A.S. Mallik, W. Weber, P.B. Messersmith, E. Mazza, N. Ochsenbein-Koelble, R. Zimmermann, M. Ehrbar, Mussel-mimetic tissue adhesive for fetal membrane repair: an ex vivo evaluation, Acta Biomater 8(12) (2012) 4365-70.

[14] Y. Shao, K. Taniguchi, K. Gurdziel, R.F. Townshend, X. Xue, K.M. Yong, J. Sang, J.R. Spence, D.L. Gumucio, J. Fu, Self-organized amniogenesis by human pluripotent stem cells in a biomimetic implantation-like niche, Nat Mater 16(4) (2017) 419-425.

[15] N. Ochsenbein-Kolble, J. Jani, L. Lewi, G. Verbist, L. Vercruysse, B. Portmann-Lanz, Enhancing sealing of fetal membrane defects using tissue engineered native amniotic scaffolds in the rabbit model, Am J Obstet Gynecol 196 (2007) 263-7.

[16] A. Zisch, R. Zimmermann, Bioengineering of foetal membrane repair, Swiss Med Wkly 138 (2008) 596-601.

[17] A.C. Engels, L. Joyeux, J. Van der Merwe, J. Jimenez, S. Prapanus, D.W. Barrett, C. Connon, T.T. Chowdhury, A.L. David, J. Deprest, Tissuepatch is biocompatible and seals iatrogenic membrane defects in a rabbit model, Prenat. Diagn. 38(2) (2018) 99-105.
[18] R. Devlieger, L. Gucciardo, E. Done, T. Van Mieghem, J. Deprest, Sealing fetal membrane defects with collagen following fetoscopic endoluminal tracheal occlusion (FETO) treatment for severe congenital diaphragmatic hernia (CDH), Reprod Sci 15(2) (2008) 102a-102a.
[19] F. Breathnach, S. Daly, E. Griffin, N. Gleeson, Intracervical application of synthetic hydrogel sealant for preterm prelabor rupture of membranes: a case report, Journal of Perinatal Medicine 33(5) (2005) 458-460.
[20] L.K. Mann, R. Papanna, K.J. Moise, Jr., R.H. Byrd, E.J. Popek, S. Kaur, S.C.G. Tseng, R.J. Stewart, Fetal membrane patch and biomimetic adhesive coacervates as a sealant for fetoscopic defects, Acta Biomaterialia 8(6) (2012) 2160-2165.
[21] A. Kivelio, P. Dekoninck, M. Perrini, C.E. Brubaker, P.B. Messersmith, E. Mazza, J. Deprest, R. Zimmermann, M. Ehrbar, N. Ochsenbein-Koelble, Mussel mimetic tissue adhesive for fetal membrane repair: initial in vivo investigation in rabbits, European Journal of Obstetrics & Gynecology and Reproductive Biology 171(2) (2013) 240-245.
[22] H.K. Carnaghan, M.R. Harrison, Presealing of the chorioamniotic membranes prior to fetoscopic surgery: Preliminary study with unfertilised chicken egg models, European Journal of Obstetrics & Gynecology and Reproductive Biology 144 (2009) S142-S145.
[23] R. Papanna, L.K. Mann, S.C.G. Tseng, R.J. Stewart, S.S. Kaur, M.M. Swindle, T.R. Kyriakides, N. Tatevian, K.J. Moise, Cryopreserved human amniotic membrane and a bioinspired underwater adhesive to seal and promote healing of iatrogenic fetal membrane defect sites, Placenta 36(8) (2015) 888-894.
[24] N. Ochsenbein-Kolble, J. Jani, L. Lewi, G. Verbist, L. Vercruysse, B. Portmann-Lanz, M. Marquardt, R. Zimmermann, J. Deprest, Enhancing sealing of fetal membrane defects using tissue engineered native amniotic-scaffolds in the rabbit model, American Journal of Obstetrics and Gynecology 196(3) (2007) 263-265.
[25] V. Pensabene, P.P. Patel, P. Williams, T.L. Cooper, K.C. Kirkbride, T.D. Giorgio, N.B. Tulipan, Repairing Fetal Membranes with a Self-adhesive Ultrathin Polymeric Film: Evaluation in Mid-gestational Rabbit Model, Ann Biomed Eng 43(8) (2015) 1978-1988.
[26] A.C. Engels, P.D. Brady, M. Kammoun, J.F. Ferreiro, P. DeKoninck, M. Endo, J. Toelen, J.R. Vermeesch, J. Deprest, Pulmonary transcriptome analysis in the surgically induced rabbit model of diaphragmatic hernia treated with fetal tracheal occlusion, Dis Model Mech 9(2) (2016) 221-228.
[27] T. Najrana, L.M. Ramos, R. Abu Eid, J. Sanchez-Esteban, Oligohydramnios compromises lung cells size and interferes with epithelial-endothelial development, Pediatr Pulm 52(6) (2017) 746-756.
[28] C.M. Haller, W. Buerzle, A. Kivelio, M. Perrini, C.E. Brubaker, R.J. Gubeli, A.S. Mallik, W. Weber, P.B. Messersmith, E. Mazza, N. Ochsenbein-Koelble, R. Zimmermann, M. Ehrbar, Mussel-mimetic tissue adhesive for fetal membrane repair: An ex vivo evaluation, Acta Biomaterialia 8(12) (2012) 4365-4370.
[29] A.E. Crowley, R.M. Grivell, J.M. Dodd, Sealing procedures for preterm prelabour rupture of membranes, Cochrane Db Syst Rev (7) (2016).
[30] I. Strehin, D. Gourevitch, Y. Zhang, E. Heber-Katz, P.B. Messersmith, Hydrogels formed by oxo-ester mediated native chemical ligation, Biomaterials science 1(6) (2013) 603-613.

[31] Y. Zhang, I. Strehin, K. Bedelbaeva, D. Gourevitch, L. Clark, J. Leferovich, P.B. Messersmith, E. Heber-Katz, Drug-induced regeneration in adult mice, Sci Transl Med 7(290) (2015).

CHAPTER FOUR – SYNTHESIS AND CHARACTERIZATION OF MUSSEL-INSPIRED ADHESIVE HYDROGELS AND PATCHES FOR FETAL MEMBRANE PRESEALING

4.1 Summary

An enduring challenge in developing surgical adhesives, and especially fetal membrane sealants, is the formation of a robust adhesive interface in a wet environment. To address this, we turn to marine organisms for inspiration, particularly mussels. Mussels secrete adhesive protein plaques to anchor themselves to organic and inorganic underwater surfaces. These adhesive proteins are rich in the amino acid 3,4-dihydroxyphenalanine (DOPA); DOPA's side chain catechol is notoriously reactive and has long been thought to be the main mediator of mussels' extraordinary adhesion. A comprehensive review on previous mussel-inspired adhesive materials from our lab and others can be found in Chapter 2 [1].

We sought to incorporate DOPA into the PEG-Cys/PEG-NHS gels used in Chapter 3 to further improve their wet adhesion. These adhesive hydrogels were synthesized and purified, measured in lap shear adhesive tests with wet bovine pericardium tissue, analyzed for *in vitro* cytocompatibility, and evaluated in the rabbit model of fetal membrane presealing introduced in Chapter 3. These adhesives adhered robustly to wet tissue and were cytocompatible with human fibroblasts *in vitro*. In the rabbit studies, these mussel-inspired adhesives appeared fetotoxic, which is likely attributed to longer-term *in vivo* catechol oxidation.

We also developed a multi-lamellar adhesive patch in which a commercial elastomer is coupled to a tissue-adhesive methacrylate surface through a polyphenol coating. With extensive work adjusting the monomer composition of the adhesive surface, we achieve a tissue-adhesive patch with an adhesive strength of 20 kPa. Ultimately, the adhesive strength of this patch was limited by the strength of its weakest layer, the polyphenol coating. Building upon the findings in the development of this patch, we developed a supramolecularly crosslinked mussel-inspired tissue adhesive patch, which is detailed in Chapter 5.

4.2 Bioinspired hydrogel adhesives

Polymer design

Previous work with native chemical ligation hydrogels indicated that they have several properties that make them promising candidates for fetal membrane presealing [2, 3]. These hydrogels are formed upon mixing of cysteine-terminated and N-hydroxysuccinimide-terminated multi-arm PEGs. They have tunable gelation times of around 1 minute and are cytocompatible, well-tolerated *in vivo*, injectable, and relatively straightforward to synthesize. The synthesis of the cysteine-terminated PEG (detailed in Chapter 3) can be easily adapted to incorporate additional amino functionality. Specifically, we sought to incorporate amino acids commonly found in the adhesive plaques of marine mussels. In these proteins, there is a high percentage of DOPA and of lysine, which has been shown to act synergistically with DOPA to further improve adhesion [4]. Thus, we sought to synthesize cysteine-terminated PEGs with short amino acid sequences that can combine with PEG-NHS via native chemical ligation crosslinking to form adhesive hydrogels.

Hydrogel synthesis and formation

Initially, we pursued solid-phase peptide synthesis to synthesize these cysteine-terminated mussel-inspired sequences before coupling them to multi-arm PEG backbones. However, there were a few issues with this approach that we ultimately could not overcome. First, we sought to

use the Liberty Blue peptide synthesizer, but quickly realized that excess of protected amino acids required to ensure coupling on this instrument was prohibitive given the cost of Fmoc-DOPA(acetonide)-OH ($500/g at the time; later available from ChemPep for $1000/5g). Then, we used a small reactor and did the couplings to the 2-chlorotrityl chloride resin by hand; both synthesizer and small-batch couplings were performed following the protocols outlined in Coin, et al. [5]. While this was time consuming, MALDI-TOF mass spectrometry confirmed the successful couplings, which was encouraging. However, we were not able to optimize the deprotection protocol due to the fact that we needed to cleave the peptide from the resin in acid while leaving the peptide protecting groups (particularly acetonide, which is highly acid labile) intact for subsequent coupling to PEG. Despite trying cleavage protocols with various reaction times (as little as 2 minutes) and concentrations of hexafluoroisopropanol, we were not able to identify a method that led to appreciable yield of protected peptide.

In an alternative approach, we tried directly coupling amino acids one at a time to multi-arm PEG amine. This is the approach that was used by former lab member Iossif Strehin to synthesize PEG-Cys [3]. However, this published synthesis had a yield of just 50% and a coupling efficiency of 86% as measured by NMR. If we were to do multiple coupling steps (eg., to synthesize PEG-DOPA-Lys-Cys), yield would be insufficient, and few PEG arms would have the expected amino acid sequences.

To improve upon the published synthesis, we made several changes to both the synthesis and workup steps. Key insights were the importance of a water-free coupling reaction, reducing loss in the many workup steps, and incorporating acetic acid into the final precipitation steps to prevent Cys and/or catechol oxidation and increase the polymers' shelf life in the freezer. The modified synthesis and workup protocol is in the methods section, below, and though it varied from batch to batch, total yield after three coupling steps (i.e. PEG-DOPA-Lys-Cys) was around 60-75% and conversion of around 90-95% for each coupling step.

To form native chemical ligation hydrogels from the synthesized cysteine-terminated PEGs and PEG-NHS, polymers were dissolved at 15 wt% in tissue culture grade PBS as described in Chapter 3 and mixed 1:1 to form gels. As needed, buffer strength was adjusted with molecular biology grade water to achieve the desired gelation time, which was measured by mixing with a 200 µl pipette tip until it clogged.

Lap shear adhesion measurements

In selecting adhesive candidates for fetal membrane presealing, adhesion strength to wet tissue is a critical metric. Previous reports of native chemical ligation and catechol/sodium periodate crosslinked multi-arm PEG hydrogels reported lap shear adhesion strengths of 46 kPa and 35 kPa, respectively [3, 6]. However, despite the existence of a standard for lap shear testing of surgical adhesives (ASTM 2255), it is quite difficult to compare adhesive strength measurements across different publications, labs, or researchers. In our experience, the following experimental conditions can influence the final, measured shear strength in these experiments: tissue type, tissue surface, strut material, strut geometry, cyanoacrylate choice, clamping device, incubation time, incubation temperature, shear rate, and tissue wetness. The detailed method that we developed for measuring the lap shear adhesive strength of hydrogel tissue adhesives is in the methods section, below.

We measured the lap shear adhesive strength of PEG-Cys, PEG-DOPA-Cys, and PEG-DOPA-Lys-Cys. When lap joints were incubated under light pressure (100g weight/strut), measured adhesive strength was less than when incubated under higher pressure (clamped with

mini binder clip – also permitted by the ASTM standard) (**Figure 1**). Looking at failed lap joints, we found that all formulations failed cohesively, indicating that future work to improve the cohesive strength of the materials would likely lead to increases in overall adhesive strength. Adhesive strengths are shown in **Figure 2**. We found that catechol-containing gels are more adhesive than non-DOPA gels, but not significantly so. More importantly, we found a large difference in adhesive strength depending on which standard incubation method was used. This underscores the need for side-by-side comparisons of different adhesive formulations, rather than relying on literature reports, as well as tissue-specific measurements and/or *in situ* tests. While lap shear adhesive strength measurements are useful for comparing different adhesive formulations, especially when measurements are performed using the exact same method, they provide little information about whether a given glue is adhesive enough for a specific clinical application.

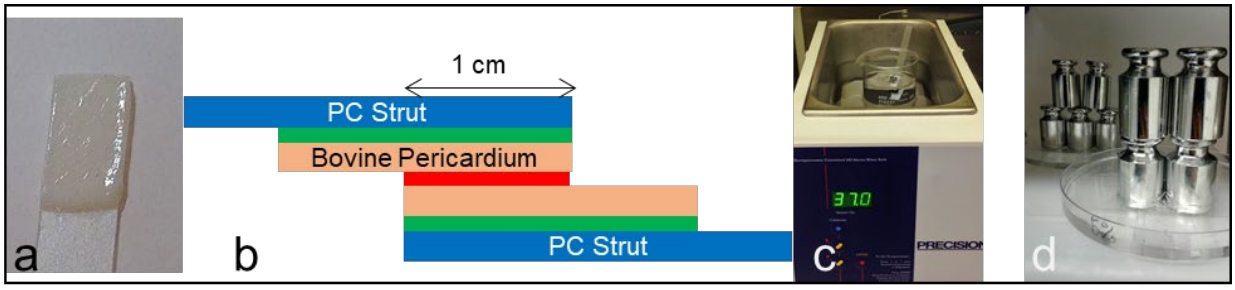

Figure 1. Preparation of lap joints for wet tissue adhesion. A. A tissue-polycarbonate strut. B. Schematic of a lap joint formed with two polycarbonate (PC, blue) struts with bovine pericardium adhered with cyanoacrylate (green). The lap joints are joined with the experimental adhesive (red). Lap joints were incubated at 37C in PBS for 1h while clamped with a binder clip (C) or under weights (D). This figure is adapted from Balkenende, Winkler, et al., "Supramolecular crosslinks in mussel-inspired tissue adhesives" (Chapter 5).

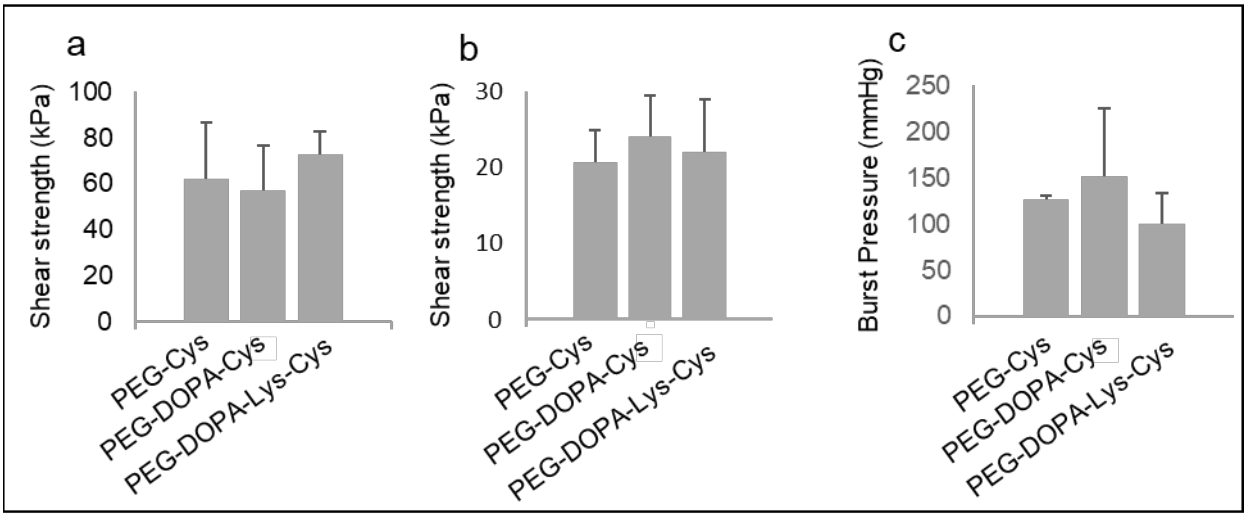

Figure 2. Lap shear and burst strength of mussel-inspired PEG adhesives. Lap shear adhesive strength to wet bovine pericardium tissue of PEG-Cys, PEG-DOPA-Cys, and PEG-DOPA-Lys-Cys hydrogels formed with upon PEG-NHS. During the 1h incubation in 37C PBS, lap joints were

held together with binder clips (A) or weights (B). The burst strength of these adhesives was studied in a custom burst chamber with bovine pericardium (C).

Burst device testing

Lap shear adhesion is a useful metric for comparing the relative strengths of different adhesives, but it does not provide much context for whether or not a given adhesive will have appropriate mechanical or adhesive properties for a given *in vivo* application. In the context of fetal membrane sealing, for example, maintaining a watertight seal is critical. To understand how our adhesives might perform in vivo, we used a custom-designed burst device similar to that in ASTM Standard F2392. A surrogate tissue is punctured, sealed, and stretched over a chamber and secured with gaskets. Then, as the chamber is slowly inflated with saline, the pressure at which the system leaks at the defect site is recorded (**Figure 3**). Intrauterine pressure during pregnancy is around 10 mmHg [7], with the maximum pre-labor pressure being around 30 mmHg during Braxton-Hicks contractions [7]. Thus, 30 mmHg was chosen as a benchmark for performance of our adhesives.

We sought to use human fetal membranes in our burst device; however, this was challenging because, upon inflation of the burst chamber, fluid would leak out through the tissue, making measurement challenging. Membranes began to burst or leak at around 10 mmHg. Using bovine pericardium tissues, we were able to collect higher-quality data, but many trials had to be eliminated because they leaked through the tissue-gasket interface or elsewhere on the device, rather than at the tissue-adhesive interface. While the results had high variability, we see that all three of the sealants evaluated (PEG-Cys, PEG-DOPA-Cys, and PEG-DOPA-Lys-Cys) burst at pressures far higher than the 30 mmHg benchmark, indicating that they likely have adhesive and cohesive strengths sufficient wet tissue sealing (**Figure 2c**).

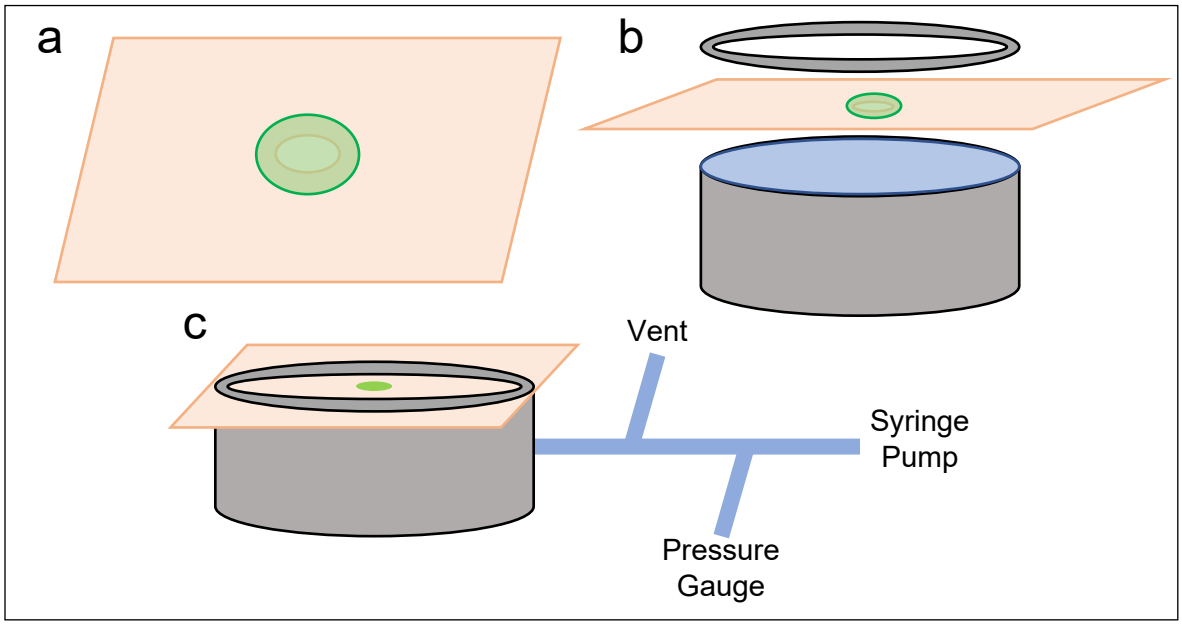

Figure 1. Schematic of burst device chamber. **a**, Bovine pericardium (orange) is punctured with a 3mm biopsy punch and sealed with the adhesive (green). **b**, Loading of the tissue-patch into the fluid-filled burst device chamber. **c**, Diagram showing burst chamber inflation and measurement setup. This figure is adapted from Balkenende, Winkler, et al., "Supramolecular crosslinks in mussel-inspired adhesives." (See Chapter 5)

Cytocompatibility testing

Prior to evaluating a material in an animal model, it is crucial to confirm that the materials are cytocompatible *in vitro*. In developing these materials, each batch was tested in a conditioned media assay with both NIH3T3 and CCD32-sk fibroblasts per ISO 10993-05. Viability was quantified using neutral red dye uptake analyses. All batches met the standard's benchmark of 70% viability relative to untreated cells.

We also sought to study the effect of these sealants on cells isolated from human amnions. These cells were a more precious resource, so not every batch was tested, but we also saw no cytotoxic effect of our materials on these cells. More details about amnion cell cytocompatibility and culture of these cells can be found in Chapter 5.

Rabbit studies

The mussel-inspired native chemical ligation hydrogel PEG-DOPA-Lys-Cys was also studied in the *in vivo* rabbit model discussed in detail in Chapter 3. The formulation was tested on two rabbit does, with the presealant applied minimally invasively between the uterus and membranes with a 23g needle, and a ~5mm uterus and membrane defect created with a scalpel blade. Both mothers remained morphologically normal, but it appeared that the sealant caused significant fetotoxicity, which is why the majority of does in the rabbit study were treated with the PEG-Cys control formulation.

In the first doe, 0 of 3 punctured fetuses survived, and 0 of 3 presealed-and-punctured fetuses survived; 2 of 2 fetuses who received no intervention survived. In the second doe, again 2 of 2 no-intervention fetuses survived, along with 3 of 3 puncture-only and 1 of 5 preseal-and-

puncture fetuses. Additionally, at the sacrifice surgery, the uterus appeared shrunken and dark (**Figure 4a**), and when excised, the adhesive, which was clear upon injection, was dark brown, an indicator that the catechol had undergone significant oxidation (**Figure 4b**).

To confirm that these materials were cytotoxic over longer timescales than the 24h used in prior neutral red studies, above, we conducted a longer-term cytocompatibility study, in which media was conditioned with adhesive gels for >24 h before being applied to cells. As shown in **Figure 5**, viability decreases significantly over time, likely due to material oxidation. While these results were initially surprising, over the last few years, a growing body of evidence has emerged that unoxidized catechols contribute to cell toxicity *in vitro*; this has been attributed, at least in part, to generation of H_2O_2 [8].

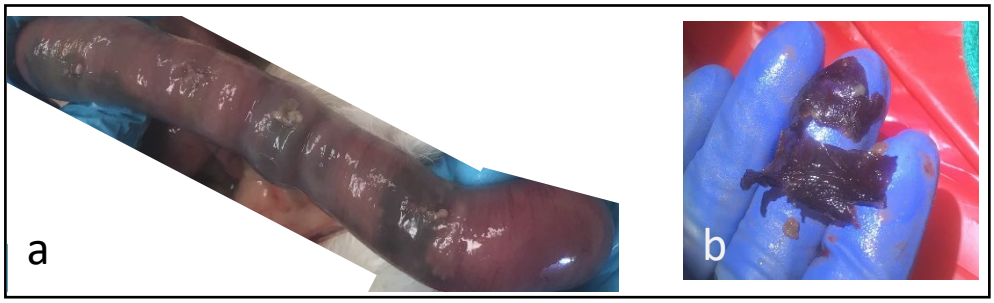

Figure 4. Explanted tissue and adhesive. A.) Uterus of rabbit treated with PEG-DOPA-Lys-Cys. Note the narrow uterus indicates the fetuses have started to resorb, as does the dark color. B.) Explanted PEG-DOPA-Lys-Cys adhesive appears dark, likely due to oxidized catechols.

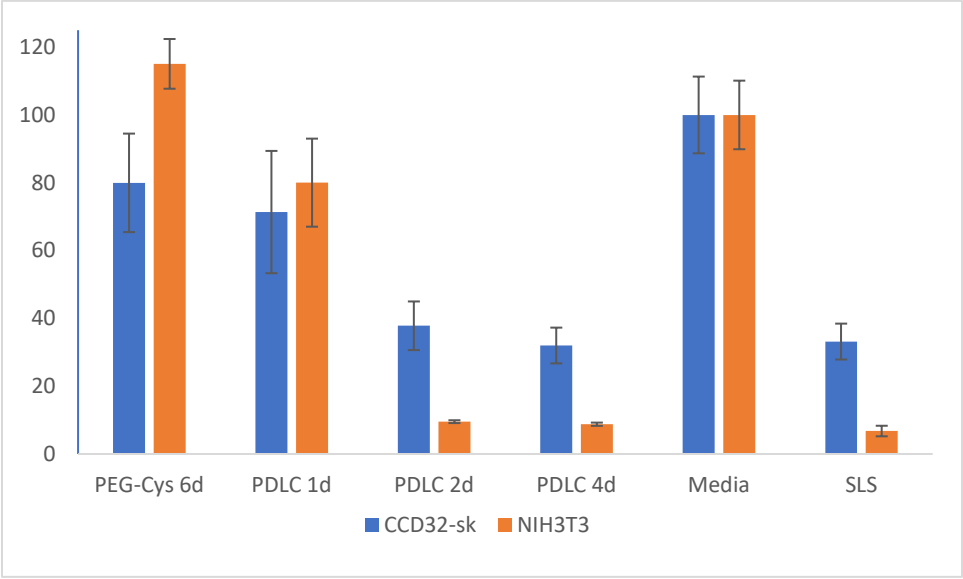

Figure 5. Longer term cytocompatibility of PEG-DOPA-Lys-Cys/PEG-NHS (PDLC) and PEG-Cys/PEG-NHS (PEG-Cys) gels compared with media only and sodium lauryl sulfate (SLS) controls. (d = days). Note that PEG-Cys was cytocompatible for 6 days while PDLC showed significant cytotoxicity after just 2 days.

Conclusions

The mussel-inspired PEG adhesives developed here have some distinct advantages over many existing mussel-inspired adhesive systems; namely, their gelation kinetics are appropriate for surgical applications, they avoid the use of harsh oxidants or other stimuli (pH, UV) for gelation, and they adhere robustly to wet tissue. However, the fact that these materials proved fetotoxic in a rabbit model of fetal membrane presealing and that the control (DOPA-free) native chemical ligation PEG hydrogel was about as adhesive as these mussel-inspired formulations are strong arguments for pursuing different avenues in future investigations. While this type of mussel-inspired adhesive may not be suitable for clinical translation at this time, there are still many underwater adhesive strategies yet to be explored that may one day yield even more powerful surgical tissue glues.

4.3 Bioinspired, multilamellar adhesive patches

While injectable liquid adhesives have great clinical potential, including in fetal surgery, adhesive patches have some distinct advantages. For example, an adhesive patch could confer a greater deal of mechanical support to and/or be tuned to match the mechanical properties of the underlying tissue. In an effort to create a novel, mussel-inspired tissue-adhesive patch, we took two approaches: a supramolecularly crosslinked polymethacrylate patch and a multi-layer elastomeric patch that used polyphenol coatings to couple a UV-cured free-radical polymer adhesive layer to an underlying elastomer.

In one approach, postdoctoral scholar Dr. Diederik Balkenende synthesized a novel polymethacrylate adhesive patch from a monomer mixture containing catechols for tissue adhesion (dopamine methacrylamide) and supramolecular ureido-4-pyrimidinone (UPy) crosslinkers (UPy methacrylate). The polymers also contained hydrophobic (2-ethylhexyl-methacrylate) and hydrophilic (oligoethylene glycol methacrylate) monomers that enabled phase separation, allowing supramolecular crosslinking to occur in a hydrophobic environment and tissue adhesion in a hydrophilic environment. This approach was ultimately successful; we developed a patch with robust adhesion to wet tissue, strong tissue sealing ability, and dose-dependent cytocompatibility with fibroblasts *in vitro*. The full development and characterization of this material is highlighted in Chapter 5.

While the supramolecular patch ultimately worked quite well, we were also interested in developing adhesive patches with tunable mechanical properties and facile syntheses. We hoped to develop an adhesive coating that could be attached to any elastomeric surface; the mechanical properties of the patch would be dictated primarily by the elastomer, which could be adapted to adhere to diverse tissue types. To avoid some of the polymer synthesis and processing hurdles faced in the development of the supramolecular patch, we used free radical polymerization under UV to cure the monomers onto the elastomer surface. To robustly couple the adhesive to the elastomer, we first coated the elastomer with dopamine methacrylamide (DMA); we hypothesized that the catechols could sufficiently coat the patch surface, leaving pendant methacrylamide groups available for polymerization. Then, when a mixture of DMA and other monomers were UV-cured onto the surface of the DMA-coated patch, some surface-bound DMA would be incorporated, anchoring the polymer chains to the elastomer surface. A schematic of the synthesis is shown in **Figure 6**.

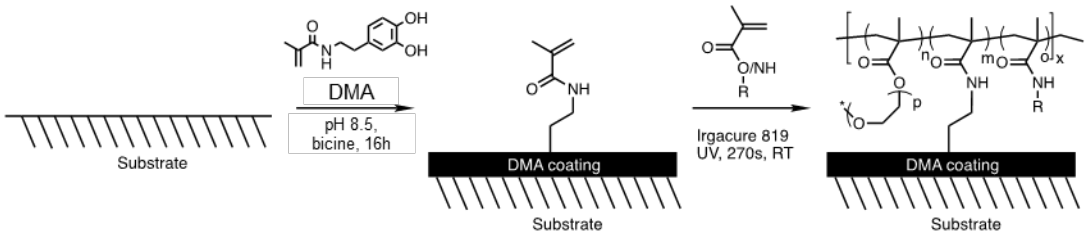

Figure 6. Multilamellar adhesive patch synthesis protocol. This figure is courtesy of Cody Higginson and Dirk Balkenende. R can be DMA or acDMA.

Ultimately, the patches had appreciable adhesion to wet tissue, but did not approach the adhesiveness of the supramolecular patches (Chapter 5) or the mussel-inspired adhesive hydrogels (Section 4.2). Some of our multi-lamellar formulations had measured lap shear adhesive strengths in the 10s of kPa range, but this was only when the tissue-patch lap joints were incubated with a clamp; adhesive strengths were lower when incubated under a 200 g weight. The mini binder clip used for clamping exerted far more force than would be clinically relevant (and is recommended by the ASTM standard; more on these measurement methods can be found in **Chapter 5**). This relatively low adhesion is likely because, in designing a multi-lamellar patch (elastomer, DMA coating, adhesive surface), the strength of the weakest interface will dictate the strength of the bulk material. We know that while catechols and other polyphenols are able to coat numerous organic and inorganic surfaces [9, 10], their mechanical strength is quite poor [11, 12]; they can often be scratched off with a fingernail. Recent work from our lab has demonstrated that there are ways to improve the mechanical properties of polyphenol coatings, including thermal annealing and the incorporation of metal ions [11], but significant strides are needed before these new findings could be incorporated into a tissue-adhesive application.

Here, we outline the general processing and synthesis schemes used to form the DMA coatings, adhere the adhesive layer, test the adhesives, and optimize our formulations. Of the many formulations, monomer mixtures, and monomer ratios we attempted, it was sometimes difficult to get reliable data, but the data presented here does represent the strongest findings from this work. This work was started in collaboration with Diederik Balkenende and our team of four masters' students, and continued with my undergraduate students Sarah Spivak and Sasha Demeulenaere.

Elastomer selection

For simplicity, we wanted to use commercially available elastomers, and at first, we tried both polyurethane (Smooth-On Rheoflex 60) and silicone commercial kits, in which two components are mixed, poured into films, and cured. While these materials could be coated with DMA (see below), subsequent XPS analysis revealed that the polyurethane material contained a significant amount of heavy metals (likely as a catalyst), so we instead used a pre-formed 1 inch wide PDMS tape (X-Treme Tape TPE-XZLCLR Silicone Rubber Self Fusing Tape) for the patches described here.

DMA coating

Elastomers were coated overnight in a solution of 2 mg/mL DMA in pH 8.5 bicine buffer in a petri dish. Some samples floated to the top of the dish, so the bottom side (no coating) was marked and taped to the bottom of the petri dish with double-sided tape so that the top side could be coated. The coatings were nearly colorless, and their presence was confirmed by incubating samples overnight in a silver nitrate solution, which forms a layer of nanoparticles on the coatings' surface that can be easily identified (**Figure 7**).

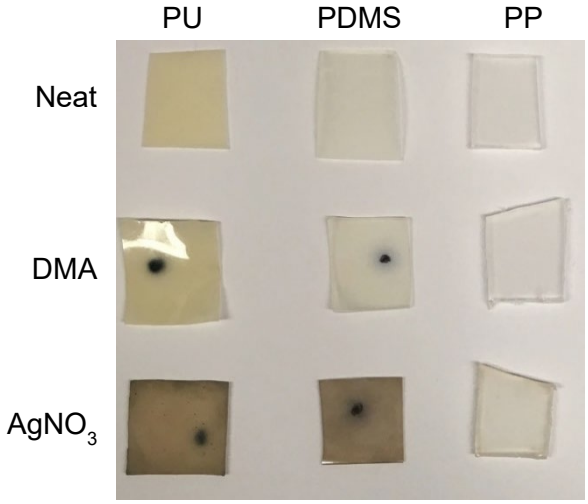

Figure 7. Neat, DMA-coated, and AgNO3-stained samples of polyurethane (PU), polydimethylsiloxane (PDMS), and polypropylene (PP) are shown. Note that the black dot seen on some samples is a fiduciary mark used to indicate the back (uncoated) side of the film.

Adhesive monomer mixture

On top of the DMA-coated elastomer, we wanted to affix a tissue-adhesive layer. To form this layer, a methacrylate monomer mixture with a radical initiator was applied to the surface of the coated patch, covered with a coverslip to fully wet the surface, and reacted under UV to form adhesive polymers, ideally incorporating DMA that had already been attached to the elastomer surface into the polymer chains. The monomer mixture contained DMA and PEG (500Da) methyl ether methacrylate (PEGma). We also made some patches with acetonide-protected DMA (acDMA), hypothesizing that by using protected DMA in the UV polymerization step, more catechol reactivity would be retained for tissue adhesion, and catechol quenching of the polymerization would be reduced. These patches were deprotected in 1M HCl prior to adhesive characterization This improved lap shear adhesion from 3.9 ± 1.7 kPa (DMA) to 12.0 ± 7.6 kPa (acDMA) (**Table 1**). Note that PEGma-only samples had adhesion of 4.5 ± 3.5 kPa, indicating that DMA alone is not sufficient for tissue adhesion in this application.

Adhesive layer			Adhesion (kPa)	SD (kPa)	n
DMA %		PEGma%			
none		100	4.5	3.5	10
DMA	20	80	3.9	1.7	8
acDMA	20	80	12.0	7.6	10
acDMA *$NaIO_4$	20	80	20.0	7.5	7

Table 1. Lap shear adhesive strength of PDMS-bound adhesive patch formulations. *$NaIO_4$ indicates that deprotected patches were brushed with $NaIO_4$ before adhering to tissue.

Finally, we studied the effect of pre-oxidizing the patch's surface to prime catechols for tissue adhesion. Deprotected acDMA-containing patches were briefly brushed with $NaIO_4$ before being formed into tissue-patch lap joints. This improved adhesion to 20.0 ± 7.6 kPa, indicating that oxidized catechols improve tissue adhesion. Similar experiments on the supramolecular patches in Chapter 5 found the same result ($NaIO_4$ treatment improves adhesion); this may be a promising avenue for future exploration, as relying on autooxidation to activate catechols may not be sufficient for robust adhesion in all applications.

Conclusions and outlook

Polyphenol coatings are a powerful tool to confer robust chemical functionality to inert surfaces. However, in this study, we see that the multi-lamellar structure of our adhesive patches was only as strong as its weakest interface, likely, the DMA-elastomer interface. Future work developing these adhesives could focus on their use as a UV-curable adhesive for non-biological applications, or could benefit from the findings of the supramolecular adhesive polymethacrylate polymers synthesized and discussed in Chapter 5. UV polymerization of these (or similar) monomer mixtures directly onto textured or functionalized surfaces, without the intermediate polyphenol layer, could result in the truly robust adhesive coating we sought in this work.

4.4 Methods

Mussel-inspired adhesive hydrogels

Synthesis of amino acid-terminated multi-arm PEGs

The general synthesis scheme for adding an amino acid to amine-terminated PEG was based on previous reports [3], and is detailed in Chapter 3, including the additional modifications to improve yield and coupling efficiency. DOPA (from Fmoc-DOPA(acetonide)-OH) or lysine (from Fmoc-Lys(Boc)-OH) was coupled to PEG-amine (or PEG-[amino acid]-amine) using the protocol from Chapter 3. Fmoc deprotection was accomplished by dissolving the dry polymer a 20% piperidine solution in DMF and stirring at room temperature for 4h; workup following the deprotection was the same as after the coupling, with only 2-3 precipitation steps. After coupling the last amino acid (usually Boc-Cys(trt)-OH), deprotection of all protection groups was performed in TFA with EDTA and TIPS and the polymer was dried and prepared for use as described in Chapter 3. Following the final deprotection, ~1% acetic acid was added to precipitation solutions (MeOH, diethyl ether) to prevent oxidation of Cys and catechol groups. In some batches, 1-4 additional wash steps with cold diethyl ether were necessary to remove trace acetic acid (identified

on NMR). If trace acetic acid is present following lyophilization, gelation times will be significantly slowed.

Lap shear adhesive strength of hydrogel adhesives

Bovine pericardium was chosen as a surrogate tissue because it is readily available, not fatty, and relatively thin and collagenous. It was shipped fresh on wet ice from Animal Technologies (Tyler, TX). Upon arrival, tissue was individually flash frozen in liquid nitrogen and stored at -80C. Prior to use, tissue was thawed in room temperature PBS. Polycarbonate sheets (PC, one side textured, one side smooth, from McMaster Carr) were cut into 1 cm-wide struts, about 10 cm long. The rough (non-cardiac-facing) side of the pericardium tissue was blotted dry and adhered to one end of the PC strut (rough PC surface) with cyanoacrylate adhesive (Loctite Super Glue, liquid all purpose [N.B.: Loctite gel does not work]). We found that metal struts do not work well as there is a high rate of sample failure upon loading into the tensile tester, and they are hard to clean; the PC struts are single-use. Excess tissue was trimmed to the same size as the strut (**Figure 1a**) Tissue struts were stored in PBS until use (< 1 h).

To form lap joints (**Figure 1b**), two tissue struts were wicked dry to remove excess surface water (place the corner of a Kimwipe on the edge of the tissue and wick away water without blotting tissue surface). Then, 20 μL of each PEG component (Cys-terminated PEG and PEG-NHS, 15 wt % each) were mixed 1:1 and applied to the tissue; a lap joint was quickly formed, with an overlap area of 1 cm^2. Lap joints were weighted using either brass weights totaling 100 g/cm^2 or clamped with a mini binder clip (Office Depot [N.B.: the "small" size is too strong; use mini]). Clamped/weighted joints were submerged in PBS and incubated at 37C for 1h (**Figure 1c, d**). Joints were removed from the bath, and excess gel was carefully trimmed from the sides. Overlap area was measured with a caliper. Using an Instron 3345 tensile tester (50N load cell), joints were loaded at 5mm/min (50%/min) until failure; lap shear strength was recorded as maximum force/overlap area. After failure, joints were observed to determine failure mode. All were found to have failed cohesively (adhesive residue on both joints, indicating a rupture of cohesive, rather than adhesive bonds). In some samples, this was also confirmed via Arnow's stain (see Chapter 5 for more details about this method).

Burst device measurements

Bovine pericardium tissues were prepared and thawed as described above. Human fetal membrane tissues were acquired and prepared as discussed in Chapter 6. A 3mm defect was cut into the tissue with a biopsy punch. A cylindrical mold was created from a rubber septum, lined with petroleum jelly to prevent it from sticking to the adhesives, and placed on the tissue around the defect. Adhesive components were mixed 1:1 at 15 wt% in PBS, cast into the mold, and allowed to set for 1-3 minutes. The mold was removed and the tissue/adhesive was loaded into the filled burst device, while minimizing bubbles. The chamber was inflated at 10 ml/min and the pressure was recorded with a pressure gauge throughout. A diagram of this setup is in **Figure 3**. Maximum pressure at burst or leak was recorded. Samples which first leaked or ruptured through the tissue/gasket interface or at sites distal to the adhesive/tissue interface were not included in the final calculations. All studies on human fetal membranes were conducted in sterile cell culture hoods, with the sash down during inflation, and with appropriate PPE.

Neutral red cytocompatibility analysis

Gels were formed using sterile buffers and cast into small molds made from the lids of Eppendorf tubes. Then, these gels were added to growth media and incubated at 37 C for 24h (30 mg gel/200 µl media). Meanwhile, cells were grown to subconfluence; NIH 3T3 and CCD32-sk cells were cultured in DMEM supplemented with 10% fetal bovine serum and 1% penicillin/streptavidin at 37 C in 5% CO_2. After 24h, conditioned media was added to cells and cultured for an additional 24h. Then, cells were analyzed with a neutral red dye uptake cell viability assay, and viability of cells treated with conditioned media was compared with cells cultured in untreated media and cells cultured with sodium lauryl sulfate (SLS, negative control). To quantify viability, conditioned media was removed and cells were rinsed with warmed PBS. Then, serum-free media with neutral red (0.2 mg/mL) was filtered, warmed, and added to cells to incubate for 3h. After 3h, media was removed, cells were rinsed with warm PBS, and lysed with a mixture of 50% ethanol, 40% DI water, and 10% acetic acid. Dye uptake was measured at 540 nm after 10 minutes of shaking, and normalized to the absorbance of control cells cultured in media. SLS-treated cells serve as negative control. Potential issues and troubleshooting solutions are shown in **Table 2**.

Issue	**Potential solution**
No absorbance is found in any well, including controls and/or is really variable	Check filters. PVDF membranes work great, but some cellulose filters interfere with the dye
	Check confluence of cells. Overconfluent cells can peel off or clump up, especially after the 3h neutral red incubation, and be sucked away during rinsing. If this is not visible with the naked eye, check wells under the microscope after each rinsing step to ensure cell layer is still there
Material is unexpectedly cytotoxic	Confirm sterile technique is being used wherever possible. Eg., weigh into tared sterile tubes in the biosafety cabinet, use sterile buffers, etc.
	Material could be adversely affecting pH. Measure pH of conditioned media. Consider adding HEPES buffer, but proceed with caution (may still be cytotoxic *in vivo*)
	Confirm material has been properly purified (no residual solvents, acid, etc.).
	Material oxidation could contribute to cytotoxicity. Consider adding antioxidants, but proceed with caution.

Table 2. Troubleshooting issues with neutral red cytocompatibility analysis.

Multilamellar adhesive patches

Adhesive patch preparation

Elastomers (PDMS, PU, PP) were coated in dopamine methacrylamide (DMA) overnight (2 mg/mL polyphenols; pH 8.5 bicine buffer). Methacrylate monomers were then deposited on the coated surface; as needed a glass cover slip was used to enable the polymers to fully wet the surface. The monomer mixture contained a radical initiator (Irgacure 819) and the monomer

mixture (usually 80% PEGma, 20% DMA or acDMA) was irradiated under UV light (90 – 270 s, λ = 365 nm, 100 mW/cm^2). Then, the cover slip was removed and the patches were gently rinsed with water and soaked for 1h in water or 1 M HCl for DMA or acDMA-containing patches, respectively, to remove polymer chains not bound to the surface and deprotect acDMA. Samples were dried and then studied in lap shear adhesion assays to wet bovine pericardium tissue.

Lap shear adhesion analysis

We measured the lap shear adhesive strength of the adhesive patches, including $NaIO_4$ pre-treatment of some patches, using the method outlined in Chapter 5.

4.5 References

[1] D.W.R. Balkenende, S.M. Winkler, P.B. Messersmith, Marine-inspired polymers in medical adhesion, Eur Polym J 116 (2019) 134-143.
[2] Y. Zhang, I. Strehin, K. Bedelbaeva, D. Gourevitch, L. Clark, J. Leferovich, P.B. Messersmith, E. Heber-Katz, Drug-induced regeneration in adult mice, Sci Transl Med 7(290) (2015).
[3] I. Strehin, D. Gourevitch, Y. Zhang, E. Heber-Katz, P.B. Messersmith, Hydrogels formed by oxo-ester mediated native chemical ligation, Biomaterials science 1(6) (2013) 603-613.
[4] G.P. Maier, M.V. Rapp, J.H. Waite, J.N. Israelachvili, A. Butler, Adaptive synergy between catechol and lysine promotes wet adhesion by surface salt displacement, Science 349(6248) (2015) 628-632.
[5] I. Coin, M. Beyermann, M. Bienert, Solid-phase peptide synthesis: from standard procedures to the synthesis of difficult sequences, Nat Protoc 2(12) (2007) 3247-3256.
[6] S.A. Burke, M. Ritter-Jones, B.P. Lee, P.B. Messersmith, Thermal gelation and tissue adhesion of biomimetic hydrogels, Biomedical Materials 2(4) (2007) 203-210.
[7] R.M. Moore, J.M. Mansour, R.W. Redline, B.M. Mercer, J.J. Moore, The physiology of fetal membrane rupture: insight gained from the determination of physical properties, Placenta 27(11-12) (2006) 1037-51.
[8] H. Meng, Y. Li, M. Faust, S. Konst, B.P. Lee, Hydrogen peroxide generation and biocompatibility of hydrogel-bound mussel adhesive moiety, Acta Biomater 17 (2015) 160-9.
[9] T.S. Sileika, D.G. Barrett, R. Zhang, K.H.A. Lau, P.B. Messersmith, Colorless Multifunctional Coatings Inspired by Polyphenols Found in Tea, Chocolate, and Wine, Angew Chem Int Edit 52(41) (2013) 10766-10770.
[10] J.H. Ryu, P.B. Messersmith, H. Lee, Polydopamine Surface Chemistry: A Decade of Discovery, Acs Appl Mater Inter 10(9) (2018) 7523-7540.
[11] K.G. Malollari, P. Delparastan, C. Sobek, S.J. Vachhani, T.D. Fink, R.H. Zha, P.B. Messersmith, Mechanical Enhancement of Bioinspired Polydopamine Nanocoatings, ACS Appl Mater Interfaces 11(46) (2019) 43599-43607.
[12] K. Lee, M. Park, K.G. Malollari, J. Shin, S.M. Winkler, Y. Zheng, J.H. Park, C.P. Grigoropoulos, P.B. Messersmith, Laser-induced Graphitization of Polydopamine: Enhancing Mechanical Performance While Preserving Multifunctionality, Nature Communications *In Press,* (2020).

CHAPTER FIVE – SUPRAMOLECULAR CROSSLINKS IN MUSSEL-INSPIRED TISSUE ADHESIVES

N.B. *This chapter also appeared as a manuscript of the same title that has been submitted for publication. Diederik W.R. Balkenende and I are co-first authors on the manuscript, along with Yiran Li and Phillip Messersmith. Dirk designed and synthesized the polymers and performed most characterization experiments except AFM analysis (Yiran) and cytocompatibility (me). Dirk and I both contributed to the development of the lap shear adhesion and burst device testing methods, and co-wrote the manuscript. The ways that this chapter contribute to and inform my thesis as a whole are discussed in the Introduction.*

Abstract

Here we introduce a tissue-adhesive patch with orthogonal cohesive and adhesive chemistries; supramolecular ureido-4-pyrimidinone (UPy) crosslinks provide cohesive strength and catechols provide mussel-inspired tissue adhesion. In the development of tissue-adhesive biomaterials, prior research has focused on forming strong adhesive interfaces in wet conditions, leaving the use of supramolecular crosslinks for cohesive strength underexplored. In developing this adhesive patch, the influence of comonomers' composition and amphiphilicity on adhesion was investigated by lap shear adhesion to wet tissue. We determined failed lap joints' failure mechanism using catechol-specific Arnow's stain, and identified formulations with improved cohesive strength. The adhesive materials were cytocompatible in mammalian cell conditioned media viability studies. We found that using orthogonal motifs to independently control adhesives' cohesive and adhesive strengths resulted in stronger tissue adhesion. The design principles presented here advance the development of wet tissue adhesives and could allow for the future design of biomaterials with desirable stimuli-responsive properties.

Introduction

Forming a strong cohesive network is important for effective and durable adhesion of medical adhesives, but the relative contributions of cohesive and adhesive interactions to overall bond strength has received little attention. The majority of clinically approved adhesives rapidly adhere after mixing a two-component solution in which a single covalent reactive motif establishes both the adhesive interface and the cohesive network.[1] To improve cohesion, several approaches have been tested including negatively swelling polymers, semi-crystalline block copolymers, and double network hydrogels.[2-4] We hypothesized that incorporating supramolecular crosslinks would improve the cohesive strength of and induce phase separation in wet-adhesive mussel-inspired materials, yielding cohesive, strong adhesive materials with biological properties appropriate for surgical applications.

Supramolecular biomaterials have potential applications in tissue engineering,[5] regenerative medicine,[6] therapeutics,[7] and controlled drug release.[8] However, the potential of supramolecular crosslinks to orthogonally control the cohesive strength of tissue adhesives has been largely unexplored.[9] Compared to covalent crosslinks, supramolecular interactions remain dynamic after crosslinking, leading to adaptive properties. Dynamic supramolecular crosslinking motifs used in adhesives[10, 11] include hydrogen bonding,[12] metal ligand coordination,[13] and host guest interactions.[14, 15] In particular, extensive work from the Meijer and Dankers groups has established ureido-4-pyrimidinone (UPy), which forms four-fold hydrogen bonding moieties upon dimerization, as a supramolecular crosslinker in a biological context.[16-19] For

example, UPy functionalized hydrogels that incorporated UPy derivatized bioactive molecules were successfully used as artificial extracellular matrix with bioactive properties.[5, 20, 21] Recently, the Dankers group reported the incorporation of catechol-functionalized UPy small molecules into supramolecular hydrogels, resulting in increased cell adhesion and attachment,[21] and created bioactive catechol-UPy films.[22]

Marine mussels (genus *Mytilus)* anchor to diverse underwater surfaces via secreted protein threads and adhesive plaques. The proteins of these byssal threads, particularly those at the adhesive interface, are rich in the amino acid L-3,4-dihidroxyphenylalanine (DOPA).[23] The catechol side chain of DOPA mediates robust adhesion both in the native mussel proteins and in synthetic materials.[24] Our group and others have shown that the incorporation of catechol into mussel-inspired synthetic polymers promotes wet tissue adhesiveness, with target applications including ligament reconstruction, hemostasis, and fetal membrane sealing.[25-29] In one example, branched PEG polymers were end-functionalized with DOPA motifs; upon mixing with a solution of $NaIO_4$, an oxidant, tissue-adhesive hydrogels were formed.[29, 30] $NaIO_4$ is commonly used as an oxidative reagent in catechol-containing adhesives to form both adhesive catechol-tissue bonds and cohesive catechol-catechol covalent crosslinks. This reduces the tunability of a material's mechanical properties, which may explain why catechol-PEG hydrogel adhesives fail cohesively.[31] Overall adhesive performance of catechol-containing tissue adhesives may benefit from the incorporation of orthogonal crosslinking strategies, rather than relying on catechols for both cohesion (catechol-catechol crosslinks) and adhesion (catechol-tissue bonds).

There is biological precedent for incorporating noncovalent interactions to strengthen the bulk properties of catechol-containing adhesive materials and other biological structures. For example, mussels and sandcastle worms secrete charged proteins that aggregate via noncovalent interactions to establish load-bearing plaques.[32] To form their byssal threads and adhesive plaques, mussels also utilize metal coordination bonding, cation-π interactions, and hydrogen bonding.[33] Several labs have reported synthetic materials that use these powerful interactions to form adhesives, stimuli-responsive materials, and other bioinspired materials.[13, 33-36]

Inspired by the contribution of non-covalent bonds to load bearing underwater bioadhesives, here we introduce hydrogen bonding supramolecular crosslinks into mussel-inspired wet tissue adhesives. Our design approach combines catechol (tissue adhesion) and UPy (hydrogen bonded crosslinks) into one adhesive polymer. Using a catechol specific stain (Arnow's stain), we identified the failure mechanism (cohesive failure vs. adhesive failure) after tissue shear adhesive tests, allowing us to understand the influence of each comonomer and optimize the formulation to improve adhesion. We found that the best performing adhesive relies not only on catechol and UPy, but also on an amphiphilic comonomer mixture, that lead to a phase separated morphology upon contact with physiological fluid. The design principles employed here – incorporating modular and orthogonal adhesive and cohesive elements to systematically improve overall adhesive strength – are generalizable and could be replicated for other adhesive systems.

Results & Discussion

Copolymer composition influences tissue adhesive strength.

The adhesive materials studied here are based on polymethacrylates in which UPy-methacrylate (UPy-MA) is the supramolecular crosslinker, and dopamine methacrylamide (DMA) provides tissue adhesive properties (**Figure 5.1**). UPy crosslinks are inherently dynamic, with their interaction strength and the fraction of UPy dimers being dependent on hydrophobicity, presence

of water, temperature, and pH.[37] In a wet environment, the choice and molar ratio of comonomers greatly influences the strength of UPy supramolecular crosslinks, and thus, overall cohesive properties. To probe the influence of comonomers, we synthesized a series of polymers containing hydrophilic methacrylate monomers with different oligoethylene glycol (OEG) chain lengths (3, 9 or 20 repeating units) and hydrophobic methacrylate comonomers with various alkyl lengths (butyl, 2-ethylhexyl, and lauryl) (**Supplemental Methods**). For comparative analysis, the weight ratio between hydrophobic and hydrophilic monomers was kept constant throughout the series.

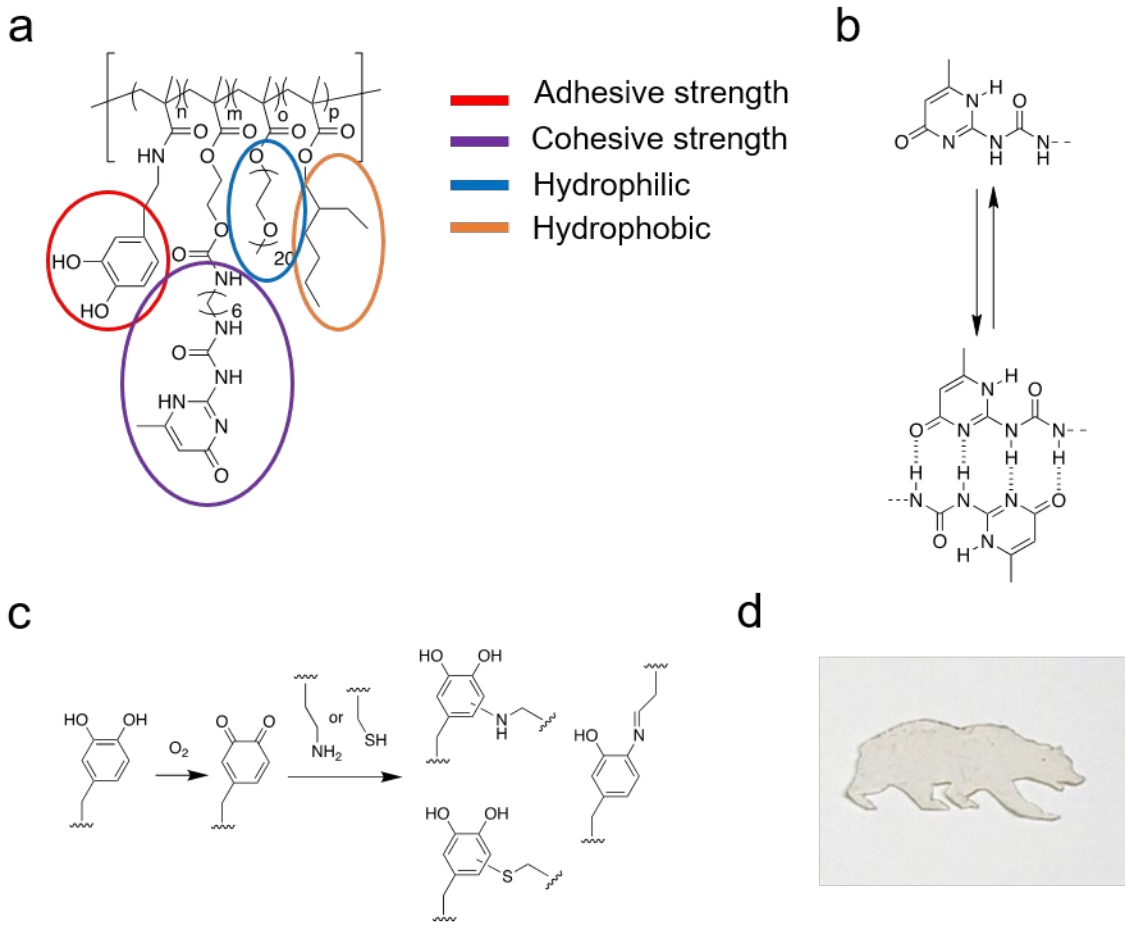

Figure 5.1. Mussel inspired supramolecular adhesive polymers. a, Chemical structure and functionality of an amphiphilic random copolymer containing DMA and UPy. **b,** Hydrogen bonding between UPy monomers on two polymer chains form dynamic, noncovalent crosslinks. **c,** Synthetic pathway to form covalent interfacial bonds via autoxidative reactions between DMA and tissue-pendant lysine or thiol residues. **d,** Photo of a cut polymer film prepared by compression molding at 80 °C.

To identify a formulation with optimal high adhesive strength, polymers were compression molded into adhesive patches, and lap shear adhesion to wet tissue was measured for each adhesive. The failed lap joint was analyzed to determine its failure mode. Using this screening method, we were able to identify a formulation that failed adhesively (i.e., cohesive strength

exceeded adhesive strength), an indication that an optimal UPy comonomer composition had been achieved.

As-prepared polymers were compression molded at 80 ºC into clear elastomeric patches. To measure the wet tissue lap shear adhesive strength of these patches, joints were constructed by compression of a polycarbonate strut with bovine pericardium tissue attached to another strut with a piece of adhesive film (**Figure 5.S1**). The adhesive joints were then incubated under compression in phosphate buffered saline (PBS) at 37 ºC for 1 h and sheared apart to measure the adhesive strength. After lap shear tests, the adhesive failure mode was visualized by Arnow's Assay which stains catechols red. Following Arnow's staining,[38] red residue on the tissue indicates cohesive failure, and conversely, no redness suggests an adhesive failure mechanism (**Figure 5.2a**). If a material failed cohesively, the formulation was modified to improve cohesive strength. This was iterated until a formulation that failed adhesively was identified.

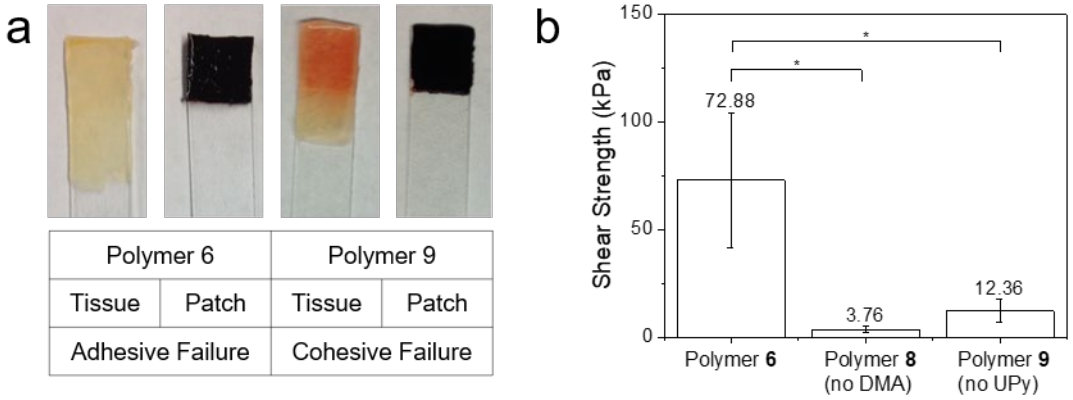

Figure 5.2. Lap shear adhesion to wet tissue. a, Arnow's staining of failed lap joints. Stained tissue from Polymer **6** has no red coloration, indicating adhesive failure; tissue from Polymer **9** is stained red, indicating cohesive failure. Both adhesives patches **6** and **9** stain dark red, indicating the presence of catechols. **b**, Tissue shear adhesive strength of Polymer **6**, Polymer **8**, and Polymer **9** towards wet bovine pericardium. During incubation (for 1h in 37 ºC PBS), lap joints were secured under a 200 g weight. Mean shear adhesion strengths are displayed above each bar. *P* values were determined by students *t*-test (*: $p < 0.05$) (n = 10).

Previous research has shown that the interaction strength of supramolecular crosslinks in a hydrophobic phase is higher than in a swollen hydrophilic phase due to a shift in the dynamic equilibrium in water.[39] Thus, in an initial attempt to maximize the UPy interaction strength, hydrophobic Polymer **1** consisting of UPy-MA, DMA, and butyl methacrylate (Bu-MA) was synthesized (**Table 5.1**). Lap joints of Polymer **1** failed before they could be loaded into the mechanical tester for adhesion tests. We hypothesized that this poor adhesion is because catechol may not be available for interfacial adhesion to tissue in a purely hydrophobic polymer. In contrast, hydrophilic Polymer **2**, composed of UPy-MA, DMA, and hydrophilic OEG methacrylate (OEG9-MA), (in which catechol would be more available for interfacial adhesion) swelled and began to disintegrate when exposed to excess DI water. After 1 hour, an adhesive strength of 16.6 ± 7.5 kPa (mean ± sd) was recorded, and Arnow's stain showed red staining on the tissue side, indicative of cohesive failure (**Table 5.1**, **Figure 5.S2**). This result makes sense given the high adhesive strength induced by DMA, and the low cohesive strength due to a low fraction of bound UPy dimers when

exposed to water. The adhesion tests of Polymers **1** and **2** confirmed that both hydrophobic and hydrophilic comonomers are necessary to 1) allow catechol to react to tissue and 2) shield UPy motifs from water to shift the dynamic equilibrium to the bound state. Based on this, we hypothesized that a phase separated morphology would result in high adhesion strength. To that end, further iterations of the polymer design contain both hydrophobic and hydrophilic comonomers that self-assemble into a phase separated structure upon contact with water.[39-41]

Table 5.1. Polymer composition and tissue adhesive properties

Sample	Methacrylate Comonomer Composition (mol%)[1]								Tissue adhesion strength (kPa)[2]	F.M.[3]
	DMA	UPy	OEG3	OEG9	OEG20	Butyl	EH	Lauryl		
Polymer **1**	8.0	8.6	-	-	-	83.3	-	-	N/A[4]	Ad
Polymer **2**	10.7	8.3	-	81.0	-	-	-	-	16.6 ± 7.5	Co
Polymer **3**	8.6	10.6	45.0	-	-	35.4	-	-	60.0 ± 8.1	Co
Polymer **4**	9.8	7.5	-	31.0	-	52.0	-	-	51.4 ± 14.8	Co
Polymer **5**	10.0	9.6	-	-	13.6	66.7	-	-	109.9 ± 36.5	Co
Polymer **6**	11.3	10.5	-	-	23.3	-	54.9	-	122.4 ± 42.4	Ad
Polymer **7**	17.1	13.9	-	-	24.7	-	-	56.0	50.9 ± 15.1	Co
Polymer **8**	-	11.0	-	-	21.8	-	67.2	-	3.8 ± 1.3	N/A[5]
Polymer **9**	12.3	-	-	-	23.2	-	64.5	-	12.4 ± 5.4	Co

[1]Monomer composition was determined by ^{1}H-NMR in $CDCl_3$.
[2]Values are mean ± standard deviation.
[3]F.M.: Failure mechanism. Ad: Adhesive failure. Co: Cohesive failure. The failure mechanism was determined using Arnow's staining after shear adhesion tests.
[4]Polymer **1** failed before shear adhesion tests could be performed.
[5]Polymer **8** does not contain catechol, therefore staining cannot reveal the failure mechanism.

We also sought to understand how the chain length of OEG-MA comonomers, even at the same overall OEG weight fraction, could impact the adhesives' ability to effectively phase separate. Three different polymers consisting of UPy-MA, DMA, Bu-MA, and OEG-MA with 3, 9 or 20 repetitive units were synthesized (Table 1). Tissue adhesion tests of Polymers **3** and **4**, prepared with OEG3-MA or OEG9-MA respectively, showed lap shear adhesive strengths of 60.0 ± 8.1 kPa (Polymer **3**) and 51.4 ± 14.8 kPa (Polymer **4**). However, when incorporating OEG20-MA (Polymer **5**), a higher adhesion strength of 109.9 ± 36.5 kPa was observed. Staining of failed lap joints showed red tissue coloration for all three polymers, indicating cohesive failure (see **Table 5.1** and **Figure 5.S2**). While OEG20-MA performed best, these materials' cohesive failure indicated that further improvement of overall tissue adhesive strength was still possible through optimization of cohesive properties.

Heinzmann et al. showed that UPy functionalized polybutyl- and polyhexyl methacrylate copolymers had glass transition temperatures above room temperature, suggesting that short hydrophobic chains in our materials (i.e. butyl-MA) may result in glassy phases with worse mechanical properties relative to similar materials with longer hydrophobic chains.[42] To test the influence of the hydrophobic comonomer on our adhesive materials, Polymer **5** (hydrophobic component: butyl-MA) was compared to polymers containing 2-ethylhexyl-MA (EH-MA, Polymer **6**) or lauryl-MA (L-MA, Polymer **7**).[43] Gratifyingly, Polymer **6** resulted in an improvement of the average tissue adhesive strength (122.4 ± 42.4 kPa), and, more importantly, Arnow's staining of Polymer **6** after the adhesion test revealed an adhesive failure mechanism, indicating the cohesive contribution exceeded the adhesive interfacial strength (**Figure 5.2a**).

Polymer **7** showed a significantly lower adhesive strength of 50.9 ± 15.1 kPa. Together, these results indicate the existence of an optimum alkyl length of the hydrophobic comonomer. and the importance of incorporating both hydrophobic and hydrophilic groups to allow for efficient UPy/catechol phase separation. Although outside the scope of this study, further optimization may improve the adhesive interface through higher concentrations of DMA or more reactive adhesive motifs.

Detailed characterization of the materials properties of Polymer 6

Wet tissue adhesion strengths can vary greatly due to small changes in test conditions and biological variation among tissues.[44] In our initial screening studies, a clamp (mini binder clip) was used during incubation. While ASTM standard 2255-05 allows this, the force applied easily exceeds 2N, which is recommended by the same standard. To probe the effect of the force applied during incubation, adhesive joints were weighed down by brass weights (**Figure 5.S1c**), the standard's preferred method. Indeed, a lower tissue adhesion strength of 73 ± 31.3 kPa was observed, suggesting that intimate interfacial contact between patch and tissue, and perhaps lower water content, improve adhesion[45] (**Figure 5.2b; Figure 5.S3**).

The adhesive polymers presented here all rely on auto-oxidation for the formation of an adhesive interface; however, many reported catechol containing adhesives are treated with $NaIO_4$ prior to adhesion.[28-30] Work from Lee and coworkers on DOPA containing semi-crystalline polymers demonstrated that solely relying on auto-oxidation of catechol significantly reduces the adhesive strength.[3] To test whether this finding applies to our adhesive polymers, the surface of the patches was brushed with a solution of $NaIO_4$ (0.1 M, 20 mg ml^{-1}) for 5s, and 2N force was applied during incubation (**Figure 5.S1c**). Tissue lap shear adhesion measurements revealed an insignificant increase in adhesive strength after one hour of incubation (88.6 ± 16.3 kPa, $P > 0.05$) compared to untreated patches. This result suggests that, in previously reported catecholic tissue adhesives, $NaIO_4$ mostly served to increase cohesive strength (e.g., catechol-catechol bonds), and that, in our materials, adequate crosslinking is already present due to UPy-UPy supramolecular bonding.

To test the contributions of UPy and DMA in Polymer **6**, tissue adhesive tests of analogs which lack either DMA or UPy (Polymers **8** and **9**, respectively) were performed (**Table 5.1**). The absence of DMA in Polymer **8** resulted in a low adhesion strength of 3.8 ± 1.3 kPa ($P < 0.05$), confirming DMA is essential for the formation of an adhesive interface in Polymer **6**. Complementary to these results, Polymer **9** (without UPy) also showed a significantly lower adhesion strength of 12.4 ± 5.4 kPa ($P < 0.05$ relative to Polymer **6**) and cohesive failure. These results are as expected since DMA-containing Polymers **6** and **9** can adhere to wet tissue, while UPy can improve the cohesive properties but is not able to form tissue-adhesive bonds. DMA and UPy are both required for a high tissue adhesive strength in Polymer **6** and serve an orthogonal functional role.

Without the use of $NaIO_4$, the formation of an adhesive interface with a tissue surface is limited by the autoxidation of DMA. Furthermore, the mechanical force exerted by swelling may lead to breaking of interfacial bonds. To test the influence of autoxidation and swelling, we studied the time dependence of tissue adhesion strength of Polymer **6** in neat and oxidized samples (**Figure 5.S4**). Interestingly, we found that for the neat sample, an initial increase in adhesive strength was followed by a decrease in adhesive strength (**Figure 5.S4a**). This result may indicate that the adhesive interface is strained and ruptures as the material swells. Time dependent measurements of samples that were brushed with $NaIO_4$ show a high shear strength of 171.9 ± 35.8 kPa after 30

min followed by a steady decease to 54.2 ± 17.2 kPa after 4 hours (**Figure 5.S4b**). Both of the time dependent tissue adhesion tests show a decrease in adhesive strength as a function of time. However, upon oxidizing the surface, fast formation of interfacial and cohesive crosslinks may be essential to withstand interfacial stress caused by swelling.

A detailed materials characterization of Polymer **6** provided further insight into its swelling kinetics, mechanical properties, and morphology (**Figure 5.3**). To monitor the speed and extent of swelling, films of Polymer **6** were swollen in excess phosphate buffered saline (PBS, pH 7.4) and the mass was monitored as function of time (**Figure 5.3a**). Rapid equilibrium swelling was observed, with a water content of 266 ± 4 wt% after 8 hours. The effect of swelling on the mechanical properties was probed by tensile testing of dogbone-shaped samples swollen overnight in PBS (**Figure 5.3b, c**). Both the dry and swollen samples show tensile properties typical for crosslinked elastomers (**Figure 5.3c, Table 5.2**).[46] Swelling did not significantly affect the elastic modulus (**Table 5.2**), confirming a phase separated morphology in which the UPy crosslinked hydrophobic phases provide tensile strength, even in a swollen state. However, a decrease in the stress and strain at break in swollen samples implies lower UPy-UPy interaction strengths and crosslink densities. Interestingly, the tensile properties in the swollen state are close to those reported for the amniotic sac; these adhesives may eventually be used to seal the sac following fetal surgery.[47] In addition, strain at break for dry samples exceeded 2000% when using slow strain rates (5% min^{-1}), confirming the dynamic character of UPy crosslinks (**Figure 5.S5**).

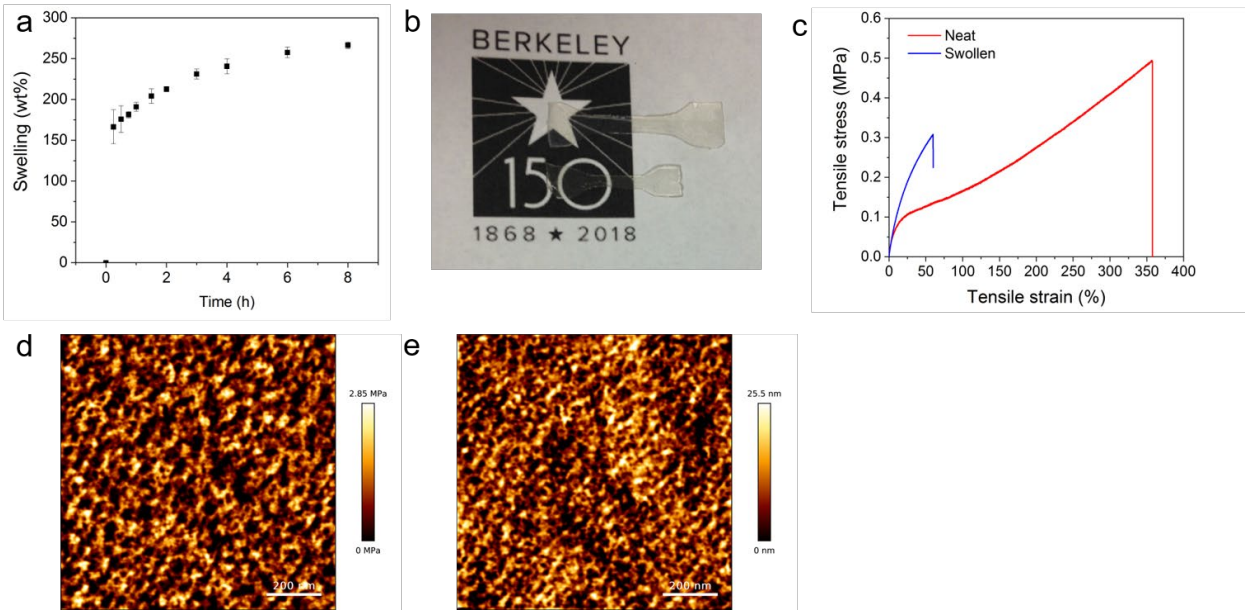

Figure 5.3. Effect of equilibrium swelling on material properties. a, Equilibrium swelling of Polymer **6** (n = 3) upon submersion in phosphate buffered saline (PBS). **b**, Photo of polymer film before (bottom) and after swelling (top) in PBS. **c**, Representative stress-strain curves of polymer **6** in the dry (—) and swollen (—) state at a strain rate of 25% min^{-1}. **d**, Atomic force spectroscopy map of the elastic modulus of a drop casted film of Polymer **6** that was swollen in PBS. **e**, AFM height map of the same area as displayed in **d**. Note that features do not overlap, indicating the modulus results from a phase-separated morphology.

Table 5.2. Mechanical characterization

Sample	Elastic Modulus (MPa)[1]	Stress at Break (MPa)	Strain at Break (%)
Polymer **6** - neat	1.28 ± 0.14	0.48 ± 0.05	410 ± 84
Polymer **6** - swollen	1.31 ± 0.12	0.28 ± 0.04	52 ± 13

[1]The elastic modulus was determined from the initial 5% strain of the stress strain curve.

To investigate the presence of a phase separated morphology, differential scanning calorimetry (DSC) measurements and atomic force microscopy (AFM) of the polymer films were performed. The DSC trace of the dry material shows one broad glass transition temperature (T_g) at -31 ºC indicating a single phase, and a shallow first order transition at 118 ºC, corresponding to the melting of (small) crystalline stacks of UPy crosslinks. Upon equilibrium swelling, the DSC trace shows the appearance of a T_g around 20 ºC, suggestive of a phase separated morphology (**Figure 5.S6**). To gain further insight into the phase separation, AFM images of drop cast, swollen films of Polymer **6** recorded in force mode (**Figure 5.3d**). The swollen material showed a nanophase separated morphology in which each phase appears to be interconnected. Furthermore, a height image of the same area (**Figure 5.3e**) does not align with the force map when superimposed, indicating that the measured stiffness profiles are not simply related to surface topology. In summary, these results imply that films of Polymer **6** maintain their elastic properties when swollen due to efficient nanophase separation, confirming our earlier hypothesis that phase separation allows for both DOPA and UPy monomers to be in their preferred hydrophilic or hydrophobic environment, respectively.

Wet tissue sealing

Tissue adhesives can seal tissues and prevent fluid flow when there is a pressure difference across a tissue, such as in intestinal peristalsis (20 mmHg)[48] or the amniotic sac during pregnancy (9 mmHg).[49] Earlier work from our group has established mussel-inspired adhesives as a potential sealant for fetal surgery to close procedural wounds in the amniotic sac.[50-53] To test the sealing properties of Polymer **6**, burst pressure measurements were performed on a custom made burst device that was inflated with PBS at 10 ml min^{-1} (**Figure 5.4a, 5.S7**). Round samples of Polymer **6** (d = 15 mm, thickness = 200 μm) showed significant deformation due to swelling and led to adhesive failure during a 1h incubation at 37 ºC in PBS.

We hypothesized that swelling of the adhesive patches could reduce their ability to resist burst pressures. We attempted two strategies to reduce swelling. First, to increase the speed at which the adhesive interface forms, patches were brushed with $NaIO_4$ (0.1 M) for 5s before they were applied to the tissue surface. A burst pressure of 50.3 ± 4.9 mmHg was observed, and the tissue stretched significantly to accommodate inflowing fluid. This demonstrates that speed of adhesion matters when fast swelling occurs. Second, since most surgical applications only require the adhesive to adhere on one side, we applied a biodegradable polycaprolactone (PCL, M_n = 80 kg mol^{-1}) backing material to reduce the adhesive patch's swelling in the *x*-*y* plane. Films of Polymer **6** and PCL were compression molded together (10 s, 500 psi, 80 ºC). Round samples of PCL-backed Polymer **6** films were tested on the burst device, resulting in burst pressures of 107.8 ± 19.2 mmHg, (**Figure 5.4b**). When the two swelling-resistant approaches were combined ($NaIO_4$ treatment and a PCL backing, 102.4 ± 19.4 mmHg), no significant increase in adhesion was seen relative to PCL-backed samples, indicating that $NaIO_4$ oxidation is not necessary when alternate

strategies to control swelling are available and that catechol auto-oxidation alone is enough to result in robust adhesion when swelling is limited. The burst pressure values measured here are sufficient for a variety of surgical applications (≤20 mmHg) and have strong potential for eventual clinical translation.

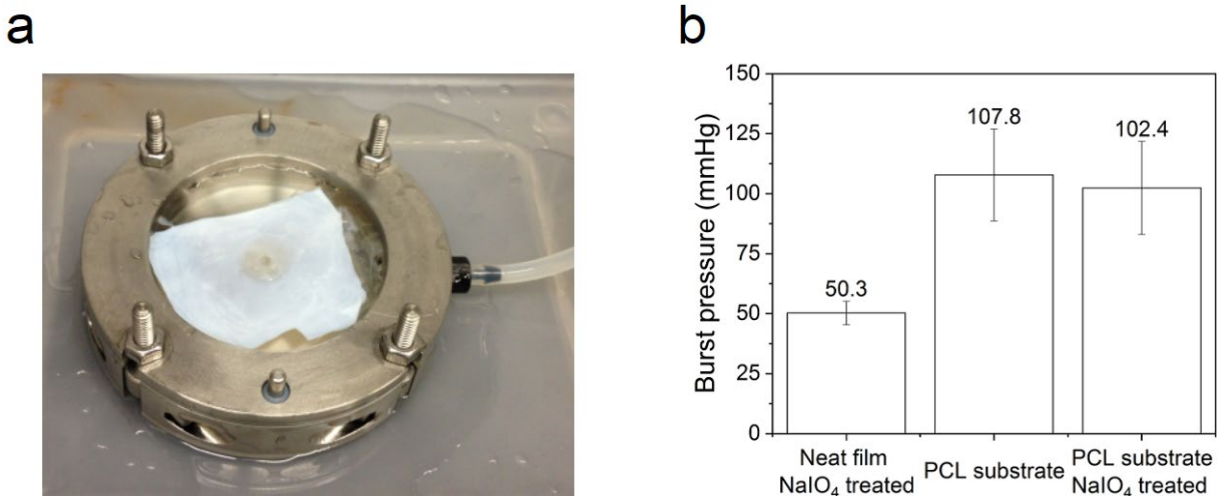

Figure 5.4. Sealing properties of bioinspired adhesive patches. a, Photo of the burst device that was used to measure the maximum pressure. A round film of Polymer **6** that was brushed with $NaIO_4$ (c = 0.1 M, 5s) is adhered to bovine pericardium on a disk of polycarbonate with a 3 mm hole. The pressure was increased using a syringe pump with PBS (10 ml min^{-1}) until failure of the adhesive patch. **b**, Burst pressure tests (n = 3) comparing burst pressure of Polymer **6** when material swelling is controlled using $NaIO_4$ (c = 0.1 M,) and/or a polycaprolactone (PCL) backing. Use of the backing was sufficient to control swelling as using both $NaIO_4$ and PCL did not further improve burst pressure.

Cytocompatibility studies.

Catechol-containing materials have performed well in animal studies with little inflammatory or other negative cell response seen.[50, 54] We performed a conditioned media experiment (per ISO standard 10993-5) to determine the cytocompatibility of neat Polymer **6** with NIH 3T3 (mouse) and CCD-32sk (human) fibroblasts. Polymer **6** was cytocompatible at 10 mg/mL (viability >70% relative to untreated controls) with both NIH3T3 and CCD32-sk cells (**Figure 5.S9**). Upon changing the polymer concentration during media conditioning, a dose-dependent viability response was observed (**Figure 5.S8**), which is in accordance to a report from Meng, et al., for other catechol containing polymers, and was attributed to H_2O_2 generation during (auto)oxidation of DMA.[55] To improve the cytocompatibility, future materials could incorporate antioxidants to decrease H_2O_2 generation.

Conclusion

In summary, we have introduced a new strategy to crosslink mussel-inspired wet tissue adhesives using supramolecular crosslinks. Careful iteration and tuning of hydrophilic and hydrophobic comonomers resulted in adhesive patches with a wet tissue adhesive strength of 122 kPa. Incorporating supramolecular crosslinks improved the patches' cohesive strength, and thus

overall adhesiveness. We identified the adhesive failure mechanism by staining failed tissue-patch lap joints using Arnow's stain; this method could be applied to optimize adhesion of other mussel-inspired adhesives. The strength of supramolecular crosslinks resulted from efficient phase separation between hydrophobic (UPy/alkyne) and hydrophyllic (DMA/OEG) phases upon contact with physiological fluid. The resulting material has high wet tissue adhesive strength, tissue sealing properties sufficient for numerous clinical applications, and suitable cytocompatibility. In addition, the orthogonal crosslinking (UPy) and adhesive (catechol) chemistries reduce the reliance on oxidative agents to form catechol-catechol crosslinks; indeed, the UPy-UPy crosslinks are sufficient to form a strong, cohesive network. We expect that the incorporation of supramolecular crosslinks can be extended to improve the performance of other surgical adhesives and anticipate future applications that exploit other supramolecular chemistries capable of providing tissue adhesives with advanced adaptive properties such as self-healing and stress relaxation.

References

1. Ghobril, C.; Grinstaff, M. W., The chemistry and engineering of polymeric hydrogel adhesives for wound closure: a tutorial. Chem. Soc. Rev. 2015, 44 (7), 1820-35.
2. Barrett, D. G.; Bushnell, G. G.; Messersmith, P. B., Mechanically robust, negative-swelling, mussel-inspired tissue adhesives. Adv. Healthc. Mater. 2013, 2 (5), 745-55.
3. Murphy, J. L.; Vollenweider, L.; Xu, F.; Lee, B. P., Adhesive performance of biomimetic adhesive-coated biologic scaffolds. Biomacromolecules 2010, 11 (11), 2976-84.
4. Li, J.; Celiz, A. D.; Yang, J.; Yang, Q.; Wamala, I.; Whyte, W.; Seo, B. R.; Vasilyev, N. V.; Vlassak, J. J.; Suo, Z.; Mooney, D. J., Tough adhesives for diverse wet surfaces. Science 2017, 357 (6349), 378-381.
5. Dankers, P. Y.; Harmsen, M. C.; Brouwer, L. A.; van Luyn, M. J.; Meijer, E. W., A modular and supramolecular approach to bioactive scaffolds for tissue engineering. Nat Mater 2005, 4 (7), 568-74.
6. Boekhoven, J.; Stupp, S. I., 25th anniversary article: supramolecular materials for regenerative medicine. Adv Mater 2014, 26 (11), 1642-59.
7. Rühs, P. A.; Adamcik, J.; Bolisetty, S.; Sánchez-Ferrer, A.; Mezzenga, R., A supramolecular bottle-brush approach to disassemble amyloid fibrils. Soft Matter 2011, 7 (7), 3571-3579.
8. Mann, J. L.; Yu, A. C.; Agmon, G.; Appel, E. A., Supramolecular polymeric biomaterials. Biomater Sci 2017, 6 (1), 10-37.
9. Duarte, A. P.; Coelho, J. F.; Bordado, J. C.; Cidade, M. T.; Gil, M. H., Surgical adhesives: Systematic review of the main types and development forecast. Prog Polym Sci 2012, 37 (8), 1031-1050.
10. Heinzmann, C.; Weder, C.; de Espinosa, L. M., Supramolecular polymer adhesives: advanced materials inspired by nature. Chemical Society reviews 2016, 45 (2), 342-358.
11. Li, Z. W.; Lu, W.; Ngai, T.; Le, X. X.; Zheng, J.; Zhao, N.; Huang, Y. J.; Wen, X. F.; Zhang, J. W.; Chen, T., Mussel-inspired multifunctional supramolecular hydrogels with self-healing, shape memory and adhesive properties. Polym Chem-Uk 2016, 7 (34), 5343-5346.
12. Cheng, S. J.; Zhang, M. Q.; Dixit, N.; Moore, R. B.; Long, T. E., Nucleobase Self-Assembly in Supramolecular Adhesives. Macromolecules 2012, 45 (2), 805-812.
13. Holten-Andersen, N.; Jaishankar, A.; Harrington, M. J.; Fullenkamp, D. E.; DiMarco, G.; He, L. H.; McKinley, G. H.; Messersmith, P. B.; Leei, K. Y. C., Metal-coordination: using one of nature's tricks to control soft material mechanics. J Mater Chem B 2014, 2 (17), 2467-2472.

14. Liu, J.; Scherman, O. A., Cucurbit[n]uril Supramolecular Hydrogel Networks as Tough and Healable Adhesives. Advanced Functional Materials 2018, 28 (21).
15. Takashima, Y.; Sahara, T.; Sekine, T.; Kakuta, T.; Nakahata, M.; Otsubo, M.; Kobayashi, Y.; Harada, A., Supramolecular Adhesives to Hard Surfaces: Adhesion Between Host Hydrogels and Guest Glass Substrates Through Molecular Recognition. Macromol Rapid Comm 2014, 35 (19), 1646-1652.
16. Spaans, S.; Fransen, P. P. K. H.; Schotman, M. J. G.; van der Wulp, R.; Lafleur, R. P. M.; Kluijtmans, S. G. J. M.; Dankers, P. Y. W., Supramolecular Modification of a Sequence-Controlled Collagen-Mimicking Polymer. Biomacromolecules 2019, 20 (6), 2360-2371.
17. Sijbesma, R. P.; Beijer, F. H.; Brunsveld, L.; Folmer, B. J. B.; Hirschberg, J. H. K. K.; Lange, R. F. M.; Lowe, J. K. L.; Meijer, E. W., Reversible polymers formed from self-complementary monomers using quadruple hydrogen bonding. Science 1997, 278 (5343), 1601-1604.
18. de Greef, T. F.; Nieuwenhuizen, M. M.; Sijbesma, R. P.; Meijer, E. W., Competitive intramolecular hydrogen bonding in oligo(ethylene oxide) substituted quadruple hydrogen bonded systems. J Org Chem 2010, 75 (3), 598-610.
19. Semenov, A. N.; Rubinstein, M., Thermoreversible gelation in solutions of associative polymers. 1. Statics. Macromolecules 1998, 31 (4), 1373-1385.
20. Bakker, M. H.; Tseng, C. C. S.; Keizer, H. M.; Seevinck, P. R.; Janssen, H. M.; Van Slochteren, F. J.; Chamuleau, S. A. J.; Dankers, P. Y. W., MRI Visualization of Injectable Ureidopyrimidinone Hydrogelators by Supramolecular Contrast Agent Labeling. Adv Healthc Mater 2018, 7 (11), e1701139.
21. Spaans, S.; Fransen, P.; Ippel, B. D.; de Bont, D. F. A.; Keizer, H. M.; Bax, N. A. M.; Bouten, C. V. C.; Dankers, P. Y. W., Supramolecular surface functionalization via catechols for the improvement of cell-material interactions. Biomater Sci 2017, 5 (8), 1541-1548.
22. van Gaal, R. C.; Fedecostante, M.; Fransen, P. P. K. H.; Masereeuw, R.; Dankers, P. Y. W., Renal Epithelial Monolayer Formation on Monomeric and Polymeric Catechol Functionalized Supramolecular Biomaterials. Macromol Biosci 2019, 19 (2).
23. Waite, J. H., Mussel adhesion - essential footwork. J Exp Biol 2017, 220 (4), 517-530.
24. Zhang, W.; Wang, R.; Sun, Z.; Zhu, X.; Zhao, Q.; Zhang, T.; Cholewinski, A.; Yang, F. K.; Zhao, B.; Pinnaratip, R.; Forooshani, P. K.; Lee, B. P., Catechol-functionalized hydrogels: biomimetic design, adhesion mechanism, and biomedical applications. Chemical Society reviews 2020, 49 (2), 433-464.
25. Shin, M.; Park, S. G.; Oh, B. C.; Kim, K.; Jo, S.; Lee, M. S.; Oh, S. S.; Hong, S. H.; Shin, E. C.; Kim, K. S.; Kang, S. W.; Lee, H., Complete prevention of blood loss with self-sealing haemostatic needles. Nat. Mater. 2017, 16 (1), 147-152.
26. Li, H.; Chen, S.; Chen, J.; Chang, J.; Xu, M.; Sun, Y.; Wu, C., Mussel-Inspired Artificial Grafts for Functional Ligament Reconstruction. ACS Appl Mater Interfaces 2015, 7 (27), 14708-19.
27. Lee, B. P.; Messersmith, P. B.; Israelachvili, J. N.; Waite, J. H., Mussel-Inspired Adhesives and Coatings. Annu. Rev. Mater. Res. 2011, 41 (1), 99-132.
28. Brubaker, C. E.; Kissler, H.; Wang, L. J.; Kaufman, D. B.; Messersmith, P. B., Biological performance of mussel-inspired adhesive in extrahepatic islet transplantation. Biomaterials 2010, 31 (3), 420-7.
29. Kivelio, A.; Dekoninck, P.; Perrini, M.; Brubaker, C. E.; Messersmith, P. B.; Mazza, E.; Deprest, J.; Zimmermann, R.; Ehrbar, M.; Ochsenbein-Koelble, N., Mussel mimetic tissue

adhesive for fetal membrane repair: initial in vivo investigation in rabbits. European Journal of Obstetrics & Gynecology and Reproductive Biology 2013, 171 (2), 240-245.
30. Lee, B. P.; Dalsin, J. L.; Messersmith, P. B., Synthesis and gelation of DOPA-Modified poly(ethylene glycol) hydrogels. Biomacromolecules 2002, 3 (5), 1038-1047.
31. Barrett, D. G.; Bushnell, G. G.; Messersmith, P. B., Mechanically Robust, Negative-Swelling, Mussel-Inspired Tissue Adhesives. Advanced Healthcare Materials 2013, 2 (5), 745-755.
32. Balkenende, D. W. R.; Winkler, S. M.; Messersmith, P. B., Marine-Inspired Polymers in Medical Adhesion. European Polymer Journal 2019.
33. Forooshani, P. K.; Lee, B. P., Recent approaches in designing bioadhesive materials inspired by mussel adhesive protein. J Polym Sci Pol Chem 2017, 55 (1), 9-33.
34. Holten-Andersen, N.; Harrington, M. J.; Birkedal, H.; Lee, B. P.; Messersmith, P. B.; Lee, K. Y. C.; Waite, J. H., pH-induced metal-ligand cross-links inspired by mussel yield self-healing polymer networks with near-covalent elastic moduli. Proceedings of the National Academy of Sciences of the United States of America 2011, 108 (7), 2651-2655.
35. Harrington, M. J.; Masic, A.; Holten-Andersen, N.; Waite, J. H.; Fratzl, P., Iron-Clad Fibers: A Metal-Based Biological Strategy for Hard Flexible Coatings. Science 2010, 328, 216-220.
36. Hofman, A. H.; van Hees, I. A.; Yang, J.; Kamperman, M., Bioinspired Underwater Adhesives by Using the Supramolecular Toolbox. Adv Mater 2018, 30 (19), e1704640.
37. Krieg, E.; Bastings, M. M.; Besenius, P.; Rybtchinski, B., Supramolecular Polymers in Aqueous Media. Chem Rev 2016, 116 (4), 2414-77.
38. Yoo, H. Y.; Iordachescu, M.; Huang, J.; Hennebert, E.; Kim, S.; Rho, S.; Foo, M.; Flammang, P.; Zeng, H.; Hwang, D.; Waite, J. H.; Hwang, D. S., Sugary interfaces mitigate contact damage where stiff meets soft. Nat Commun 2016, 7, 11923.
39. Goor, O. J. G. M.; Hendrikse, S. I. S.; Dankers, P. Y. W.; Meijer, E. W., From supramolecular polymers to multi-component biomaterials. Chemical Society reviews 2017, 46 (21), 6621-6637.
40. ter Huurne, G. M.; Voets, I. K.; Palmans, A. R. A.; Meijer, E. W., Effect of Intra- versus Intermolecular Cross-Linking on the Supramolecular Folding of a Polymer Chain. Macromolecules 2018, 51 (21), 8853-8861.
41. Matsumoto, M.; Terashima, T.; Matsumoto, K.; Takenaka, M.; Sawamoto, M., Compartmentalization Technologies via Self-Assembly and Cross Linking of Amphiphilic Random Block Copolymers in Water. J Am Chem Soc 2017, 139 (21), 7164-7167.
42. Heinzmann, C.; Salz, U.; Moszner, N.; Fiore, G. L.; Weder, C., Supramolecular Cross-Links in Poly(alkyl methacrylate) Copolymers and Their Impact on the Mechanical and Reversible Adhesive Properties. ACS Appl Mater Interfaces 2015, 7 (24), 13395-404.
43. Balkenende, D. W.; Monnier, C. A.; Fiore, G. L.; Weder, C., Optically responsive supramolecular polymer glasses. Nat Commun 2016, 7, 10995.
44. ASTM Interntional, F2255-05(2015) Standard Test Method for Strength Properties of Tissue Adhesives in Lap-Shear by Tension Loading. ASTM International: West Conshohocken, PA, 2015; Vol. F2255-05(2015).
45. Michel, R.; Poirier, L.; van Poelvoorde, Q.; Legagneux, J.; Manassero, M.; Corte, L., Interfacial fluid transport is a key to hydrogel bioadhesion. Proceedings of the National Academy of Sciences of the United States of America 2019, 116 (3), 738-743.

46. Chen, Q. Z.; Liang, S. L.; Thouas, G. A., Elastomeric biomaterials for tissue engineering. Prog Polym Sci 2013, 38 (3-4), 584-671.
47. Haller, C. M.; Buerzle, W.; Kivelio, A.; Perrini, M.; Brubaker, C. E.; Gubeli, R. J.; Mallik, A. S.; Weber, W.; Messersmith, P. B.; Mazza, E.; Ochsenbein-Koelble, N.; Zimmermann, R.; Ehrbar, M., Mussel-mimetic tissue adhesive for fetal membrane repair: an ex vivo evaluation. Acta Biomater 2012, 8 (12), 4365-70.
48. Scott, S. M.; Knowles, C. H.; Wang, D.; Yazaki, E.; Picon, L.; Wingate, D. L.; Lindberg, G., The nocturnal jejunal migrating motor complex: defining normal ranges by study of 51 healthy adult volunteers and meta-analysis. Neurogastroenterol Motil 2006, 18 (10), 927-35.
49. Sideris, I. G.; Nicolaides, K. H., Amniotic fluid pressure during pregnancy. Fetal Diagn Ther 1990, 5 (2), 104-8.
50. Kivelio, A.; Dekoninck, P.; Perrini, M.; Brubaker, C. E.; Messersmith, P. B.; Mazza, E.; Deprest, J.; Zimmermann, R.; Ehrbar, M.; Ochsenbein-Koelble, N., Mussel mimetic tissue adhesive for fetal membrane repair: initial in vivo investigation in rabbits. Eur. J. Obstet. Gynecol. Reprod. Biol. 2013, 171 (2), 240-5.
51. Bilic, G.; Brubaker, C.; Messersmith, P. B.; Mallik, A. S.; Quinn, T. M.; Haller, C.; Done, E.; Gucciardo, L.; Zeisberger, S. M.; Zimmermann, R.; Deprest, J.; Zisch, A. H., Injectable candidate sealants for fetal membrane repair: bonding and toxicity in vitro. Am. J. Obstet. Gynecol. 2010, 202 (1), 85 e1-9.
52. Perrini, M.; Barrett, D.; Ochsenbein-Koelble, N.; Zimmermann, R.; Messersmith, P.; Ehrbar, M., A comparative investigation of mussel-mimetic sealants for fetal membrane repair. J. Mech. Behav. Biomed. Mater. 2016, 58, 57-64.
53. Winkler, S. M.; Harrison, M. R.; Messersmith, P. B., Biomaterials in fetal surgery. Biomaterials science 2019, 7 (8), 3092-3109.
54. Brubaker, C. E.; Messersmith, P. B., Enzymatically Degradable Mussel-Inspired Adhesive Hydrogel. Biomacromolecules 2011, 12 (12), 4326-4334.
55. Meng, H.; Li, Y.; Faust, M.; Konst, S.; Lee, B. P., Hydrogen peroxide generation and biocompatibility of hydrogel-bound mussel adhesive moiety. Acta Biomater. 2015, 17, 160-9.

Acknowledgements and contributions

D.W.R.B. acknowledges support from the Swiss National Science Foundation early and advanced postdoc mobility grants (P2FRP2_165141 and P300P2_174468). This project is also supported by the NIH (R01-EB022031), the NSF (Graduate Research Fellowship DGE 1752814 to S.M.W.), and the Siebel Foundation (Siebel Scholars Fellowship to S.M.W.).

D.W.R.B. synthesized all materials. D.W.R.B, S.M.W, and Y.L. contributed to the experimental work and data analysis. All authors contributed to the conception of the experiments and discussion of the results, and commented on the manuscript. D.W.R.B and S.M.W wrote the manuscript and contributed equally. D.W.R.B. and P.B.M. conceived and designed the concepts. The authors declare no competing financial interests.

CHAPTER FIVE – SUPPORTING INFORMATION

Supporting Materials & Methods

Unless indicated otherwise, all chemicals and anhydrous solvents were obtained from Sigma Aldrich and used as received. All other non-anhydrous solvents were purchased from Macron Chemicals and used as received. Films of polycarbonate (PC) and Teflon were purchased from McMaster Carr.

Characterization

NMR

^{1}H-NMR (400 MHz) spectra were recorded on a 400 MHz Bruker Avance spectrometer in $CDCl_3$ or DMSO-*d*6. ^{1}H NMR spectra were referenced against the signal for residual $CHCl_3$ at 7.26 ppm or DMSO at 2.50 ppm.

GPC

Gel Permeation Chromatography was performed on a Viscotek GPC Max equipped with Agilent Technologies PLgel 5 μm Mixed-C columns in THF and calibrated on polystyrene standards.

Compression Molding

Compression molding was performed on a custom-made compression molder at 2000 psi and 80 °C for 1 min unless noted otherwise.

Photography

All photos were recorded on an Apple iPhone.

Tensile and shear adhesion tests

Tensile tests and shear adhesion tests were performed on an Instron 3345 tensile tester equipped with a 50N load cell. Raw data from shear adhesion or tensile tests were processed using Bluehill 3 software. The elastic modulus was determined as the slope of the initial 5% strain from the stress strain curves. The adhesion strength (in kPa) was calculated as the maximum force divided by the overlapped area (as measured with a digital caliper).

Data processing

All raw data has been processed using Originlab or Microsoft Excel and statistical significance ($p < 0.05$) was determined using Students t-test.

Differential scanning calorimetry

Differential scanning calorimetry (DSC) measurements were performed using a Mettler-Toledo instrument operating at a heating/cooling rate of 10 °C min^{-1} with a range from -100 to 200 °C under an atmosphere of N_2. Data from the second heating cycle are reported unless indicated otherwise.

Atomic force microscopy (AFM) imaging

AFM imaging experiments were carried out on a commercial AFM (JPK Nanowizard 3 Ultra) in QI mode. A silicon cantilever (ScanAsyst Fluid+, Bruker) with typical tip radii of ~ 2 nm

and resonance frequencies of ~150 kHz was used for imaging. Before AFM imaging experiments, polymer film was compression molded at onto a silicon wafer at 80 °C for less than 10s. The polymer film on the wafer was then glued to a small petri dish. The petri dish was filled with 2-3 ml of PBS. AFM imaging was conducted after 30 min of equilibration. The image data and elastic modulus were analyzed using JPK data processing software.

Synthetic methods

General polymerization procedure (Polymer 6)

Radical inhibitors were removed from commercial monomers by passage through activated basic alumina. DMA, 2-(6-isocyanatohexylaminocarbonylamino)-6-methyl-4[1H]pyrimidinone, and UPy methacrylate (UPy-MA; (ureido-4-pyrimidinone)-hexyl-amide-ethylmethacrylate) were synthesized as previously reported.[56-58] An oven dried Schlenk flask equipped with a magnetic stirring bar was charged with UPy-MA (891 mg, 2.11 mmol), DMA (932 mg, 4.21 mmol), 2-ethylhexyl methacrylate (2.83 ml, 1.26 mmol), OEG20-MA (950 g mol^{-1}, 4.00 g, 4.21 mmol), AIBN (17 mg, 0.11 mmol) and anhydrous DMF (20 mL). The flask was sealed with a rubber septum and four freeze-pump-thaw cycles were performed after which the Schlenk was backfilled with nitrogen. The reaction mixture was heated to 80 °C for 5 hours and allowed to cool to room temperature. The crude mixture was precipitated into ice cold ether (350 mL) and additionally reprecipitated 2 times from a DCM/methanol mixture (8:2, 30 mL) into ice cold ether (350 mL). All volatiles were removed *in vacuo* for 36 hours to obtain a semi-clear elastic polymer. Colorless films (thickness = 200 μm) were prepared by compression molding between sheets of PTFE at 80 °C, 2000 psi for 1 min. We found that during polymerizations, only about half of the DMA in the reaction gets incorporated into the polymer; therefore, DMA feed amounts were doubled for all polymerizations. ^{1}H NMR (400 MHz, $CDCl_3$) δ 13.18, 11.88, 10.16, 6.84, 6.61, 5.89, 4.11, 3.85, 3.84, 3.68, 3.23, 2.70, 2.28, 2.07, 1.33, 0.93. GPC (RI) M_n = 42.6 kg/mol; polydispersity index, PDI = 1.4.

Polymers 1-5, 7-9

The same procedure was as in 6 (above) was followed, with varying monomer compositions. Any changes are noted below.

Polymer 1. Reactants: UPy-MA (600 mg, 1.42 mmol), DMA (627 mg, 2.83 mmol), butyl methacrylate (1.41 g, 9.92 mmol), AIBN (16.5 mg, 0.14 mmol) and DMF (20 mL). Product: The general polymerization procedure was used to yield Polymer **1** as brittle and light orange transparent solid. ^{1}H NMR (400 MHz, $CDCl_3$) δ 13.19, 11.91, 10.17, 6.84, 6.79, 6.65, 5.88, 4.36, 3.98, 3.30, 3.28, 2.77, 2.27, 1.67 - 0.90. GPC (RI) M_n = 10.5 kg/mol; polydispersity index, PDI = 1.9.

Polymer 2. Reactants: UPy-MA (600 mg, 1.42 mmol), DMA (630 mg, 2.83 mmol), OEG9-MA (500 g mol^{-1}, 4.96 g, 9.92 mmol), AIBN (17 mg, 0.15 mmol) and anhydrous DMF (10 mL). Product: The general polymerization procedure yielded Polymer **2** as transparent elastomeric solid. Due to the low glass transition and resulting stickiness of this material, it was necessary after compression molding to cool the polymer film and PTFE sheets to -80 °C to remove the PTFE sheets. ^{1}H NMR (400 MHz, $CDCl_3$) δ 13.14, 11.87, 10.12, 6.83, 6.81, 6.76, 6.59, 5.88, 4.11, 4.10, 3.67, 3.58, 3.41, 2.73, 2.28, 1.53, 1.39, 1.28, 1.02, 0.91. GPC (RI) M_n = 34.3 kg/mol; polydispersity index, PDI = 3.2.

Polymer 3. Reactants: UPy-MA (300 mg, 0.71 mmol), DMA (314 mg, 1.42 mmol), butyl methacrylate (282 mg, 1.98 mmol), OEG3-MA (200 g mol^{-1}, 596 mg, 2.98 mmol), AIBN (8mg, 0.07 mmol) and DMF (10 mL). Products: The general polymerization procedure was used to yield Polymer **3** as transparent hard solid. ^{1}H NMR (400 MHz, $CDCl_3$) δ 13.14, 11.87, 10.14, 6.85, 6.78, 6.77, 6.61, 5.88, 4.13, 3.97, 3.68, 3.59, 3.42, 3.27, 2.72, 2.27, 1.98, 1.63, 1.42, 0.98, 0.89. GPC (RI) M_n = 5.9 kg/mol; polydispersity index, PDI = 2.3.

Polymer 4. Reactants: UPy-MA (446 mg, 1.05 mmol), DMA (465 mg, 2.10 mmol), butyl methacrylate (484 mg, 3.40 mmol), OEG9-MA (500 g mol^{-1}, 1.98 g, 3.97 mmol), AIBN (12 mg, 0.11 mmol), and anhydrous DMF (10 mL). Products: The general polymerization procedure was used to yield Polymer **4** as transparent elastomeric solid. ^{1}H NMR (400 MHz, $CDCl_3$) δ 13.17, 11.87, 10.11, 6.85, 6.78, 6.61, 5.89, 4.13, 3.97, 3.68, 3.41, 2.70, 2.29, 2.28, 2.07, 2.03, 1.64, 1.63, 1.42, 1.29, 0.98, 0.92, 0.91, 0.91, 0.90, 0.89. GPC (RI) M_n = 23.6 kg/mol; polydispersity index, PDI = 3.4.

Polymer 5. Reactants: UPy-MA (200 mg, 0.47 mmol), DMA (209 mg, 0.95 mmol), butyl methacrylate (382 mg, 2.69 mmol), OEG20-MA (950 g mol^{-1}, 591 mg, 0.62 mmol), AIBN (8 mg, 47 μmol) and DMF (10 mL). Product: The general polymerization procedure was used to yield Polymer **5** as elastomeric solid. ^{1}H NMR (400 MHz, $CDCl_3$) δ 13.16, 11.88, 10.15, 6.85, 6.78, 6.61, 5.88, 3.97, 3.68, 3.60, 3.41, 3.27, 2.71, 1.98, 1.64, 1.42, 0.98, 0.89. GPC (RI) M_n = 9.7 kg/mol; polydispersity index, PDI = 2.3.

Polymer 7. Reactants: UPy-MA (600 mg, 1.41 mmol), DMA (627 mg, 2.83 mmol), lauryl methacrylate (2.40 ml, 8.49 mmol), OEG20-MA (950 g mol^{-1}, 2.89 g, 3.04 mmol), AIBN (12 mg, 0.07 mmol) and DMF (10 mL). Product: The general polymerization procedure was used to yield Polymer **7** as transparent elastomeric solid. ^{1}H NMR (400 MHz, $CDCl_3$) δ 13.17, 11.87, 10.14, 6.82, 6.77, 6.59, 5.88, 3.94, 3.66, 3.59, 3.41, 3.23, 2.73, 2.26, 1.63, 1.29, 0.91. Reliable PDI and molecular weight measurements could not be completed as polymer showed interaction with the GPC column.

Polymer 8. Reactants: UPy-MA (287 mg, 0.68 mmol), 2-ethylhexyl methacrylate (1.13 ml, 5.04 mmol), PEG20-MA (950 g mol^{-1}, 1.00 g, 1.05 mmol), AIBN (11 mg, 68 μmol) and DMF (10 mL). Product: The general polymerization procedure was used to yield Polymer **8** as white elastomeric solid. ^{1}H NMR (400 MHz, $CDCl_3$) δ 13.17, 11.91, 10.20, 5.87, 4.11, 3.86, 3.68, 3.42, 3.28, 2.29, 1.78, 1.58, 1.40, 1.33, 1.06, 0.93. GPC (RI) M_n = 33.3 kg/mol; polydispersity index, PDI = 1.3.

Polymer 9. Reactants: DMA (337 mg, 1.52 mmol), 2-ethylhexyl methacrylate (1.13 ml, 5.03 mmol), PEG20-MA (950 g mol^{-1}, 1.00 g, 1.05 mmol), AIBN (13 mg, 76 μmol) and DMF (10 mL). Product: The general polymerization procedure was used to yield Polymer **9** as transparent elastomeric solid. Due to the low glass transition and resulting stickiness of this material it was necessary after compression molding to cool the polymer film and PTFE sheets to -80 °C to remove the PTFE sheets. ^{1}H NMR (400 MHz, $CDCl_3$) δ 6.85, 6.77, 6.63, 4.11, 3.85, 3.68, 3.60, 3.42, 2.76, 1.89, 1.58, 1.41, 1.33, 1.06, 0.93. GPC (RI) M_n = 53.8 kg/mol; polydispersity index, PDI = 1.6.

Swelling of polymer films

PBS powder concentrate (Fisher) and DI water were used to prepare 1X PBS solution. Dry and films of polymer (between 5 and 10 mg each, n = 3) were submerged into PBS (20 mL) and the sample mass was monitored at pre-set intervals. Prior to weighing the samples, surface water was removed using a laboratory tissue (Kimwipe). The swelling ratio (in wt%) was calculated by subtracting the original dry mass from the swollen mass and dividing by the original dry mass.

Tissue adhesion studies

Lap shear tissue adhesion studies were conducted according to ASTM-2255-05 (Figure **S1**). In short, large polycarbonate (PC) films were cut into rectangular struts (6 x 1 cm) to which tissue and adhesives could be attached for mounting into the Instron. Untreated and freshly harvested bovine pericardium was purchased from Animal Technologies Inc. (Tyler, TX, USA), shipped on wet ice, frozen in liquid nitrogen, and stored at -80 ^{o}C. Prior to use, frozen tissue was thawed in excess PBS for at least 60 min. Freshly thawed and moist bovine pericardium was adhered on the rough (and fatty) side to the textured side of the PC strut with Loctite all-purpose liquid super glue. Subsequently, the tissue was trimmed around the edges to obtain struts with rectangular strip of bovine pericardium (**Figure 5.S1a**). As prepared struts were temporarily stored in PBS solution prior to use. Polymer films (200 μm thickness) were cut into 1 x 1 cm squares and adhered to polycarbonate struts using super glue. In cases in which $NaIO_4$ was used as oxidant, a piece of cotton wool soaked with $NaIO_4$ solution (0.1 M) was brushed on the adhesive polymer film for 5s and excess solution was removed via gentle blotting with a Kimwipe. Lap joints were prepared by overlapping (1 cm overlap) a strut with bovine pericardium with a strut with a polymer adhesive film and hand pressed together for 5 sec (**Figure 5.S1f**). Samples were submerged into PBS solution at 37 ^{o}C for 1h either using a mini binder clip (Office Depot brand) as clamping device or a 200g brass weight for each sample (**Figure 5.S1c**). After incubation, lap joints were removed from solution and subjected to a shear tensile test (strain rate = 5 mm min^{-1}) until failure. The shear adhesion strength (in kPa) was calculated as the maximum load divided by the initial overlapped area.

Determination of failure mode after shear adhesion tests

To determine the mode of failure, both the tissue strut and the strut with the adhesive patch were subjected to Arnow's stain after shear adhesion tests. The lap joints were submerged into a HCl solution (0.5M, 5mL) for 5 min, then transferred into a nitrating solution ($NaNO_2$, 0.1 g ml^{-1}; $NaMoO_4$, 0.1 g ml^{-1}) for 5 min and finally transferred into a NaOH solution (1 M, 5 mL) for 5 min. Images were recorded immediately after the staining on a white paper background. Cohesive failure was determined when reddish color was observed on the tissue surface, indicating that the adhesive patch had separated, leaving polymer residue (and therefore Arnow-stainable catechol) on the tissue surface. Adhesive failure was determined when the tissue only showed a light-yellow color due to the presence of phenolic amino acids and the absence of adhesive patch residue.

Burst tests

A piece of bovine pericardium was secured to a large piece of polycarbonate with super glue (Loctite liquid all-purpose); the edges were glued securely, and an area of approximately 4 sq cm was left unglued in the center. A 3 mm hole was punched through center of the tissue and PC using a biopsy punch (**Figure 5.S8a**). A round film of adhesive was shortly hand-pressed onto the pericardium, and incubated under a 200g brass weight for 1h in PBS at 37 ^{o}C. Then the PC/tissue/adhesive patch setup was mounted into the custom-made burst device, with a fluid-tight

seal forming between the device's gaskets and the PC (**Figure 5.S8b**). The device was inflated with PBS using an Orion Sage syringe pump at 10 ml min^{-1} until the adhesive polymer patch failed (**Figure 5.S8c**). The pressure at adhesive failure was measured in-line using an Additel 680 pressure gauge.

Adhesive patches with a polycaprolactone (PCL) backing were prepared by separately preparing thin (100 μm) films of adhesive polymer and of PCL (both at 80 ºC, 2000psi, 1 min) and then shortly compression molded in a sandwiched fashion at 500 psi for 15s to attach the 2 films together and form a PCL-backed adhesive patch.

Cytocompatibility studies

NIH 3T3 and CCD-32sk cells were cultured to sub-confluence in 96 well plates. Polymer films were conditioned in cell culture media (DMEM with 10% fetal bovine serum, 1% penicillin/streptomycin, and 10 mM HEPES) at a known concentration for 24 h at 37 ºC. Then, 100 μL of conditioned media was applied to cells. After growing with exposure to conditioned media for 24 hours, cells were cultured an additional 3 h in serum-free, neutral red supplemented media, following the protocol in ISO 10993-5. Control samples included cells with untreated media and cells cultured with media supplemented with sodium laurel sulfate (0.2 mg ml^{-1}, negative control). After neutral red staining, cells were rinsed with warm PBS, and lysed in a solution of 50% ethanol, 40% distilled water, and 10% acetic acid. Absorbance at 540 nm was measured on a plate reader and all wells were compared with untreated cells to calculate relative viability.

Supplemental Figures

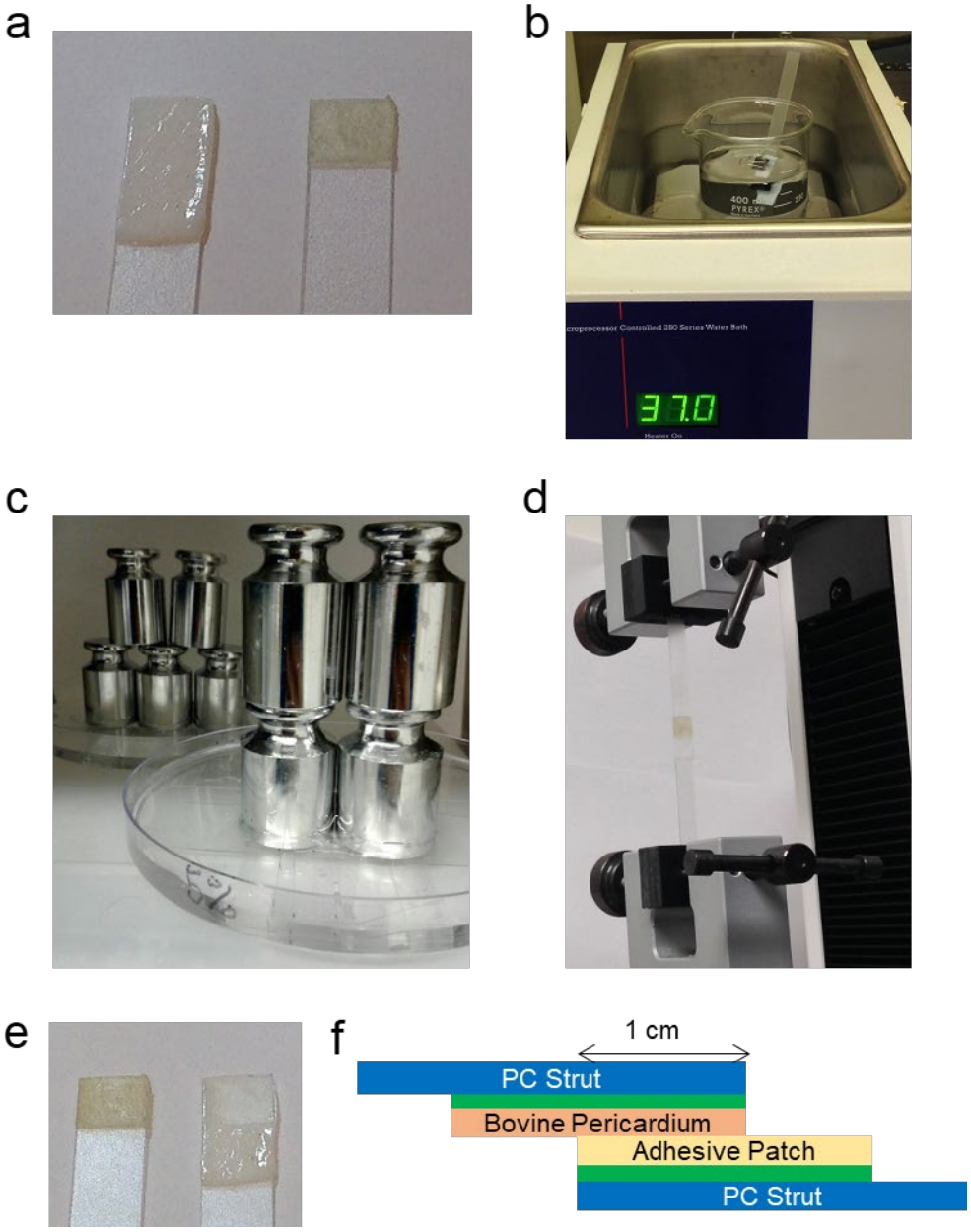

Figure 5.S1. Method used for tissue lap shear adhesion tests. a, Struts with bovine pericardium (left) and adhesive polymer (right) prior to formation of a lap joint. **b**, Incubation of a lap joint held together by a binder clip in PBS in a 37 ºC bath. **c,** Incubation of a set of lap joints pressed together with one 200g brass weight for each sample in PBS in an incubator at 37 ºC. **d**, Shear adhesion tensile test setup on an Instron mechanical tester. **e**, Image of a failed lap joint before Arnow's staining. **f,** Schematic of a cross-section of a lap joint of bovine pericardium tissue and adhesive patch samples, each adhered to a polycarbonate (PC) strut with super glue (green).

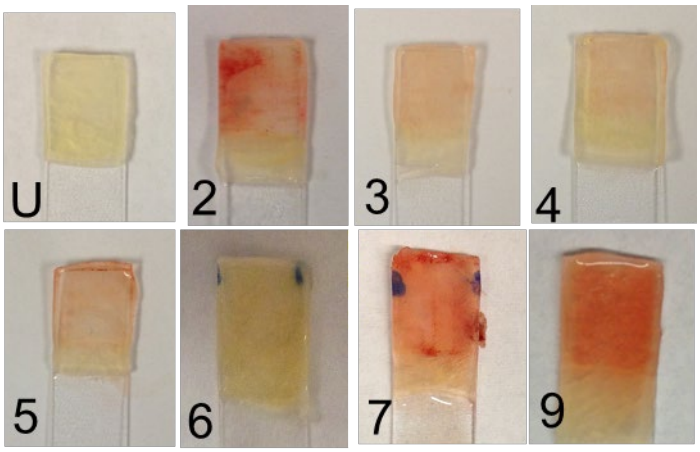

Figure 5.S2. Tissue from failed lap joints after Arnow's staining. Failed lap joints were stained with Arnow's stain. Unstained (U) tissue is shown along with tissue that had been in lap joints with the adhesive polymer patches (numbered). Data not shown for patches **1** and **8** due to low adhesion (**1**) and lack of catechols (**8**). Blue marks seen in **6** and **7** are Sharpie marks leftover from cutting the PC struts and do not influence samples or staining.

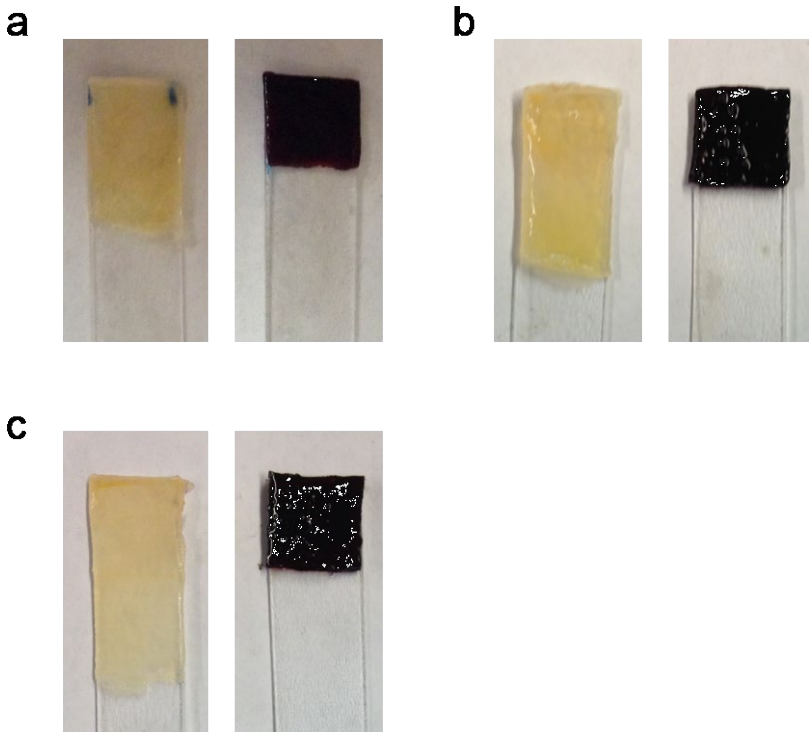

Figure 5.S3. Arnow's stain of lap joints after shear adhesion tests of Polymer 6 using different methods of incubation. During incubation for 1h in 37 ºC PBS, lap joints were (**a**) clamped with binder clips, (**b)** compressed with 200g brass weights, and (**c)** compressed with 200g brass weights after brushing adhesive polymer surface with $NaIO_4$ (0.1 M) for 5s before forming the lap joint with the tissue. Note that all samples exhibit cohesive failure (no reddish residue on tissue surface).

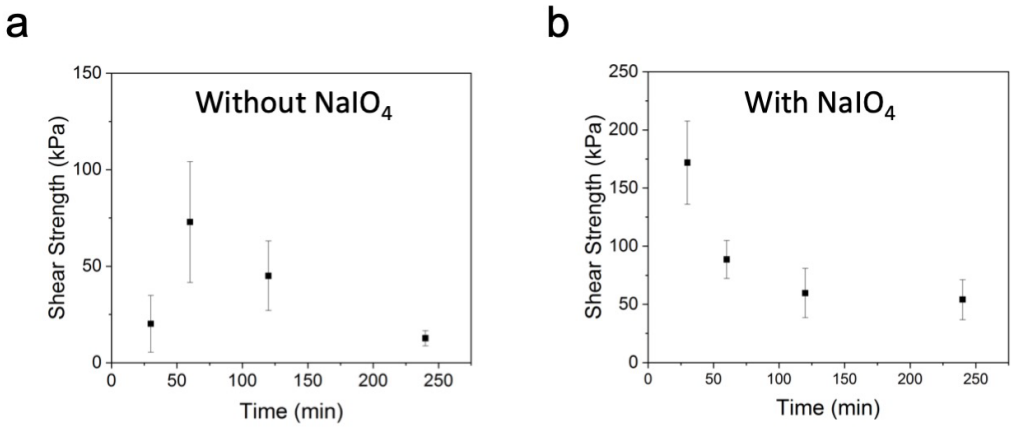

Figure 5.S4. Time dependent tissue adhesion experiments with and without oxidative crosslinker. a, Time dependent tissue adhesion strength of Polymer **6** that was incubated with 200g weights. **b**, Time dependent tissue adhesion strength of Polymer **6** that was incubated with 200g weights and brushed with $NaIO_4$ (c = 0.1 M, 5s).

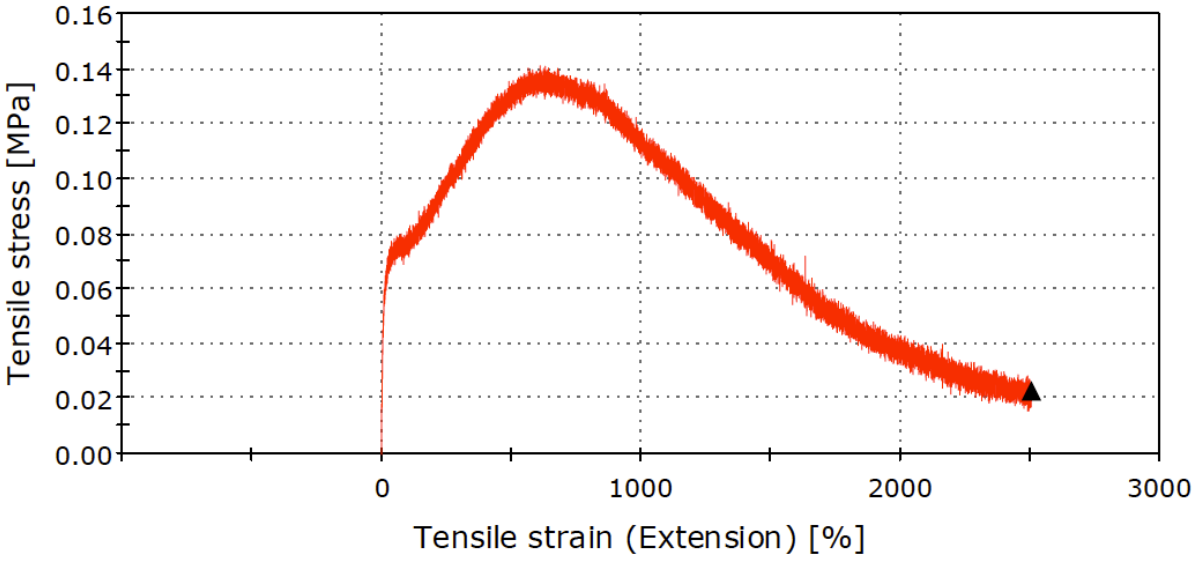

Figure 5.S5. Representative tensile test of Polymer 6 in the dry state (5% min^{-1}). Triangle indicates last collected datapoint, at the limits of the instrument.

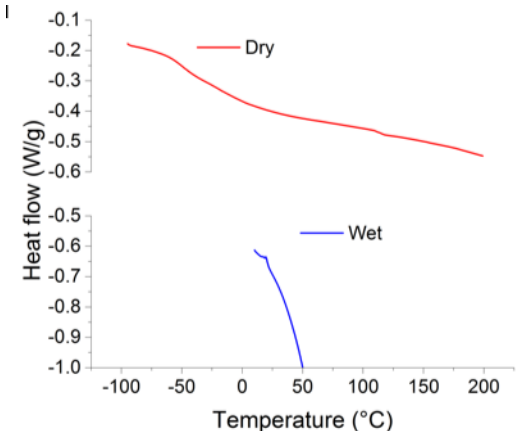

Figure 5.S6. Differential scanning calorimetry (DSC) traces of the second heating of Polymer **6** in the dry (—) and swollen (—) state at a heating rate of 10 ºC min^{-1} under a N_2 atmosphere.

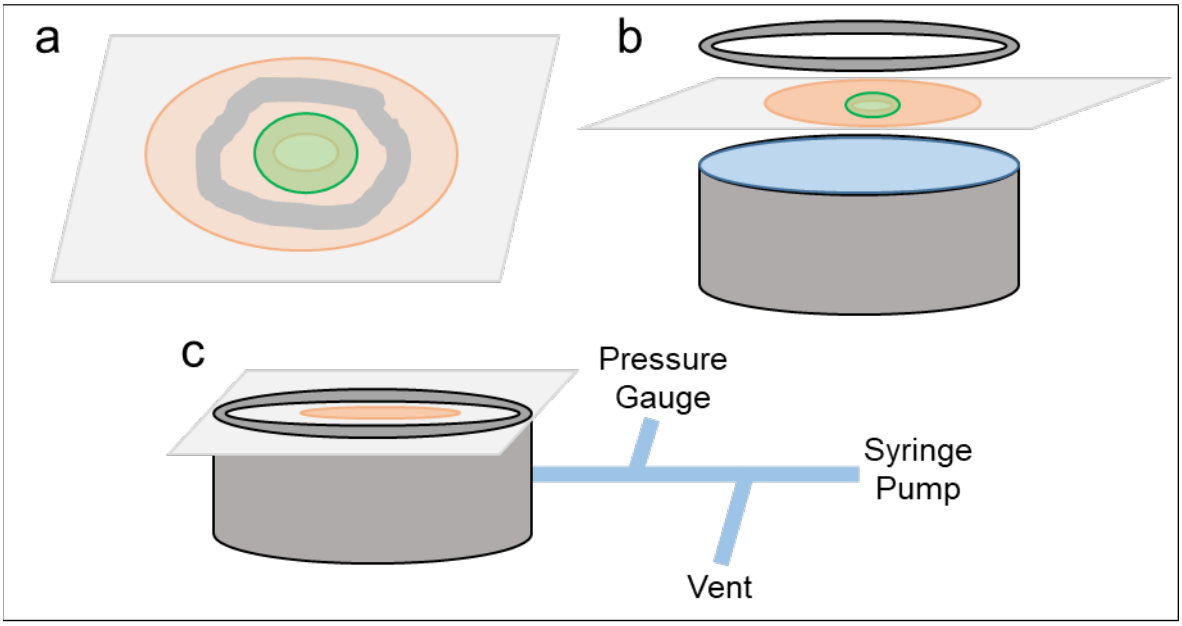

Figure 5.S7. Schematic of burst device chamber. **a,** Bovine pericardium (orange) affixed to polycarbonate (grey) with superglue. A 3mm hole is punched through the tissue and strut, and an adhesive patch (green) adheres to the tissue, covering the hole. **b,** Loading of the polycarbonate-tissue-patch into the fluid-filled burst device chamber. **c,** Diagram showing burst chamber inflation and measurement setup; the vent (liquid inlet) is closed during operation.

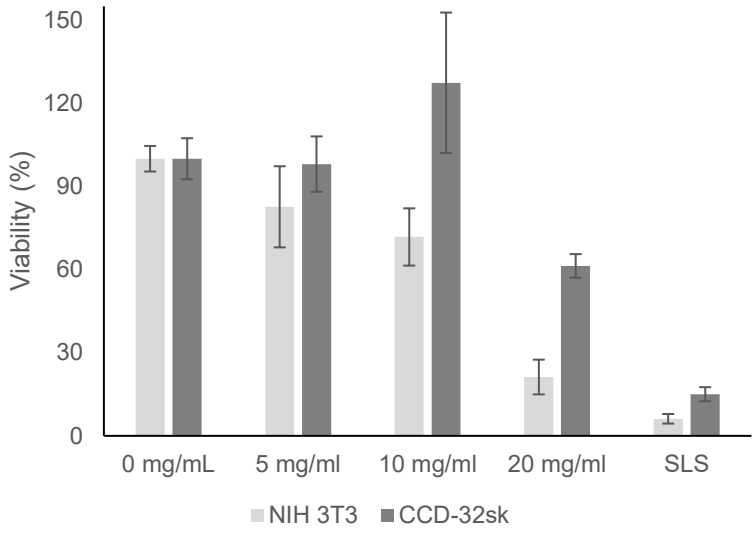

Figure 5.S8. Dose-dependent cytocompatibility of Polymer 6. NIH 3T3 and CCD-32sk cells were grown for 24h in media conditioned with Polymer **6**. Dose-dependent cell viability was seen. SLS = sodium lauryl sulfate. Mean ± SD of n ≥ 4 samples/condition.

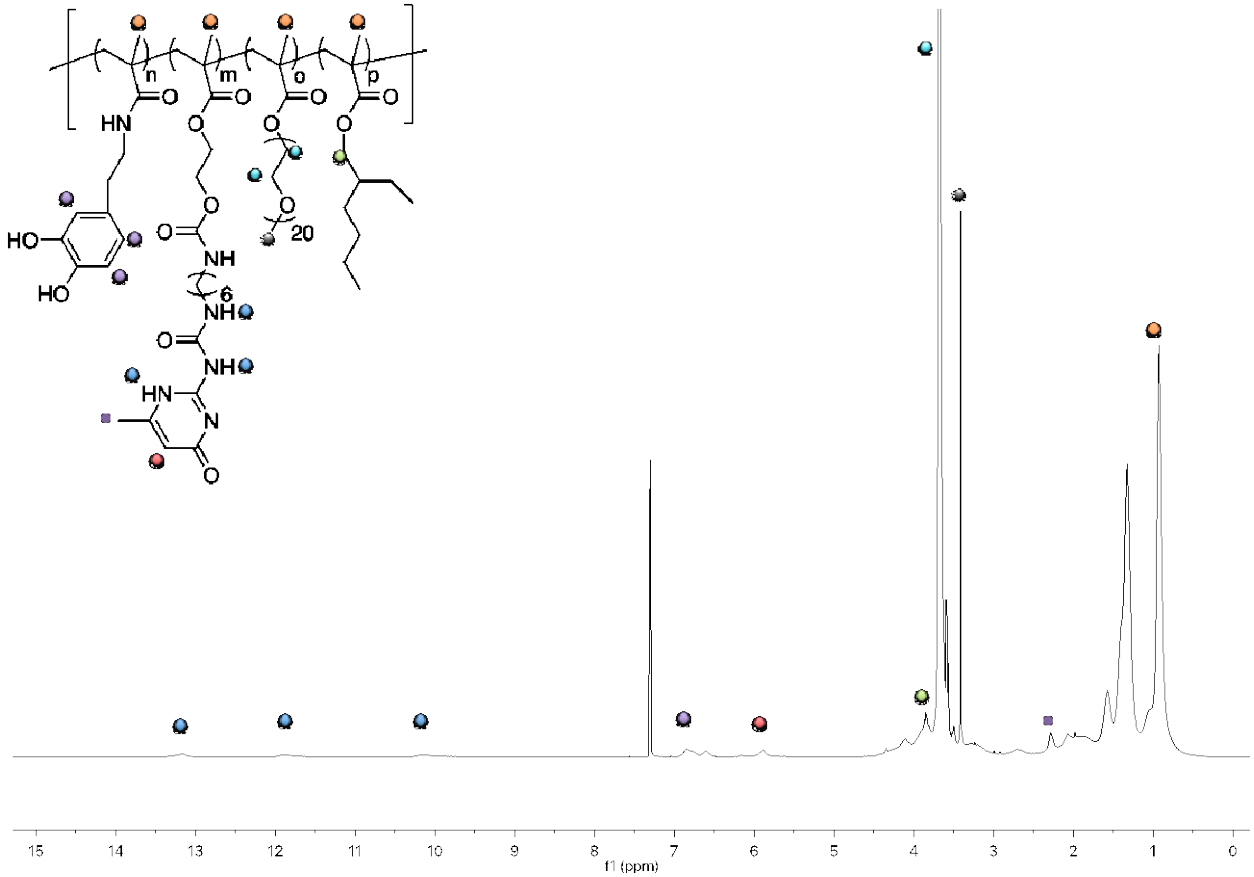

Figure 5.S9. ^{1}H-NMR spectrum of Polymer 6.

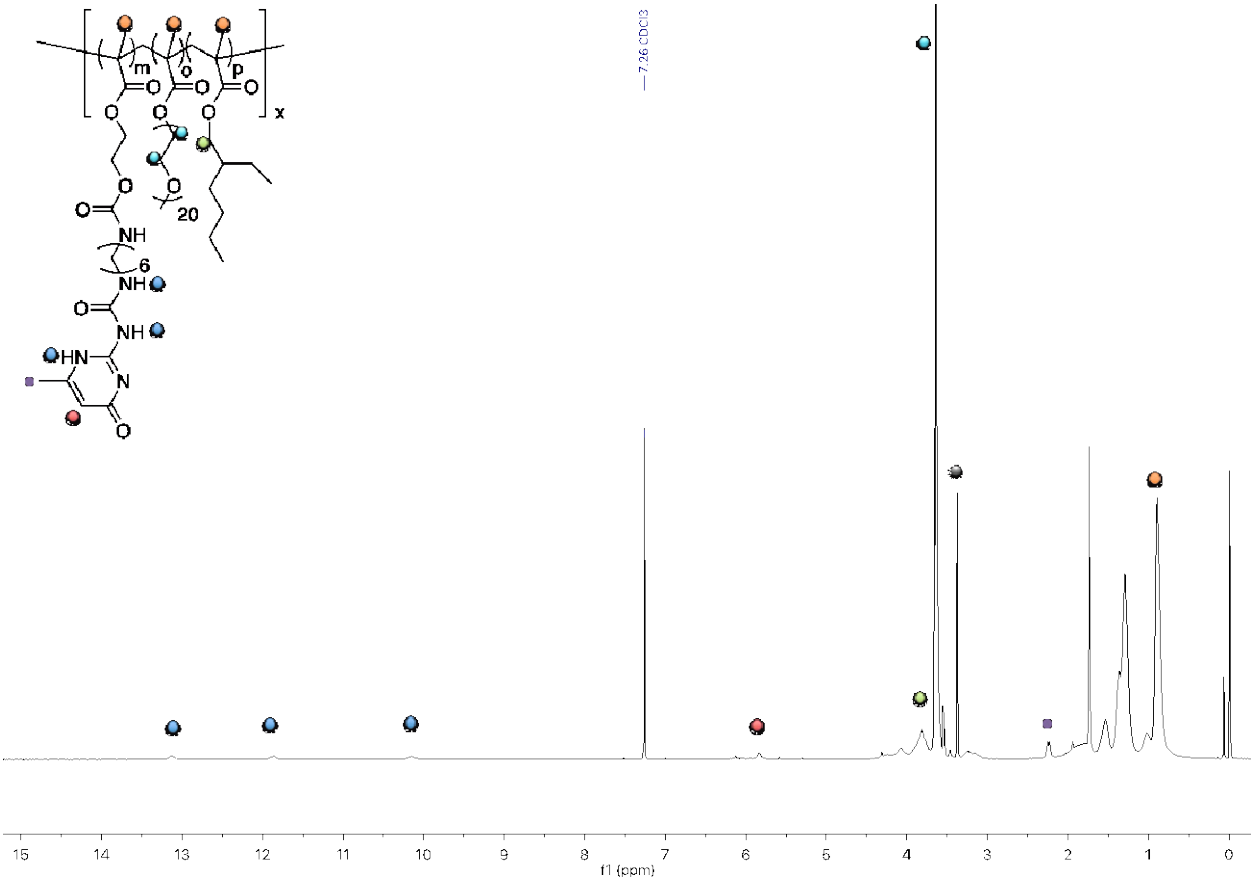

Figure 5.S10. ^{1}H-NMR spectrum of Polymer 8

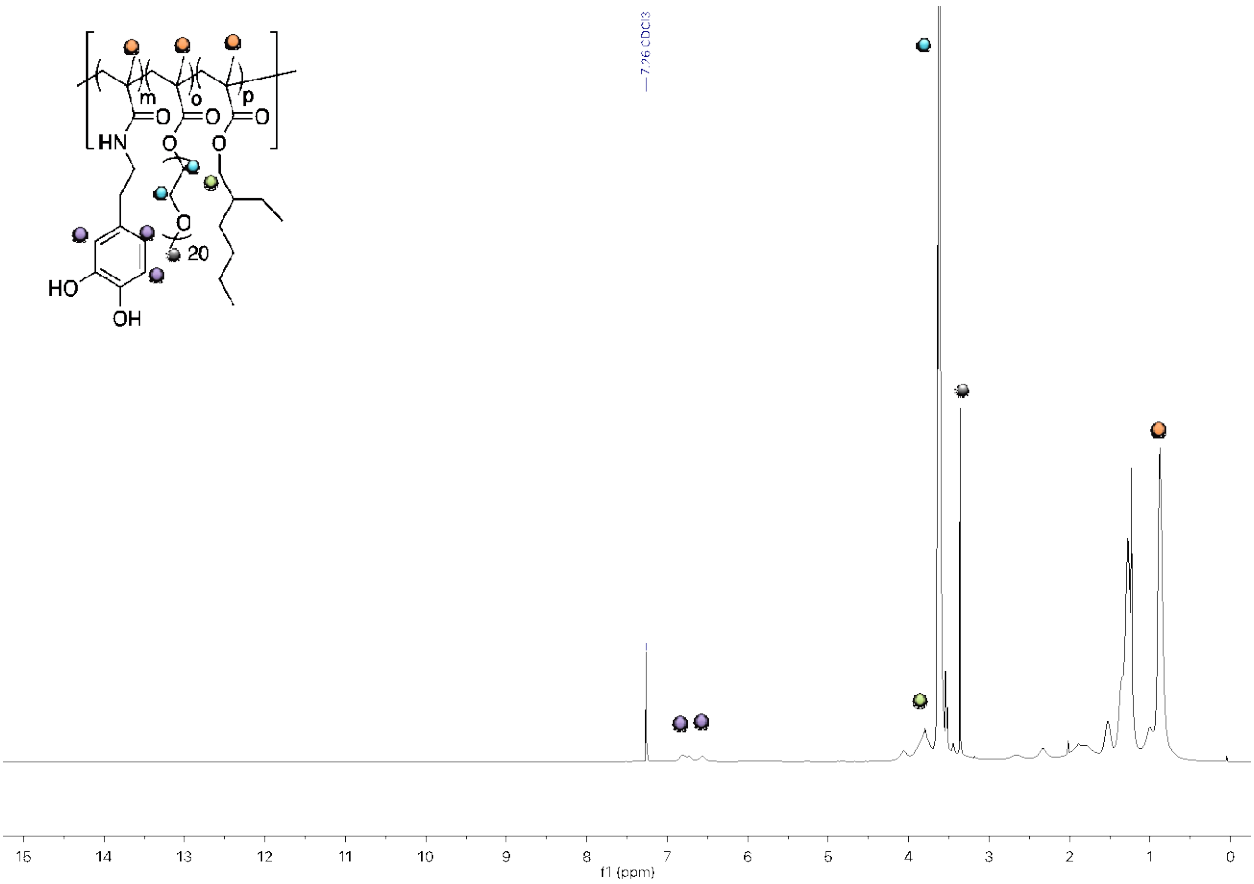

Figure 5.S11. ^{1}H-NMR spectrum of Polymer 9

Supplemental References

[56] H. Wu, V. Sariola, C. Zhu, J. Zhao, M. Sitti, C.J. Bettinger, Transfer Printing of Metallic Microstructures on Adhesion-Promoting Hydrogel Substrates, Adv. Mater. 27(22) (2015) 3398-3404.

[57] H.M. Keizer, R. van Kessel, R.P. Sijbesma, E.W. Meijer, Scale-up of the synthesis of ureidopyrimidinone functionalized telechelic poly(ethylenebutylene), Polymer 44(19) (2003) 5505-5511.

[58] E.B. Berda, E.J. Foster, E.W. Meijer, Toward Controlling Folding in Synthetic Polymers: Fabricating and Characterizing Supramolecular Single-Chain Nanoparticles, Macromolecules 43(3) (2010) 1430-1437.

CHAPTER SIX – HUMAN FETAL MEMBRANES AS A MODEL FOR BIOMATERIALS ANALYSIS AND DRUG-TISSUE RESPONSE

6.1 Summary

In developing adhesives for presealing the human fetal membranes, it is important to be able to learn as much as possible about the effect of these materials on the fetal environment before progressing to *in vivo* studies. In particular, the cells of the fetal membranes are in close contact with the adhesives and understanding these tissue-material interactions is key. We obtained fresh human fetal membranes from patients undergoing elective Cesarean sections at UCSF Moore Women's hospital, and developed methods to culture the membranes *ex vivo* and to extract amnion cells from these tissues and culture them *in vitro*. These cells and tissues were used to assess the cytocompatibility of novel polymer tissue adhesives developed in Chapters 3 and 4. We are also interested in understanding how the small-molecule regenerative drug 1,4-dihydrophenonthrolin-4-one-3-carboxylic acid (DPCA) interacts with the human fetal membranes and if it can induce an *in vitro* healing response in these tissues, which notoriously do not heal *in vivo*. Here, we also discuss the development of an *ex vivo* organ culture model to study DPCA-human fetal membrane interactions.

6.2 Background and innovation

The fetal membranes, the amnion and chorion, are two closely-associated membrane tissues that line the uterus and surround the fetus and amniotic fluid during pregnancy. Spontaneous or iatrogenic damage to these membranes can lead to preterm labor, membrane infection, amniotic fluid leakage, and poor fetal outcomes [1, 2]. Studying fetal membrane properties as a means for understanding the health of the mother and fetus goes back centuries. For example, in 1869, Scottish obstetrician James Matthews Duncan, studied the burst strength of 100 membrane samples from 36 patients, in an attempt to calculate the forces exerted by the mother and experienced by the "adult fetus" during term labor [3]. He calculated the "power of the labour" that would have been required to burst each membrane (mean: 16.7 lbs), and noted that amnions from mothers who delivered less than 0.5 h after membrane rupture had stronger mechanical properties. Subsequent work has analyzed the mechanical properties of the human fetal membranes [4], investigated decellularized fetal membranes as a scaffold for wound healing and tissue engineering [5], explored the membranes as a source of human stem cells [6, 7], and sought to understand the membranes' crucial role in maintaining and supporting pregnancy [2]. A new area of investigation crucial to the development of fetal membrane sealants is the use of fetal membranes in biocompatibility or cytocompatibility studies of novel biomaterials [8] and to analyze drug-tissue responses *in vitro*.

Compared to other tissues, the fetal membranes are relatively available for researchers' study. Following vaginal or Cesarean section births, they are usually discarded along with the placenta as medical waste. For studies of the biological and mechanical properties of the membranes or membrane-derived cells or materials, membranes from planned (elective) Cesarean sections are preferred, since they have not undergone the strains of labor. Additionally, since the membranes are thin, almost two-dimensional structures, culturing them *ex vivo* and extracting their cells for *in vitro* culture is more straightforward than other tissue types. *Ex vivo* cells and tissues of the fetal membrane are unique tools to study and develop new biomaterials and drug therapies.

They can address some of the limitations of animal models, *in vivo* studies with established cell lines, and placenta- and membrane-on-a-chip technologies [9, 10]. Thus far, these opportunities have been largely underexplored. Here, we cultured *ex vivo* fetal membranes and extracted amnion cells with media conditioned with experimental fetal membrane adhesives to achieve a more clinically relevant tissue- and cytocompatiblity profile. We also performed initial assessments of how these cells and tissues would respond when treated with DPCA, a small molecule drug target that has been shown to initiate regenerative healing in adult mammals, and could potentially be used for healing fetal membrane defects *in vivo*.

6.3 Development of cell and tissue culture models of human fetal membranes

Human fetal membranes were obtained from patients undergoing non-emergent (planned) C-section deliveries at UCSF Moore Women's Hospital. Patients were deidentified, so no informed consent was needed per the UCSF IRB; however, per the UCSF maternal-fetal medicine research guidelines, staff asked patients' permission and patients were free to donate their membranes or not.

There are published protocols for culturing human fetal membranes *ex vivo* and for extracting amnion and chorion cells from these membranes [11-17]. Working from these protocols, our optimized protocols for culturing membranes and extracting and culturing cells are below (Methods and Appendix 6A). Key insights in the development of these methods include decreasing the time between membrane harvest and culture, ensuring sterile work flow, and careful filtration techniques. In our hands, amnions, chorions, and the membrane bilayer could be cultured *ex vivo* in pieces approximately 1 cm^2 for 10 days, as measured with calcein am/ethidium homodimer 1 live/dead staining (**Figure 6.3.1**). This tracks with other reported studies of amnion membranes. [14]. Some protocols called for culturing these membranes in transwell plates or other substrates [14, 18], but we had success in regular tissue culture plates of 12 or even 24 wells.

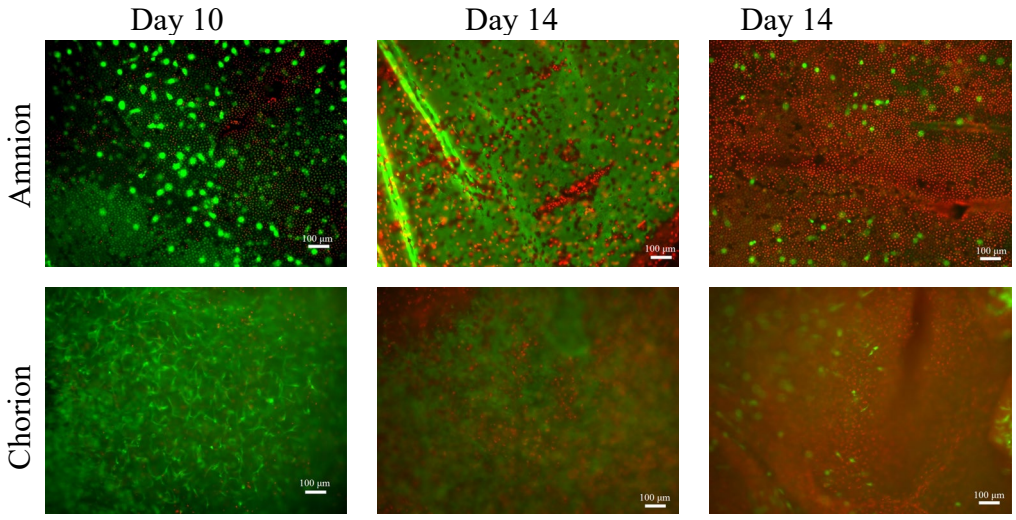

Figure 6.3.1. Live/dead staining to monitor viability of amnion and chorion membranes in culture over time. Cell viability remained robust up to 10 days, but some samples exhibited significant cell death after 14 days. All images are composite images of red (ethidium homodimer 1) and green (calcein AM) channels. Scale bar is 100 µm.

We also sought to isolate cells from fetal membranes. Despite repeated efforts, extraction of chorion cells was not as successful as amnion cell extraction. We attributed this to the thinner amnion membranes being more susceptible to digestion and cell release in the collagenase cocktails. After mincing and serial digestion, amnion tissue is usually almost completely liquefied, but a significant fraction of chorion tissues remained undigested, and must be filtered. Future efforts for chorion cell culture could focus on longer incubation times, or better filtration methods. Our optimized method for amnion cell extraction is in Appendix 6A. We could culture amnion cells for up to two weeks with excellent viability (**Figure 6.3.2**), as measured with calcein am/ethidium homodimer 1 live/dead staining.

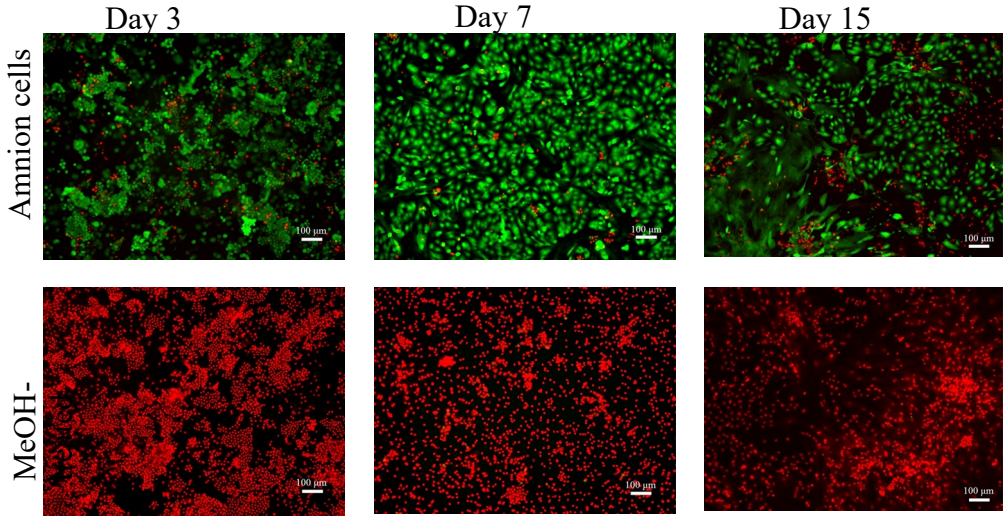

Figure 6.3.2. Live/dead staining to monitor viability of extracted amnion cells for up to 15 days. Cell viability remained robust throughout the experimental timeline. All images are composite images of red and green channels. Negative control images contain cells that were killed with 70% methanol. Scale bar is 100 µm.

Future work in this area is ongoing, and includes separately extracting and culturing amnion epithelial and mesenchymal cells, and using antibody staining, FACS sorting, and qPCR to identify stem cell marker expression in these tissues. Identifying reliable stem cell markers in these tissues *in vitro* and how they change in the membranes over time will be key in our efforts to study regenerative drugs and their potential to heal the fetal membranes (see Section 6.4). Additionally, our cultures were successful despite using a relatively simple culture medium with few additives; other reported protocols call for including additional growth factors and nutrients, particularly when maintaining stem-like cell populations [12, 16, 18]. This could be an avenue for additional future exploration as we seek to enable regeneration of these tissues.

6.4 Human fetal membranes for biomaterials analysis

Once we established *ex vivo* human fetal membrane and amnion cell cultures, we sought to study cyto- and tissue-compatibility of the experimental fetal membrane sealants developed in Chapters 2 and 3. Amnion cell cultures were tested in conditioned media assays with experimental sealants, and viability was measured with both live/dead and neutral red assays. Characteristic results for live/dead and neutral red staining are shown in **Figures 6.4.1** and **6.4.2**, respectively.

For all adhesives tested, viability was above the 70% threshold prescribed by the ISO standard (10993-5). In fetal surgery biomaterial compatibility studies, cultures of amnion cells also are more clinically relevant than using other established mammalian cell lines. However, one disadvantage is that they grow more slowly than other cell types, so longer culture times may be necessary to reveal potential cytotoxicity effects.

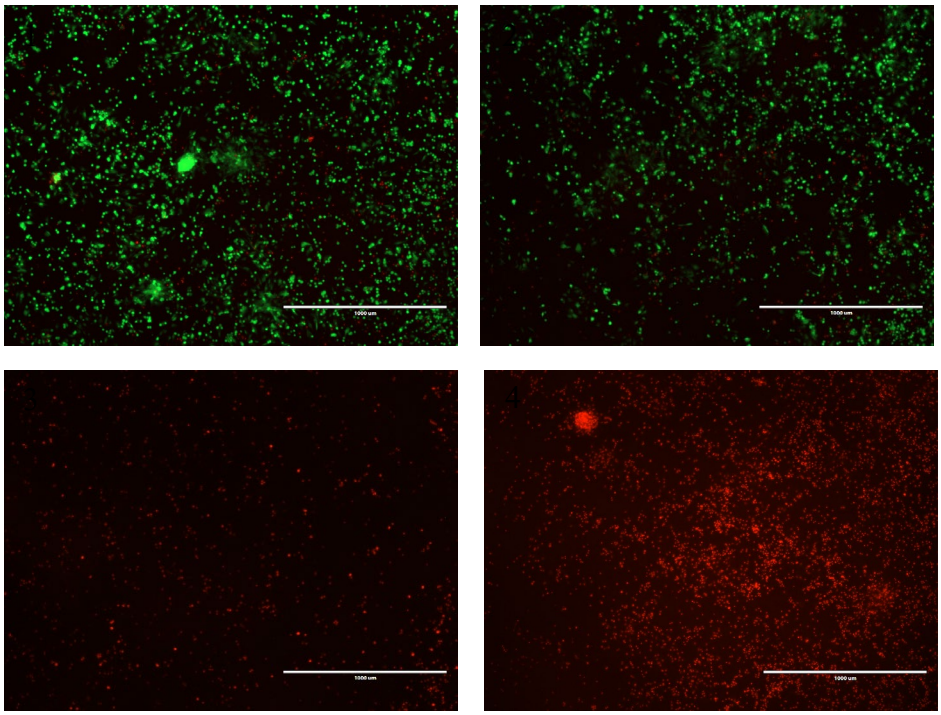

Figure 6.4.1. Live-dead staining of extracted amnion cells with conditioned media. Images are overlays between red (ethidium homodimer 1) and green (calcein AM) channels. Top left: Media conditioned with PEG-DOPA-Cys for 24. Top right: Control cells conditioned with untreated media. Bottom left: Dead control with added SLS. Bottom right: Dead control with added MeOH. Scale bar: 1000 µm

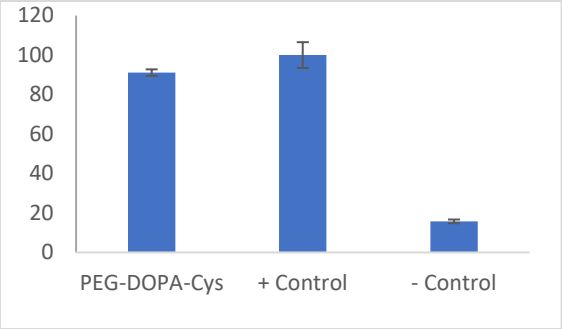

Figure 6.4.2. Viability of extracted amnion cells cultured with media conditioned with mussel-inspired adhesives. Values are normalized to the positive control (media only). Negative control cells were grown with SLS to kill cells. Error bars: SD of ≥3 wells.

Whole membranes, amnions, and chorions were also cultured in direct contact with adhesive gels (PEG-Cys/PEG-NHS) for 24-48h and then live/dead stained to monitor cell viability, which appeared robust (Figure 6.4.3). Further work in this space could include additional staining

to understand what, if any, cellular or immune response the adhesives induce in the cells and tissues. Understanding the effect of these materials on *ex vivo* human fetal membrane tissues is a huge advantage relative to cell culture, as is the relative availability of tissue samples compared to other tissue types.

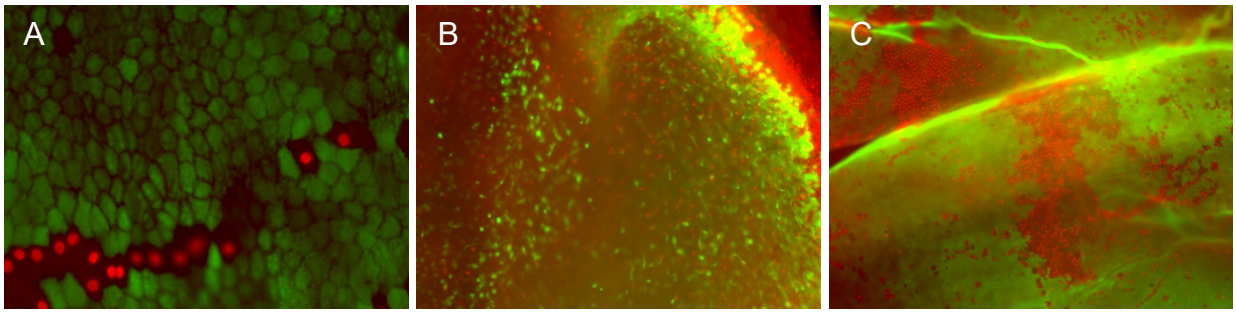

Figure 6.4.3. Characteristic images of live/dead staining of fetal membranes cultured in direct contact with PEG-Cys/PEG-NHS. Amnion (A, C) and chorion (B) tissues were cultured for 24 (A) or 48 (B, C) hours. Images were acquired through the adhesive gel (A, B), or after the gel had been gently removed (C). Overall, viability was good, but some cell death was noted, especially after 48h of culture in direct contact with the gel.

6.5 Regenerating human fetal membrane cells and tissues with DCPA

After tissue or limb injury or disease, adult mammals cannot usually heal regeneratively, and scarring or loss of function are common [19]. In particular, the human fetal membranes do not heal following surgical or spontaneous cut, puncture, or rupture [20, 21]. In parallel to our efforts to develop fetal membrane sealants, we sought to study the regenerative drug 1,4-dihydrophenonthrolin-4-one-3-carboxylic acid (DPCA) in *ex vivo* tissue culture models of the human fetal membrane cells and tissues, with the aim of eventual translation to animal models, then clinical use. This would not only be the first study of DPCA in human tissues (past studies of DPCA have been in rodent models and established human and other mammalian cell lines [22-25]), but also could establish the human fetal membranes as an *in vitro* model for understanding drug-tissue interactions, bridging the gaps between 2D cell culture, animal models, and human clinical trials. Work on this project was unfortunately halted due to COVID-19 campus closures. While incomplete, the progress thus far will provide a significant stepping stone for other lab members to continue this work once labs (and particularly human fetal membrane collection) can fully reopen.

Hypoxia-inducible factor 1-alpha (HIF1a) is a transcription factor and important regulator of many cell processes including development, hypoxic response, and regenerative healing [26]. Extensive work from our collaborator Dr. Ellen Heber-Katz and others has identified DPCA as a potent, indirect regulator of HIF1a. DPCA inhibits the activity of prolyl hydroxylases (PHDs), preventing PHDs from tagging HIF1a for degradation. Treatment with DPCA is expected to increase basal HIF1a levels in the cytoplasm and nucleus, leading to increased expression of regenerative genes at an injury site [22]. Previous work has identified several stem cell markers that are upregulated in mammalian cells after treatment with DPCA, including NANOG, Pax7, Nestin, Oct3/4, Pref-1, and CD133 [22, 23]. We wanted to see if a similar change in protein expression could be identified following DPCA treatment of our human fetal membrane cells and tissues.

We successfully cultured both human fetal membranes and extracted amnion cells with DPCA and developed antibody staining methods for cells and tissues. We were able to incorporate DPCA, which is fairly insoluble, into cell culture media at up to 50 µg/mL. We found that amnion cells were cytocompatible (>70% viability relative to untreated cells) with DPCA for 24h at up to the highest studied dose, 50µg/ml (**Figure 6.5.1**). We also sought to understand whether DPCA was acting on these cells to change expression of relevant proteins, HIF1a and stem cell markers. In protocols culturing DPCA with amnion cells or tissues for 24h at 20-50 µg/mL, antibody staining results were inconclusive, despite extensive optimization. Antibody staining of membrane tissue and extracted amnion cells are shown in **Figures 6.5.2** and **6.5.3**, respectively. Our optimized protocol for directly imaging the tissues is in Appendix 6B, though obtaining clear images with an entire field of view in focus remained challenging. Frustratingly, staining results were highly variable from day to day, but ultimately, no robust evidence that DPCA caused upregulation of HIF1a or of these stem cell markers was found in amnion cells or fetal membrane tissues at the studied concentrations or timescales (20-40 µg/mL, 24h), which was surprising given past literature findings that DPCA causes these changes in protein expression in other cell types [22].

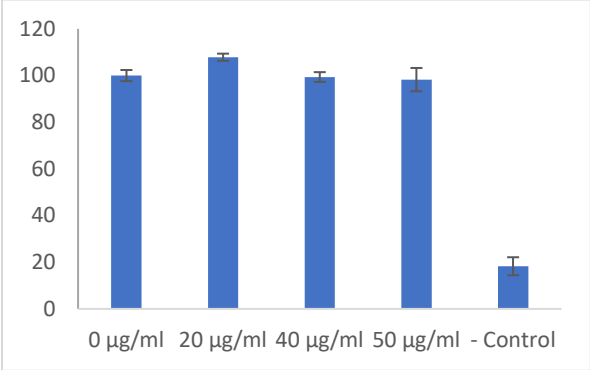

Figure 6.5.1. Dose-response viability of amnion cells cultured with DPCA for 24h. Amnion cells *in vitro* appear to have higher tolerance for DPCA than other cell lines; this could be due to their slower growth. Values are normalized to 0 µg/mL; negative control cells treated with SLS.

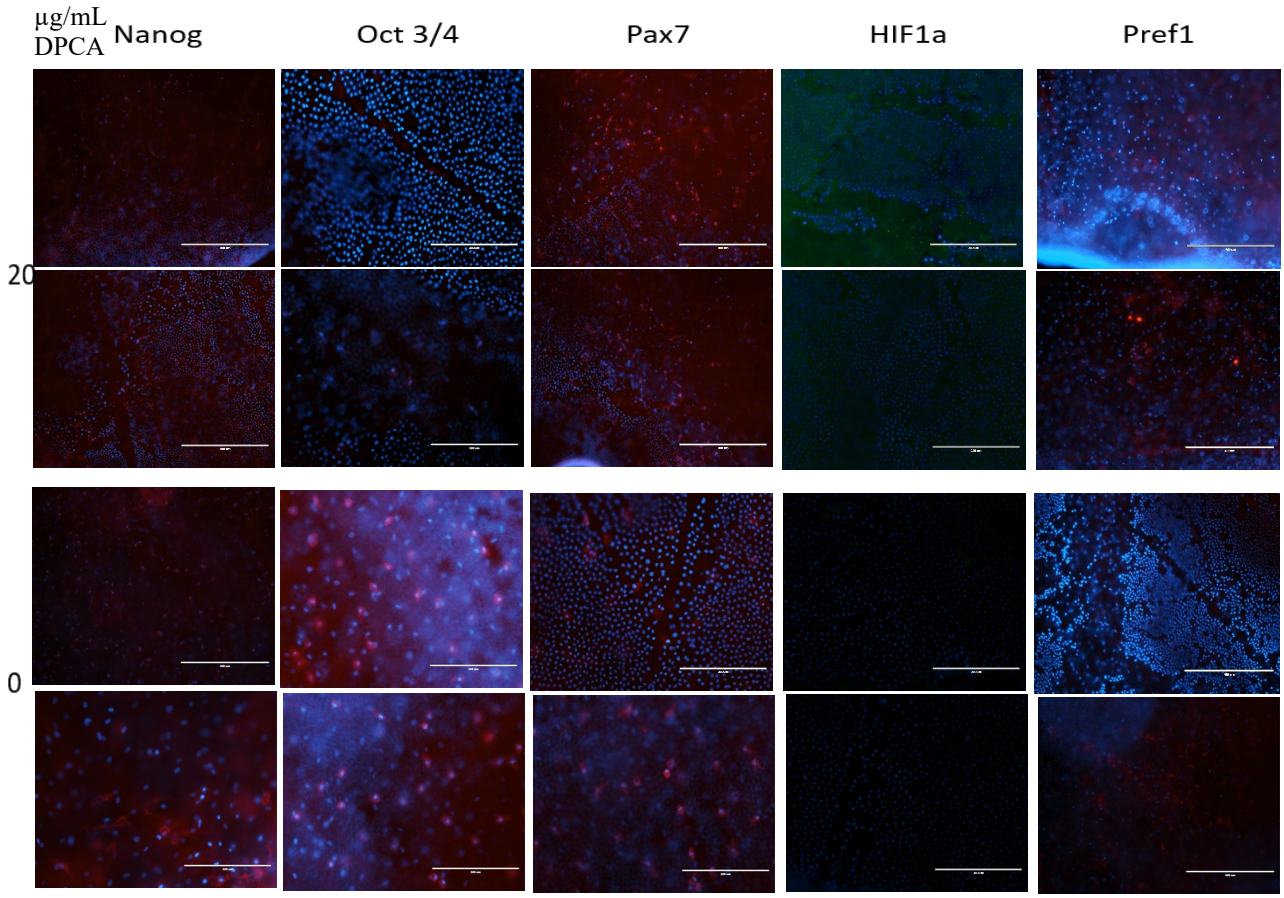

Figure 6.5.2. Antibody staining of fetal membranes cultured with DPCA. These images are characteristic of our findings in multiple attempts to quantify changes in protein expression after treatment of fetal membrane tissue with DPCA. In addition to difficulties imaging through membrane tissues (optimized protocol shown in Appendix 6B), results were highly variable day-to-day and membrane-to-membrane. Blue: DAPI. Red, green: secondary antibody fluorophores. Scale bar: 200 µm.

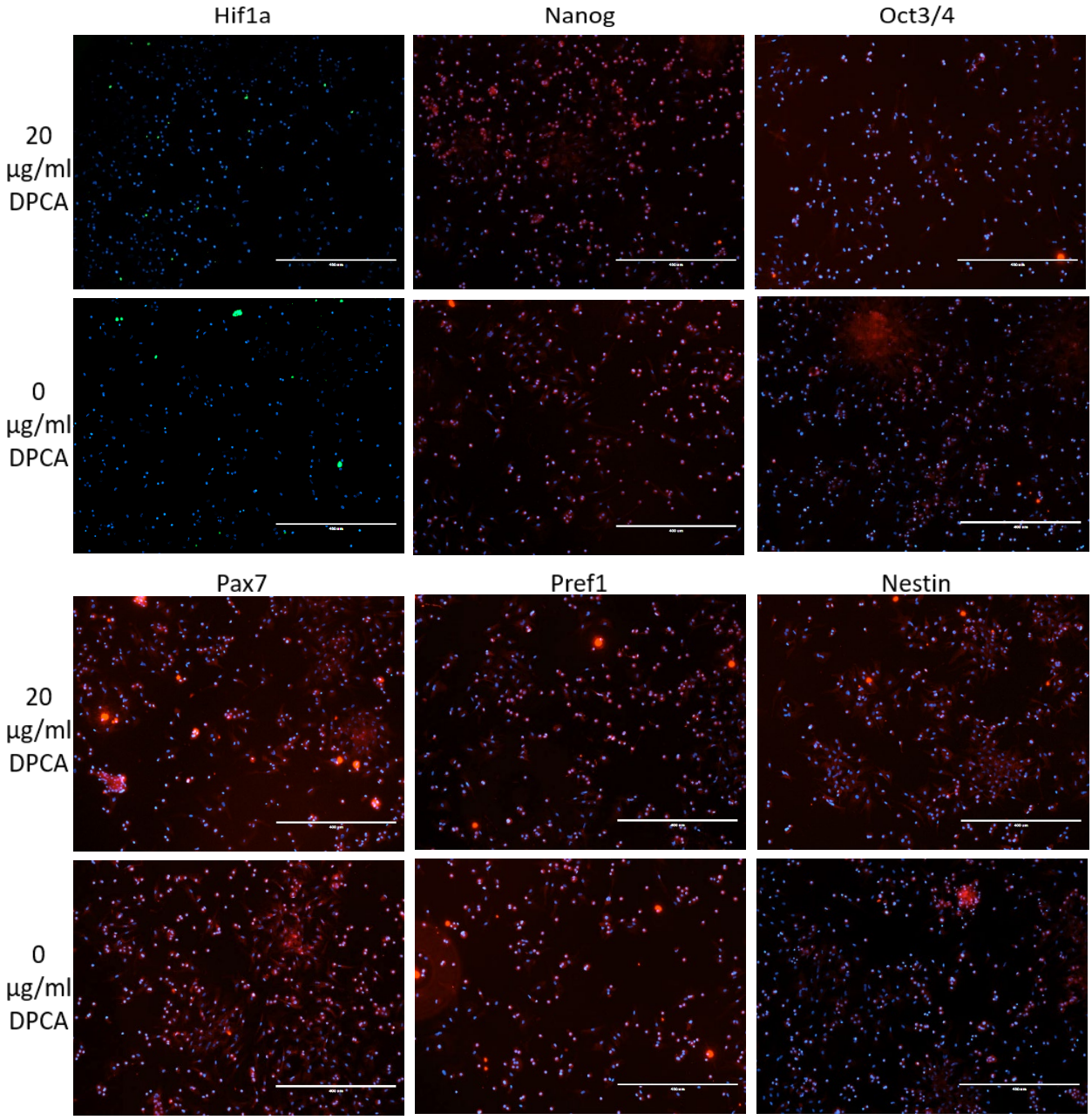

Figure 6.5.3. Antibody staining of DCPA-treated amnion cells. These images are representative of what we found in repeated attempts at multiple doses of DPCA; it was challenging to identify differences protein expression between DPCA-treated and untreated cells. Blue: DAPI. Red, green: secondary antibody fluorophores. Scale bar: 200 µm.

In an effort to overcome this and identify changes in protein expression, we pursued two alternate strategies. The first was to increase the concentration of DPCA, without affecting cell viability. To do this, DPCA was first dissolved in DMSO, further diluted into cell culture media up to 200 µg/mL, and cultured on cells for shorter times (e.g., 4h). Another strategy was to use

qPCR to identify RNA expression of the target genes of interest. Both of these avenues were cut short due to the coronavirus pandemic, but postdoctoral scholar Jisoo Shin has been successfully pursuing them in recent weeks.

6.6 Conclusions, threads to pick up, and future work

This work has established human fetal membrane cells and tissues as a valuable research and discovery tool for our lab, not only as a primary tissue for investigating tissue-biomaterial interactions, but also as a way to evaluate the effects of small molecule drugs on readily available *ex vivo* human tissues. Following on the work presented here, we identified that the next steps would be to use DMSO to enable higher DPCA concentrations in culture; establish protocols to separate extracted amnion cells into epithelial and mesenchymal cultures; perform qPCR analysis DPCA-treated cells and tissues; and monitor *ex vivo* healing of scratched and punctured human fetal membrane tissues. While this work was put on hold due to the global coronavirus pandemic, exacerbated because of ongoing restrictions on tissue collection at UCSF, since the lab's reopening, postdoctoral scholar Jisoo Shin has made excellent progress validating many of our hypotheses. Specifically, in treating amnion cells with higher concentrations of DPCA for shorter times, she was able to induce HIF1a and stem cell marker expression, as verified by the antibody staining. Also, she successfully separated and identified amnion mesenchymal and epithelial cells in culture. qPCR analysis of DPCA-treated cells is also ongoing. Extracted amnion mesenchymal and epithelial cells are stored in liquid nitrogen, but any work with fresh tissues remains on hold until the reopening of research sample collections at UCSF. We are the first to treat human tissues and primary cells with DPCA, and going forward, healing the human fetal membrane, a non-healing tissue, with DPCA remains a promising avenue of investigation for our lab.

6.7 Methods

<u>Membrane procurement, processing, and culture</u>

Membranes were dissected from the placenta by UCSF research staff, leaving approximately 1-2 inches of membrane attached to the placenta. Membranes were rinsed in HBSS buffer supplemented with amphotericin B (0.2 µg/mL) and penicillin/streptavidin (1%) and stored in a sealed container with fresh supplemented HBSS buffer in the refrigerator. Membranes were stored for less than 1 hour, and then transferred to a cooler with ice packs and brought by car to the research lab. In a tissue culture hood, membranes were further rinsed with PBS, and large blood clots were removed. When necessary, amnion and chorion were separated bluntly. Membranes were cut (either as a bilayer or individually) using a scalpel and straight edge and put in 12-well tissue culture plates (~1 cm squares) for longer-term culture or 10 cm tissue culture dishes (~5 cm squares) for subsequent cell extraction. Cells and membranes were cultured in 1:1 DMEM:F12 media with 10% FBS, 1% penicillin/streptavidin, 100 mM HEPES, and 0.2 µg/mL amphotericin B. Incubators were kept at 37 C, 5% CO_2, and media was changed every day. Membranes from which cells were extracted for *in vitro* culture were incubated from 0.5-24h prior to cell extraction; amnion cell extraction and culturing protocols are included in Appendix 6A.

<u>Media conditioning, direct-contact cytocompatibility, and DPCA preparation</u>

Media conditioned with biomaterials was prepared as described in Chapter 3. Subsequent viability analysis was performed with neutral red (see Chapter 3) or live/dead (see below) staining assays.

Direct-contact cytocompatibility tests were performed by combining ~20 µL of each adhesive component, rapidly mixing, and pipetting onto amnion, chorion, or whole membrane (amnion/chorion bilayer) tissues. Then tissues were cultured as described above.

To add DPCA to the media, DPCA was first added to a solution of cell culture media at about 1 mg/ml, vortexed for around 5 minutes, and incubated at 37 C for 0.5-18h. The solution was then sterile filtered with at 0.2 µm filter, and returned to 37 C while an aliquot was further diluted in ACN and water for HPLC analysis. HPLC traces were compared to a standard curve of known DPCA concentrations to determine the concentration of the solution. Following this process, final DPCA concentration was usually around 40-80 µg/ml. This solution was further diluted in warm cell culture media to 20-50 µg/mL before being added to pre-plated cells or fetal membrane pieces, usually for a 24h incubation.

Calcein AM/ethidium homodimer 1 staining

Cells and tissues were stained with calcein AM and ethidium homodimer 1 to detect cells that are metabolically active (i.e., live) or have damaged membranes (i.e., dead), respectively (Kit: LIVE/DEAD ® Viability/Cytotoxicity Kit for mammalian cells, Thermo Fisher). Adherent amnion cells were stained following the kit's protocol. Briefly, cells were gently rinsed with warm PBS, then stained with a warmed PBS or serum-free media solution containing 2 µM calcein AM and 4 µM ethidium homodimer 1. Cells and dyes were incubated for 10-20m at 37 C, rinsed again with warmed PBS, and imaged with the Keyence or Evos microscopes using the appropriate green and red fluorescence filter cubes. Cells killed with 70% methanol (room temperature, 30m) served as a negative control.

After working optimize the protocol for fetal membrane live/dead staining, we found the following protocol works well. Fetal membrane tissues were rinsed 3 times in warmed PBS, and then incubated at 37 C for 15-30 minutes in a solution of warmed serum-free media with 6 µM calcein and 20 µM ethidium homodimer 1. When staining of the membrane bilayer, it is best to separate the amnion and chorion prior to the first PBS rinsing step so that dyes can better penetrate the tissues. To image, tissues were again rinsed in warmed PBS, then placed on a dry tisssue culture plate. If nuclear staining is desired, 1-2 drops of DAPI diamond anti-fade stain were placed on each side of each tissue.

Antibody staining of cells and tissues

Following DPCA treatment of extracted amnion cells, cells were fixed either in methanol or with formalin and stained with primary antibodies against HIF1a, Oct3/4, Nanog, Pax7, CD133, Nestin, and Pref-1. Following primary and secondary antibody staining, plated amnion cells were treated with 1 drop of DAPI diamond anti-fade mountant per well, and membranes were prepared for imaging as in the live/dead staining, above. Stained cells and tissues were imaged on the Keyence using the blue (DAPI) and red or green (secondary probe) filter settings. All images from the same antibody were imaged using the same settings so that relative fluorescent amounts could be accurately compared. For the specific antibodies used, incubation concentrations, and our optimized fixation, staining, and imaging protocols, please see Appendices 6B and 6C.

Appendix 6A – Protocol for extracting and culturing amnion cells from human fetal membranes

This protocol was adapted from Bilic, et al. [14]. This protocol is for one membrane piece, approximately 5cm x 5cm; multiple (4-6) amnion pieces can be run in parallel.

Note: It is recommended that you check each membrane for general membrane quality using the procedure described in Motedayyen, et al. [11]. This procedure can also be used to monitor membrane quality after subsequent days of culture *in vitro*.

1. Membrane preparations: Human fetal membranes are collected from UCSF as described above. In a large tissue culture dish, carefully mince one piece of tissue into ~1mm chunks using a scalpel and straight edge. Transfer minced tissue in 1-2 mL PBS to a 15 mL tube. (Best transfer method is to cut the tip (~4mm) off of a 1 mL pipette tip and use this to suck up the pieces).
2. Four trypsin digestions: add 7ml of warmed 0.25% trypsin to the tube and incubate for 15 m at 37 C. If you are diluting the trypsin from a more concentrated solution, do so in serum-free membrane culture media. Gently remove most of the excess trypsin with a pipette. Repeat for a total of 4 digestions.
    a. Discard the supernatant from the first digestion; retain supernatant from subsequent digestions. This solution can be expected to contain epithelial cells; these can be plated following the instructions from step 6, below.
3. Following the last incubation, centrifuge at 1000 rpm for 5m. Gently remove the supernatant without disturbing the cell pellet or streak at the bottom.
    a. Keep the supernatant, as described in step 2a, combining with supernatant from 2a.
4. During above incubations, prepare 2 mg/mL collagenase in serum free media. You'll need ~8 ml per sample.
    a. Weigh collagenase powder, dissolve, then sterile filter with a 0.2 µm syringe filter.
    b. Pure human collagenase is expensive, but we found success with collagenase from *Clostridium histolyticum*, a bacterially derived combination of collagenase, trypsin, clostripain, and other digesting enzymes (Affymetrix/USB™ J1382003).
5. Gently resuspend the cell pellet from step 3 in ~7 mL of warmed collagenase solution from step 4. Incubate at 37 C for 2h.
6. Centrifuge for 5m at 1000 rpm. Gently remove supernatant from each tube, leaving cell pellet behind (err on the side of leaving liquid behind to not disturb the cell pellet/streak).
7. Then add ~1-2 mL media (growth media not serum-free!) to each tube, and gently pipette well to resuspend all the cells. At this stage, separate tubes from the same membrane can be combined if desired.
8. Count the number of cells on Countess cytometer and record cell numbers for each sample. Take the average of at least 2 measurements/tube.
9. For plating, we generally have success putting about 10^6 cells/mL in the wells of a 96 well plate and around 3-5 * 10^5 cells/well in larger flasks or wells.
10. To maintain cell cultures of extracted cells, follow usual cell culture best practices. Note that these cells usually take longer to settle, so take care when changing media that you don't accidentally suck all the not-yet-adhered cells away. Once cells settle, media should be changed every 48-72h.

11. To passage these cells, note that trypsin (e.g., TrypLExpress) alone usually is not enough to loosen cells from the plates; we found that serum-free media supplemented with 0.125% trypsin and 1 mg/mL collagenase incubated at 37 C for 10-20 minutes was sufficient to loosen cells for passaging.

Appendix 6B – Protocol for antibody staining of human fetal membrane cells and tissues

1. Rinse cells or tissues 3x with warmed PBS, leaving each wash in for 2-5 minutes.
2. Fix the samples in methanol or formalin. If you had been culturing an amnion-chorion tissue bilayer, gently use tweezers to separate the two layers before fixing to improve Ab penetration to each layer.
    a. Methanol: Add cold methanol (-20 C) to each sample and incubate at -20 C for 10 minutes (cells) or 20-30 minutes (tissues).
    b. Formalin: Add formalin fixative solution and incubate 4h at RT or overnight in the refrigerator.

Then, rinse with PBS three times, leaving each rinse in for 2-5 minutes.

3. Add 0.1% Triton solution diluted in 5% goat serum in PBS (96 well plates – 100 µL; tissues – 300 µL)
4. Incubate for 30 minutes at room temperature
5. Aspirate Triton solution and wash with 100 µl 5% goat serum in PBS, leaving first two washes in for 2-5 minutes. Leave the last wash in the plate.
6. Incubate for 1 hour at room temperature or overnight at 4 C.
7. Aspirate 5% goat serum from all wells and add antibody solution diluted in 5% goat serum PBS
    a. Cells: add 30 µL Ab solution per well (see Appendix 6C for details)
    b. Membranes: place in 48 well plates and add 80-90 µl/well (enough to cover tissue). Larger membrane pieces can be cut at this stage, placed in separate wells, and stained separately.
8. Incubate plate for 2 hours at room temperature OR overnight at 4°C
9. Remove antibody solution from all wells and wash 3x with 1% goat serum diluted in PBS, leaving each wash in for 2-5 minutes
10. Add secondary antibody diluted 1:300 in PBS. (Volumes as in Step 7.)
11. Incubate for 1 hour at room temperature; once the secondary antibody is added, take care to protect the plate from light (eg, cover with aluminum foil, keep hood dark, etc).
12. Remove secondary antibody solution from all wells and wash 2x with PBS, leaving each wash in for 2-5 minutes.
13. Stain with DAPI ProLong Diamond Antifade Mountant.
    a. For membranes, after the rinse, place a drop of antifade mountant on a slide or empty culture plate; place a membrane on top; place another drop on top. Up to 2 membranes can be placed on each slide but be careful that they don't slip off the slide.
    b. For cells, add one drop per well, then seal plate for imaging.

14. Image cells or membranes using the appropriate blue and red or green fluorescence filters on the Keyence. You may need to carefully flip the membrane over to image both sides of the membrane to capture all cell types for imaging

Appendix 6C –Antibody concentrations for staining of DPCA-treated cells

These antibody concentrations are based off of the suppliers' recommendations and optimization experiments performed by Kelsey DeFrates; Kelsey also supplied the below table. All antibodies were stored per manufacturer's recommendations; antibodies stored at -20 C were thawed upon first use and aliquoted into ~10 µL aliquots and frozen. Aliquots were used within a week of thawing and not refrozen.

Table A6C: Antibodies used in immunofluorescence staining of human fetal membrane cells and tissues.

	Primary			Secondary		
Marker	Supplier	Antibody	Dilution	Supplier	Antibody	Dilution
HIF-1a	Abcam	Ab2185 Rabbit polyclonal IgG	1:500	M. Probes	A11008 Goat anti-Rabbit IgG (H+L) Cross-Adsorbed Alexa Fluor 488	1:300
NANOG	Novus Biologics	NB100-588	1:150	M. Probes	A11036 Goat anti-Rabbit IgG (H+L) Highly Cross-Adsorbed, Alexa Fluor 568	1:300
Oct-3/4	Santa Cruz Biotech	Sc-5279 Mouse monoclonal IgG2b	1:150	M. Probes	A11005 Goat anti-Mouse IgG (H+L) Cross-Adsorbed Alexa Fluor 594	1:300
CD133	Invitrogen	PA5-38014 Rabbit polyclonal IgG	1:150	M. Probes	A11008 Goat anti-Rabbit IgG (H+L) Cross-Adsorbed Alexa Fluor 488	1:300
PAX7	RD Systems	MAB1675 Mouse monoclonal IgG1	1:50	M. Probes	A11005 Goat anti-Mouse IgG (H+L) Cross-Adsorbed Alexa Fluor 594	1:300
PREF-1	Thermo Scientific	MA515915	1:200	M. Probes	A11005 Goat anti-Mouse IgG (H+L) Cross-Adsorbed Alexa Fluor 594	1:300

NESTIN	Thermo Scientific	PIMA1110 Mouse monoclonal IgG1 kappa	1:50	M. Probes	A11005 Goat anti-Mouse IgG (H+L) Cross-Adsorbed Alexa Fluor 594	1:300

References

[1] G. Bryant-Greenwood, L.K. Millar, Human fetal membranes: Their preterm premature rupture, Biology of Reproduction 63 (2000) 1575-79.
[2] R. Menon, L.S. Richardson, Preterm prelabor rupture of the membranes: A disease of the fetal membranes, Seminars in Perinatology 41(7) (2017) 409-419.
[3] J.M. Duncan, 5. On a lower limit to the power exerted in the function of parturition., Proceedings of the Royal Society of Edinburgh 6 (1869) 163-164.
[4] R.M. Moore, J.M. Mansour, R.W. Redline, B.M. Mercer, J.J. Moore, The physiology of fetal membrane rupture: insight gained from the determination of physical properties, Placenta 27(11-12) (2006) 1037-51.
[5] J.H. Arrizabalaga, M.U. Nollert, Human Amniotic Membrane: A Versatile Scaffold for Tissue Engineering, Acs Biomater Sci Eng 4(7) (2018) 2226-2236.
[6] T. Miki, Amnion-derived stem cells: in quest of clinical applications, Stem Cell Res Ther 2 (2011).
[7] R. Lim, Concise Review: Fetal Membranes in Regenerative Medicine: New Tricks from an Old Dog?, Stem Cell Transl Med 6(9) (2017) 1767-1776.
[8] G. Bilic, C. Brubaker, P.B. Messersmith, A.S. Mallik, T.M. Quinn, C. Haller, E. Done, L. Gucciardo, S.M. Zeisberger, R. Zimmermann, J. Deprest, A.H. Zisch, Injectable candidate sealants for fetal membrane repair: bonding and toxicity in vitro, American Journal of Obstetrics and Gynecology 202(1) (2010).
[9] R.L. Pemathilaka, D.E. Reynolds, N.N. Hashemi, Drug transport across the human placenta: review of placenta-on-a-chip and previous approaches, Interface Focus 9(5) (2019) 20190031.
[10] J.S. Gnecco, A.P. Anders, D. Cliffel, V. Pensabene, L.M. Rogers, K. Osteen, D.M. Aronoff, Instrumenting a Fetal Membrane on a Chip as Emerging Technology for Preterm Birth Research, Curr Pharm Des 23(40) (2017) 6115-6124.
[11] H. Motedayyen, N. Esmaeil, N. Tajik, F. Khadem, S. Ghotloo, B. Khani, A. Rezaei, Method and key points for isolation of human amniotic epithelial cells with high yield, viability and purity, BMC Res Notes 10(1) (2017) 552.
[12] R. Devlieger, E. Gratacos, J. Wu, L. Verbist, R. Pijnenborg, J.A. Deprest, An organ-culture for in vitro evaluation of fetal membrane healing capacity, Eur J Obstet Gynecol Reprod Biol 92(1) (2000) 145-50.
[13] B.K. Koo, I.Y. Park, J. Kim, J.H. Kim, A. Kwon, M. Kim, Y. Kim, J.C. Shin, J.H. Kim, Isolation and Characterization of Chorionic Mesenchymal Stromal Cells from Human Full Term Placenta, J Korean Med Sci 27(8) (2012) 857-863.
[14] G. Bilic, N. Ochsenbein-Kolble, H. Hall, R. Huch, R. Zimmermann, In vitro lesion repair by human amnion epithelial and mesenchymal cells, American Journal of Obstetrics and Gynecology 190(1) (2004) 87-92.
[15] S.V. Murphy, A. Kidyoor, T. Reid, A. Atala, E.M. Wallace, R. Lim, Isolation, cryopreservation and culture of human amnion epithelial cells for clinical applications, J Vis Exp (94) (2014).
[16] E. Boldenow, K.A. Hogan, M.C. Chames, D.M. Aronoff, C. Xi, R. Loch-Caruso, Role of cytokine signaling in group B Streptococcus-stimulated expression of human beta defensin-2 in human extraplacental membranes, Am J Reprod Immunol 73(3) (2015) 263-72.

[17] M. Castillo-Castrejon, N. Meraz-Cruz, N. Gomez-Lopez, A. Flores-Pliego, J. Beltran-Montoya, M. Viveros-Alcaraz, F. Vadillo-Ortega, Choriodecidual Cells From Term Human Pregnancies Show Distinctive Functional Properties Related to the Induction of Labor, American Journal of Reproductive Immunology 71(1) (2014) 86-93.
[18] C.K. Roseblade, M.H.F. Sullivan, H. Khan, M.R. Lumb, M.G. Elder, Limited Transfer of Prostaglandin E2 across the Fetal Membrane before and after Labor, Acta Obstet Gyn Scan 69(5) (1990) 399-403.
[19] S.E. Iismaa, X. Kaidonis, A.M. Nicks, N. Bogush, K. Kikuchi, N. Naqvi, R.P. Harvey, A. Husain, R.M. Graham, Comparative regenerative mechanisms across different mammalian tissues, Npj Regen Med 3 (2018).
[20] E. Gratacos, J. Sanin-Blair, L. Lewi, N. Toran, G. Verbist, L. Cabero, A histological study of fetoscopic membrane defects to document membrane healing, Placenta 27 (2006) 452-6.
[21] R. Devlieger, L.K. Millar, G. Bryant-Greenwood, L. Lewi, J.A. Deprest, Fetal membrane healing after spontaneous and iatrogenic membrane rupture: A review of current evidence, American Journal of Obstetrics and Gynecology 195(6) (2006) 1512-1520.
[22] Y. Zhang, I. Strehin, K. Bedelbaeva, D. Gourevitch, L. Clark, J. Leferovich, P.B. Messersmith, E. Heber-Katz, Drug-induced regeneration in adult mice, Sci Transl Med 7(290) (2015).
[23] I. Strehin, D. Gourevitch, Y. Zhang, E. Heber-Katz, P.B. Messersmith, Hydrogels formed by oxo-ester mediated native chemical ligation, Biomaterials science 1(6) (2013) 603-613.
[24] E. Heber-Katz, P. Messersmith, Drug delivery and epimorphic salamander-type mouse regeneration: A full parts and labor plan, Adv Drug Deliver Rev 129 (2018) 254-261.
[25] J. Cheng, D. Amin, J. Latona, E. Heber-Katz, P.B. Messersmith, Supramolecular Polymer Hydrogels for Drug-Induced Tissue Regeneration, Acs Nano 13(5) (2019) 5493-5501.
[26] E. Heber-Katz, Oxygen, Metabolism, and Regeneration: Lessons from Mice, Trends Mol Med 23(11) (2017) 1024-1036.